Tilo Strutz

# Data Fitting and Uncertainty

A practical introduction to weighted least squares and beyond

► With Online-Service

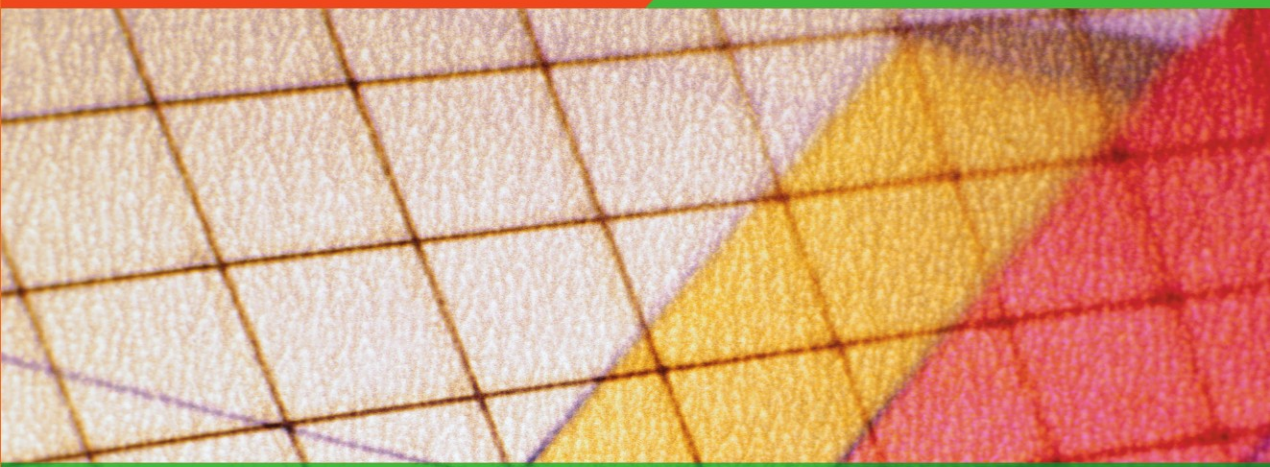

VIEWEG+
TEUBNER

Tilo Strutz

# Data Fitting and Uncertainty

## Aus dem Programm

Weitere Titel des Autors:

**Bilddatenkompression**
von T. Strutz

---

**Verschlüsselungsalgorithmen**
von G. Brands

**Einführung in die Computergrafik**
von H.-J. Bungartz, M. Griebel und C. Zenger

**Statistische Datenanalyse**
von W.-M. Kähler

**Digitale Signalverarbeitung**
von K. D. Kammeyer und K. Kroschel

**Kommunikationstechnik**
von M. Meyer

**Signalverarbeitung**
von M. Meyer

**Digitale Sprachsignalverarbeitung**
von P. Vary, U. Heute und W. Hess

**Information und Codierung**
von M. Werner

**Digitale Signalverarbeitung mit MATLAB®**
von M. Werner

**Nachrichtentechnik**
von M. Werner

**Digitale Audiosignalverarbeitung**
von U. Zölzer

**www.viewegteubner.de**

Tilo Strutz

# Data Fitting and Uncertainty

A practical introduction to weighted least squares and beyond

With 124 figures, 23 tables and 71 test questions and examples

VIEWEG+
TEUBNER

Bibliographic information published by the Deutsche Nationalbibliothek
The Deutsche Nationalbibliothek lists this publication in the Deutsche Nationalbibliografie; detailed bibliographic data are available in the Internet at http://dnb.d-nb.de.

1st Edition 2011



Editorial Office: Reinhard Dapper | Walburga Himmel

Vieweg+Teubner Verlag is a brand of Springer Fachmedien.
Springer Fachmedien is part of Springer Science+Business Media.
www.viewegteubner.de




Cover design: KünkelLopka Medienentwicklung, Heidelberg
Layout: FROMM MediaDesign, Selters/Ts.
Printed on acid-free paper
Printed in Germany

ISBN 978-3-8348-1022-9

# Preface

The method of least squares has been developed by Carl-Friedrich Gauß in 1795 and has been published 1809 in volume two of his work on celestial mechanics *Theoria Motus Corporum Coelestium in sectionibus conicis solem ambientium*. Although it is a rather old technique, it is used still today in many practical applications and has lost nothing in its importance, but has been developed further in several directions.

The idea of this method is to determine the behaviour of systems for which just a limited number of samples, i.e. pairs of input and output, are given. If a certain model function describing the system is presumed, then the parameters of this function are searched which explain the system best in terms of minimisation of the quadratic error. In case of simple systems, applying the method of least squares reduces to, for instance, drawing an approximating curve through a scatter plot of data points.

The early fields of application included, for instance, astronomy (modelling of celestial bodies' movement) and geodesy with the purpose of alleviating measurement errors. Nowadays, this method of approximating data points is probably applied in all sciences, especially those dealing traditionally with statistics as, for instance, physics, biology, economy, or psychology, but also in more recent fields as computer vision. There is basically no difference between experimental data and computer generated data with respect to the data analysis via the method of least squares.

The principle of least squares is generally straightforward, however, its computational intricacy is heavily dependent on the character and complexity of the model function which should describe the behaviour of the system under investigation. So, from the introduction of this data-fitting method in the 19th century until now many numerical techniques for proper and elegant treatment have been developed. In addition, mathematical tools for the evaluation of the fitting results have had to be derived.

The intention of this textbook is to introduce the topic in a more comprehensible manner enabling the reader to solve his/her own specific data-fitting problem. It describes the method of least squares and the treatment of uncertainty in a recipe-like way. Emphasis is put on the unified and generic approach from which the solutions for particular applications can be derived. The book fills the gap between those explaining only very simple data-fitting techniques and those looking at the topic at very high mathematical level. The text discusses many real-life and simulated examples and is accompanied with working source code in

the programming language C, which is provided on the publishers website (see 'OnlinePlus' area).

The book addresses mainly engineers and software programmers or corresponding undergraduates, which are not primarily interested in proofs and derivations of the formulae, but want to quickly become acquainted with the topic and its pitfalls in order to solve a particular fitting problem. A basic mathematical background, especially a familiarity with matrices and partial derivatives as well as some knowledge about variances and standard deviations, is beneficial. Readers, not yet familiar with the method of least squares, are recommended to start with the first chapter followed by the others in sequential order. Every chapter finishes with a list of test questions, enabling a cross-check of whether the subject has been understood.

The material is organised in two parts. The generic basics of data fitting by the Gaussian method of least squares are introduced in the first part. Several examples of linear systems as well as of nonlinear systems are discussed thoroughly in order to enable the reader to solve similar problems.
Chapter 1 explains the general idea of data fitting and defines the terminology and the notation. Chapter 2 presents all principal formulae for the application of the least-square method. In Chapter 3, methods for the estimation of weights are proposed. This is essential, for instance, when uncertainties of recorded data points are not known in advance or the data contain outliers. A clustering approach is discussed, which separates the possible outliers from the bulk of useful data points. An assessment of the results of the data fitting is described in Chapter 4.

The second part of the book is mostly dedicated to the underlying theory and also some numerical methods are discussed in more detail.
It starts with Chapter 5 which is about basic linear algebra and algorithms for matrix inversion. Chapter 6 explains the idea of least squares introducing the principle of maximum likelihood. On this basis, different techniques for the solution of linear and nonlinear fitting problems (i.e. optimisation) are discussed. In Chapter 7 some methods and tools are collected which are helpful in connection with data fitting.

The appendix contains two chapters. The first is about investigations regarding a cluster-based outlier-detection method. The second chapter describes a data-fitting software and discusses several issues of implementing the least-squares method. It concludes with a detailed performance tests of the software.

Leipzig, July 2010 Tilo Strutz

*to my family*

# Contents

# Part I

# Framework of Least-Squares Method

# Chapter 1

# Introduction to Data-Fitting Problems

## 1.1 What is data fitting?

The classical setup for data fitting is based on an experiment or measurement. The measurements yield different results, dependent on the experimental conditions. For instance, we can think of measuring the electrical current $I$ (*observation*) in a resistor $R$ dependent on the given voltage $U$ (*condition*) across this resistor.

Typically, the underlying functional relation between the outcome of the measurement and the corresponding conditions is known or assumed. This relation is described by a mathematical model, which is called *model function* throughout the book. If we expect, for instance, the resistor $R$ to be constant, the functional connection would be $I = U/R$ according to Ohm's law. If the electrical component is of any other type, the relation between $I$ and $U$ could be different and another suitable model has to be used.

The goal of data fitting is to find those parameters of the model function that best describe the connection between observations and conditions.

The mathematical description is as follows.
The outcome of the measurement or experiment is called observation $y$. It is dependent on several conditions, described by a vector $\mathbf{x}$. The parameters of the model are combined in a vector $\mathbf{a}$ with $M$ elements $a_j$, $j = 1 \ldots M$. They are unknown and have to be determined by data fitting methods. Thus, the model function is

$$y = f(\mathbf{x}|\mathbf{a}) \,. \tag{1.1}$$

In case of the aforementioned Ohm's law, the current $I$ is equivalent to the observation $y$, the vector of conditions reduces to a scalar $x = U$, and $\mathbf{a} = a = R$ is the only parameter to be determined.

T. Strutz, *Data Fitting and Uncertainty*, DOI 10.1007/978-3-8348-9813-5 _1,

Sometimes more than one value is observed for a single experiment. We could, for instance, think of measuring not only the current $I$ flowing through the resistor, but also its temperature $T$. However, since the corresponding model function $T = f(I)$ will be different, $y$ is only considered as a scalar for the moment and not as a vector of observations.

It is impossible to change the experimental conditions continuously in practice. Discrete points indicated by variable $i$ have to be selected instead. Besides of this, the observations are affected by random errors (noise). That is why the problem has to be re-formulated as

$$y_i = f(\mathbf{x}_i|\mathbf{a}) + \varepsilon_i \; . \tag{1.2}$$

The vector $\mathbf{x}_i$ contains the condition for experiment $i$ and can be regarded as a set of independent variables, whereas the $y_i$ are considered as dependent variables. It is assumed that $\mathbf{x}_i$ is known exactly or that the error in $\mathbf{x}_i$ is at least negligibly small compared to the error in the measured observation $y_i$. Only $\mathbf{a}$ is unknown and has to be calculated using suitable data-fitting methods. The repetition of a certain experiment under the same condition $\mathbf{x}_i$ leads to different values of $y_i$, because observations are subject to the random error $\varepsilon_i$. Doing the experiment an infinite number of times would reveal the true *parent distribution* of $y_i$. In practice, however, the parent distribution is unknown and can only be estimated to a certain accuracy.

Since we are looking for an optimal solution for $\mathbf{a}$, data fitting is a kind of optimisation problem. Strictly speaking, it concerns minimisation, as will be shown later on. It must be emphasized that the optimum of $\mathbf{a}$ is never absolute, but rather always related to the measured data and the assumptions taken with regard to the reliability of the observations $y_i$ or the distribution of their errors [Mey84]. When the model parameters $\mathbf{a}$ are found, the model function can be used for the interpolation and, provided that the model is not only an approximation for a limited subset of conditions, also for the extrapolation of data.

Data fitting is often referred as *data reduction*, since the number of $N$ observations is reduced to a mere $M$ parameters plus the selection of a suitable model function. Keeping in mind that the model does not represent all observations exactly, but instead, acts as approximation, it also can be regarded as special kind of lossy data compression [Str09a].

In some applications, the true functional connection between the experimental conditions $\mathbf{x}_i$ and the observations $y_i$ is not known. In this case, it is a common method to approximate $y$ for a limited range of $\mathbf{x}$ by using a superposition of special functions of higher order like polynomials, trigonometric functions, or

something else. However, the decision for or against a certain model function must be made very carefully, since it will heavily influence the result of the data-fitting procedure. In particular, model functions that are not based on a true or realistic physical, chemical, or other model must not be used extrapolate data!

## 1.2 Notation

Three basic types of variables are used in this book. Scalar variables are always denoted in *italics*, for instance, $y$, $f(x)$, $a_1$ etc. Vectors are expressed in small, bold-faced letters, such as $\mathbf{x} = (x_1, x_2, \ldots x_N)^{\mathrm{T}}$. The exponent T means "transposed", making $\mathbf{x}$ a column vector. Please note that T is not in *italics* because it is not a variable. The same holds true for indices, which are not consecutive numbers such as $i$ in $y_i$ but rather simply indicate that a certain variable is related to something else, like $\sigma_{\mathrm{y}}^2$. y is not a serial number here; it signals that $\sigma^2$ is the variance in $y$. Finally, matrices are denoted with capital, bold-faced letters such as $\mathbf{J}$ and $\mathbf{W}$, for example.

The elements of matrices are scalars, thus the elements of matrix $\mathbf{A}$ are denoted by $a_{ij}$ with $i = 1, \ldots, N$ and $j = 1, \ldots, M$ as the row and column indices, respectively. The set of integers is denoted by $\mathbb{Z}$. $||\mathbf{x}||$ is the Euclidean norm of column vector $\mathbf{x}$, i.e., $||\mathbf{x}|| = \left(\mathbf{x}^{\mathrm{T}} \cdot \mathbf{x}\right)^{1/2} = \left(\sum_i x_i^2\right)^{1/2}$. Pages 235f list most of the variables, which are used throughout the book.

Readers who are not familiar with matrix algebra are requested to read Section 5.1 first.

## 1.3 Linear vs. nonlinear problems

The discussion of the linearity of a data-fitting problem is indispensable, since the kind of treatment and its complexity depend heavily on this property.

In engineering, the term "linear" is associated with things like linear time invariant (LTI) systems or linear signal transformations and indicates that an additive superposition of input signals leads to an additive superposition of the according output signals. In addition, a characteristic curve $y = f(x)$ is called linear if it is a straight line, which is basically the same because of

$$y_1 = f(x_1)\,, \qquad y_2 = f(x_2) \qquad \longrightarrow \qquad y_1 + y_2 = f(x_1 + x_2)\,. \tag{1.3}$$

In the field of data fitting, the terms "linear" and "nonlinear" are used with different meanings. They are not assigned to the relation between the observation

$y$ and the vector of conditions $\mathbf{x}$ of the model function $y = f(\mathbf{x}|\mathbf{a})$, but instead to the relation between $y$ and the model parameters $a_j$ $(j = 1 \ldots M)$! For instance, the exponential function

$$y = f(\mathbf{x}|\mathbf{a}) = a_1 \cdot \mathrm{e}^{-x} \tag{1.4}$$

is regarded as linear in $\mathbf{a}$, despite the nonlinear term $\mathrm{e}^{-x}$, since the first derivative is $\partial y/\partial a_1 = \mathrm{e}^{-x}$ and no longer dependent on $\mathbf{a}$. In contrast to that

$$y = \mathrm{e}^{a_2 \cdot x} \tag{1.5}$$

is obviously nonlinear due to $a_2$, because $\partial y/\partial a_2 = x \cdot \mathrm{e}^{a_2 \cdot x}$ is still dependent on $a_2$.

Sometimes a chosen model function seems to be nonlinear at first glance, but turns to linear if treated properly. Since data fitting of nonlinear functions is in general more difficult than data fitting of linear ones, the desired model should always be inspected carefully to determine whether it is in fact nonlinear or simply *pseudo-nonlinear*.

**Example (1)**:
The model function

$$y = b_1 + (x - b_2)^2 \ , \tag{1.6}$$

for example, seems to be nonlinear, since $b_2$ is part of a squared term. However, the function can be transformed into

$$\begin{aligned} y &= b_1 + x^2 - 2 \cdot b_2 \cdot x + b_2^2 \\ &= b_1 + b_2^2 - 2 \cdot b_2 \cdot x + x^2 \end{aligned}$$

and at closer look it becomes apparent that the equation can be rewritten as

$$y = a_1 + a_2 \cdot x + x^2 \ . \tag{1.7}$$

with

$$a_1 = b_1 + b_2^2 \quad \text{and} \quad a_2 = -2 \cdot b_2 \ .$$

It turns out that the model is linear in $\mathbf{a}$!
□□□

**Example (2)**:
Another example is the cosine function

$$y = b_1 + b_2 \cdot \cos(x - b_3) \ . \tag{1.8}$$

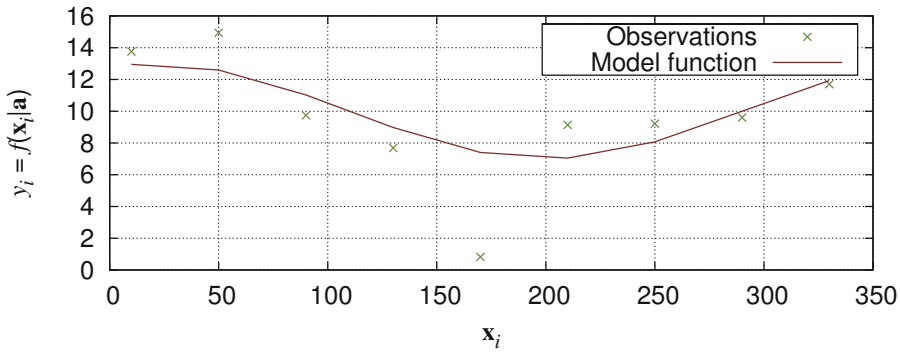


Figure 1.1: Example of a pseudo-nonlinear model function: $y = b_1 + b_2 \cdot \cos(x - b_3)$

This model could be used to describe a circular movement, if the observation is restricted to the projection of the movement onto a screen perpendicular to the plane of movement as for instance described in [Pot06]. **Figure 1.1** shows the recording of nine observations in dependence of known rotation angles $x_i$.

There are three unknowns to be determined via data fitting: $b_2$ is the radius of the circular movement, $b_3$ is a phase offset dependent on the direction of the projection, and $b_1$ indicates the centre of the performed movement.

It is somewhat more difficult to discover a proper transformation here. Looking for a suitable trigonometric operation, we find

$$\cos(a - b) = \cos(a)\cos(b) + \sin(a)\sin(b)$$

and after its application to the initial model function (1.8)

$$y = b_1 + b_2 \cdot [\cos(x)\cos(b_3) + \sin(x)\sin(b_3)] \ .$$

Using

$$a_1 = b_1, \quad a_2 = b_2 \cdot \cos(b_3), \quad \text{and} \quad a_3 = b_2 \cdot \sin(b_3)$$

we get

$$y = f(\mathbf{x}|\mathbf{a}) = a_1 + a_2 \cdot \cos(x) + a_3 \cdot \sin(x) \ , \tag{1.9}$$

which is a linear model function with respect to $\mathbf{a}$. After fitting of (1.9) it is straightforward to determine $b_j$ from $a_j$.
□□□

**Example (3)**:
Many applications require the fitting of points belonging to a circle, whose function is given as

$$(y_1 - a_1)^2 + (y_2 - a_2)^2 = r^2 \,, \tag{1.10}$$

with $r$ as the radius and $(a_1, a_2)$ as centre of the circle. The main problem here is that there are no conditions, but only observations. Therefore, this formula can not be used directly with respect to the setup $y = f(\mathbf{x}|\mathbf{a})$. A trick is needed, and it will turn out that the problem can be converted in a linear one. Subsection 1.5.3 discusses the details.
□□□

In contrast to pseudo-nonlinear problems, real nonlinear model functions can be linearised only if alterations are permitted on the left side of the function. This is a valid operation; however, it leads also to a different optimisation problem with different results compared to the original model.

The exponential function

$$y = b_1 \cdot \exp(b_2 \cdot x) \tag{1.11}$$

is the standard example to demonstrate the linearisation of nonlinear models. In order to release $b_2$ from the exponent, the logarithm has to be applied to both sides of the equation

$$\begin{aligned} \ln(y) &= \ln\left[b_1 \cdot \exp(b_2 \cdot x)\right] = \ln(b_1) + b_2 \cdot x \\ &= a_1 + a_2 \cdot x \end{aligned} \tag{1.12}$$

which is a linear straight-line problem. However, since the logarithm of $y$ is now fed into the computations instead of $y$ itself, the errors in $y$ are also weighted differently. The points of lower values of $y$ influence the determination of the slope and intercept of the line now too strongly compared to higher values of $y$.

The data fitting is no longer optimised according to $b_1$ and $b_2$ and yields different results.

Even a variation of the exponential model

$$y = b_1 \cdot \exp(b_2 \cdot x + b_3) \tag{1.13}$$

can be linearised. Upon closer inspection, it becomes apparent that $b_1$ and $b_3$ are indistinguishable

$$\begin{aligned} \ln(y) &= \ln\left[b_1 \cdot \exp(b_2 \cdot x + b_3)\right] \\ &= \ln(b_1) + b_2 \cdot x + b_3 \\ &= a_1 + a_2 \cdot x \end{aligned}$$

Table 1.1: Transformations for linearisation of nonlinear functions leading to $v = a_1 + a_2 \cdot u$

| Function | $u$ | $v$ | $a_1$ | $a_2$ |
|---|---|---|---|---|
| $y = b_1 \cdot x^{b_2}$ | $\ln(x)$ | $\ln(y)$ | $\ln(b_1)$ | $b_2$ |
| $y = b_1 + \frac{b_2}{x}$ | $\frac{1}{x}$ | $y$ | $b_1$ | $b_2$ |
| $y = \frac{b_2}{x + b_1}$ | $x$ | $\frac{1}{y}$ | $\frac{b_1}{b_2}$ | $\frac{1}{b_2}$ |
| $y = \frac{b_1 \cdot x}{x + b_2}$ | $\frac{1}{x}$ | $\frac{1}{y}$ | $\frac{1}{b_1}$ | $\frac{b_2}{b_1}$ |

with $a_1 = \ln(b_1) + b_3$ and $a_2 = b_2$.
In fact, the ambiguity of parameters in this example might even inhibit the success of solving the data-fitting problem numerically. It must be emphasized once again that model functions should be selected carefully and simplified as much as possible.

Other functions can also be linearised in a similar manner. Setting

$$v = a_1 + a_2 \cdot u$$

as (linear) target model, the true model function can be converted using suitable substitutions for $x$ and $y$. For instance, equation (1.11) was linearised by applying $v = \ln(y)$, $u = x$, $a_1 = \ln(b_1)$ and $a_2 = b_2$. **Table 1.1** provides solutions for the linearisation of some other functions (based on [Pap01]).

## 1.4 Example applications of linear data fitting

This Section and the next are intended to explain the broad field of data fitting applications and are not required for the comprehension of the subsequent chapters. Impatient readers may wish to skip to Chapter 2. Nevertheless, the author recommends reading these sections after the reader has familiarised himself or herself with the method of least squares. Some of the explanations therein touch on special problems that might be relevant to the reader's setup.

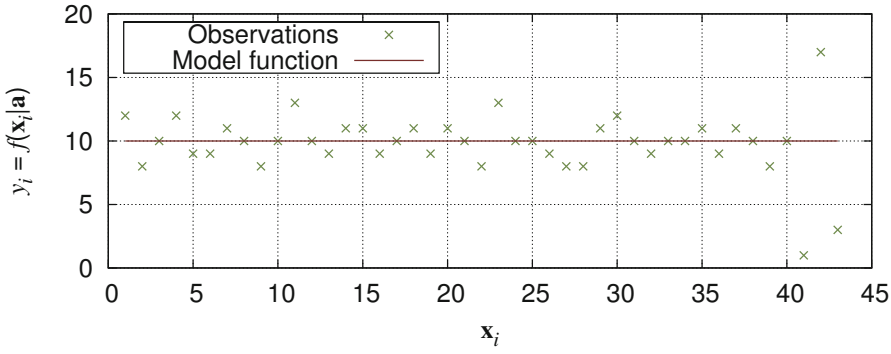


a)

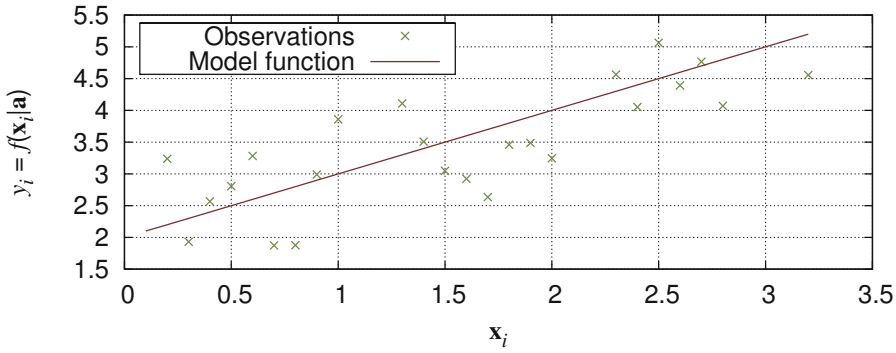


b)

Figure 1.2: Example for model functions: a) determination of a constant value, b) fitting of a straight line.

### 1.4.1 Estimation of a constant value

The simplest problem in data fitting is to determine a certain constant value, which could be the mean of some observations.

Let us assume that we want to find out how often people working in an office look out of the window during the day. We employ a statistics trainee to watch the people and let her count the occurrences of looking-out-of-the-window separately for each person. The result of a ten-day experiment watching six people each day yields the observations depicted in **Figure 1.2**a)[1]. Furthermore, we should disregard that special conditions can influence the counted numbers dramatically, for instance, if the office staff were exclusively male and the window pointed to

[1] The values are chosen arbitrarily and are not the result of a real experiment.

a street with shops typically attracting young women.[2] Generally, some observations deviate from the mean stronger than others. Somebody may have spotted a beautiful bird and wants to keep track of it. Alternatively, another person could only have eyes for the trainee and does not look out of the window at all. This 'anomalous' behaviour disturbs the statistics. If we get lucky, these so-called *outliers* balance each other out. However, outliers are very often biased to one side (birds are of higher interest than the trainee is). It is therefore essential to detect these mavericks and to treat them properly, as it is discussed in Chapter 3.

The mathematical description of (1.1) simplifies to

$$y = f(\cdot|\mathbf{a}) = \text{const.} = a_1 \; . \tag{1.14}$$

No special conditions are distinguished and the outcome $y$ of the measurement is equal to a constant value $a_1$ representing the entire model.

### 1.4.2 Parameter estimation for a straight line (linear regression)

Another very famous example of data fitting, often used in economics and medical science, for example, deals with straight lines.

The mathematical description is still very elementary

$$y = f(\mathbf{x}|\mathbf{a}) = a_1 + a_2 \cdot x \; . \tag{1.15}$$

The variable $y$ is linearly dependent on a single condition $x$ and two parameters $(a_1, a_2)$ have to be determined. **Figure 1.2** b) depicts an example.

### 1.4.3 Polynomial function

There are scenarios where the relation between the experimental conditions and the experiment results (observations) has to be described without knowing the underlying model function. In these cases, the chosen range of conditions is approximated by a linear combination of special functions, which could be polynomials of degree $M-1$, for instance

$$y = f(\mathbf{x}|\mathbf{a}) = a_1 + a_2 \cdot x + \ldots + a_M \cdot x^{M-1} \; . \tag{1.16}$$

After the data fitting, values $a_j$ very close to zero can indicate, for instance, that the corresponding part of the polynomial is not required to describe the examined problem. This, however, only holds true if the standard uncertainty of the

[2] The results for the summer and winter seasons will also differ dramatically in that scenario.

observations is rather low. Additional model parameters are quickly integrated in order to fit the random component of the data. The standard uncertainty of single estimated parameters in percent (see Chapter 4) is a somewhat more reliable indication of unnecessary parts of the model function. If the random error in the observations is not too high, then the uncertainties of suspicious parameters are high in comparison to other parameters.

### 1.4.4 Multiple linear regression

So far, the condition vector $\mathbf{x}$ had contained one single element only. We can also conceive of ($M$-1)-dimensional problems

$$y = f(\mathbf{x}|\mathbf{a}) = a_1 + a_2 \cdot x_1 + a_3 \cdot x_2 + \ldots + a_M \cdot x_{M-1} \; . \tag{1.17}$$

#### Approximation of planes

One example of multiple linear regression is the approximation of planes, which is in fact two-dimensional. The setup is

$$y = f(\mathbf{x}|\mathbf{a}) = a_1 + a_2 \cdot x_1 + a_3 \cdot x_2 \; , \tag{1.18}$$

where $x_1$ and $x_2$ might be coordinates. $a_2$ and $a_3$ are the gradients with different orientation according to the used coordinate system and $a_1$ is merely an offset. An example is shown in **Figure 1.3**.

#### Supervised classification

Typically, classification is not associated with data fitting. Nevertheless, data fitting is applicable for the distinction between objects of two classes, for instance.

According to equation (1.17) the classification is based on $M-1$ features forming the condition vector $\mathbf{x}$. The parameters $a_j$ must be determined using a training set of objects with known assignments to one of the classes. The class numbers are the observed values $y_i$. Once the parameters are known, the classification of objects not included in the training set becomes possible.

Practical applications typically require several independent features to distinguish the objects. As an explanation, we consider here the simplest case of classification using a single feature $x$. Since in supervised classification the class membership is known for the training set of objects, we can determine the distribution of the feature for each class separately (**Figure 1.4**).

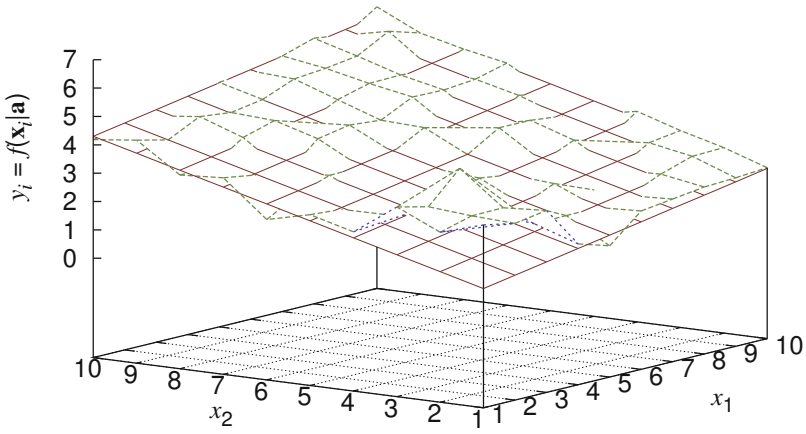


Figure 1.3: Example for a two-dimensional model function: plane approximation. The green vertices indicate the (noisy) observations $y_i$.

Now let us assign the observation value $y_i = 1$ to the first class and the value 2 to the second class. The numbers are slightly randomised for better visualisation in **Figure 1.4**b) affecting the spread around 1 and 2. Albeit the scatter plot in Figure 1.4b) does not follow a straight line, the model function

$$y = a_1 + a_2 \cdot x$$

has to be fitted to the data.

After model parameters $a_1$ and $a_2$ are determined, new objects can be classified by using their feature value as condition $x$. The resulting value of $y$ has to be compared to the threshold of 1.5: if $y$ is larger, the object is assigned to class 2; otherwise it belongs to class 1. Even a rejection of objects could be managed, if two thresholds are applied.

There are only two prerequisites for a successful distinction.

First, the training set must comprise a comparable number of objects in each class. In the example of Figure 1.4b) $N_1 = N_2 = 200$ objects are used for each class. If class 1 only contained very few training objects compared to class 2, then they had only weak influence on the fitting procedure and the straight line would be almost entirely captured by the second class, i.e., $a_1 \approx 2$ and $a_2 \approx 0$.

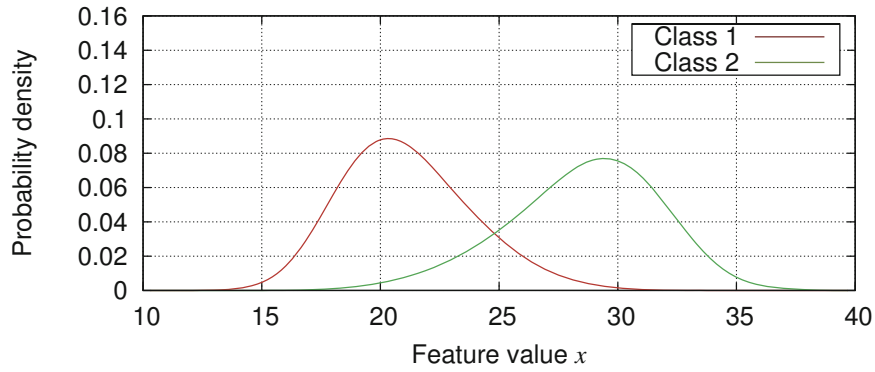


a)

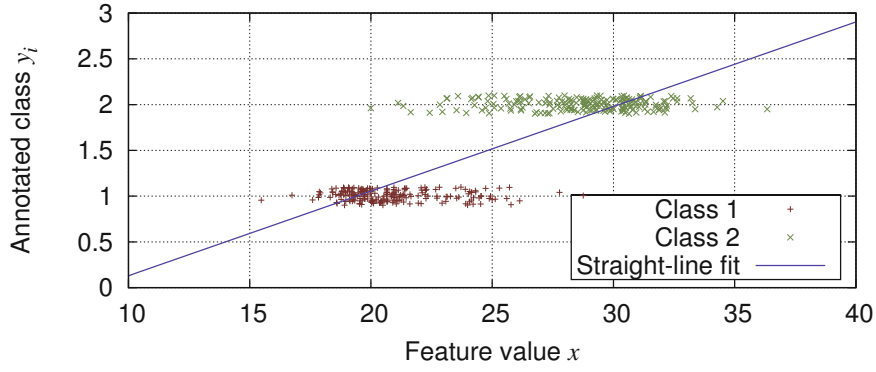


b)

Figure 1.4: Supervised classification: a) distributions of same feature for different classes; b) assignment of class numbers; see text for details

This problem could be overcome simply by using different weights[3] for the classes $c$ in order to balance their influence, i.e. $w_c = 1/N_c$.

The second prerequisite concerns the linear separability of the two classes. If, for instance, the feature values were distributed as depicted in **Figure 1.5**a), it would be impossible to make a linear decision based on only one feature. Either two or more features have to be used or a nonlinear[4] approach must be applied. However, the selection of a proper model function has to be made carefully, when using the least-squares method for fitting. A parabola does not result in good distinction between these two classes, as can be seen in **Figure 1.5**b). However, applying a least-squares-based neural network (see Subsection 1.5.4) with one input and three hidden neurons (10 parameters in total) yields excellent distinction.

[3] The use of weights is discussed in detail in Chapter 3.
[4] Either nonlinear with respect to $x$ or a nonlinear model function (see Section 1.3).

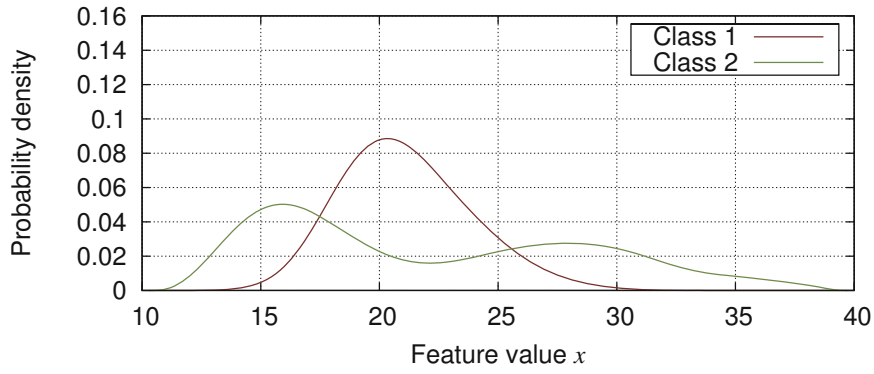


a)

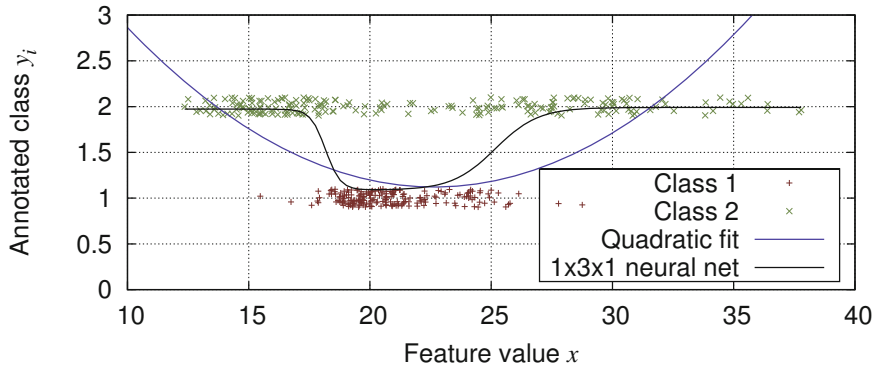


b)

Figure 1.5: a) Class distributions that cannot be linearly separated by a single feature; b) Discrimination using a parabola vs. a neural network

**Affine transformation**

Another example for multiple linear regression is the modelling of affine transformations of coordinates, for instance (**Figure 1.6**). For two-dimensional problems, this can be described via

$$\begin{pmatrix} x \\ y \end{pmatrix} = \begin{pmatrix} a_1 \\ a_2 \end{pmatrix} + \begin{pmatrix} a_3 & a_5 \\ a_4 & a_6 \end{pmatrix} \cdot \begin{pmatrix} u \\ v \end{pmatrix} \tag{1.19}$$

or in matrix notation

$$\mathbf{x} = \mathbf{A} \cdot \mathbf{u} = \begin{pmatrix} x \\ y \end{pmatrix} = \begin{pmatrix} a_1 & a_3 & a_5 \\ a_2 & a_4 & a_6 \end{pmatrix} \cdot \begin{pmatrix} 1 \\ u \\ v \end{pmatrix} . \tag{1.20}$$

Given a set of pairs of coordinates $(u_i; v_i)$ and $(x_i; y_i)$, the parameters of the geometrical transformation have to be determined. The vectors $\mathbf{u}$ and $\mathbf{x}$ are the

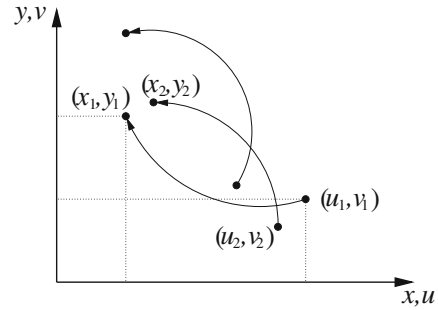


Figure 1.6: Affine transformation of coordinates

coordinates of points before and after the transformation, respectively. $(a_1\ a_2)^{\mathrm{T}}$ introduces a translational displacement to the points, whereas $a_3 \ldots a_6$ are responsible for more complex changes, like rotation, scaling and sheering. Based on given corresponding points $\mathbf{u}_i$ and $\mathbf{x}_i$, the coefficients $a_1 \ldots a_6$ have to be estimated. The components of $\mathbf{x}$ in equation (1.20) can be calculated independently of each other using

$$\begin{aligned} x &= a_1 + a_3 \cdot u + a_6 \cdot v \\ y &= a_2 + a_4 \cdot u + a_6 \cdot v \ , \end{aligned} \tag{1.21}$$

which is in fact the same fitting problem as the plane approximation (eq. 1.18). Only the interpretation of the data is different.

In the case of a translation combined with a pure rotation with an angle of $\theta$, $\mathbf{A}$ would be

$$\mathbf{A} = \begin{pmatrix} a1 & \cos(\theta) & -\sin(\theta) \\ a_2 & \sin(\theta) & \cos(\theta) \end{pmatrix} .$$

However, since there are now constraints on the parameter determination, namely

$$a_3 = a_6 = \cos(\theta) \qquad \text{and} \qquad a_4 = -a_5 = \sin(\theta) \ ,$$

the two equations in (1.21) are therefore dependent on each other and the linear affine transformation has changed into a nonlinear model.

### Linear prediction

A special application of data fitting is the prediction of time series (or other sequences of data, such as in image-compression algorithms [Str09a]). The experimental conditions are specified here by the time-series samples $x[\cdot]$ that have

already be seen, i.e., which lie in the past. The linear prediction problem can be expressed with

$$\hat{x}[n] = f(\mathbf{x}_n|\mathbf{a}) = \mathbf{x}_n^{\mathrm{T}} \cdot \mathbf{a} \;, \tag{1.22}$$

if $\mathbf{x}$ and $\mathbf{a}$ are column vectors. $\hat{x}[n]$ is the predicted value of $x[n]$. Taking only three samples from the past for prediction, i.e. $\mathbf{x}_n^{\mathrm{T}} = (x[n-1]\; x[n-2]\; x[n-3])$, the model function is

$$\hat{x}[n] = f(\mathbf{x}_n|\mathbf{a}) = a_1 \cdot x[n-1] + a_2 \cdot x[n-2] + a_3 \cdot x[n-3] \;. \tag{1.23}$$

The idea behind the procedure of prediction is to forecast the current sample value $x[n]$ dependent on its $M$ predecessors $x[n-1] \ldots x[n-M]$. Before the predictor can be applied, the model-parameters vector $\mathbf{a}$ has to be determined using a training set of known combinations of $x[n]$ and its predecessors. Please note that the mean value of the prediction error $e[n] = x[n] - \hat{x}[n]$ is assumed to be zero in general. If, however, the prediction is performed in dependence on different contexts, then the mean of the prediction might deviate from zero and the correction of $\hat{x}[n]$ by an additional parameter $a_0$ in equation (1.23), i.e. $\hat{x}_c[n] = \hat{x}[n] + a_0$, should be considered. This is called bias cancellation [ISO00].

The scenario of predicting single pixel values in images is depicted in **Figure 1.7**. The setup is based on the presumption that the single pixel positions are scanned starting with the top-left corner, row-by-row downwards to the bottom-right corner of the image. Let us assume that the scanning process has reached the position marked with 'X'. All pixels above the thick line have been already processed and 'X' is the next value $x[n, m]$ to be predicted. A template defines which of the neighbouring pixels are involved in the computation of the estimation value $\hat{x}[n, m]$. That means these values act as conditions with respect to the model function (1.1). Given the template in Figure 1.7, the model function is

$$\begin{aligned} \hat{x}[n,m] \;=\; & a_1 \cdot x[n-1,m] + a_2 \cdot x[n,m-1] + \\ & a_3 \cdot x[n-1,m-1] + a_4 \cdot x[n+1,m-1] + \\ & a_5 \cdot x[n-2,m] + a_6 \cdot x[n,m-2] + \\ & a_7 \cdot x[n-2,m-1] + a_8 \cdot x[n-1,m-2] + \\ & a_9 \cdot x[n+1,m-2] + a_{10} \cdot x[n+2,m-1] \;. \end{aligned}$$

The setup further presumes that the characteristics of the image signal do not change very much within the vicinity of the current position. Thus the model parameters $a_j$ can be determined based on the relations between the pixel values in the window defined by $L_1$, $L_2$, and $L_3$ in Figure 1.7. This window contains all pixel positions from which the pixel values are taken as observations. The conditions arise from the values at the corresponding template positions. In total,

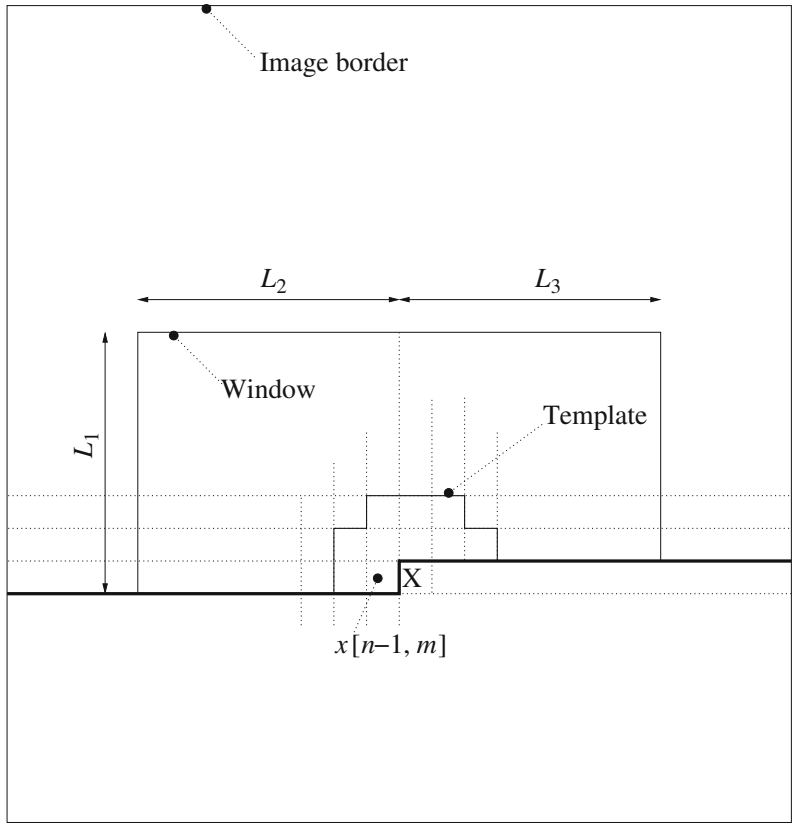


Figure 1.7: Environment for the prediction of single pixel values

there are $L_1 \times L_2 + (L_1 - 1) \times L_3$ observations available for the determination of the model parameters $a_1 \ldots a_{10}$, which are used afterwards for the computation of the estimation value $\hat{x}[n, m]$.

In case that the template (or the window) is not completely located inside the image area, an exception handling is required.

## 1.5 Selected nonlinear data-fitting problems

### 1.5.1 Exponential functions

Subsection 3.5.7 operates with an exponential function of type

$$y = a_1 \cdot \exp(a_2 \cdot x) \tag{1.24}$$

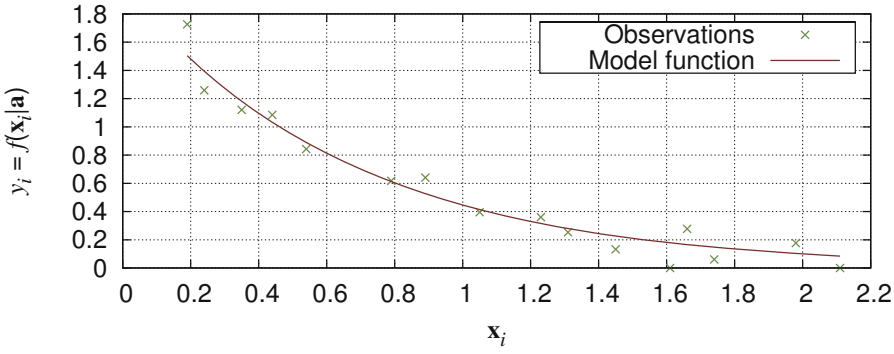


a)

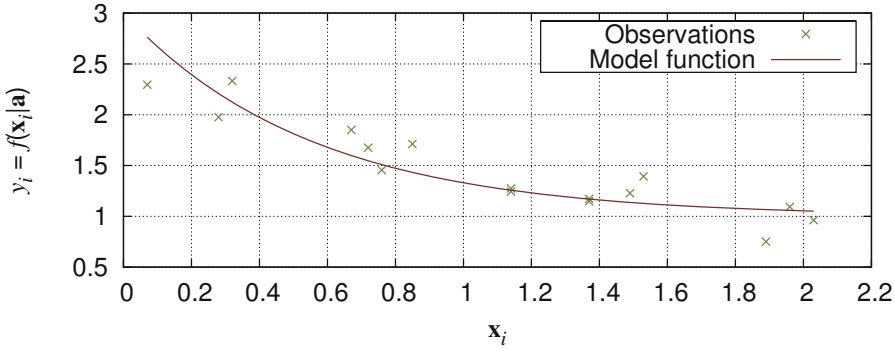


b)

Figure 1.8: Examples of exponential functions: a) $y = a_1 \cdot \exp(a_2 \cdot x)$; b) $y = a_1 + a_2 \cdot \exp(a_3 \cdot x)$

in order to study the effects of linearisation (see Section 1.3) for the selected case of $a_1 = 2, a_2 = -1.5$ (**Figure 1.8**a). The conditions are also randomised in the test-data set used in this example. Nevertheless, it is assumed that the conditions $x_i$ are exactly known and only the observations $y_i$ are uncertain according to the statements in Section 1.1. There are techniques that can also deal with uncertain conditions. However this goes beyond the scope of this book and is discussed only briefly in Section 7.6.

A simple variation of equation (1.24)

$$y = a_1 + a_2 \cdot \exp(a_3 \cdot x) \tag{1.25}$$

eludes from linearisation and methods for nonlinear data fitting have to be used. **Figure 1.8**b) shows an example with $a_1 = 1.0$, $a_2 = 2.0$, and $a_3 = -1.8$.

### 1.5.2 Composite Gaussian bell functions

Another nonlinear problem is the fitting of distributions, which can be modelled, for instance, via superposition of two Gaussian bells with different amplitudes $c$, mean values $\mu$ and variances $\sigma^2$

$$y = c_1 \cdot \exp\left[-\frac{(x-\mu_1)^2}{2\cdot\sigma_1^2}\right] + c_2 \cdot \exp\left[-\frac{(x-\mu_2)^2}{2\cdot\sigma_2^2}\right] .$$

In the language of data fitting this can be written as

$$y = a_1 \cdot \exp\left[a_2 \cdot (x-a_3)^2\right] + a_4 \cdot \exp\left[a_5 \cdot (x-a_6)^2\right] \qquad a_2, a_5 < 0 .$$

**Figure 1.9** shows two examples of superposition: additive and subtractive. Despite the very different model parameters $a_1 \ldots a_6$, the modelled functions look very similar. This leads to the conclusion that the fitting of those data sets is ambiguous.

### 1.5.3 Circle function

The function of a circle is given by

$$(y_1 - a_1)^2 + (y_2 - a_2)^2 = r^2 , \tag{1.26}$$

with $r$ as radius of the circle centred at $(a_1, a_2)$ (**Figure 1.10**). It is obvious that there are only observations ($y_1$ and $y_2$), but no conditions. $r$ is just another parameter, say $r = a_3$. In order to fit this function into the framework of model functions a trick is required. We exchange conditions and observations and rewrite (1.26) as

$$y = 0 = (x_1 - a_1)^2 + (x_2 - a_2)^2 - a_3^2 . \tag{1.27}$$

Consequently, the observations are in principle correct, whereas the conditions are erroneous. The evaluation of the fitting results becomes more complicated (e.g. see [Kas76]).

[Coo93] and others have shown that it is also possible to linearise the model function (1.27) in the manner that was discussed in Subsection 1.3. Let us rewrite equation (1.27) as

$$\begin{aligned} 0 &= (x_1^2 - 2\cdot x_1 \cdot a_1 + a_1^2) + (x_2^2 - 2\cdot x_2 \cdot a_2 + a_2^2) - a_3^2 . \\ &= x_1^2 + x_2^2 - 2\cdot x_1 \cdot a_1 - 2\cdot x_2 \cdot a_2 + a_1^2 + a_2^2 - a_3^2 . \end{aligned} \tag{1.28}$$

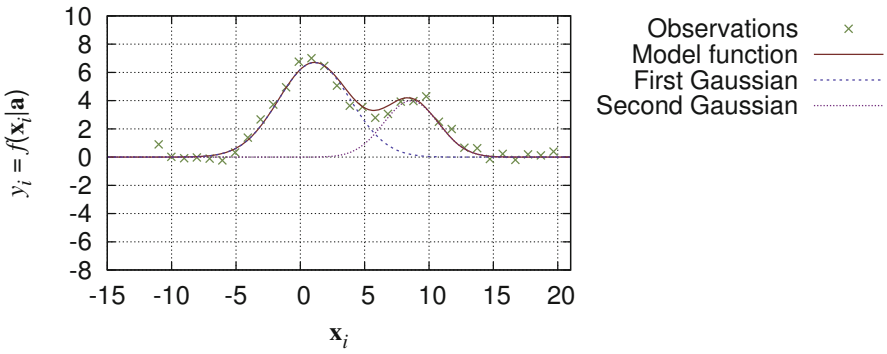


a)

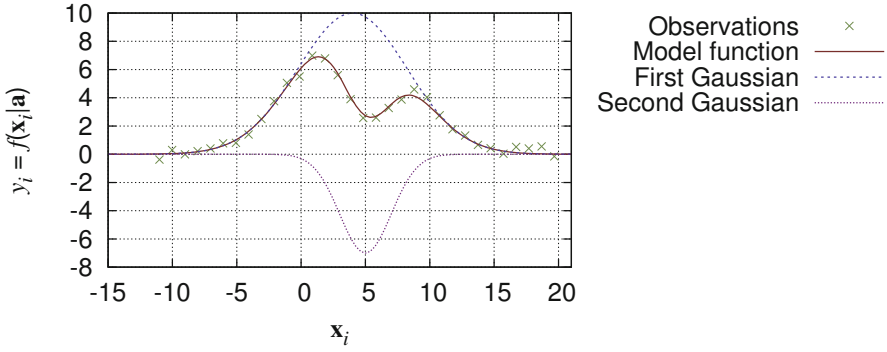


b)

Figure 1.9: Example of composite Gaussian functions; a) sum of two positive Gaussian bells with $a_1 = 6.7$, $a_2 = -0.06378$, $a_3 = 1.1$, $a_4 = 4$, $a_5 = -0.11125$, $a_6 = 8.6$ and $\sigma_\varepsilon^2 = 0.25$; b) difference of two Gaussian bells $a_1 = 10$, $a_2 = -0.27778$, $a_3 = 4$, $a_4 = -7$, $a_5 = -0.125$, $a_6 = 5$ and $\sigma_\varepsilon^2 = 0.25$

Using $b_1 = 2 \cdot a_1$, $b_2 = 2 \cdot a_2$, and $b_3 = a_1^2 + a_2^2 - a_3^2$ results to

$$-(x_1^2 + x_2^2) = -b_1 \cdot x_1 - b_2 \cdot x_2 + b_3 \,, \tag{1.29}$$

which is linear in $\mathbf{b} = (b_1 \;\; b_2 \;\; b_3)^{\mathrm{T}}$.

Please remember that $x_1$ and $x_2$ are observations, which now appear on both sides of the equation. The fitting of a linear model function is not applicable if all observations (values on the left side) are equal to zero as in equation (1.28), thus the term $(x_1^2 + x_2^2)$ must be moved to the left side of the model function.

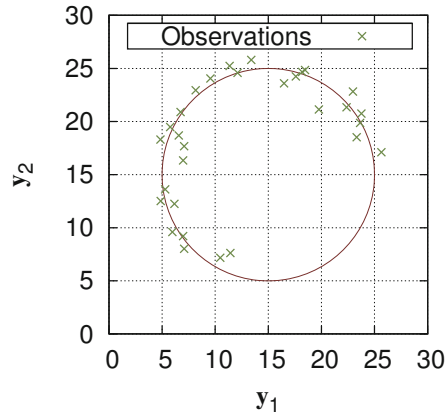


Figure 1.10: Observed points of a circular object

After fitting with this linearised version, the values of the original variables $a_1$, $a_2$, and $a_3$ can then be recovered from the formulas

$$a_1 = 0.5 \cdot b_1 \qquad a_2 = 0.5 \cdot b_2 \qquad a_3 = \sqrt{a_1^2 + a_2^2 - b_3}\,.$$

### 1.5.4 Neural networks

For a long time, artificial neural networks were regarded as a completely new method of signal processing. Because of the variety of different possible topologies of networks and kinds of signal propagation, this belief is true to a certain extend. The mostly used type of *feed-forward networks* (**Figure 1.11**), however, is nothing other than a weighted superposition of typically nonlinear functions and can be easily converted into a data-fitting task. The network in Figure 1.11 has nine parameters in total, four weights $w_{lk}$ propagating the input values $x_l$ to the hidden neurons, three offset parameters $w_{0k}$ and $v_0$ introducing bias into the summation indicated by $\Sigma$, and two parameters $v_k$ weighting the intermediate values $h_k$. $l$ and $k$ are the indices of input and hidden neurons, respectively. The intermediate values result from the weighted summation of the input values followed by a limitation of the dynamic range, which can be achieved for instance using the sigmoid function

$$h_k(t_k) = \frac{1}{1 + \mathrm{e}^{-t_k}} \tag{1.30}$$

with the intermediate value

$$t_k = \sum_l w_{lk} \cdot x_l = \mathbf{w}^{\mathrm{T}} \cdot \mathbf{x}\,. \tag{1.31}$$

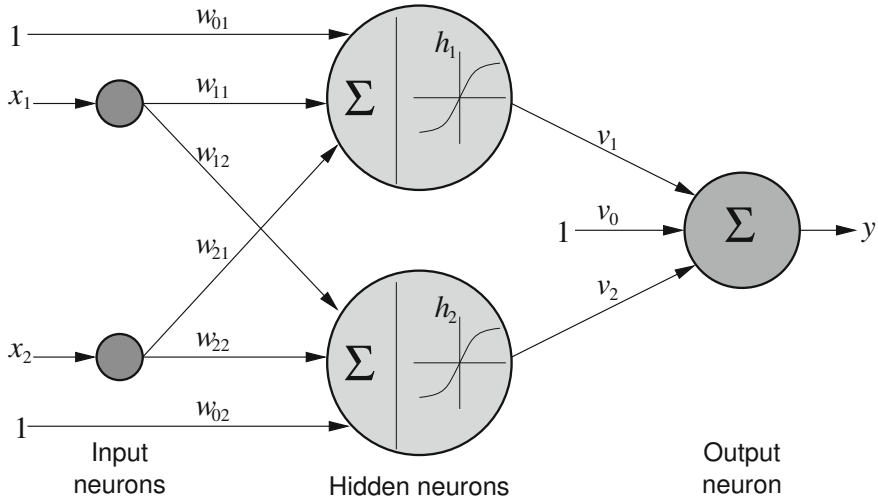


Figure 1.11: Feed-forward 2-2-1 neural network with two input neurons, one hidden layer consisting of two neurons, and a single output neuron

The output is merely the weighted sum of the intermediate values

$$y = \sum_k v_k \cdot h_k = \mathbf{v}^{\mathrm{T}} \cdot \mathbf{h} \,. \tag{1.32}$$

In order to simplify the computations, the sigmoid function (eq. 1.30) can be replaced by the hyperbolic-tangent function

$$h_k(t_k) = \tanh(t_k) = \frac{2}{1 + \mathrm{e}^{-2 \cdot t_k}} - 1 \;, \tag{1.33}$$

by linear transformations of the input

$$0.5 \cdot t_k \quad \mapsto \quad t_k$$

and of the output

$$2 \cdot h_k(t_k) - 1 \quad \mapsto \quad h_k(t_k)$$

(**Figure 1.12**). A neural network using (1.33) is equivalent to a network using (1.30), but having different values for the resulting weights [Bis95].

Putting the equations (1.31), (1.32), and (1.33) together and replacing the $w_{lk}$ and $v_k$ by $a_j$, a nonlinear model function can be derived for the example given in Figure 1.11

$$\begin{aligned} y = f(\mathbf{x}_n|\mathbf{a}) \;\; &= \;\; \tanh(a_1 x_1 + a_2 x_2 + a_3) \cdot a_4 + \\ &\quad\;\; \tanh(a_5 x_1 + a_6 x_2 + a_7) \cdot a_8 + a_9 \;. \end{aligned} \tag{1.34}$$

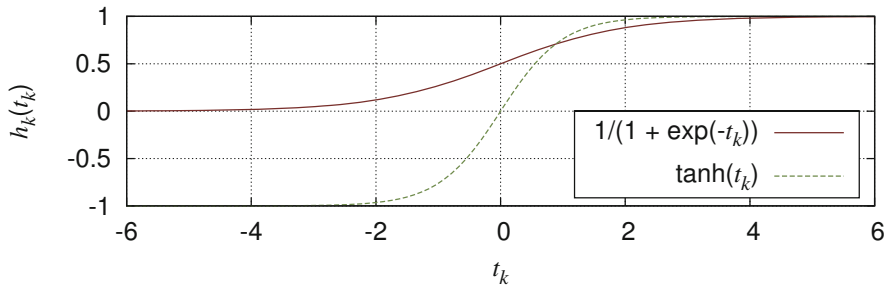


Figure 1.12: Comparison of sigmoid and hyperbolic-tangent function

Instead of presenting single pairs of $\mathbf{x}_i$ and $y_i$ followed by weights adjustment using back-propagation of errors through the single layers as described in many textbooks, the training of the neural network can now be performed simply using a data-fitting procedure. Combined with a suitable weighting scheme (see Chapter 3), outliers in the training set can also be treated properly.

## 1.6 Test questions

**1.1** What is the difference between conditions and observations?

**1.2** The least-squares method deals with model functions. Which values have to be determined?

**1.3** What are linear and nonlinear problems in the sense of the least-squares method? Give two examples each.

**1.4** What does "linearisation of a model function" mean?

**1.5** Give an example application (i.e. model function) with more than one observation per measurement.

**1.6** Which values are expected to be error-free in least-squares calculations: observations, parameters, or conditions?

**1.7** Itemise three practical applications that could make use of data fitting.

# Chapter 2

# Estimation of Model Parameters by the Method of Least Squares

## 2.1 What are "Least Squares"?

It is well known that the determination of $N$ unknown variables requires a set of $N$ linearly independent equations. If the number of equations is lower than the number of unknowns, the problem is said to be under-determined. If there are more linearly independent equations than unknown variables, it is over-determined.

The least-squares method deals with the latter case. Since experimental observations $y_i$ are typically affected by errors expressed by $\varepsilon_i$

$$y_i = f(\mathbf{x}_i|\mathbf{a}) + \varepsilon_i \ , \tag{2.1}$$

it is beneficial to have as many equations (i.e., pairs of $y_i$ and $\mathbf{x}_i$) available as possible in order to get better and more reliable statistics[1]. That means the parameters $\mathbf{a}$ can be estimated more accurately.

Suppose we are given a set of observations $y_i$ with corresponding conditions $\mathbf{x}_i$, under which the observations have been made. The goal of data fitting using the least-squares method is to minimise the squared residual error between the observations and the values calculated via the model function

$$\chi^2 = \sum_i w_i \cdot [f(\mathbf{x}_i|\mathbf{a}) - y_i]^2 \longrightarrow \text{Min} \tag{2.2}$$

Based on the maximum-likelihood principle, which is discussed in more detail in Chapter 6, the fitting problem corresponds to a minimisation problem. The value of $\chi^2$ is dependent on the selection of a hopefully appropriate model function $f(\mathbf{x}_i|\mathbf{a})$ and on random fluctuations in the measured values of variable $y_i$. In

[1] It is assumed that the mean of $\varepsilon$ is equal to zero.

T. Strutz, *Data Fitting and Uncertainty*, DOI 10.1007/978-3-8348-9813-5 _2,

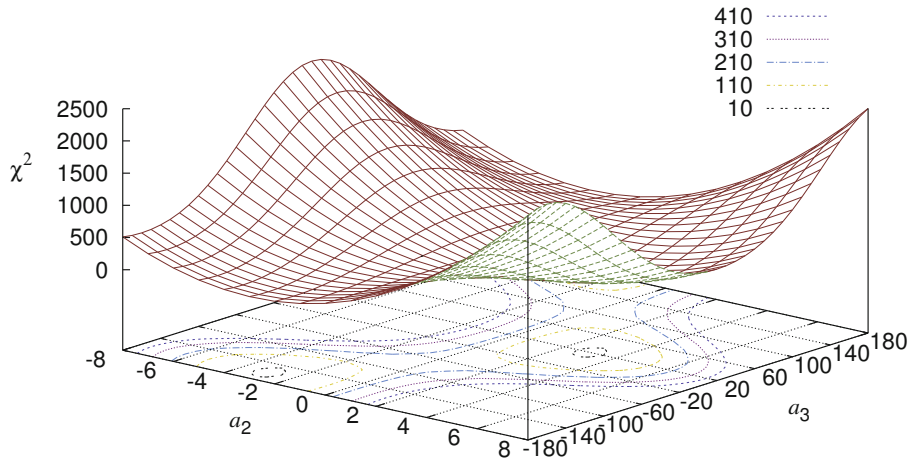


Figure 2.1: Error surface of $\chi^2 = \sum_i [a_2 \cdot \cos(x_i - a_3) - y_i]^2$ with a global minimum at $(a_2, a_3) = (3, 20)$

addition to the already introduced variables, equation (2.2) contains weights $w_i$. Each weight should express the reliability of the observation to which it is assigned. The more uncertain an outcome $y_i$ of the experiment, the lower $w_i$ should be. For example, the weight has to be close to or equal to zero when a particular observation shows indication of being an outlier. However, in a large number of cases, this reliability is not known in advance, which means the weights have to be estimated (see Chapter 3).

When observations are weighted, the procedure is primarily called *generalised least squares* or *weighted least squares* in contrast to *ordinary least squares* with $w_i = w = \text{const}$.

The influence of a chosen set of parameters $\mathbf{a}$ on $\chi^2$ can be visualised using what are called error surfaces. The procedure for minimising $\chi^2$ has to find the global minimum in that surface. **Figure 2.1** shows an example of the cosine model function $f(\mathbf{x}|\mathbf{a}) = a_2 \cdot \cos(x_i - a_3)$ with a global minimum at the position $(a_2, a_3) = (3, 20)$. Since the cosine is a periodic function, it is evident that this is not the only minimum. Minima can be found at $(3, 20 + k \cdot 360)$ and $(-3, 200 + k \cdot 360)$ with $k \in \mathbb{Z}$. Another example is depicted in **Figure 2.2**. When more than two parameters are involved, then we speak of hyper-surfaces.

For linear problems, the position of the global minimum (i.e., the desired parameter vector $\mathbf{a}$) can be calculated directly. Simple problems, such as fitting a constant or a straight line, can easily be treated analytically by setting the par-

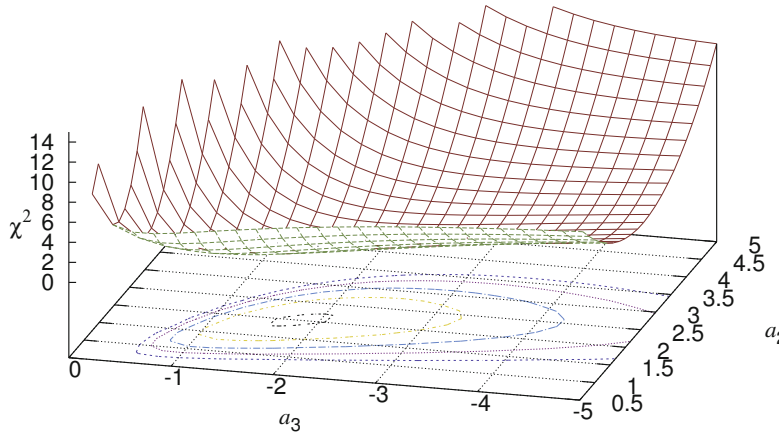


Figure 2.2: Error surface of $\chi^2 = \sum_i [a_2 \cdot \exp(a_3 \cdot x_i) - y_i]^2$ with a global minimum at $(a_2, a_3) = (2, -1.8)$

tial derivatives $\partial\chi^2/\partial a_j$ of equation (2.2) to zero and solving the corresponding equation system by hand. Section 7.4 explains one example in detail.

Nonlinear model functions require the application of a gradient descent, walking from a starting point gradually towards the global minimum. It is obvious that an initial estimation of parameters **a** is needed and should be as close as possible to that minimum.

The theoretical basis of least squares is explained in more detail in Chapter 6. The following text presents the final formulae to use.

## 2.2 A general algorithm for minimisation problems

This section presents a general solution for the fitting of nonlinear model functions to data without any proofs or derivations in order to provide the reader with basic information required for their own software developments and implementations. Linear problems can be regarded as a subset simplifying the least-squares procedure in different terms, as will be discussed in the following.

Solving minimisation problems via the least-squares method requires a so-called *Jacobian matrix*[2]. It is of size $N$ (number of observations) times $M$ (number of

[2] named after the German mathematician Karl Gustav Jacob Jacobi (1804-1851)

parameters) and contains all partial derivatives of each equation $y_i = f(\mathbf{x}_i|\mathbf{a}) + \varepsilon_i$ with respect to the observation condition $\mathbf{x}_i$

$$\mathbf{J} = \begin{pmatrix} \frac{\partial f(\mathbf{x}_1|\mathbf{a})}{\partial a_1} & \frac{\partial f(\mathbf{x}_1|\mathbf{a})}{\partial a_2} & \cdots & \frac{\partial f(\mathbf{x}_1|\mathbf{a})}{\partial a_M} \\ \frac{\partial f(\mathbf{x}_2|\mathbf{a})}{\partial a_1} & \frac{\partial f(\mathbf{x}_2|\mathbf{a})}{\partial a_2} & \cdots & \frac{\partial f(\mathbf{x}_2|\mathbf{a})}{\partial a_M} \\ \vdots & \vdots & \ddots & \vdots \\ \frac{\partial f(\mathbf{x}_N|\mathbf{a})}{\partial a_1} & \frac{\partial f(\mathbf{x}_N|\mathbf{a})}{\partial a_2} & \cdots & \frac{\partial f(\mathbf{x}_N|\mathbf{a})}{\partial a_M} \end{pmatrix} . \tag{2.3}$$

In addition, a vector containing all residuals has to be prepared

$$\mathbf{r} = \begin{pmatrix} y_1 - f(\mathbf{x}_1|\mathbf{a}) \\ y_2 - f(\mathbf{x}_2|\mathbf{a}) \\ y_3 - f(\mathbf{x}_3|\mathbf{a}) \\ \vdots \\ y_N - f(\mathbf{x}_N|\mathbf{a}) \end{pmatrix} . \tag{2.4}$$

A residual is expressed by the difference between the observation $y_i$ and the value resulting from the model function using the current vector of parameters

$$\mathbf{a} = (a_1\ a_2\ \cdots\ a_j\ \cdots\ a_M)^{\mathrm{T}} .$$

The parameter vector $\mathbf{a}$ has to be filled with initial estimates in the beginning. A diagonal matrix

$$\mathbf{W} = \begin{pmatrix} w_1 & 0 & 0 & \cdots & 0 \\ 0 & w_2 & 0 & \cdots & 0 \\ 0 & 0 & \ddots & \cdots & \vdots \\ \vdots & \vdots & \vdots & \ddots & 0 \\ 0 & 0 & \cdots & 0 & w_N \end{pmatrix} \tag{2.5}$$

is the third (optional) component for solving the minimisation problem. It contains one weight for each of the $N$ observations and expresses how important or reliable the corresponding observation is for the determination of the model parameters.[3] If all observations have the same impact, this matrix can be ignored by setting all $w_i$ equal to one. Otherwise, proper weights have to be chosen as will be discussed in Chapter 3.

[3] Setting $\mathbf{W}$ to a diagonal matrix implicates the assumption of independent observations. If there are dependencies between single measurements, then the off-diagonal elements may also be non-zero.

Putting everything together, we have to compute[4]

$$\mathbf{\Delta a} = \left(\mathbf{J}^{\mathrm{T}} \cdot \mathbf{W} \cdot \mathbf{J}\right)^{-1} \cdot \mathbf{J}^{\mathrm{T}} \cdot \mathbf{W} \cdot \mathbf{r} \,. \tag{2.6}$$

The result is a vector of parameter adjustments

$$\mathbf{\Delta a} = (\Delta a_1 \; \Delta a_2 \; \cdots \; \Delta a_j \; \cdots \; \Delta a_M)^{\mathrm{T}}$$

and the new vector of parameters is given by

$$\mathbf{a} \longleftarrow \mathbf{a} + \mathbf{\Delta a} \,. \tag{2.7}$$

The alternating computation of (2.6) and (2.7) has to be performed iteratively until the adjustments are close to zero. The stop criterion could be, for instance,

$$|\Delta a_j| < \epsilon \qquad \forall\, j \tag{2.8}$$

with $\epsilon$ close to the CPU precision. In addition, a safeguard against an infinite loop has to be implemented, restricting the number of iterations to a maximum value. The description above is the general procedure for solving least-squares problems of nonlinear functions. Section 2.4 will describe how the computation can be simplified for linear model functions.

The term $\mathbf{J}^{\mathrm{T}}\mathbf{W}\mathbf{J}$ in equation (2.6) is also called *normal matrix* $\mathbf{N}$. It is quadratic with $M \times M$ elements according to the number of parameters of $f(\mathbf{x}|\mathbf{a})$. Substituting $f(\mathbf{x}_i|\mathbf{a})$ by $f_i$ this matrix is

$$\mathbf{N} = \begin{pmatrix} \sum_{i=1}^{N} w_i \left(\frac{\partial f_i}{\partial a_1}\right)^2 & \sum_{i=1}^{N} w_i \left(\frac{\partial f_i}{\partial a_1}\frac{\partial f_i}{\partial a_2}\right) & \cdots & \sum_{i=1}^{N} w_i \left(\frac{\partial f_i}{\partial a_1}\frac{\partial f_i}{\partial a_M}\right) \\ \sum_{i=1}^{N} w_i \left(\frac{\partial f_i}{\partial a_2}\frac{\partial f_i}{\partial a_1}\right) & \sum_{i=1}^{N} w_i \left(\frac{\partial f_i}{\partial a_2}\right)^2 & \cdots & \sum_{i=1}^{N} w_i \left(\frac{\partial f_i}{\partial a_2}\frac{\partial f_i}{\partial a_M}\right) \\ \vdots & \vdots & \ddots & \vdots \\ \sum_{i=1}^{N} w_i \left(\frac{\partial f_i}{\partial a_M}\frac{\partial f_i}{\partial a_1}\right) & \sum_{i=1}^{N} w_i \left(\frac{\partial f_i}{\partial a_M}\frac{\partial f_i}{\partial a_2}\right) & \cdots & \sum_{i=1}^{N} w_i \left(\frac{\partial f_i}{\partial a_M}\right)^2 \end{pmatrix} . \tag{2.9}$$

$\mathbf{N}$ is obviously a symmetric matrix with respect to the main diagonal.

[4] In theory, the second derivatives of the function to be minimised also have to be taken into account for nonlinear models. This is discussed more in detail in Section 6.4. However, there are justified reasons to ignore them.

## 2.3 Pitfalls

Although the given solution for nonlinear least-square problems looks very convincing, attention has to be paid to some details.

One of the main problems is the assignment of suitable starting parameters $\mathbf{a}$. Obviously, the initial values should already be as close as possible to the global minimum, (i) to avoid getting trapped in a local minimum and (ii) to ensure fast convergence of the iterative procedure. This can be achieved by using either an appropriate functional connection between parameters and observations, i.e., making some assumption leading to a rough guess of $\mathbf{a}$, or a grid search in the parameter space for promising coordinates.

For instance, given a trigonometric model function $y_i = a_1 + \sin(x_i - a_2)$, the mean value $a_1$ could be simply estimated by averaging all observed values $y_i$, under the presumption that the observations are almost equally distributed over the full range of oscillation. In contrast, a grid search requires some knowledge about the range of the parameters $a_j$. For each $a_j$ a certain number of points (e.g., equidistant) in that range are selected leading to a finite set of different parameter vectors $\mathbf{a}$. The vector resulting in the smallest $\chi^2$ is then used as starting point $\mathbf{a}_{\text{start}}$ for the fitting procedure. As an alternative to an equidistant grid, randomly generated sets of seed points in the parameter space could also be considered. If possible, the estimation based on some a priori knowledge is preferred. The grid-search method is tricky for complex model functions with many parameters and should only be applied when necessary.

The initialisation of parameters is especially crucial when there are lots of local minima on the error surface of the model function. Under certain conditions, the minimisation process will converge to undesirable values or not at all. Getting stuck in a local minimum or in a flat region of the error surface is very aggravating. In case of an unsatisfactory fit, the randomised re-initialisation of the parameters can be considered; the randomisation of the resulting parameter vector $\mathbf{a}_{\text{result}}$ with deviations of $\sigma_j \geq |a_{j,\text{start}} - a_{j,\text{result}}|$ might also be an option. The fitting must be repeated until the remaining error falls below a given threshold or the maximum number of allowed iterations is reached.

The range of the parameters is another matter to be considered. If the limits of the parameters are known, they should also be supervised in order to avoid convergence to futilely large or infinitesimally small values. The most elegant method is to fake the gradients of the error hyper-surface in such a manner that the critical regions do not attract the optimisation procedure. An example is provided in Subsection 2.6.8.

The third potential problem concerns the matrix inversion involved. Very large values in $\mathbf{N} = \mathbf{J}^{\mathrm{T}}\mathbf{W}\mathbf{J}$ become very small values in $\mathbf{N}^{-1}$. In some applications, it might be required to scale the values in order to combine the data at a comparable level of magnitude. Otherwise, the limited precision of numbers in computers will lead to unpredictable effects.

Further details about the minimisation procedure can be found in Chapter 6 as well as in Section B.7.

## 2.4 Simplifications for linear model functions

In case of linear model functions, the computation according to (2.6) and (2.7) can be simplified a great deal. The main advantage of this is that iterative computations are not necessary. Equation (2.6) leads automatically to the final parameter values

$$\mathbf{a} = \left(\mathbf{J}^{\mathrm{T}} \cdot \mathbf{W} \cdot \mathbf{J}\right)^{-1} \cdot \mathbf{J}^{\mathrm{T}} \cdot \mathbf{W} \cdot \mathbf{r} \,. \tag{2.10}$$

Therefore, (i) the initial values $a_j$ can be set to zero and (ii) as a result of doing so, $f(\mathbf{x}_i|\mathbf{a})$ is equal to zero and $\mathbf{r}$ reduces to

$$\mathbf{r} = \mathbf{y} = \begin{pmatrix} y_1 \\ y_2 \\ \vdots \\ y_N \end{pmatrix} \tag{2.11}$$

All the pitfalls discussed in the previous section vanish when a linear model function is used instead of a nonlinear one. Therefore, the model function should always be selected carefully. As already mentioned in Section 1.5, it is sometimes possible to convert (pseudo-)nonlinear functions into linear ones.

When the model function is linear with respect to all parameters $a_j$, then it can be expressed by

$$y_i = f(\mathbf{x}_i|\mathbf{a}) = a_1 \cdot f_1(\mathbf{x}_i) + a_2 \cdot f_2(\mathbf{x}_i) + \ldots + a_M \cdot f_M(\mathbf{x}_i)$$

with arbitrary functions $f_j(\mathbf{x}_i) = \partial f(\mathbf{x}_i|\mathbf{a})/\partial a_j$. In this case, the Jacobian matrix is obviously equal to

$$\mathbf{J} = \begin{pmatrix} f_1(\mathbf{x}_1) & f_2(\mathbf{x}_1) & \cdots & f_M(\mathbf{x}_1) \\ f_1(\mathbf{x}_2) & f_2(\mathbf{x}_2) & \cdots & f_M(\mathbf{x}_2) \\ \vdots & \vdots & \cdots & \vdots \\ f_1(\mathbf{x}_N) & f_2(\mathbf{x}_N) & \cdots & f_M(\mathbf{x}_N) \end{pmatrix}$$

and the fitting problem is reduced to a system of linear equations

$$\mathbf{y} = \mathbf{J} \cdot \mathbf{a}$$

$$\begin{pmatrix} y_1 \\ y_2 \\ \vdots \\ y_N \end{pmatrix} = \begin{pmatrix} f_1(\mathbf{x}_1) & f_2(\mathbf{x}_1) & \cdots & f_M(\mathbf{x}_1) \\ f_1(\mathbf{x}_2) & f_2(\mathbf{x}_2) & \cdots & f_M(\mathbf{x}_2) \\ \vdots & \vdots & \cdots & \vdots \\ f_1(\mathbf{x}_N) & f_2(\mathbf{x}_N) & \cdots & f_M(\mathbf{x}_N) \end{pmatrix} \cdot \begin{pmatrix} a_1 \\ a_2 \\ \vdots \\ a_M \end{pmatrix}. \quad (2.12)$$

Section 6.3 will discuss this more in detail, especially the origin of equation (2.10).

The columns of the Jacobian matrix can be regarded as different basis vectors. $\mathbf{y}$ is a weighted superposition of these basis vectors with $a_j$ as weights.

If the observations have to be weighted according to their uncertainties, both sides of the equation must be divided by the standard deviation $\sigma_i$

$$\begin{pmatrix} \frac{y_1}{\sigma_1} \\ \frac{y_2}{\sigma_2} \\ \vdots \\ \frac{y_N}{\sigma_N} \end{pmatrix} = \begin{pmatrix} \frac{f_1(\mathbf{x}_1)}{\sigma_1} & \frac{f_2(\mathbf{x}_1)}{\sigma_1} & \cdots & \frac{f_M(\mathbf{x}_1)}{\sigma_1} \\ \frac{f_1(\mathbf{x}_2)}{\sigma_2} & \frac{f_2(\mathbf{x}_2)}{\sigma_2} & \cdots & \frac{f_M(\mathbf{x}_2)}{\sigma_2} \\ \vdots & \vdots & \cdots & \vdots \\ \frac{f_1(\mathbf{x}_N)}{\sigma_N} & \frac{f_2(\mathbf{x}_N)}{\sigma_N} & \cdots & \frac{f_M(\mathbf{x}_N)}{\sigma_N} \end{pmatrix} \cdot \begin{pmatrix} a_1 \\ a_2 \\ \vdots \\ a_M \end{pmatrix} \quad (2.13)$$

$$\mathbf{y}' = \mathbf{J}' \cdot \mathbf{a} \quad (2.14)$$

$\mathbf{J}'$ is also called the *design matrix*.

## 2.5 Curve approximation in case of unknown model function

In the ideal case of data fitting, the functional relation between the conditions of the measurement and its outcome, i.e., the observations, is known. The aim of applying the method of least-squares approximation is determining the parameters of this functional relation. There are, however, many practical scenarios, in which this relation is unknown, i.e., no model function is available.

**Example 1**

The typical goal in such cases is to approximate the functional behaviour between the taken measurements based on a series of related functions, for example, as a

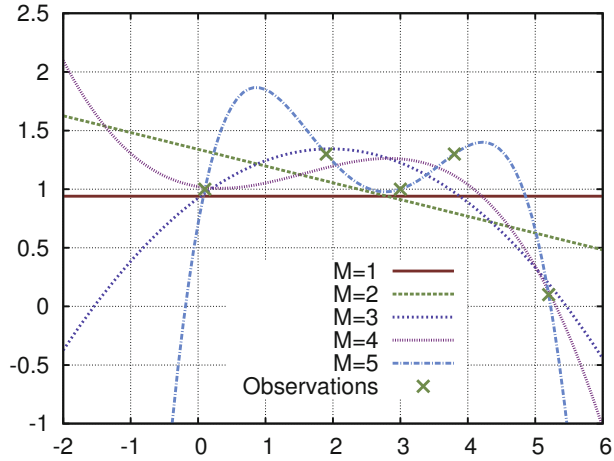


Figure 2.3: Polynomial data fitting with increasing order of model function

polynomial

$$y = f(x|\mathbf{a}) = \sum_{j=1}^{M} a_j \cdot x^{j-1} = a_1 + a_2 \cdot x + a_3 \cdot x^2 + a_4 \cdot x^3 + \cdots .$$

The more elements are involved, i.e., the higher $M$ is, the better the observations $y_i$ $(i = 1, 2, \ldots, N)$ are represented. If the number $M$ of model parameters approaches the number $N$ of observations $(M = N)$, then the curve $f(x|\mathbf{a})$ can be drawn exactly through all the observed data points.

**Figure 2.3** shows the fitting results for a signal with five samples $y_i$

| $x_i$ | 0.1 | 1.9 | 3.0 | 3.8 | 5.2 |
|---|---|---|---|---|---|
| $y_i$ | 1.0 | 1.3 | 1.0 | 1.3 | 0.1 |

taken under conditions $x_i$. The order of the polynomial used as the model function was changed from zero $(M = 1)$ to four $(M = 5)$. The zero-order model simply determines the average of all observations; the polynomial of order one fits a straight line and so on. It can be clearly seen that the curve is closer to the data points the higher the number of model parameters becomes. However, the property of generalisation between observed data points becomes unreliable. With $M = 5$, for example, the model function oscillates between the first two samples, which does not seem to be a sufficient approximation. If $M$ is too high compared to $N$, we talk of *over-fitting*.

Using a superposition of elementary functions as a model also forbids the extrapolation of the behaviour beyond the range of available conditions, as can be concluded from Figure 2.3.

**Example 2**

In some applications of data fitting, there is no actual mathematical relation based on a law of nature between the data taken as conditions and the data interpreted as observations. In economics, for example, the costs of a project often have to be estimated in the planning process. In such cases, meaningful features of products from former projects can be used as conditions and the related actual costs as observations. We can now assume that each of the features has a linear or quadratic influence on the costs. Restricting the conditions to three significant features yields, for instance,

$$\begin{aligned} y = f(x|\mathbf{a}) \quad = \quad & a_1 + a_2 \cdot x_1 + a_3 \cdot x_1^2 + a_4 \cdot x_2 + a_5 \cdot x_2^2 + a_6 \cdot x_3 + a_6 \cdot x_3^2 + \\ & a_7 \cdot x_1 \cdot x_2 + a_8 \cdot x_1 \cdot x_3 + a_9 \cdot x_2 \cdot x_3 \; . \end{aligned}$$

The estimated parameters $a_1 \ldots a_9$ can be used to determine the costs of the new project. If there is some degree of freedom, for example, if feature $x_3$ is not fixed yet, it can be set to a value that minimises the total costs.

**Example 3**

Trigonometric polynomials are also able to approximate arbitrary functions

$$y = f(x|\mathbf{a}, \phi) = \frac{a_0}{2} + \sum_{j=1}^{p} [a_j \cdot \cos(j\omega x - \varphi_j)] \tag{2.15}$$

with $\phi = \{\varphi_j\}$ and $\omega = 2 \cdot \pi / T$, where $T$ is the assumed period of the periodic function $f(x|\mathbf{a}, \phi)$. For $p = \infty$, this polynomial corresponds to the Fourier series. Since the extrapolation outside the range of given conditions $[x_{\min} \ldots x_{\max}]$ is not recommended, this presumed periodicity does not harm the approximation of the curve. The variables $a_0$, $a_j$, $\varphi_j$, and $\omega$ are the model parameters, which have to be estimated.

## 2.6 Example computations

This section is devoted to some example calculations according to the model functions introduced in the first chapter, making the mode of functioning somewhat clearer. For nonlinear model functions, the initialisation of parameters and their limitation to reasonable ranges are also discussed.

### 2.6.1 Constant value

The model function is

$$y = f(\cdot|\mathbf{a}) = \text{const.} = a_1 \ .$$

There is a single model parameter $a_1$. In case of $N$ observations $y_i$, the size of the Jacobian matrix $\mathbf{J}$ is $N \times 1$ and the elements are equal to $\partial f_i / \partial a_1 = 1$

$$\mathbf{J} = \begin{pmatrix} 1 \\ 1 \\ \vdots \\ 1 \end{pmatrix} \ .$$

Feeding $\mathbf{J}$ into equation (2.10) yields

$$\begin{aligned} a_1 &= \left( (1\ 1\ \cdots\ 1) \cdot \mathbf{W} \cdot \begin{pmatrix} 1 \\ 1 \\ \vdots \\ 1 \end{pmatrix} \right)^{-1} \cdot (1\ 1\ \cdots\ 1) \cdot \mathbf{W} \cdot \begin{pmatrix} y_1 \\ y_2 \\ \vdots \\ y_N \end{pmatrix} \\ &= \left( \sum_{i=1}^{N} w_i \right)^{-1} \cdot (w_1\ w_2\ \cdots\ w_N) \cdot \begin{pmatrix} y_1 \\ y_2 \\ \vdots \\ y_N \end{pmatrix} \\ &= \frac{\sum_{i=1}^{N} (w_i \cdot y_i)}{\sum_{i=1}^{N} w_i} \ . \end{aligned}$$

This result is not very surprising. The constant $a_1$ is equal to the weighted average of all observations $y_i$. The denominator $\sum_{i=1}^{N} w_i$ simply normalises to the sum of all weights.

### 2.6.2 Straight line

Now let us increase the number of parameters from one to two for the straight-line example

$$y_i = f(\mathbf{x}_i|\mathbf{a}) = a_1 + a_2 \cdot x_i + \varepsilon_i \qquad i = 1, 2, \ldots, N \ .$$

The partial derivatives are

$$\frac{\partial f_i}{\partial a_1} = 1 \qquad \text{and} \qquad \frac{\partial f_i}{\partial a_2} = x_i$$

and the Jacobian becomes

$$\mathbf{J} = \begin{pmatrix} 1 & x_1 \\ 1 & x_2 \\ \vdots & \vdots \\ 1 & x_N \end{pmatrix} .$$

Fed into equation (2.6), we get

$$\begin{aligned} \mathbf{a} &= \left( \begin{pmatrix} 1 & \cdots & 1 \\ x_1 & \cdots & x_N \end{pmatrix} \mathbf{W} \begin{pmatrix} 1 & x_1 \\ 1 & x_2 \\ \vdots & \vdots \\ 1 & x_N \end{pmatrix} \right)^{-1} \cdot \begin{pmatrix} 1 & \cdots & 1 \\ x_1 & \cdots & x_N \end{pmatrix} \mathbf{W} \begin{pmatrix} y_1 \\ y_2 \\ \vdots \\ y_N \end{pmatrix} \\ &= \begin{pmatrix} \sum_{i=1}^{N} w_i & \sum_{i=1}^{N} w_i \cdot x_i \\ \sum_{i=1}^{N} w_i \cdot x_i & \sum_{i=1}^{N} w_i \cdot x_i^2 \end{pmatrix}^{-1} \cdot \begin{pmatrix} \sum_{i=1}^{N} w_i \cdot y_i \\ \sum_{i=1}^{N} w_i \cdot x_i y_i \end{pmatrix} . \end{aligned} \tag{2.16}$$

Applying equation (5.6) for matrix inversion results to

$$\begin{aligned} \mathbf{a} &= \frac{1}{d} \cdot \begin{pmatrix} \sum_{i=1}^{N} w_i (x_i)^2 & -\sum_{i=1}^{N} w_i x_i \\ -\sum_{i=1}^{N} w_i x_i & \sum_{i=1}^{N} w_i \end{pmatrix} \begin{pmatrix} \sum_{i=1}^{N} w_i y_i \\ \sum_{i=1}^{N} w_i x_i y_i \end{pmatrix} \\ &= \frac{1}{d} \cdot \begin{pmatrix} \sum_{i=1}^{N} w_i (x_i)^2 \cdot \sum_{i=1}^{N} w_i y_i - \sum_{i=1}^{N} w_i x_i \cdot \sum_{i=1}^{N} w_i x_i y_i \\ \sum_{i=1}^{N} w_i \cdot \sum_{i=1}^{N} w_i x_i y_i - \sum_{i=1}^{N} w_i x_i \sum_{i=1}^{N} w_i y_i \end{pmatrix} . \end{aligned}$$

with

$$d = \sum_{i=1}^{N} w_i (x_i)^2 \cdot \sum_{i=1}^{N} w_i - \left( \sum_{i=1}^{N} w_i x_i \right)^2 .$$

Without a question, the equation for **a** can also be derived manually without using the matrix approach (see Section 7.4).

### 2.6.3 Polynomial approximation

After reading the two preceding Subsections, the principle of the numerical solution of least-squares problems should be clear by now and we can restrict the exemplifications to the Jacobian matrix. For combinations of polynomials

$$y_i = f(\mathbf{x}_i|\mathbf{a}) = a_1 + a_2 \cdot x_i + \ldots + a_M \cdot x_i^{M-1} + \varepsilon_i \qquad i = 1, 2, \ldots, N$$

the Jacobian is

$$\mathbf{J} = \begin{pmatrix} 1 & x_1 & x_1^2 & \cdots & x_1^{M-1} \\ 1 & x_2 & x_2^2 & \cdots & x_2^{M-1} \\ \vdots & \vdots & \vdots & \cdots & \vdots \\ 1 & x_N & x_N^2 & \cdots & x_N^{M-1} \end{pmatrix} .$$

### 2.6.4 Plane approximation

The plane approximation is an example for multiple regression, as the condition vector is two-dimensional here, namely $\mathbf{x} = (x_1, x_2)^{\mathrm{T}}$, and the model function is

$$y_i = f(\mathbf{x}_i|\mathbf{a}) = a_1 + a_2 \cdot x_{1,i} + a_3 \cdot x_{2,i} + \varepsilon_i \; . \tag{2.17}$$

The Jacobian matrix must reflect that different conditions (namely $x_{1,i}$ and $x_{2,i}$) are assigned to the parameters. The gradients are

$$\frac{\partial f_i}{\partial a_1} = 1 \; , \qquad \frac{\partial f_i}{\partial a_2} = x_{1,i} \qquad \text{and} \qquad \frac{\partial f_i}{\partial a_3} = x_{2,i} \; .$$

Please note that the first index of $x$ discriminates between the variables $x_1$ and $x_2$, while the second index is related to the different observations. The Jacobian matrix is accordingly

$$\mathbf{J} = \begin{pmatrix} 1 & x_{1,1} & x_{2,1} \\ 1 & x_{1,2} & x_{2,2} \\ \vdots & \vdots & \vdots \\ 1 & x_{1,N} & x_{2,N} \end{pmatrix} .$$

### 2.6.5 Linear prediction

The linear prediction of order $M$ is described by

$$x[n] = f(\mathbf{x}_n|\mathbf{a}) = a_1 \cdot x[n-1] + a_2 \cdot x[n-2] + \cdots + a_M \cdot x[n-M] \; .$$

in which $M$ preceding samples of a sequence of values are used to predict the current sample $x[n]$. The underlying assumption is that the sequence $\{x[n]\}$ was produced by an one-dimensional auto-regressive (AR) process of $M$th order. In contrast to other model functions, the observation and the experimental conditions only differ in the time index $n$ here.

The Jacobian matrix has to be written as

$$\mathbf{J} = \begin{pmatrix} x[m-1] & x[m-2] & \cdots & x[m-M] \\ x[m-2] & x[m-3] & \cdots & x[m-(M+1)] \\ \vdots & \vdots & \cdots & \vdots \\ x[m-N] & x[m-(1+N)] & \cdots & x[m-(M+N)] \end{pmatrix}$$

with $m, n \in \mathbb{Z}$, $m \leq n$. Parameter $m$ defines the context of the prediction. Typically, it starts directly before the value to be predicted, i.e., $m = n$.

### 2.6.6 Cosine function

It was shown in Section 1.3 that function

$$y_i = b_1 + b_2 \cdot \cos(x_i - b_3) + \varepsilon_i \ ,$$

which is nonlinear in $b_3$, can be expressed as

$$y_i = a_1 + a_2 \cdot \cos(x_i) + a_3 \cdot \sin(x_i) + \varepsilon_i \tag{2.18}$$

simplifying the fitting to a linear problem. The partial derivatives according to the parameters $a_j$ are

$$\frac{\partial f_i}{\partial a_1} = 1 \ , \qquad \frac{\partial f_i}{\partial a_2} = \cos(x_i) \qquad \text{and} \qquad \frac{\partial f_i}{\partial a_3} = \sin(x_i) \ .$$

Therefore, the Jacobian matrix is simply

$$\mathbf{J} = \begin{pmatrix} 1 & \cos(x_1) & \sin(x_1) \\ 1 & \cos(x_2) & \sin(x_2) \\ \vdots & \vdots & \vdots \\ 1 & \cos(x_N) & \sin(x_N) \end{pmatrix} \ .$$

### 2.6.7 Rotation and translation of coordinates

As already stated in Subsection 1.4.4, the fitting of a rotation matrix is not trivial, since not only the conditions but also the observations appear in pairs.

Let us assume that the vectors $\mathbf{u}_i = (u_i\ v_i)^{\mathrm{T}}$ are given coordinates in a first image (conditions) and the vectors $\mathbf{x}_i = (x_i\ y_i)^{\mathrm{T}}$ are the corresponding coordinates in a second image (observations) found by a matching algorithm. If the second image is a translated and slightly rotated version of the first image,

$$\begin{pmatrix} x \\ y \end{pmatrix} = \begin{pmatrix} a_1 \\ a_2 \end{pmatrix} + \begin{pmatrix} \cos(a_3) & -\sin(a_3) \\ \sin(a_3) & \cos(a_3) \end{pmatrix} \cdot \begin{pmatrix} u \\ v \end{pmatrix}$$

has to be used as model function with $a_3$ being the rotation angle. Actually, there are two model functions, namely

$$f_{\mathrm{x}}(\mathbf{u}|\mathbf{a}) = \quad x \quad = a_1 + \cos(a_3) \cdot u - \sin(a_3) \cdot v \tag{2.19}$$

and

$$f_{\mathrm{y}}(\mathbf{u}|\mathbf{a}) = \quad y \quad = a_2 + \sin(a_3) \cdot u + \cos(a_3) \cdot v\ , \tag{2.20}$$

which are coupled via $a_3$. Since (2.19) and (2.20) are nonlinear functions with respect to $\mathbf{a}$, the partial derivatives

$$\begin{aligned} &\frac{\partial x_i}{\partial a_1} = 1\ , \quad &&\frac{\partial x_i}{\partial a_2} = 0 \quad &&\text{and} \quad &&\frac{\partial x_i}{\partial a_3} = -u_i \cdot \sin(a_3) - v_i \cdot \cos(a_3) \\ &\frac{\partial y_i}{\partial a_1} = 0\ , \quad &&\frac{\partial y_i}{\partial a_2} = 1 \quad &&\text{and} \quad &&\frac{\partial y_i}{\partial a_3} = \quad u_i \cdot \cos(a_3) - v_i \cdot \sin(a_3)\ . \end{aligned}$$

are dependent on the parameters. Therefore, a suitable initialisation of $\mathbf{a}$ is required. It could be assumed, for example, that there is no rotation, but only a translational displacement

$$a_{1,\mathrm{init}} = \frac{1}{N}\sum_{i=1}^{N}(x_i - u_i)\ , \qquad a_{2,\mathrm{init}} = \frac{1}{N}\sum_{i=1}^{N}(y_i - v_i)\ , \qquad a_{3,\mathrm{init}} = 0\ .$$

The two model functions (2.19) and (2.20) must be combined into a single framework for the fitting procedure

$$\mathbf{r} = \begin{pmatrix} x_1 - f_{\mathrm{x}}(\mathbf{u}_1|\mathbf{a}) \\ x_2 - f_{\mathrm{x}}(\mathbf{u}_2|\mathbf{a}) \\ \vdots \\ x_N - f_{\mathrm{x}}(\mathbf{u}_N|\mathbf{a}) \\ y_1 - f_{\mathrm{y}}(\mathbf{u}_1|\mathbf{a}) \\ y_2 - f_{\mathrm{y}}(\mathbf{u}_2|\mathbf{a}) \\ \vdots \\ y_N - f_{\mathrm{y}}(\mathbf{u}_N|\mathbf{a}) \end{pmatrix} \qquad \mathbf{J} = \begin{pmatrix} 1 & 0 & -u_1 \cdot \sin(a_3) - v_1 \cdot \cos(a_3) \\ 1 & 0 & -u_2 \cdot \sin(a_3) - v_2 \cdot \cos(a_3) \\ \vdots & \vdots & \vdots \\ 1 & 0 & -u_N \cdot \sin(a_3) - v_N \cdot \cos(a_3) \\ 0 & 1 & u_1 \cdot \cos(a_3) - v_1 \cdot \sin(a_3) \\ 0 & 1 & u_2 \cdot \cos(a_3) - v_2 \cdot \sin(a_3) \\ \vdots & \vdots & \vdots \\ 0 & 1 & u_N \cdot \cos(a_3) - v_N \cdot \sin(a_3) \end{pmatrix}\ .$$

Using this setup, the problem can be handled in the same manner as those with only one observation per condition. However, the $x$ and $y$ coordinates are treated separately. In the case of weighted fitting, possibly combined with the detection of outliers, this will lead to the strange effect that not the point $(x, y)$ is assigned a weight, but $x$ and $y$ individually. In extreme case, one coordinate is declared as outlier and the other is not. Section 7.5 suggests an alternative treatment, which regards $(x, y)$ $(u, v)$ as inseparable pairs.

### 2.6.8 Exponential model function

The exponential function

$$y_i = a_1 \cdot \exp(a_2 \cdot x_i) + \varepsilon_i$$

describes a nonlinear model. The partial derivatives are consequently dependent on the model parameters

$$\frac{\partial f_i}{\partial a_1} = \exp(a_2 \cdot x_i) \qquad \text{and} \qquad \frac{\partial f_i}{\partial a_2} = a_1 \cdot x_i \cdot \exp(a_2 \cdot x_i)\ . \tag{2.21}$$

The corresponding Jacobian matrix reads as

$$\mathbf{J} = \begin{pmatrix} \exp(a_2 \cdot x_1) & a_1 \cdot x_1 \cdot \exp(a_2 \cdot x_1) \\ \exp(a_2 \cdot x_2) & a_1 \cdot x_2 \cdot \exp(a_2 \cdot x_2) \\ \vdots & \vdots \\ \exp(a_2 \cdot x_N) & a_1 \cdot x_N \cdot \exp(a_2 \cdot x_N) \end{pmatrix}$$

Facing the dependence on model parameters, it becomes apparent that an initial guess of $\mathbf{a} = (a_1, \ldots, a_M)^{\mathrm{T}}$ is required. Assuming, for instance, that the experiment analyses a decaying process, $a_2$ has to be negative and $a_1$ has presumably a magnitude similar to $y_1$, if $x_1$ is close to zero.

Using these estimates, the vector of residuals is in the beginning

$$\mathbf{r} = \begin{pmatrix} y_1 - (a_1 \cdot \exp(a_2 \cdot x_1)) \\ y_2 - (a_1 \cdot \exp(a_2 \cdot x_2)) \\ \vdots \\ y_N - (a_1 \cdot \exp(a_2 \cdot x_N)) \end{pmatrix}\ .$$

The application of equation (2.6) results to a vector $\mathbf{\Delta a}$ containing the updates for

$$\mathbf{a} \longleftarrow \mathbf{a} + \mathbf{\Delta a}\ .$$

As long as there are distinct changes in the parameter values (see Section 2.2, eq. 2.8), the Jacobian matrix **J** and the vector of residuals **r** have to be re-computed and fed again into (2.6).

It was already mentioned above that $a_2$ must be negative for a decaying process. Unfortunate input data[5], however, might push $a_2$ towards positive values. This can be prevented by simply modifying (2.21) slightly to

$$\begin{aligned}
\frac{\partial f_i}{\partial a_1} &= \begin{cases} \exp(a_2 \cdot x_i) & \text{if} \quad a_2 < 0 \\ 1 & \text{otherwise} \end{cases} \\
\frac{\partial f_i}{\partial a_2} &= \begin{cases} a_1 \cdot x_i \cdot \exp(a_2 \cdot x_i) & \text{if} \quad a_2 < 0 \\ a_1 \cdot x_i & \text{otherwise} \end{cases} .
\end{aligned}$$

Please note that the derivatives remain continuous at $a_2 = 0$.

Alternatively one should consider to set $a_j$ to zero before computing $\frac{\partial f_i}{\partial a_j}$, if $a_j$ is already outside the admissible range.

### 2.6.9 Composite Gaussian bell functions

In Subsection 1.5.2 the superposition of two Gaussian bells was discussed

$$y_i = a_1 \cdot \exp\left[a_2 \cdot (x_i - a_3)^2\right] + a_4 \cdot \exp\left[a_5 \cdot (x_i - a_6)^2\right] + \varepsilon_i \ ,$$

which could be used, for instance, to model the distribution of a certain variable.

Due to the nonlinear character and relative high number of parameters, the determination of the Jacobian matrix becomes a little bit more complex. The partial derivatives are

$$\begin{aligned}
&\frac{\partial f_i}{\partial a_1} = \exp\left[a_2 \cdot (x - a_3)^2\right] \ , \quad \frac{\partial f_i}{\partial a_2} = a_1 \cdot \exp\left[a_2 \cdot (x - a_3)^2\right] \cdot (x - a_3)^2 \ , \\
&\frac{\partial f_i}{\partial a_4} = \exp\left[a_5 \cdot (x - a_6)^2\right] \ , \quad \frac{\partial f_i}{\partial a_5} = a_3 \cdot \exp\left[a_5 \cdot (x - a_6)^2\right] \cdot (x - a_6)^2 \ , \\
&\frac{\partial f_i}{\partial a_3} = -a_1 \cdot \exp\left[a_2 \cdot (x - a_3)^2\right] \cdot a_2 \cdot 2 \cdot (x - a_3) \ , \\
&\frac{\partial f_i}{\partial a_6} = -a_4 \cdot \exp\left[a_5 \cdot (x - a_6)^2\right] \cdot a_5 \cdot 2 \cdot (x - a_6) \ .
\end{aligned}$$

Because of the ambiguity of additive or subtractive combination of two Gaussian bells (see subsection 1.5.2) and other effects causing an error hyper-surface with

[5] especially if the model function is not appropriate

different local minima, the accurate estimation of initial parameters **a** is an extremely important task. One feasible method neglecting the ambiguity would be to fit roughly a single Gaussian at the position of the major peak of the observed values. This Gaussian curve is then subtracted from the observations. The residual undergoes the same procedure of estimating mean, amplitude, and deviation parameters, now for the second Gaussian bell. Herewith, the initial parameters are already rather close to the –hopefully– global minimum.

### 2.6.10 Circle function

Given the model function

$$y_i = 0 = (x_{1,i} - a_1)^2 + (x_{2,i} - a_2)^2 - a_3^2 + \varepsilon_i \tag{2.22}$$

describing a circle (see also Subsection 1.5.3), the partial derivatives with respect to the model parameters are

$$\frac{\partial f_i}{\partial a_1} = 2 \cdot (a_1 - x_{1,i}) \,, \qquad \frac{\partial f_i}{\partial a_2} = 2 \cdot (a_2 - x_{2,i}) \qquad \text{and} \qquad \frac{\partial f_i}{\partial a_3} = -2 \cdot a_3 \,.$$

$a_1$ and $a_2$ define the circle centre whereas $a_3$ corresponds to its radius. Under the assumption that the points (the conditions) are fairly distributed on the circle, the centre is estimated via

$$\begin{pmatrix} a_{1,\text{init}} \\ a_{2,\text{init}} \end{pmatrix} = \begin{pmatrix} \frac{1}{N} \sum_{i=1}^{N} x_{1,i} \\ \frac{1}{N} \sum_{i=1}^{N} x_{2,i} \end{pmatrix} \,. \tag{2.23}$$

The radius estimation is a little bit more complex. It averages the distances of all points to the estimated circle centre

$$a_{3,\text{init}} = \frac{1}{N} \sum_{i=1}^{N} \sqrt{(x_{1,i} - a_{1,\text{init}})^2 + (x_{2,i} - a_{2,\text{init}})^2} \,. \tag{2.24}$$

Since the circle function (2.22) is pseudo-nonlinear, as was pointed out in Chapter 1, it would be reasonable to use instead the form

$$x_{1,i}^2 + x_{2,i}^2 = b_1 \cdot x_{1,i} + b_2 \cdot x_{2,i} - b_3 \,,$$

with

$$\frac{\partial f_i}{\partial b_1} = x_{1,i} \,, \qquad \frac{\partial f_i}{\partial b_2} = x_{2,i} \qquad \text{and} \qquad \frac{\partial f_i}{\partial b_3} = -1 \,.$$

The reconstruction of circle centre $(a_1, a_2)$ and radius $a_3$ is

$$a_1 = 0.5 \cdot b_1 \qquad a_2 = 0.5 \cdot b_2 \qquad a_3 = \sqrt{a_1^2 + a_2^2 - b_3}\ .$$

It has to be mentioned that this procedure leads in general to visually pleasing fits. If, however, one seeks for a solution that minimises the sum squared geometric distances from all points to the circle, then another approach has to be used. This will discussed in Section 7.6.

### 2.6.11 Neural networks

In dependence on the number of input and hidden neurons, neural networks are able to build rather complex nonlinear functions mapping the input (conditions $\mathbf{x}_i$) to the output (observations $y_i$). This makes it difficult to initialise the weights of the net (parameter vector $\mathbf{a}$) with reasonable values. Typically, they are randomly generated. The only constraint concerns the range of definition. The argument $t_k$ of equation (1.33)

$$h_k(t_k) = \tanh(t_k)$$

should lie in the range of $-4 \ldots 4$, see also Figure 1.12 on page 24. Otherwise, small changes of the parameters would have almost no effect on the output of the neurons, since the slope of the hyperbolic tangent is too flat outside this region. Very slow convergence would be the consequence.

**Figure 2.4** shows $3 \times 32$ points in 3D space, which correspond to feature vectors $\mathbf{x}$ with three features $(x_1, x_2, x_3)$ each. The feature vectors belong to three classes 1, 2, and 3. Using a feed-forward 3-3-1 neural network (**Figure 2.5**), it is possible to correctly classify all points. It is a kind of supervised classification. The elements of the single feature vectors (conditions) are presented to the three input neurons and the correct class is expected as output (observation). The neural net combines the three feature values in such a way that the output is smaller than 1.5 for all vectors from class 1 and higher than 2.5 for all vectors from class 3 (**Figure 2.6**a).

When reducing the number of hidden neurons from 3 to 2, some of class 1 and 2 are falsely assigned (**Figure 2.6**b).

The major problem of neural networks lies in the error surface with multiple local minima. In addition, it is not possible to guess good starting values for the parameters. The parameters must be initialised with random values. Also a target for the minimisation criterion $\chi^2$ should be set low in order to hopefully find the best combination of weights.

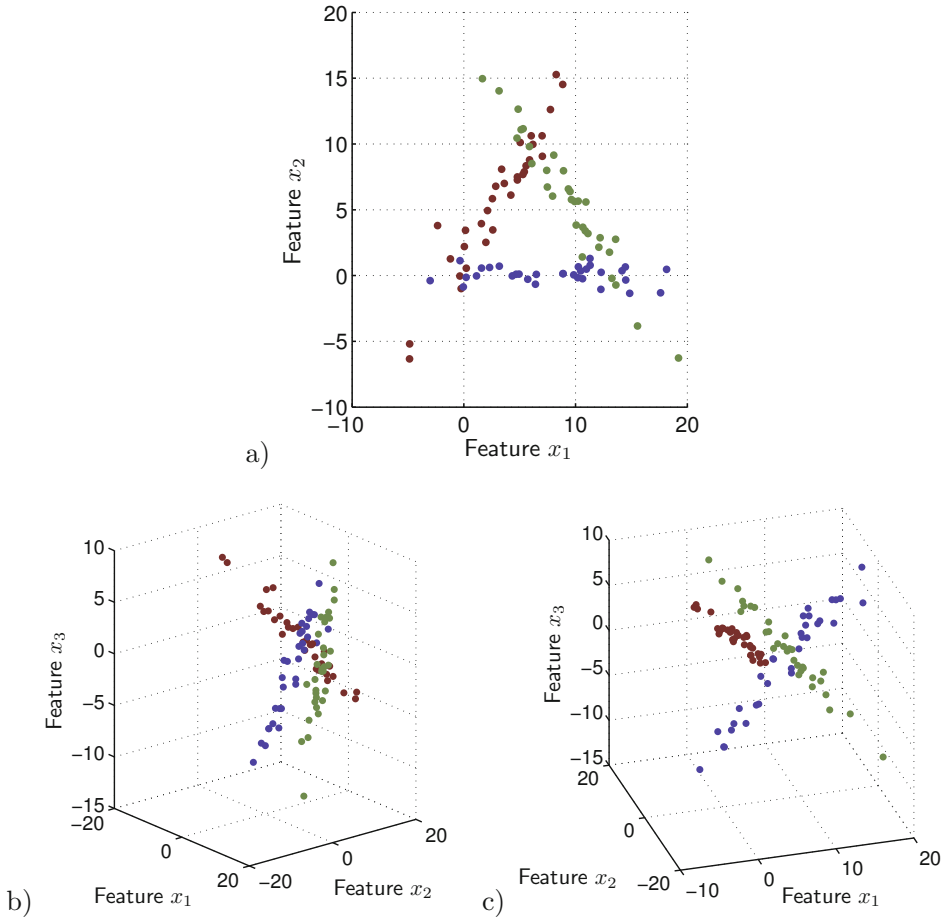


Figure 2.4: Feature vectors from three separated classes; a) view onto $x_1$–$x_2$ plane; b)+c) views illustrating the separability

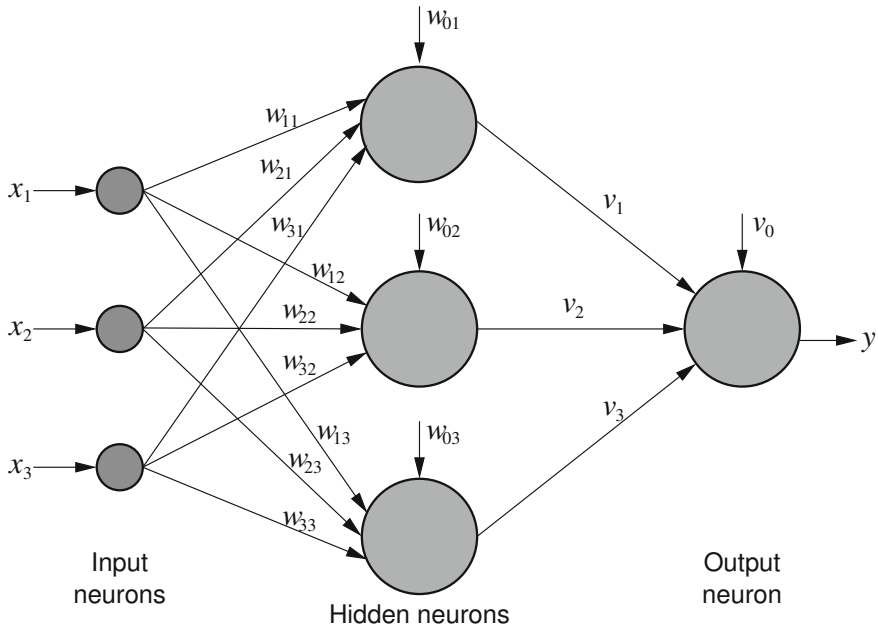


Figure 2.5: Feed-forward 3-3-1 neural network

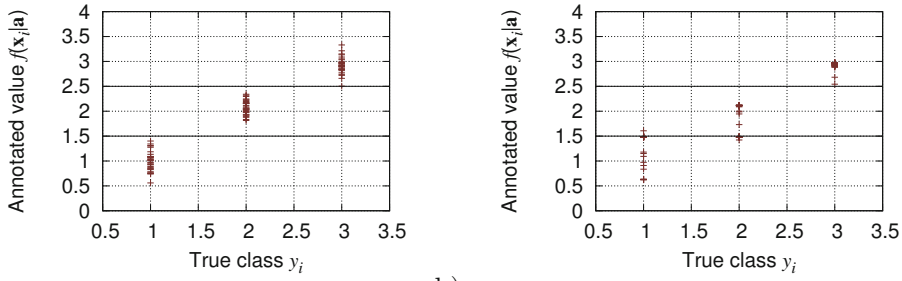


a) b)

Figure 2.6: Results of classification via neural networks; a) 3-3-1 net (16 parameters); b) 3-2-1 net (11 parameters)

## 2.7 Test questions

**2.1** Does the least-squares method concern minimisation or optimisation?

**2.2** What is the aim of least-squares fitting?

**2.3** What is an error surface? What is it dependent on?

**2.4** Why do nonlinear fitting problems require an initialisation of parameters?

**2.5** What is the content of the Jacobian matrix? What do its columns and rows depend on?

**2.6** What is the residual vector?

**2.7** Is it possible to compute the model-function parameters directly (in one pass) for linear (nonlinear) models?

**2.8** Write down the fitting equations for linear (nonlinear) fitting problems.

**2.9** What are the drawbacks of nonlinear model functions?

**2.10** Itemise different methods for the estimation of initial parameter values.

**2.11** Explain the relation between least squares and neural networks.

**2.12** How must the fitting procedure be altered if there is more than one observation per condition $\mathbf{x}$?

**2.13** Given the linear model function

$$f(\mathbf{x}|\mathbf{a}) = a_1 \cdot x + a_2 \cdot x^2 + a_3 \cdot \mathrm{e}^x + a_4 \cdot \sin(x) \ ,$$

what is the Jacobian matrix?

**2.14** How many parameters have to be estimated in a 2-3-2 neural network?

# Chapter 3

# Weights and Outliers

## 3.1 What are the weights good for?

The previous chapter has already introduced an $N \times N$ matrix

$$\mathbf{W} = \begin{pmatrix} w_1 & 0 & 0 & \cdots & 0 \\ 0 & w_2 & 0 & \cdots & 0 \\ 0 & 0 & \ddots & \cdots & \vdots \\ \vdots & \vdots & \vdots & \ddots & 0 \\ 0 & 0 & \cdots & 0 & w_N \end{pmatrix}$$

containing weights $w_i$ assigned to each of the $N$ observation $y_i = f(\mathbf{x}_i|\mathbf{a})$. This chapter explains why it is advantageous to use these weights and how to estimate them.

The underlying idea is the following. If it is known that observation $y_k$ has a higher uncertainty than $y_l$, then the weight $w_k$ should be lower than $w_l$. In other words: the more reliable value of $y_l$ may influence the data-fitting calculation more than $y_k$.

The reliability is often dependent on the experimental conditions $\mathbf{x}_i$. **Figure 3.1** visualises data of a possible experiment for the estimation of distances by eye. It is evident that the estimation error is somehow proportional to the real distance. If the true distance is one centimetre, the error will be in the range of millimetres, whereas the estimations of hundreds of metres will result to much larger errors. The uncertainty is typically indicated by error bars (the vertical lines in Fig. 3.1).

In theory, the optimal weight is independent on the single observation $y_i$, but equal to

$$w_i = \frac{1}{\sigma_i^2} \,. \tag{3.1}$$

It implies the knowledge of the standard uncertainty $\sigma_i$ of the parent distribution from which each single observation $y_i$ is drawn. This implication is rather venturous. Unfortunately, in very many practical cases, there is no chance neither to

T. Strutz, *Data Fitting and Uncertainty*, DOI 10.1007/978-3-8348-9813-5 _3,

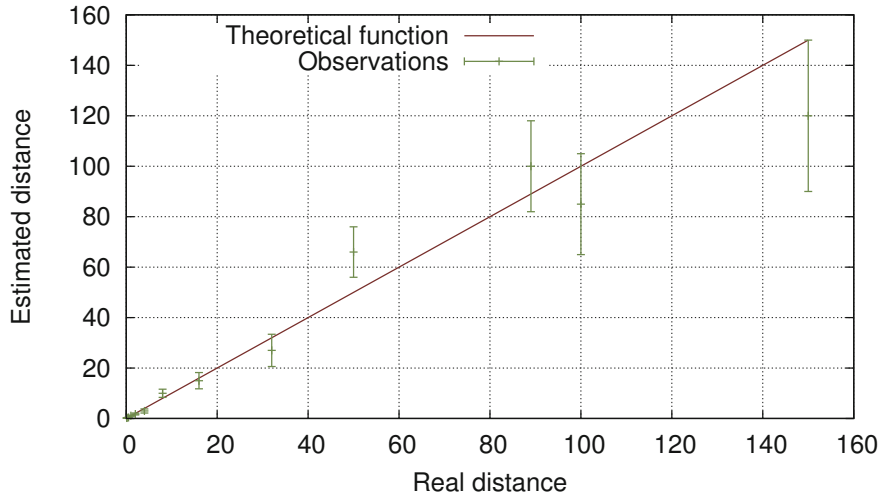


Figure 3.1: Estimation of distances: an example for uncertainties depending on the experimental condition. Uncertainties are depicted as error bars with the observed value (estimated distance) in the middle of the bars.

obtain directly $\sigma_i$ nor to get knowledge about the true parent distribution[1]. The general advise is to set $\sigma_i = \sigma = 1.0$, as long as no information is available about $\sigma_i$. However, treating all observations equally can lead to poor fitting results, especially in the presence of outliers.

Instead of ignoring the weights, they should be estimated based on the available observations in order to reflect their relative importance, especially if the detection of outliers is intended (see next section). After the removal of putative outliers, it is legitimate to forget the estimated weights and to fit the model function to the reduced set of data points.

## 3.2 Outliers

Many applications do not only require an estimation of weights but require, in addition, the detection of outliers. Outliers, also referred to as mavericks or contaminant observations, are data points that deviate so much from other points that they seem to be generated by a different mechanism than the 'good' observations.

[1] In addition, the values of $\sigma_i$ are based on the assumption that the errors in $y_i$ are normally distributed, which can be different in particular scenarios.

When observations are subject to data analysis, at least two scenarios have to be distinguished. Either (i) outliers negatively influence the results of analysis, or (ii) the search for outliers is the main task of data analysis. In data mining, for instance, outlier detection is also regarded as the detection of novelty or anomaly. In most cases, there is a set of training values available that defines 'normality'. Security applications are examples, in which atypical behaviour by people or technical systems has to be detected. In applications with a small number of observations, however, the detection method should be able to identify outliers without prior training.

With respect to scenario (i), lively discussion can be found in the past literature on outliers as to whether to reject suspicious values or always to keep all observations. Beckman and Cook give an overview of the history of attempts to find outliers in data sets [Bec83]. Unfortunately, no established standard technique has to date. A comprehensive review of the tests developed for outlier detection can be found in Barnett and Lewis [Bar94]. Outlier tests (also known as discordance tests) are mostly tailored to the statistical model generating the observations and often presume some knowledge of the number of putative outliers. Many of them can only cope with a single outlier. With the focus on machine learning and data mining, approaches to outlier detection have been surveyed by [Mar03] and [Hod04]. If the underlying model is not known in advance, for example, when dealing with biological or economical data, mild assumptions about the model will have to be made as a minimum.

With regard to the model, we must differentiate between (i) analytical models in the form of $\mathbf{y} = f(\mathbf{x}|\mathbf{a})$, that is, the vector of observations $\mathbf{y}$ is a function of a set of conditions $\mathbf{x}$ with certain model parameters $\mathbf{a}$, and (ii) more descriptive models, such as: "The observations must be clustered or connected". The latter type of model is often used in the field of machine learning; its parametrisation is usually possible to a certain extent. In these applications, the outlier detection is typically based on classification with a so-called rejection/novelty class.[Mar03, Hod04]

For each single case of application, it must be carefully judged, whether outliers are likely to occur or whether strongly deviating observations are the normal case. The on-line "Engineering Statistics Handbook" lists the following possible reasons for outliers: [ESH07]

- operator blunders,
- equipment failures,
- day-to-day effects,
- batch-to-batch differences,
- anomalous input conditions, and
- warm-up effects.

Furthermore it makes following important remark: "*The best attitude is that outliers are our 'friends'; outliers are trying to tell us something, and we should not stop until we are comfortable with the explanation for each outlier*". Everybody should therefore be keen to find outliers, since their detection and the exploration of the reason of their presence may provide new knowledge.

The enumeration above refers to real-life experiments or measurement series, and, as a minimum, must be extended by the reasons inherent in the deficiency of computational algorithms. Let us consider, for example, the tracking of objects in image sequences. A computational pattern-recognition algorithm has to analyse images taken at certain time steps. It may happen that the algorithm frequently fails to detect the desired object under certain conditions, for instance when other objects or background patterns attract the algorithm. The detection algorithm is therefore not only producing values that deviate more or less from the true object coordinates, but can also produce results that are totally wrong.

If one can expect that the number of outliers will not increase in proportion to the number of observations, the identification of outliers becomes important especially in data sets with a low number of observations. Here, the influence can typically not be neglected because the presence of outliers would strongly bias the result of data analysis.

## 3.3 Estimation of weights

Before starting with the determination of weights, let us recapitulate the procedure of data fitting.

Based on the analytical and general model function

$$y = f(\mathbf{x}|\mathbf{a}) \,, \tag{3.2}$$

the true outcome $y$ of an experiment is a function of the experimental conditions $\mathbf{x}$ and certain model parameters $\mathbf{a}$. In practice, this model function is sampled with a limited number of real observations

$$y_i = f(\mathbf{x}_i|\mathbf{a}) + \varepsilon_i \qquad i = 1, 2, \ldots, N \,, \tag{3.3}$$

deviating from the true values of $y$ by $\varepsilon_i$. Since the model parameters themselves have to be estimated based on the available observations $y_i$, only estimates $\hat{y}$ of $y$ can be determined

$$\hat{y} = f(\mathbf{x}|\hat{\mathbf{a}}) \,. \tag{3.4}$$

$\hat{\mathbf{a}}$ is the vector of estimated model parameters. The sample number $i$ indicates a particular estimate and its corresponding conditions

$$\hat{y}_i = f(\mathbf{x}_i|\hat{\mathbf{a}}) \; . \tag{3.5}$$

The residual[2]

$$\Delta_i = y_i - \hat{y}_i \tag{3.6}$$

expresses the deviation of each observation $y_i$ from its estimated value $\hat{y}_i$. Please note that $\Delta_i$ is not only dependent on the fluctuations $\varepsilon_i$, but is also influenced by the estimation of the model parameters $\mathbf{a}$.

In regression analysis, the goal is typically to find the best model parameters $a_j \in \mathbf{a}$ with respect to a certain optimisation criterion. The presence of outliers disturbs the parameter estimation, and the deviates $\Delta_i$ are influenced as well, affecting the outlier detection in turn. Robust regression methods have therefore been developed that automatically down-weight the influence of outliers and result in more accurate model parameters [Ham86]. Many robust estimators iteratively search for optimal weights [Hol77].

In the most likely case that the uncertainty $\sigma_i$ for a particular observation $y_i$ is not known in advance, the weights have to be estimated dependent on the observations themselves. Therefore, the data fitting has to be performed first with constant weights $w_i = 1.0$ calculating model parameters $\hat{\mathbf{a}}$ which are hopefully not too far from the optimal ones. Then, the observations $y_i$ have to be compared with the corresponding values of $\hat{y}_i = f(\mathbf{x}_i|\hat{\mathbf{a}})$ using the absolute differences

$$|\Delta_i| = |y_i - \hat{y}_i| \; .$$

Under consideration of the weighted and squared residuals of observations with respect to the modelled function

$$\chi^2 = \sum_i w_i \cdot [f(\mathbf{x}_i|\hat{\mathbf{a}}) - y_i]^2 = \sum_i w_i \cdot \Delta_i^2 \; , \tag{3.7}$$

the value of $\Delta_i^2$ has to be mapped to a suitable weight $w_i$. After the determination of weights and the removal of putative outliers, the least-square fitting must be performed again.

[2] The residual $(y_i - \hat{y}_i)$ is sometimes also called *deviate* to be more precisely [Sch89].

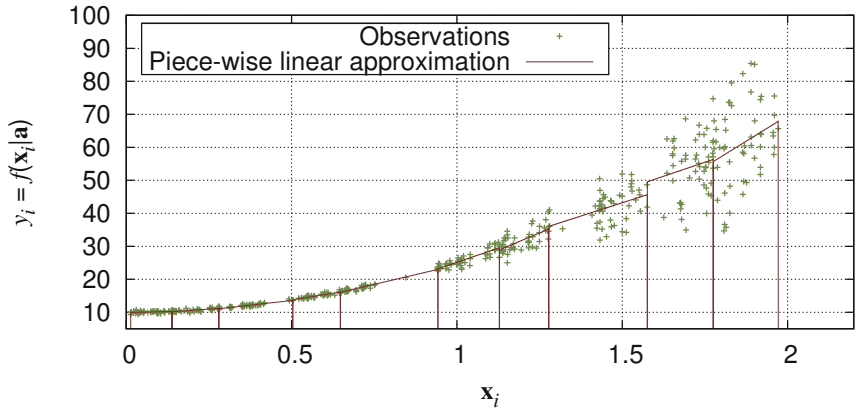


Figure 3.2: Scatter plot and piece-wise linear approximation of measured data with bins containing fifty observations each

### 3.3.1 Estimation by binning

In the favourable case of many measurements under the same (or at least similar) conditions, weights should be determined using estimated standard uncertainties.

If there are enough observations available for a given range of conditions, it is possible to segment ("to bin") the $x$ axis (conditions) into $K$ intervals. The $N_k$ data points from each bin $B_k$, $k = 1, 2, \ldots K$ can be approximated, for instance, by a straight line, using the model function

$$y_i = a_1 + a_2 \cdot x_i + \varepsilon_i \qquad \forall x_i \in B_k.$$

That means, the curve is piece-wise linearly approximated before the fitting with the correct model function is carried out. **Figure 3.2** shows the start and end position of each bin (i.e. the range of conditions) and the fitted straight lines. As can be seen, the piece-wise approximation does not necessarily result to a continuous curve.

The deviation of the observations $y_i$ from these lines indicates the uncertainty of the observations in each bin via

$$\sigma_{\mathrm{y},k} = \sqrt{\frac{1}{N_k - 2} \sum_{x_i \in B_k} \left[ y_i - (\hat{a}_1 + \hat{a}_2 \cdot x_i) \right]^2} \,.$$

Obviously, the size of the bins has to be chosen carefully. It can either be fixed in size or adapted somehow dependent on the data, for example, using a constant

number $N_k$ of observations for each bin $B_k$. In Figure 3.2, for instance, the bins comprise fifty observations each.

Alternatively, one could use overlapping bins or a window sliding along the condition axis. At each position, the uncertainty could be determined and assigned to the observation at the window centre. In maximum, each observation would get its own uncertainty, however, at the price of additional computational costs.

### 3.3.2 Weights estimation using deviates

A simple method of mapping residuals (or more precise: deviates) $\Delta = (y_i - \hat{y}_i)$ to suitable weights is to take their squared values $\Delta_i^2$ instead of $\sigma_i^2$ as weights

$$w_i = \frac{1}{\sigma_i^2} \approx \frac{1}{\Delta_i^2} \,. \tag{3.8}$$

This procedure is not correct in the sense of theoretical statistics, but under circumstances of very erroneous data a sufficient approximation. However, it turns out that a direct application of this formula can become dangerous in practice, in particular when an observation $y_i$ is by chance equal or very close to the model function. An unjustified high weight would be assigned to this observation, compared to the others. Therefore, $w_i$ has to be limited to a maximum value, reflecting the probable minimum squared uncertainty $\sigma_i^2$. This is achieved by using a lower bound $\lambda_\mathrm{L}$

$$w_i = \begin{cases} \dfrac{1}{\lambda_\mathrm{L}^2} & \text{for} \quad |\Delta_i| < \lambda_\mathrm{L} \\ \\ \dfrac{1}{\Delta_i^2} & \text{otherwise} \end{cases} \,. \tag{3.9}$$

The weights $w_i$ obtained via (3.9) are indirectly dependent on the observations $y_i$. In theory, this should be avoided, since it brings bias (systematic error) into the parameter estimation. However, in very erroneous environments this possible bias can be neglected in comparison to the effect of random errors and outliers.

#### Normally distributed deviates

The definition of $\lambda_\mathrm{L}$ could be formulated as

$$\lambda_\mathrm{L} = \kappa_\mathrm{L} \cdot \hat{\sigma}_\mathrm{y} \,,$$

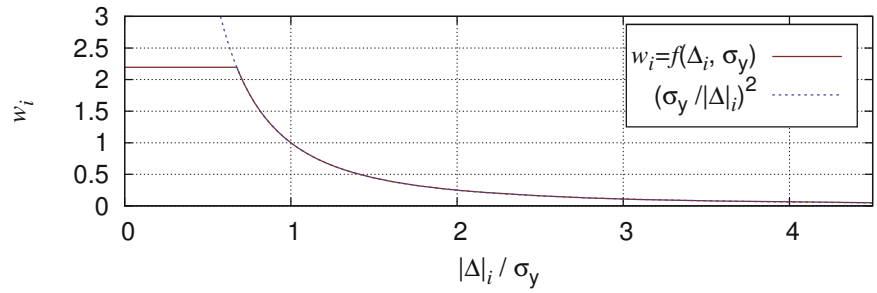


Figure 3.3: Transfer function for the mapping of deviates to suitable weights. $\kappa_L = \lambda_L/\sigma_y = 0.675$ limits the hyperbolic function (in case of normal distributed deviates).

whereas $\kappa_L$ is an application-dependent factor and $\hat{\sigma}_y$ the estimated standard deviation (e.s.d.) of the observations $y_i$ with respect to the model function

$$\hat{\sigma}_y = \sqrt{\frac{1}{N-M} \cdot \frac{\sum_{i=1}^{N} w_i \cdot [f(\mathbf{x}_i|\hat{\mathbf{a}}) - y_i]^2}{\frac{1}{N}\sum_{i=1}^{N} w_i}} \,. \tag{3.10}$$

$M$ is the number of model parameters. The sum below the fraction line normalises the weights to a mean value equal to one.

Using $\hat{\sigma}_y$ in the weighting process puts implicitly the presumption of normally distributed deviates. In addition, $\hat{\sigma}_y$ reflects only the deviation of the recorded observations, not the deviation in the parent distribution $\sigma_i$. If the number of observation $N$ is not sufficient high, both values, $\hat{\sigma}_y$ and $\sigma_i$, can differ a lot.

**Figure 3.3** depicts the weights as a function of the absolute deviates. Assuming a Gaussian distribution of deviates, the value of $\kappa_L = 0.675$ splits the observation into two halves, one getting equal weights $w_i = 1/\lambda_L^2$ and the other getting weights based on the corresponding deviate $w_i = 1/\lambda_i^2$ according to equation (3.9). Using $\kappa_L = 1.0$, for example, 68.3% of all weights would be equal.

In the beginning of Section 3.3, it was stated that the first run of data fitting must use equal weights if the uncertainty $\sigma_i$ of the single observation $y_i$ is not known. Afterwards, the estimation of the weights $w_i$ is possible in dependence on the residuals $\Delta_i = y_i - f(\mathbf{x}|\hat{\mathbf{a}})$ and $\hat{\sigma}_y$ (equation (3.10)).

Now let us imagine that a particular data set contains observations with highly varying uncertainty. If the number $N$ of observations is rather small ($N <<$

100), it is very likely that the data fitting yields suboptimal if not even wrong parameter values in the beginning. In addition, the computed value $\hat{\sigma}_\mathrm{y}$ is high and consequently the threshold $\lambda_\mathrm{L}$ as well. The discrimination between most observations (with smaller absolute residuals $|\Delta_i|$) will fail, since equal weights are assigned to them. Furthermore, the derived values $\Delta_i$ do not reflect the deviation from the true model function, but describe the distances to the current modelled function $f(\mathbf{x}|\hat{\mathbf{a}})$ which can still be entirely wrong as long as the estimated parameters $\hat{\mathbf{a}}$ are far from their optimum.

Thus, the first estimate of weights is likely to be non-optimal and it is necessary to iterate the processing with alternating execution of parameter estimation by data fitting and determination of weights. The iteration stops when the changes of the weights are negligible. This procedure is also called *iteratively re-weighted least squares* and has been firstly mentioned in the context of robust regression by [Hol77].

**Non-normally distributed deviates**

In order to avoid the dependence of $\lambda_\mathrm{L}$ on $\hat{\sigma}_\mathrm{y}$, those deviate is taken as threshold, which cuts the set of deviates in two halves, that is,

$$\lambda_\mathrm{L} = \mathrm{median}\left(|\Delta_i|\right), \qquad \Delta_i = f(\mathbf{x}_i|\hat{\mathbf{a}}) - y_i \tag{3.11}$$

In case of normally distributed deviates, this would approximately correspond to $\lambda_\mathrm{L} = \kappa_\mathrm{L} \cdot \hat{\sigma}_\mathrm{y} = 0.675 \cdot \sigma_\mathrm{y}$.

Taking the median element, fifty percent of all observations are assigned to equal weights. Of course, any element of another rank would differently influence the strength of weighting. However, $\lambda_\mathrm{L}$ should be bounded to a minimum of about $0.05 \cdot \max_i\left(|\Delta_i|\right)$ in order to prevent an unbalanced weighting if a large number of deviates is very small.

## 3.4 Approaches towards outlier detection

Let us assume, each observation $y_i$ is assigned a weight $w_i$ indicating the importance of this particular observation. In the simplest case, these weights are all equal to one. The elimination of outliers, i.e. setting their weights to zero, requires a threshold $\lambda_\mathrm{O}$ that is compared to the absolute deviates

$$w_i = \begin{cases} 0 & \text{for} \quad |\Delta_i| \geq \lambda_\mathrm{O} \\ w_i & \text{otherwise} \end{cases} . \tag{3.12}$$

$\lambda_O$ is a hard threshold and defines the range of outliers. Some application also allow soft-bounded estimations of the "degree of outlierness" [Bre00].

The determination of $\lambda_O$ is the critical task in outlier detection.

Outlier detection can be applied either directly or after the estimation of weights. In general, the estimation of weights has a positive effect on outlier detection. Observations will emerge as contaminants if the weighting procedure improves the estimation of model parameters.

It is theoretically possible but not recommended to include the outlier detection into the iterations of weights estimation because this would cause problems when applying the threshold $\lambda_O$. Turning off some observations is a nonlinear operation, which could lead to an unstable iteration with slow convergence or even oscillation in the worst case. That means, iterative weighting and outlier detection must be applied consecutively.

In the following, two methods of outlier detection will be explained. The first one is quite simple and is, despite its shortcomings, widely used in many applications. The second method is more sophisticated and improves the detection results by clustering the observations in acceptable data points and contaminants.

### 3.4.1 Standardised residuals

#### The Method

The criterion of standardised residuals assumes that the values $y$ to be inspected are normally distributed according to the distribution function

$$f(y) = \frac{1}{\sqrt{2\pi} \cdot \sigma_y} \cdot \exp\left[-0.5 \cdot \left(\frac{y - \overline{y}}{\sigma_y}\right)^2\right] \tag{3.13}$$

with a mean $\overline{y}$ and a standard deviation $\sigma_y$. The true value $\sigma_y$ is not known in advance. Since the number of observations $i = 1, \ldots, N$ is limited, $\sigma_y$ can only be estimated to a certain degree of accuracy by

$$\hat{\sigma}_y = \sqrt{\frac{1}{N-1} \sum_{i=1}^{N} (y_i - \overline{y})^2}\,. \tag{3.14}$$

The majority of all observations drawn from a normal distribution are less distant from the mean than a certain multiple of its standard deviation. The method

of standardised residuals (also called the $z$-score) utilises this fact to identify contaminants

$$\frac{|y_i - \overline{y}|}{\hat{\sigma}_\mathrm{y}} > \kappa_\mathrm{O} \ . \tag{3.15}$$

All observations leading to a standardised residual larger than $\kappa_\mathrm{O}$ are considered to be outliers. Many texts propose values in the range $3 \leq \kappa_\mathrm{O} \leq 4$. The value could also be adapted to the number of observations $N$ according to Chauvenet's criterion [Cha71] (see Section 7.2).

In the context of data fitting via least-squares approximation, $\overline{y}$ corresponds to $f(\mathbf{x}|\hat{\mathbf{a}})$ and (3.15) turns into

$$\frac{|\Delta_i|}{\hat{\sigma}_\mathrm{y}} = \frac{\Lambda_i}{\hat{\sigma}_\mathrm{y}} > \kappa_\mathrm{O} \ . \tag{3.16}$$

The threshold for outliers is therefore

$$\lambda_\mathrm{O} = \kappa_\mathrm{O} \cdot \hat{\sigma}_\mathrm{y} \tag{3.17}$$

with an esitmated standard deviation $\hat{\sigma}_\mathrm{y}$ according to equation (3.10).

### Implications of the normal distribution

Although the normal distribution has its theoretical foundation, most people are not willing to accept that a measurement can deliver a result that arbitrarily deviates from the correct value. This is, however, exactly what the range of definition $-\infty \leq y \leq +\infty$ of the normal distribution is telling us. In practical cases of limited numbers $N$ of observations $y_i$ $(i = 1, 2, \ldots, N)$, possibly everybody will reject an observation $y_i$ that is further apart than, say, a certain multiple of the standard deviation $\sigma_\mathrm{y}$. Therefore, when talking about outliers, it seems to be appropriate to consider a modification of the statistical model of the observations.

Choosing the cut-off value based on the standardised residual raises another problem. Typically, it is expected that the outlier criterion will separate the cluster of 'good' observations from contaminants, especially when inspecting the plot of residuals. There should be a certain distance between the outer border of the cluster and the outliers. The standardised residual criterion, however, does not offer a separation of this kind by definition. In **Figure 3.4** a), two out of 100 observations $y_i$ drawn from a normal distribution ($\sigma_\mathrm{y} = 1.0, \overline{y} = 0$) are declared as outliers, when using $\kappa_\mathrm{O} = 3$.[3] Intuitively, one would cut off the observation

[3] The estimated standard deviation is somewhat higher than 1.0 leading to a threshold of $\kappa_\mathrm{O} \cdot \sigma = 3.047$.

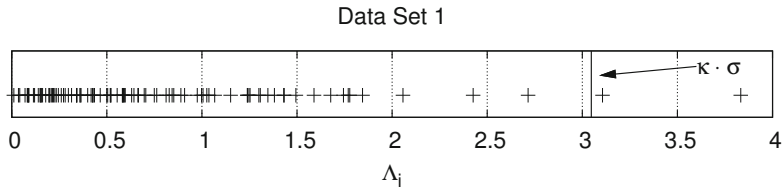


a)

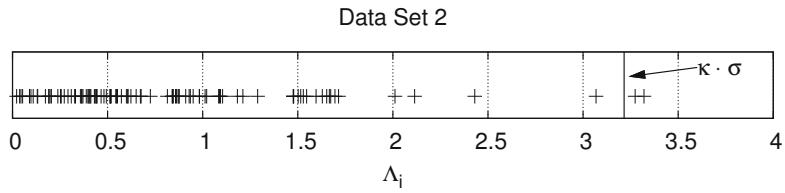


b)

Figure 3.4: The weakness of outlier detection via standardised residuals. Example distributions of deviates $\Lambda_i = |\Delta_i| = |y_i - \hat{y}_i|$ with threshold according to the $3 \cdot \hat{\sigma}_\Delta$ rule.

at $\Lambda_i = |\Delta_i| \approx 3.8$ in maximum. The opposite is true for the example in **Figure 3.4** b). Under same conditions, two out of 100 observations are again classified as outliers. Judgement by eye would suggest three, due to the large gap between 2.5 and 3.0.

The next subsection proposes an approach to outlier detection based on cluster-analysis that is independent on the estimated standard deviation $\hat{\sigma}_\mathrm{y}$ and takes into account that outliers should be apart from the bulk of 'good' observations.

### 3.4.2 Cluster criterion

Outlier detection based on the standardised residuals discussed above is dependent on the normal distribution of observations and the estimation of its standard deviation $\hat{\sigma}_\mathrm{y}$ (see eq. 3.14), which is rather uncertain in the case of low numbers of observations. In order to avoid this dependency, a method of outlier detection is required following another principle.

The basic idea is to find a pattern, or strictly speaking a gap, in the distribution of deviates that might point to the existence of outliers (**Figure 3.5**). Putative contaminants are identified by comparing the distances between the absolute deviates $\Lambda_i = |\Delta_i| = |y_i - \hat{y}_i|$ [Str09b].

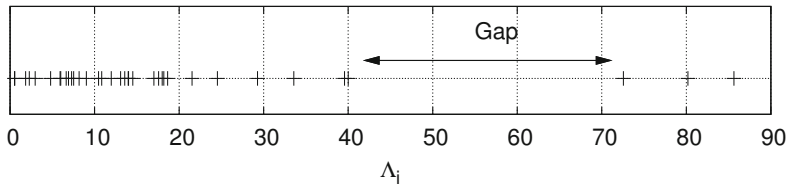


Figure 3.5: Example distribution of deviates $\Lambda_i = |\Delta_i| = |y_i - \hat{y}_i|$ with a significant gap between the bulk of deviates on the left and the three suspicious points on the right.

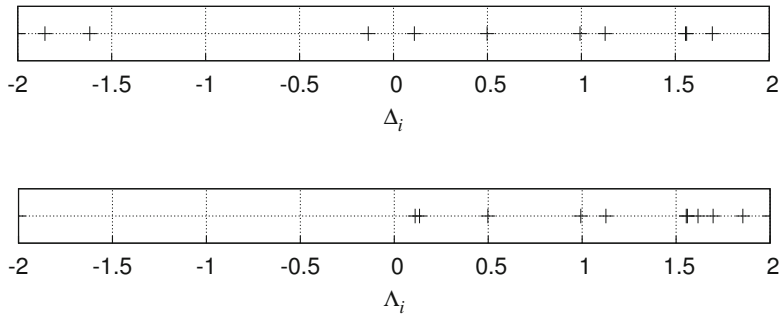


Figure 3.6: Example distribution of absolute deviates ; a) with sign, b) absolute values

### Basic approach

It is presumed that all non-outliers form a one-dimensional cluster in the sense that their corresponding absolute deviates are relatively close to each other, while the deviates of contaminant observations are more or less remote from this cluster. The sign of the deviates provides no valuable information for the process of outlier detection. In contrast, mapping all negative deviates into the range of positive numbers decreases the distances between them on average leading to fewer potential outliers, especially if they are distributed almost evenly in the negative and positive domain and their total number $N$ is low. The example in **Figure 3.6** shows that taking the absolute values integrates exposed deviates into the set of deviates.

The algorithm for clustering the observations in good data points and putative outliers will be explained in detail in the following. Afterwards, several numerical

examples will be discussed, making the procedure more transparent.

First, the absolute deviates $\Lambda = |\Delta|$ have to be sorted in ascending order

$$\ldots \leq \Lambda_j \leq \ldots \leq \Lambda_k \leq \ldots \leq \Lambda_l \leq \ldots \ .$$

These sorted values are numbered by $n$

$$\Lambda_\mathrm{s}[0] \leq \ldots \leq \Lambda_\mathrm{s}[n] \leq \Lambda_\mathrm{s}[n+1] \leq \ldots \Lambda_\mathrm{s}[N-1]$$

and the differences between them are calculated

$$d[n+1] = \Lambda_\mathrm{s}[n+1] - \Lambda_\mathrm{s}[n] \ .$$

In the sequel, only absolute deviates are considered and we will abandon on the attribute "absolute".

It is expected that the deviate of an outlier will show a significantly higher difference (distance) from its nearest neighbour downwards, i.e., the deviate will be more distant from the others than deviates of measurements drawn from the correct distribution.

What qualifies a distance $d_\mathrm{b}$ as a border (a gap) between a one-dimensional cluster of good observations and possible outliers?

1. It must be distinctly larger than a typical distance (global criterion)

$$d_\mathrm{b} \geq \kappa_1 \cdot d_\mathrm{glob} \qquad \text{with } \kappa_1 > 1 \ . \tag{3.18}$$

2. It should be substantially larger than its predecessors (local criterion)

$$d_\mathrm{b} \geq \kappa_2 \cdot d_\mathrm{loc} \qquad \text{with } \kappa_2 > 1 \ . \tag{3.19}$$

We define the typical distance for a certain deviate as the weighted average of distances belonging to deviates which are smaller than the deviate corresponding to the distance $d[n]$ under investigation

$$d_\mathrm{glob}[n] = \frac{1}{C_{1,n}} \cdot \sum_{j=1}^{n-1} d[n-j] \cdot v_j \ . \tag{3.20}$$

Considering only the smaller deviates avoids the influence of other potential outliers. The weighting $v_j$ becomes weaker with increasing $j$, i.e. with increasing distance[4] to the point under investigation

$$v_j = \exp\left[-\frac{1}{2} \cdot \left(\frac{j}{N/2}\right)^2\right] \ . \tag{3.21}$$

[4] Here, 'distance' refers to the index $n$ of the sorted set of deviates.

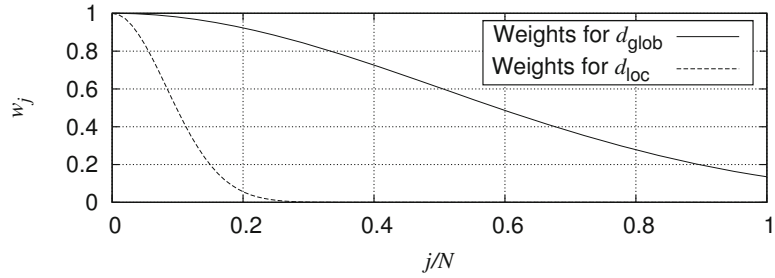


Figure 3.7: Weights $w_j$ for the determination of $d_{\mathrm{glob}}[n]$ and $d_{\mathrm{loc}}[n]$ in dependence of the distance $j$ to the difference $d[n]$ (normalised by number of observation $N$)

The slope of the exponential function in eq. (3.21) is dependent on the number of observations $N$ in order to make the calculation adaptive to this number (**Figure 3.7**). The constant $C_1$ in (3.20) normalises to the sum of weights

$$C_{1,n} = \sum_{j=1}^{n-1} v_j \ . \tag{3.22}$$

In principle, the second criterion (eq. 3.19) utilises the same averaging process, but with weights falling off more rapidly in order to express closeness

$$d_{\mathrm{loc}}[n] = \frac{1}{C_{2,n}} \cdot \sum_{j=1}^{n-1} d[n-j] \cdot \exp\left[-\frac{1}{2} \cdot \left(\frac{j}{N/12}\right)^2\right] \tag{3.23}$$

with

$$C_{2,n} = \sum_{j=1}^{n-1} \exp\left[-\frac{1}{2} \cdot \left(\frac{j}{N/12}\right)^2\right] \ . \tag{3.24}$$

The denominators $N/2$ and $N/12$ have been determined empirically. Figure 3.7 shows that $d_{\mathrm{glob}}[n]$ is dependent on all differences $d[n-j]$ with slightly decreasing weights, while $d_{\mathrm{loc}}[n]$ is mainly influenced by only few neighbouring differences. Please note that both, $d_{\mathrm{glob}}[n]$ and $d_{\mathrm{loc}}[n]$ are different for each distance $d[n]$, reflecting the adaptive character of the approach. This property is also discussed in the examples below.

In summary, the presence of one or more outliers is indicated if there is an absolute deviate $\Lambda_{\mathrm{s}}[n]$ showing a distance $d[n]$ from the next deviate down $\Lambda_{\mathrm{s}}[n-1]$, which

has the two properties

$$d[n] \geq \kappa_1 \cdot d_{\text{glob}}[n] \qquad \text{and} \qquad d[n] \geq \kappa_2 \cdot d_{\text{loc}}[n] \; . \tag{3.25}$$

The value of the corresponding deviate $\Lambda_{\text{s}}[n]$ is taken as the cut-off value $\lambda_{\text{O}}$. If there is more than one deviate satisfying both criteria, the one with the highest relation $d[n]/d_{\text{loc}}[n]$ is selected. If these values are identical as well, the decision is made dependent on the larger distance $d[n]$.

Using the approach described, even multiple outliers can be eliminated at once, because the observation $y_{\text{b}}$ corresponding to the distance $d_{\text{b}}$ fulfilling eq. (3.25) only marks the border between the two clusters of good observations and contaminants. It is evident that all observations having higher absolute deviates than $y_{\text{b}}$ also belong to the cluster of outliers.

**Parameter determination**

Experiments with different kinds of data sets have shown that $\kappa_2$ can be set to a fixed value of 2, while $\kappa_1$ should be dependent on the number of observations $N$.

Suitable values for $\kappa_1$ have been derived from computer simulations. The idea has been to choose a value for $\kappa_1$ that will lead to a probability of about $P_{\text{o}} = 0.15$ that an outlier is detected in a data set with normally distributed deviates. For different numbers of observations $N$ in the range of $8 \leq N \leq 2048$, $10^5$ random data sets have each been investigated and the resulting plots $P_{\text{o}} = f(\kappa_1)$ have been examined. Naturally, the outlier probability $P_{\text{o}}$ decreases with increasing values of $\kappa_1$. **Figure 3.8** shows the derived dependence of $\kappa_1$ on $N$. If $N$ is a number between these points, the corresponding $\kappa_1$ can be interpolated.

**Exception handling**

In experiments with integer-valued observations, several deviates typically have identical values leading to many distances equal to zero. The local change in distances would be over-estimated in theses cases and the determination of $d_{\text{loc}}[n]$ is altered to

$$d_{\text{loc}}[n] = \begin{cases} d[n]/\kappa_2 & \text{if more than the half of all} \\ & \text{predecessors } d[n-j] \text{ are equal to zero} \\ d_{\text{loc}}[n] & \text{otherwise} \end{cases} \; . \tag{3.26}$$

The alternative value is chosen such that the local criterion is fulfilled (see eq. (3.25)), but with the lowest chance of being selected as the border between the clusters of good and bad data points.

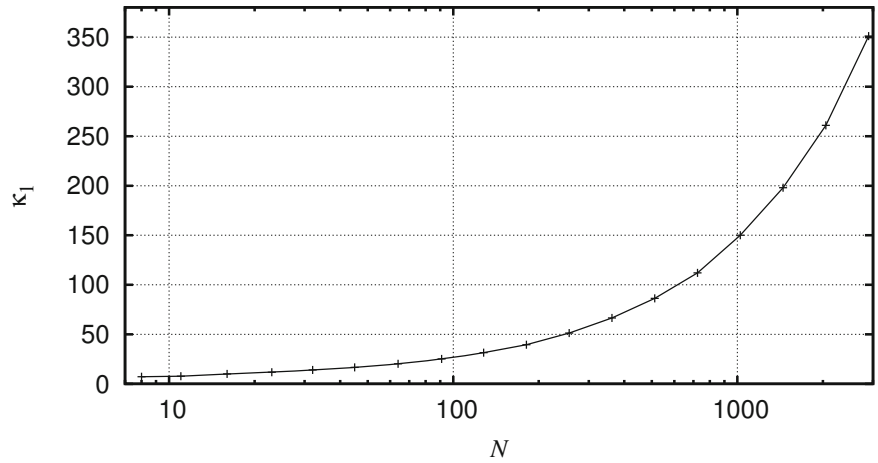


Figure 3.8: Threshold $\kappa_1$ in dependence on the Number of observations $N$.

Furthermore, the cluster-based approach described so far only separates the observations in two clusters. It does not care about the number of observations per cluster. An additional mechanism is required, which ensures that the cluster of outliers is not larger than the cluster of good observations. This can be achieved, for example, by analysing only distances $d[n]$ with $n > N/2$.

**Examples**

The entire procedure of outlier detection based on distances is explained in following examples.

**Example 1:**
The absolute deviates $\{\Lambda_i\}$ are given according to the plot in **Figure 3.9**. Inspection by eye suggests the presence of three clusters for the classification of the observations in good and bad ones.

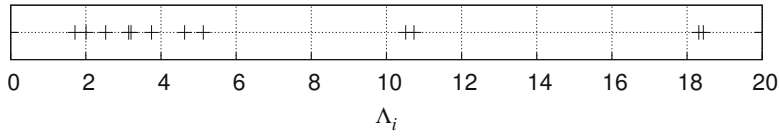


Figure 3.9: Distribution of deviates in Example 1.

Table 3.1: Intermediate values of cluster-based outlier detection, Example 1, see text for details.

| $n$ | $\Lambda_s[n]$ | $d[n]$ | $d_{glob}[n]$ | $q[n] = \frac{d[n]}{d_{glob}[n]}$ | $d_{loc}[n]$ | $r[n] = \frac{d[n]}{d_{loc}[n]}$ |
|---|---|---|---|---|---|---|
| 0 | 1.70 | 0.00 | 0.000 | 0.000 | 0.000 | 0.000 |
| 1 | 2.00 | 0.30 | 0.000 | 0.000 | 0.000 | 0.000 |
| 2 | 2.50 | 0.50 | 0.300 | 1.667 | 0.300 | 1.667 |
| 3 | 3.10 | 0.60 | 0.402 | 1.492 | 0.464 | 1.294 |
| 4 | 3.20 | 0.10 | 0.472 | 0.212 | 0.578 | 0.173 |
| 5 | 3.70 | 0.50 | 0.373 | 1.341 | 0.196 | 2.553 |
| 6 | 4.60 | 0.90 | 0.400 | 2.249 | 0.430 | 2.095 |
| 7 | 5.10 | 0.50 | 0.500 | 1.000 | 0.816 | 0.613 |
| 8 | 10.50 | 5.40 | 0.505 | 10.692 | 0.572 | 9.446 |
| 9 | 10.70 | 0.20 | 1.335 | 0.150 | 4.451 | 0.045 |
| 10 | 18.30 | 7.60 | 1.213 | 6.263 | 1.139 | 6.673 |
| 11 | 18.40 | 0.10 | 2.231 | 0.045 | 6.235 | 0.016 |
| | | | | $\kappa_1$: 8.180 | | $\kappa_2$: 2.000 |

The sorted deviates $\Lambda_s[n]$, distances $d[n]$, averaged distances $d_{glob}[n]$ and $d_{loc}[n]$, as well as the relations $q[n] = d[n]/d_{glob}[n]$ and $r[n] = d[n]/d_{loc}[n]$ for this example are listed in **Table 3.1**. The distances range from 0.10 to 7.60. Only one of them, $d[8]$, fulfils the global criterion $d[n]/d_{glob}[n] \geq \kappa_1$. Since the local criterion $d[8]/d_{loc}[8] \geq \kappa_2$ is also satisfied, a gap between two clusters has been found. In order to exclude all observations not belonging to the cluster of good points, the value of the deviate corresponding to the critical distance $d[8]$ is taken as threshold $\lambda_O$, i.e., all observations with deviates $\Lambda_i \geq \lambda_O = \Lambda_s[8] = 10.5$ are marked as outliers.

Please note that the relation $q[10] = 6.263$ is below the threshold $\kappa_1$, although the corresponding distance $d[10] = 7.6$ is higher than $d[8]$. This is caused by the effect of accommodation. As one large distance has already been seen for predecessors, the new occurrence of a similar distance is not anymore an indication of contaminant observations, but only of a sparse distribution. This is an important feature of the cluster-based method. It must also be pointed out that the local condition can also be fulfilled for small distances such as, for example, $d[5] = 0.5$ if the predecessors are even smaller by chance.
□□□

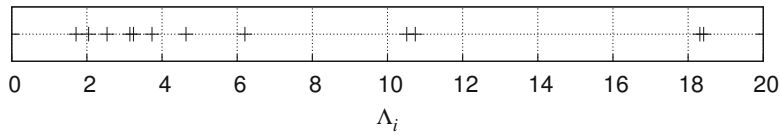


Figure 3.10: Distribution of deviates in Example 2.

Table 3.2: Intermediate values of cluster-based outlier detection, Example 2, see text for details.

| $n$ | $\Lambda_s[n]$ | $d[n]$ | $d_{glob}[n]$ | $q[n] = \frac{d[n]}{d_{glob}[n]}$ | $d_{loc}[n]$ | $r[n] = \frac{d[n]}{d_{loc}[n]}$ |
|---|---|---|---|---|---|---|
| 0 | 1.70 | 0.00 | 0.000 | 0.000 | 0.000 | 0.000 |
| 1 | 2.00 | 0.30 | 0.000 | 0.000 | 0.000 | 0.000 |
| 2 | 2.50 | 0.50 | 0.300 | 1.667 | 0.300 | 1.667 |
| 3 | 3.10 | 0.60 | 0.402 | 1.492 | 0.464 | 1.294 |
| 4 | 3.20 | 0.10 | 0.472 | 0.212 | 0.578 | 0.173 |
| 5 | 3.70 | 0.50 | 0.373 | 1.341 | 0.196 | 2.553 |
| 6 | 4.60 | 0.90 | 0.400 | 2.249 | 0.430 | 2.095 |
| 7 | 6.20 | 1.60 | 0.500 | 3.200 | 0.816 | 1.960 |
| 8 | 10.50 | 4.30 | 0.705 | 6.102 | 1.457 | 2.951 |
| 9 | 10.70 | 0.20 | 1.327 | 0.151 | 3.763 | 0.053 |
| 10 | 18.30 | 7.60 | 1.202 | 6.322 | 0.958 | 7.937 |
| 11 | 18.40 | 0.10 | 2.217 | 0.045 | 6.219 | 0.016 |
| | | | | $\kappa_1$: 8.180 | | $\kappa_2$: 2.000 |

**Example 2:**
As in any case of using thresholds, slight variation of values might cause different response of the system. Let us assume that one certain observation is somewhat more distant to the model function leading to a deviate of $\Lambda_s[7] = 6.2$ instead of 5.1 (see **Figure 3.10**). **Table 3.2** contains the resulting values. The related distance $d[8] = 4.3$ has been fallen below $\kappa_1 \cdot d_{glob} = 8.18 \cdot 0.705 = 5.7669$ which has increased itself owing to the modified value of $d_{glob}$. The local criterion $r[8] = 2.951$ still signals a distinct change in the sequence of distances, but the global distance is not fulfilled anymore. The algorithm judges the distance of 4.3 as not being significant in comparison to the other distances. Since the global criterion is never fulfilled, no outliers are identified. The gaps between $\Lambda_s[7]$ and $\Lambda_s[8]$ as well as $\Lambda_s[9]$ and $\Lambda_s[10]$ are still visible in Figure 3.10, but are interpreted as sparseness of the distribution and not as indication for outliers.
□□□

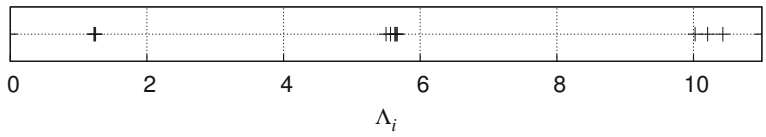


Figure 3.11: Distribution of deviates in Example 3.

Table 3.3: Intermediate values of cluster-based outlier detection, Example 3, see text for details.

| $n$ | $\Lambda_s[n]$ | $d[n]$ | $d_{\text{glob}}[n]$ | $q[n] = \frac{d[n]}{d_{\text{glob}}[n]}$ | $d_{\text{loc}}[n]$ | $r[n] = \frac{d[n]}{d_{\text{loc}}[n]}$ |
|---|---|---|---|---|---|---|
| 0 | 1.20 | 0.00 | 0.000 | 0.000 | 0.000 | 0.000 |
| 1 | 1.21 | 0.01 | 0.000 | 0.000 | 0.000 | 0.000 |
| 2 | 1.22 | 0.01 | 0.010 | 1.000 | 0.010 | 1.000 |
| 3 | 5.50 | 4.28 | 0.010 | 428.000 | 0.010 | 428.000 |
| 4 | 5.52 | 0.02 | 1.506 | 0.013 | 3.450 | 0.006 |
| 5 | 5.60 | 0.08 | 1.130 | 0.071 | 0.785 | 0.102 |
| 6 | 5.61 | 0.01 | 0.900 | 0.011 | 0.131 | 0.076 |
| 7 | 5.61 | 0.00 | 0.719 | 0.000 | 0.025 | 0.000 |
| 8 | 5.62 | 0.01 | 0.576 | 0.017 | 0.003 | 3.326 |
| 9 | 10.00 | 4.38 | 0.462 | 9.477 | 0.008 | 531.891 |
| 10 | 10.20 | 0.20 | 1.066 | 0.188 | 3.528 | 0.057 |
| 11 | 10.40 | 0.20 | 0.963 | 0.208 | 0.948 | 0.211 |
| | | | | $\kappa_1$: 8.180 | | $\kappa_2$: 2.000 |

**Example 3:**
This example reveals that the cluster-based outlier detection does not depend on the normal distribution of deviates (**Figure 3.11**). The majority of absolute residuals is in the range of $5 \ldots 6$, plus some distinctively smaller and higher deviates. The evaluation of the deviates results in the values listed in **Table 3.3**. There are two distances with $q[n] > \kappa_1$, $q[3] = 428.0$ and $q[9] = 9.477$.However, $d[9] = 4.38$ has the highest quotient of $r[9] = 531.891$ greater than $\kappa_2 = 2.0$. Therefore, all observations with deviates of $\Lambda_i \geq \Lambda_s[9] = 10.0$ are declared as contaminants.
□□□

Now let us consider an example in which many deviates are identical to another in pairs owing to integer-valued observations.

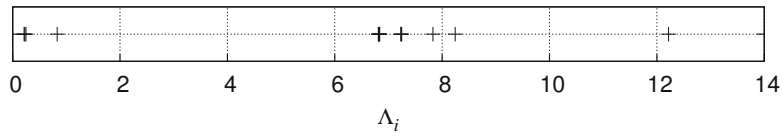


Figure 3.12: Distribution of deviates in Example 4.

Table 3.4: Intermediate values of cluster-based outlier detection, Example 4, see text for details.

| $n$ | $\Lambda_s[n]$ | $d[n]$ | $d_{glob}[n]$ | $q[n] = \frac{d[n]}{d_{glob}[n]}$ | $d_{loc}[n]$ | $r[n] = \frac{d[n]}{d_{loc}[n]}$ |
|---|---|---|---|---|---|---|
| 0 | 0.20 | 0.00 | 0.000 | 0.000 | 0.000 | 0.000 |
| 1 | 0.20 | 0.00 | 0.000 | 0.000 | 0.000 | 0.000 |
| 2 | 0.20 | 0.00 | 0.000 | 0.000 | 0.000 | 0.000 |
| 3 | 0.80 | 0.60 | 0.000 | 0.000 | 0.000 | 2.000 |
| 4 | 6.80 | 6.00 | 0.207 | 29.050 | 0.411 | 2.000 |
| 5 | 6.80 | 0.00 | 1.742 | 0.000 | 4.242 | 0.000 |
| 6 | 6.80 | 0.00 | 1.395 | 0.000 | 1.596 | 0.000 |
| 7 | 6.80 | 0.00 | 1.149 | 0.000 | 0.319 | 0.000 |
| 8 | 6.80 | 0.00 | 0.960 | 0.000 | 0.034 | 0.000 |
| 9 | 7.20 | 0.40 | 0.808 | 0.495 | 0.002 | 2.000 |
| 10 | 7.20 | 0.00 | 0.737 | 0.000 | 0.272 | 0.000 |
| 11 | 7.20 | 0.00 | 0.624 | 0.000 | 0.104 | 0.000 |
| 12 | 7.80 | 0.60 | 0.525 | 1.142 | 0.021 | 2.000 |
| 13 | 8.20 | 0.40 | 0.513 | 0.779 | 0.411 | 2.000 |
| 14 | 12.20 | 4.00 | 0.482 | 8.295 | 0.429 | 2.000 |
| | | | | $\kappa_1$: 9.620 | | $\kappa_2$: 2.000 |

**Example 4:**
**Figure 3.12** shows the absolute deviates $\{\Lambda_i\}$ used in this example. **Table 3.4** contains the intermediate values for this example. Many distances are equal to zero, because of the identical deviates. Distance $d[4] = 6.0$ exceeds the first threshold of $\kappa_1 \cdot d_{glob}[4] = 9.62 \cdot 0.207 = 1.991$ and the local criterion is satisfied as well. Since there is no other point fulfilling both criteria, the threshold $\lambda_O$ is set to $\Lambda_s[4] = 6.8$.

The result underlines the fact that the clustering of deviates works perfectly. In its application to data analysis, however, it does not seem to be appropriate to reject more that 50% of the observations. An

additional mechanism is therefore needed. The threshold $\lambda_O$ should only be set when the cluster of good observations contains at least a predefined percentage of the total number of observations. This could be achieved, for example, by only comparing the top 35% or less of the deviates with the thresholds $\kappa_1$ and $\kappa_2$. On the other hand, however, such a small cluster of 'good' observations could indicate an improperly chosen model $y = f(\mathbf{x}|\mathbf{a})$.
□□□

The described method of cluster-based outlier detection is not only applicable to deviates in the framework of least-squares approximation, but also suitable in other scenarios. The mapping of the observations $y_i$ to absolute values $\Lambda_i$ using an application-specific technique is the crucial point. The only constraint is that small values of $\Lambda_i$ must correspond to good data points and large values to suspicious observations.

The advantages of the cluster-based method for outlier detection have been proved in [Str09b] based on Monte Carlo simulations. The corresponding results are presented in the appendix, Chapter A.

## 3.5 Application of weighted data fitting and outlier detection

This section compares the least-squares fitting in dependence of the used weighting and outlier-detection scheme for a variety of test data with different model functions. The results are discussed afterwards.

The general processing pipeline is depicted in **Figure 3.13**. Each of the three blocks can be switched off independently on the other. Usage of the reset block makes sense only if both other blocks, weights estimation and outlier removal, are enabled. When using the last processing block, the weights are only exploited for a more reliable outlier detection. The final fitting is performed using equal weights. If all processing steps are bypassed, ordinary least-squares approximation is applied. Most examples, which are discussed in the following, use weights

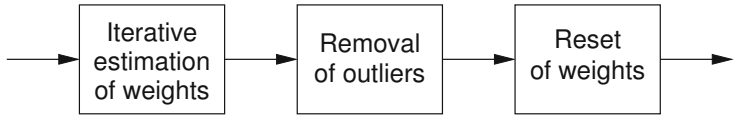


Figure 3.13: Flowchart of weighting and outlier detection

estimation based on deviates, as has been discussed in Subsection 3.3.2. Only the last example allows for the weighting via binning (Subsection 3.3.1). The detection and removal of outliers is performed either with standardised residuals (z-score) or cluster-based (ClubOD) (see Subsection 3.4). The threshold for the z-score method is adaptively chosen according to Chauvenet's criterion (see Section 7.2) with $\nu_0 = 0.15$, i.e. with the assumption of 0.15 outliers per data set on average.

### 3.5.1 Constant value

A set of forty simulated observations $y_i$ (normally distributed with $\overline{y_i} = 10.0, \sigma_\mathrm{y} = 1.340$, see Section 6.1) has been generated and extended by three outliers. It has to be fitted to the model function

$$y = f(\mathbf{x}|\mathbf{a}) = \text{const.} = a_1 \ .$$

The solution for linear model functions (see Section 2.4)

$$\mathbf{a} = \left(\mathbf{J}^\mathrm{T} \cdot \mathbf{W} \cdot \mathbf{J}\right)^{-1} \cdot \mathbf{J}^\mathrm{T} \cdot \mathbf{W} \cdot \mathbf{y}$$

simplifies to

$$a_1 = \frac{\sum\limits_{i=1}^{N} w_i \cdot y_i}{\sum\limits_{i=1}^{N} w_i} \ ,$$

as was already shown in Subsection 2.6.1. The usage of $w_i = 1.0$ for all $i$ (i.e. equal weights) yields a mean value of 9.791 (**Table 3.5**). Without estimation of suitable weights, the z-score method declares two observations as being contaminant and the estimated parameter changes to $a_1 = 9.829$. ClubOD removes three contaminants, leading to the correct value of $a_1 = 10.000$. Applying the iterated weights refinement, the result improves to $a_1 = 9.961$. ClubOD still identifies the same three outliers, while the other method now finds 5 outliers.

The error bars in the plot of **Figure 3.14** depict the uncertainties in terms of estimated weights. Outliers have an infinite uncertainty, thus, the error bars of the outlier $(x_i, y_i) = (41, 3)$, $(42, 1)$ and $(43, 17)$ cross the entire plot. The z-score approach detects two more outliers at $(x_i, y_i) = 11, 13)$ and $(23, 13)$.

The plots of deviates reveals the three distinct mavericks (**Figure 3.15**).

In this artificial example, the cluster-based method results in a solution, which is closest (identical) to the true model parameter (number is boldfaced), regardless of the application of unequal weighting.

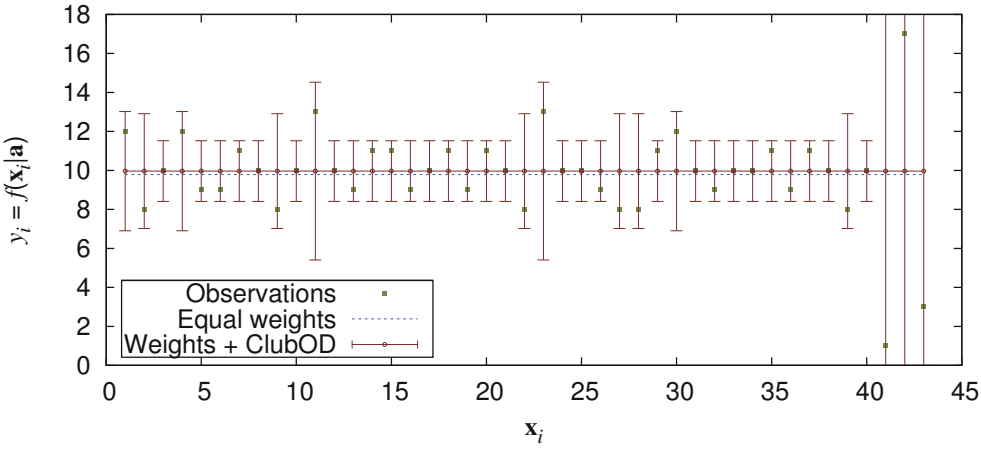


Figure 3.14: Results of fitting a constant with and without weighting of observations

Table 3.5: Results for fitting a constant

| **Constant** | $a_1$ | Detected outliers |
|---|---|---|
| True values | 10.000 | 3 |
| Equal weights | 9.791 | 0 |
| z-score | 9.829 | 2 |
| ClubOD | **10.000** | 3 |
| Estimated weights | 9.961 | 0 |
| Weights + z-score | 9.942 | 5 |
| + weights reset | 9.842 | 5 |
| Weights + ClubOD | 9.965 | 3 |
| + weights reset | **10.000** | 3 |

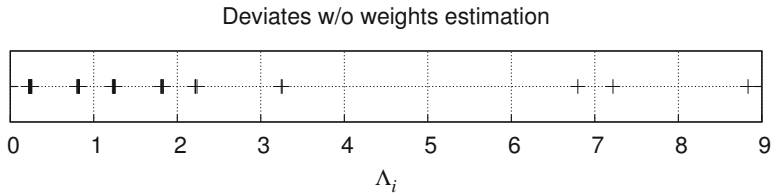


Figure 3.15: Deviates according to the example of fitting a constant without weights

Table 3.6: Datasets used for straight-line fitting

| $i$ | $x_i$ | $y$ | $y_i^{(0)}$ | $y_i^{(1)}$ | $y_i^{(2)}$ | $y_i^{(3)}$ |
|---|---|---|---|---|---|---|
| 1 | 0.1 | 2.1 | 1.704 | 1.704 | 2.113 | 2.113 |
| 2 | 0.2 | 2.2 | 2.321 | 3.000 | 2.216 | 4.000 |
| 3 | 0.3 | 2.3 | 2.208 | 2.208 | 2.345 | 2.345 |
| 4 | 0.4 | 2.4 | 2.442 | 2.442 | 2.466 | 2.466 |
| 5 | 0.5 | 2.5 | 2.577 | 2.577 | 2.581 | 4.000 |
| 6 | 0.6 | 2.6 | 2.770 | 2.770 | 2.418 | 2.418 |
| 7 | 0.7 | 2.7 | 2.493 | 2.493 | 3.076 | 3.076 |
| 8 | 0.8 | 2.8 | 2.569 | 2.569 | 2.862 | 2.862 |
| 9 | 0.9 | 2.9 | 2.888 | 4.000 | 2.342 | 2.342 |
| 10 | 1.0 | 3.0 | 3.215 | 3.215 | 1.343 | 1.343 |

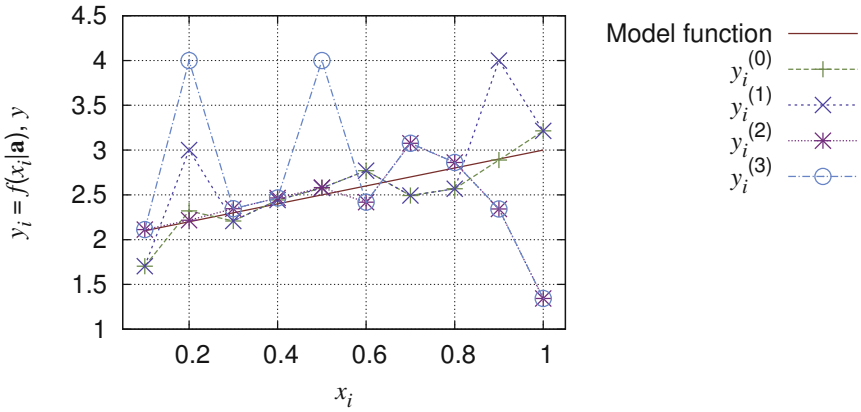


Figure 3.16: Test data for fitting of straight lines

### 3.5.2 Straight line

The performance of weighted least squares applied to the fitting of straight lines shall be demonstrated using four small data sets listed in **Table 3.6**. The corresponding plots are shown in **Figure 3.16**.

The process generating the (error-free) output is

$$y = 2.0 + 1.0 \cdot x \ .$$

The first data set $y_i^{(0)}$ is a randomised version of $y$ with normally distributed errors using a constant deviation of $\sigma_i = \sigma = 0.25$. In $y_i^{(1)}$ two additional outliers

Table 3.7: Results of straight-line fitting, function $y^{(0)}$

| $y^{(0)}$ | $a_1$ | $a_2$ | Detected outliers |
|---|---|---|---|
| True values | 2.000 | 1.00 | 0 |
| Equal weights | 1.861 | 1.195 | 0 |
| z-score | 1.861 | 1.195 | 0 |
| ClubOD | 1.861 | 1.195 | 0 |
| Estimated weights | **2.000** | 1.111 | 0 |
| Weights + z-score | 2.016 | 1.101 | 2 |
| + weights reset | 2.005 | **1.059** | 2 |
| Weights + ClubOD | 2.016 | 1.112 | 3 |
| + weights reset | 2.004 | 1.126 | 3 |

are introduced artificially at $i = 2$ and $i = 9$. For sets $y_i^{(2)}$ and $y_i^{(3)}$ the deviation starts with $\sigma_1 = 0.01$ and then doubles with increasing $i$ up to $\sigma_{10} = 5.12$. $y_i^{(3)}$ is falsified in addition by two outliers at $i = 2$ and $i = 5$.

The result of fitting these four data sets to a straight line is shown in **Figure 3.17**. The error bars indicate the estimated uncertainty of the observation (based on the estimated weight). If the error bar crosses the entire plot, then this measurement is either assigned a very low weight or it is even regarded as an outlier.

In the presence of strong outliers, the fitted curves with application of weights are distinctly closer to the model function than those without using weights.

The estimated parameters are listed in **Tables 3.7**–**3.10**. For the case of $y^{(0)}$, **Figure 3.18** shows the distribution of the deviates before outlier detection with and without the estimation of weights. The plots of deviates do not indicate any presence of outliers when equal weights are used. After weights estimation, however, three observations seem to be more distant to the model function than the other explaining the results of outlier detection. Consequently, ClubOD falsely detects three outliers (Table 3.7). Also the z-score method is adversely affected. Nevertheless, removing the three suspicious data points and re-running of ordinary least squares leads to results close to optimum. This first example underlines the usefulness of weights estimation. The estimated parameters are much closer to the true ones when using weighting.

The results for $y^{(1)}$ are listed in **Table 3.8**. Only when proper weights are estimated, both detectors are able to find the two outliers. Despite the removal of the contaminants, the estimated model parameters are not very close to the true values. This is caused by the missing influence of the correct observations

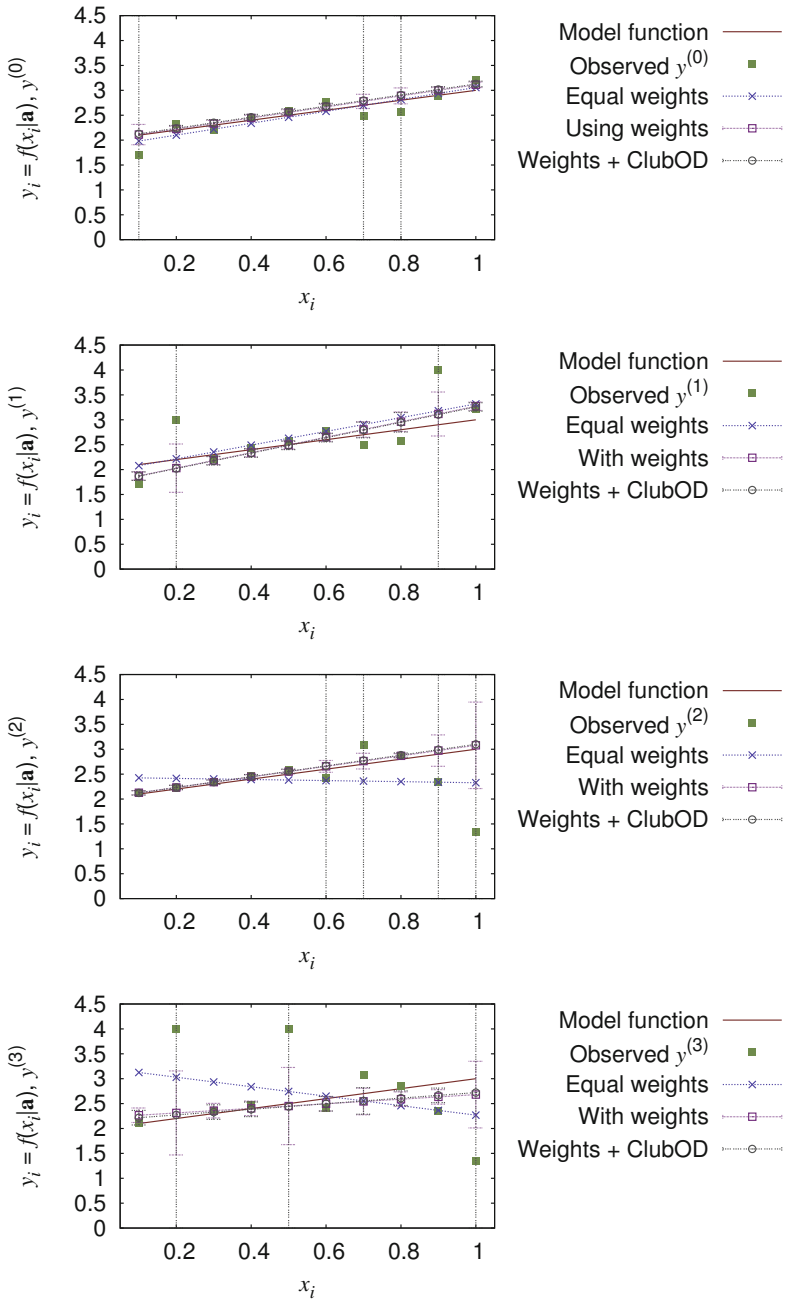


Figure 3.17: Results of fitting a straight line with and without weighting of observations and outlier detection

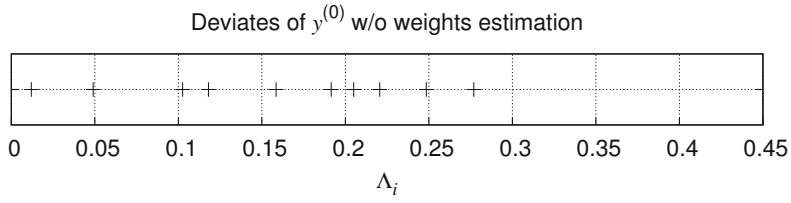


a)

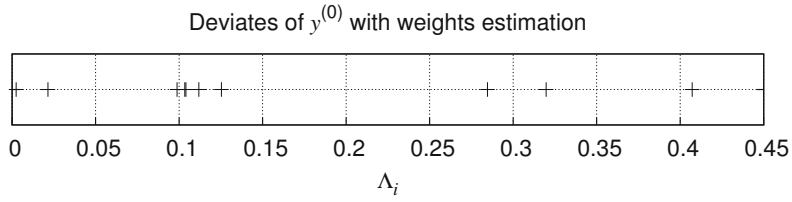


b)

Figure 3.18: Deviates according to the example of fitting a straight line $y^{(0)}$; a) without application of weights estimation, b) using the estimation of weights

Table 3.8: Results of straight-line fitting, function $y^{(1)}$

| $y^{(1)}$ | $a_1$ | $a_2$ | Detected outliers |
|---|---|---|---|
| True values | 2.000 | 1.00 | 2 |
| Equal weights | **1.939** | 1.379 | 0 |
| z-score | 1.939 | 1.379 | 0 |
| ClubOD | 1.939 | 1.379 | 0 |
| Estimated weights | 1.718 | 1.554 | 0 |
| Weights + z-score | 1.712 | 1.546 | 2 |
| Weights + ClubOD | 1.712 | 1.546 | 2 |
| + weights reset | 1.750 | **1.358** | 2 |

at these conditions $x_i$. The plots of deviates in **Figure 3.19** show that the two contaminants become more distant to the bulk of good observations after the estimation of weights, enabling their detection and removal.

**Table 3.9** shows the results for $y^{(2)}$. Four of the 'good' observations deviate much more from the model function than others after the application of proper weights misguiding both outlier detectors (**Figure 3.20**). Fitting the remaining six observations still leads to acceptable model parameters.

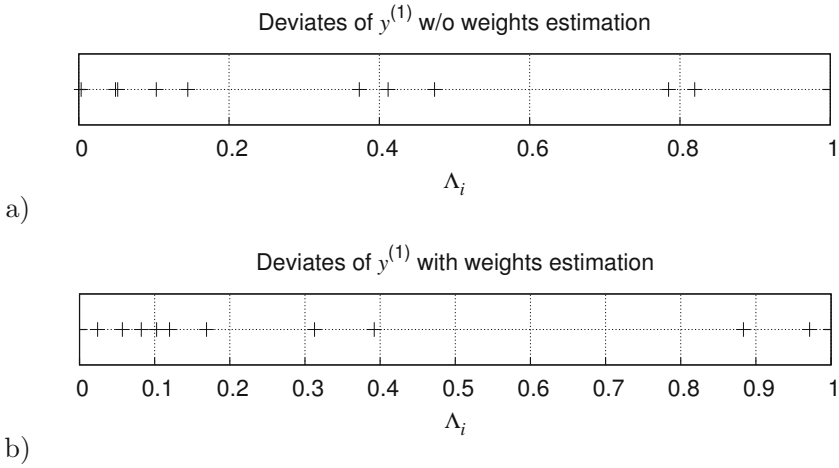


Figure 3.19: Deviates according to the example of fitting a straight line $y^{(1)}$; a) without application of weights estimation, b) using the estimation of weights

Table 3.9: Results of straight-line fitting, function $y^{(2)}$

| $y^{(2)}$ | $a_1$ | $a_2$ | Detected outliers |
|---|---|---|---|
| True values | 2.000 | 1.00 | 0 |
| Equal weights | 2.436 | −0.109 | 0 |
| z-score | 2.436 | −0.109 | 0 |
| ClubOD | 2.436 | −0.109 | 0 |
| Estimated weights | 2.021 | **1.058** | 0 |
| Weights + z-score | **2.015** | 1.084 | 4 |
| Weights + ClubOD | 2.015 | 1.084 | 4 |
| + weights reset | 2.015 | 1.084 | 4 |

The example of $y^{(3)}$ distinctly shows that the application of weights estimation can dramatically improve the data fitting (**Table 3.10**). Using equal weights results to completely wrong model parameters. As in the example of $y^{(1)}$, only weights estimation enables the proper detection of the outliers, as can be derived again from the plots of deviates (**Figure 3.21**). The best fitting is obtained in this case when we forget the weights after the removal of the contaminants.

The performance of the two outlier-detection schemes is almost the same in these examples of straight-line fitting, however, with a slight advantage of the z-score

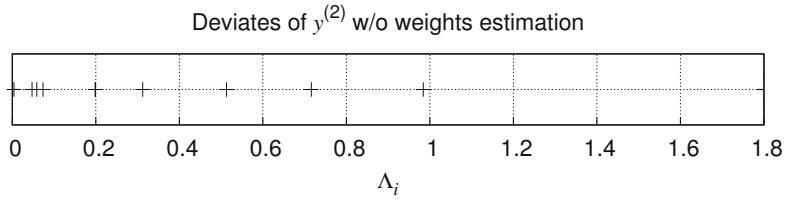


a)

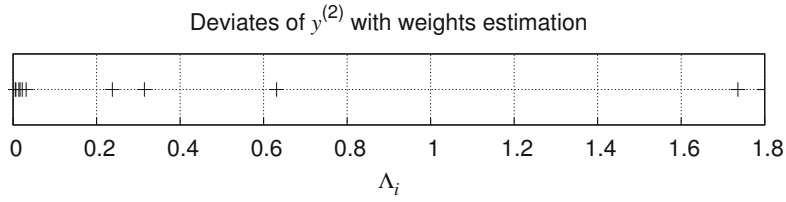


b)

Figure 3.20: Deviates according to the example of fitting a straight line $y^{(2)}$; a) without application of weights estimation, b) using the estimation of weights

Table 3.10: Results of straight-line fitting, function $y^{(3)}$

| $y^{(3)}$ | $a_1$ | $a_2$ | Detected outliers |
|---|---|---|---|
| True values | 2.000 | 1.00 | 2 |
| Equal weights | 3.220 | −0.952 | 0 |
| z-score | 3.220 | −0.952 | 0 |
| ClubOD | 3.220 | −0.952 | 0 |
| Estimated weights | 2.220 | 0.460 | 0 |
| Weights + z-score | 2.161 | 0.561 | 3 |
| Weights + ClubOD | 2.161 | 0.561 | 3 |
| + weights reset | **2.150** | **0.677** | 3 |

approach in case $y_i^{(0)}$, where it classifies only two observations falsely as outliers, while ClubOD detects three.

### 3.5.3 Plane approximation

The test data for the fitting of a plane have been generated by

$$y_i = a_1 + a_2 \cdot x_{1,i} + a_3 \cdot x_{2,i} + \varepsilon_i = 0.1 + 0.2 \cdot x_{1,i} + 0.4 \cdot x_{2,i} + \varepsilon_i$$

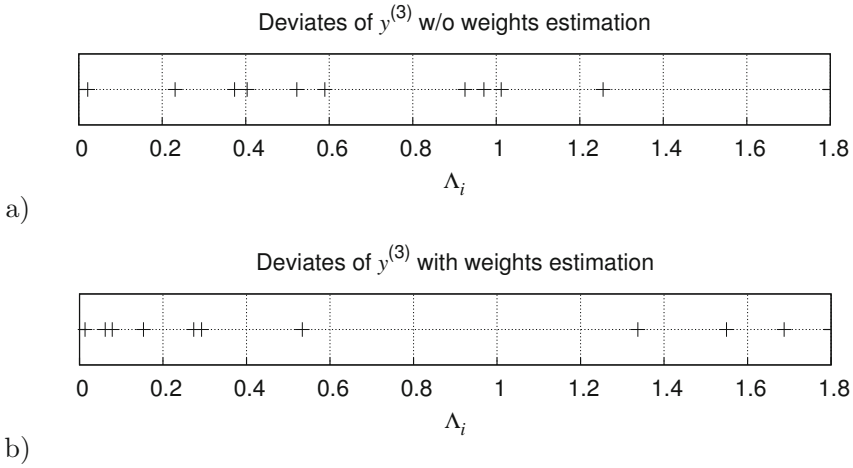


Figure 3.21: Deviates according to the example of fitting a straight line $y^{(3)}$; a) without application of weights estimation, b) using the estimation of weights

Table 3.11: Results of plane fitting

| **Plane** | $a_1$ | $a_2$ | $a_3$ | Detected outliers |
|---|---|---|---|---|
| True values | 0.1 | 0.2 | 0.4 | 9 |
| Equal weights | 0.954 | 0.142 | 0.334 | 0 |
| z-score | 0.882 | 0.147 | 0.339 | 1 |
| ClubOD | 0.954 | 0.142 | 0.334 | 0 |
| Estimated weights | 0.206 | 0.209 | 0.384 | 0 |
| Weights + z-score | 0.180 | 0.212 | 0.385 | 12 |
| Weights + ClubOD | 0.181 | 0.211 | 0.386 | 9 |
| + weights reset | **0.096** | **0.206** | **0.399** | 9 |

with a randomisation of the observation using $\sigma_{\varepsilon_i} = \sigma_\varepsilon = 0.5$. In addition, an offset of 1.5 (systematic error) was introduced for the points $(x_1; x_2) = \{(1;1) \ldots (3;3)\}$, that is, the data set contains nine outliers.

The estimated model parameters and the number of detected outliers are dependent on the schemes used for the weights estimation (**Table 3.11**). Without using weights, the outliers cannot be sufficiently detected. Only in case of weights estimation, ClubOD is able to find the nine outliers. This can be understood by examining the plots of deviates in **Figure 3.22**. The z-score method, however,

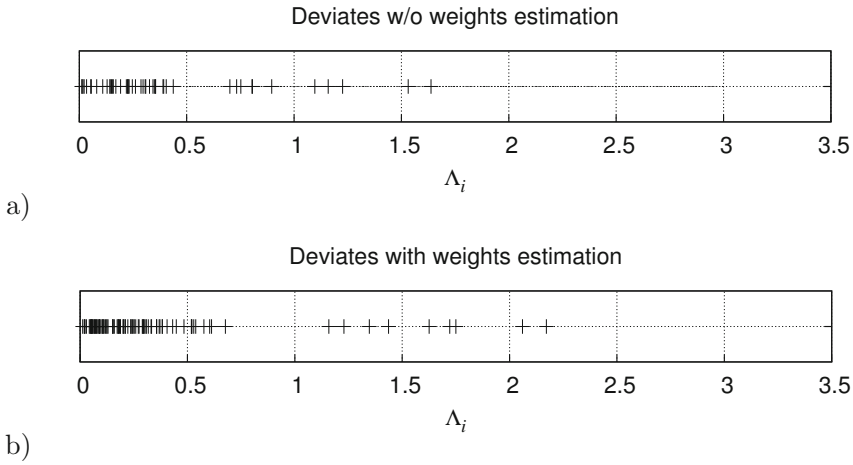


Figure 3.22: Deviates according to the example of fitting a plane; a) without application of weights estimation, b) using the estimation of weights

declares 12 data points as being contaminant.

The removal of the nine outliers in combination with resetting all weights to equal values yields the best approximation in this example.

In **Figure 3.23**a), it can be seen that the fitted plane (blue) is attracted by the contaminants (1;1) ... (3;3) causing high deviates in the opposite region when no weighting is used. **Figure 3.23**b) shows the improvement after application of weights estimation, outlier detection via ClubOD, and forgetting the weights afterwards.

### 3.5.4 Coordinates transformation

The transformation of coordinates is an example with two or more observed values per measurement (see also Subsection 1.4.4 'Affine transformation'). When dealing with images, there are two observations $(x\ y)^{\mathrm{T}}$ corresponding to two conditions $(u\ v)^{\mathrm{T}}$. The latter are coordinates in an image indicating special regions and are also called *landmarks* (see **Figure 3.24**). The task in the experiment was to find counterparts of these landmarks in a second image. The question addressed in this application is: What are the translational displacement and the angle of rotation between both images? The corresponding model function for the least-squares setup is

$$\begin{pmatrix} x \\ y \end{pmatrix} = \begin{pmatrix} a_1 \\ a_2 \end{pmatrix} + \begin{pmatrix} \cos(a_3) & -\sin(a_3) \\ \sin(a_3) & \cos(a_3) \end{pmatrix} \cdot \begin{pmatrix} u \\ v \end{pmatrix}$$

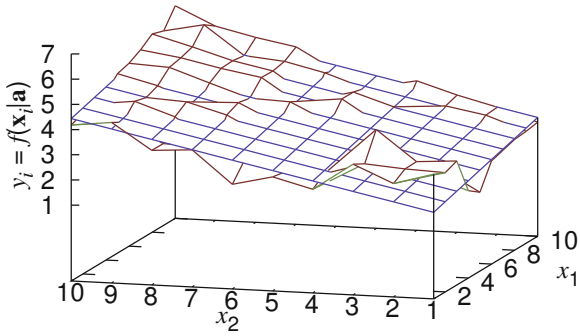


a)

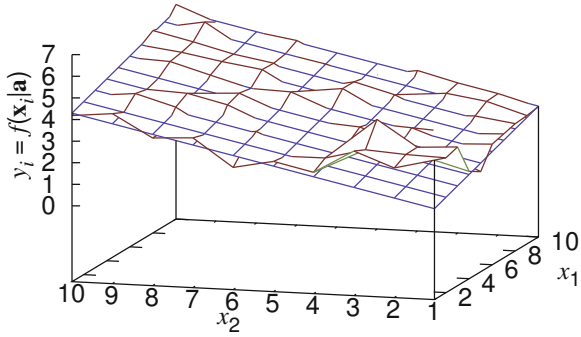


b)

Figure 3.23: Results of fitting a plane; a) without weighting; b) after removal of all nine outliers)

or

$$\begin{aligned} f_{\mathrm{x}}(\mathbf{u}|\mathbf{a}) = \quad x \quad &= a_1 + \cos(a_3) \cdot u - \sin(a_3) \cdot v \\ f_{\mathrm{y}}(\mathbf{u}|\mathbf{a}) = \quad y \quad &= a_2 + \sin(a_3) \cdot u + \cos(a_3) \cdot v \ . \end{aligned}$$

Since both equations are not independent on each other, but coupled via trigonometric functions of $a_3$, the fitting problem is nonlinear. The inspection of the landmark pattern in Figure 3.24 by eye reveals that there are obviously some mismatches, i.e. false correspondences between image regions. Indeed, nine of the 121 matched points seem to be outliers, since they show deviations of more than two image-grid points from the modelled positions in both, $x$ and $y$ direction. **Table 3.12** shows the fitting results in dependence of the chosen weighting scheme.

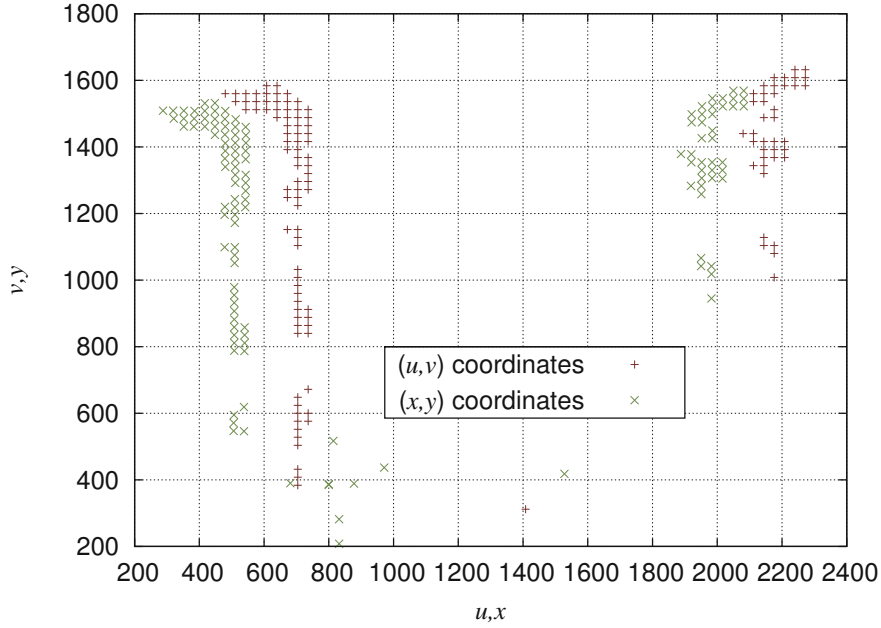


Figure 3.24: Example of two corresponding sets of coordinates with distinct outliers in the vicinity of $(x, y) = (800; 400)$; the + sign indicates coordinates in the first image (conditions), the × sign coordinates of matched regions in the second image (observations).

Table 3.12: Results of fitting coordinates

| **Coord.transf.** | $a_1$ | $a_2$ | $a_3$ | Detected outliers |
|---|---|---|---|---|
| True values | ? | ? | ? | 18 |
| Equal weights | −132.29 | −92.08 | 1.668° | 0 |
| z-score | −195.64 | −52.64 | −0.167° | 9 |
| ClubOD | −202.18 | −47.07 | −0.396° | 16 |
| Estimated weights | −201.58 | −47.57 | −0.376° | 0 |
| Weights + z-score | −201.87 | −47.62 | −0.382° | 17 |
| Weights + ClubOD | −201.87 | −47.62 | −0.382° | 17 |
| + weights reset | −201.87 | −47.62 | −0.382° | 17 |

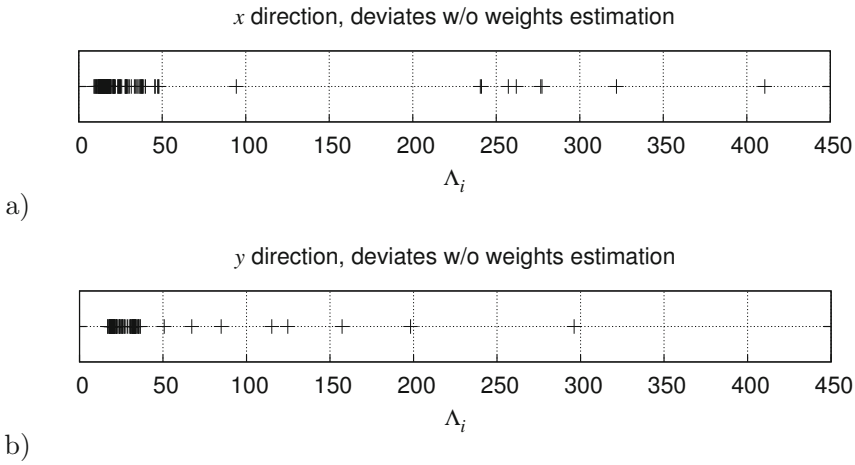


Figure 3.25: Deviates according to the fitting of coordinates without weighting; a) $x$ coordinates; b) $y$ coordinates

The number of outliers given in the table are counted separately for the $x$ and $y$ coordinates as a consequence of their independent weighting (see Subsection 2.6.7). Even though the true parameters are not known in this example, it is evident that without any weighting or outlier detection the found displacement and the rotation angle are wrong.

Based on the distribution of deviates (**Figure 3.25**), ClubOD is able to identify 16 out of 18 outliers leading to model parameters which are close to the correct ones with high probability. The z-score method finds only nine of them.

After applying the weighted least-squares procedure, the majority of all observations is very close to the model function in both coordinates (**Figure 3.26**). Only few observations (nine to be exact) deviate much stronger as can be seen in the deviates plots. The both methods are now able to detect 17 outliers. One out of the 9 mismatches deviate only in one coordinate, while the other is rather close to the correct value. That is why the 18th outlier could not be detected. This underlines that it would be beneficial to treat the (multiple) coordinates of data points in a joint manner.

The very high accuracy of the good observation leads to the fact that they all are assigned to identical weights. Only the contaminant observations are down-weighted according to their deviates. That is why the equalisation of weights after the removal of outliers does not change the parameter values anymore (**Table 3.12**).

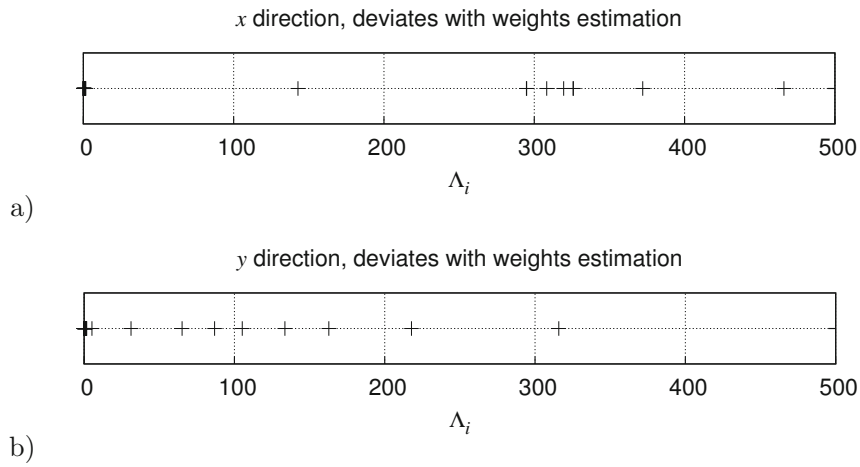


Figure 3.26: Deviates according to the fitting of coordinates with weighting; a) $x$ coordinates; b) $y$ coordinates

**Figure 3.27** depicts the result of the transformation of the $(u, v)$ coordinates using the estimated translation and rotation parameters (pure outlier removal).

### 3.5.5 Linear prediction

In Subsection 1.4.4, the prediction of pixel values for application in image compression was introduced. The observations are identical to the pixel values themselves and it is assumed that there are no outliers. In addition, all observations are typically stemming from the same image-taking process, implicating that all values have the same uncertainty. Nevertheless, the quality of prediction can be improved when weights are incorporated. The main problem lies in the assumption that the image characteristics do not change within the window region depicted in Figure 1.7. In natural pictures, i.e. photographs, the signal properties are rather similar for neighbouring pixels, but become more and more different with higher distances. The process of model-parameter determination should take this behaviour into account. Observations close to the current position should get high weights, while the weights should decrease with increasing distance. A typical relation is $w_i = d_i^{0.8}$, if $d_i$ is the Euclidean distance between the position of an observation $y_i = x[n-j, m-k]$ and the position of the value $x[n, m]$ to be predicted [Mey01].

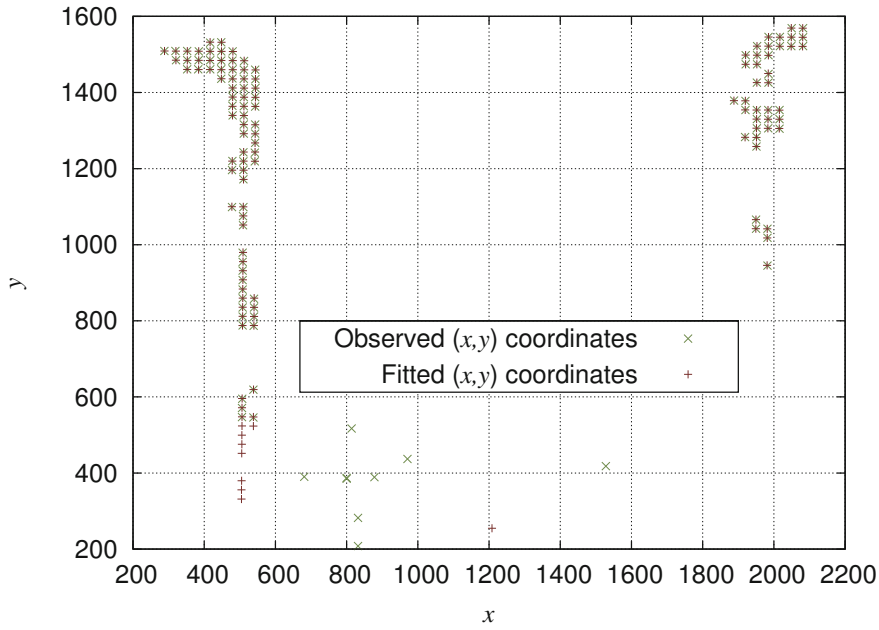


Figure 3.27: Result of the coordinates transform based on pure outlier removal

### 3.5.6 Cosine function

The model function

$$y = a_1 + a_2 \cdot \cos(x) + a_3 \cdot \sin(x)$$
$$\text{(based on } y = b_1 + b_2 \cdot \cos(x - b_3), \text{ see Section 1.3)} \tag{3.27}$$

describes a harmonic oscillation process with an oscillation frequency of $f_0 = 1/(2 \cdot \pi)$.

**Example (1)**

**Figure 3.28** shows the plot of observations generated by computational object-detection algorithms in comparison with the true object positions. The object was performing a circular movement in the $x$-$z$ plane and has been projected to a screen that was parallel to the $x$-$y$-plane such that the movement is mapped to a straight line on the screen. For each rotational position, three observations have been made by different detection algorithms. At zero and 320 degrees only two observations could be recorded. Please note that $x$, $y$, and $z$ are related to

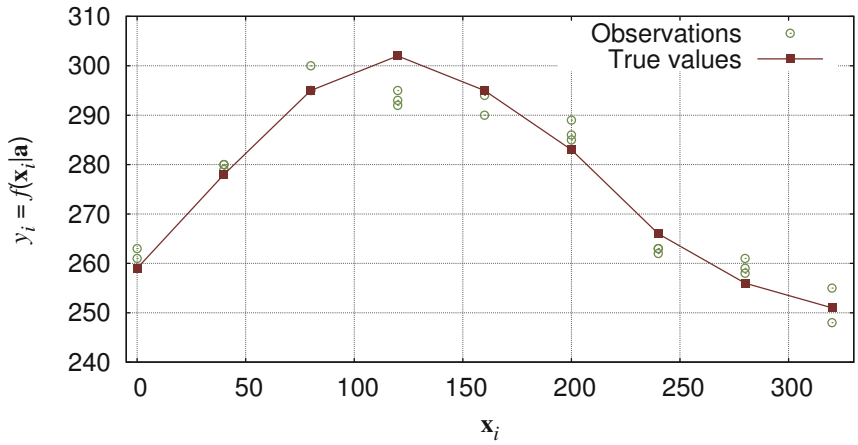


Figure 3.28: Recordings of a circular object movement. The observations $y_i$ are dependent on the rotation angle $x_i$ (in degrees)

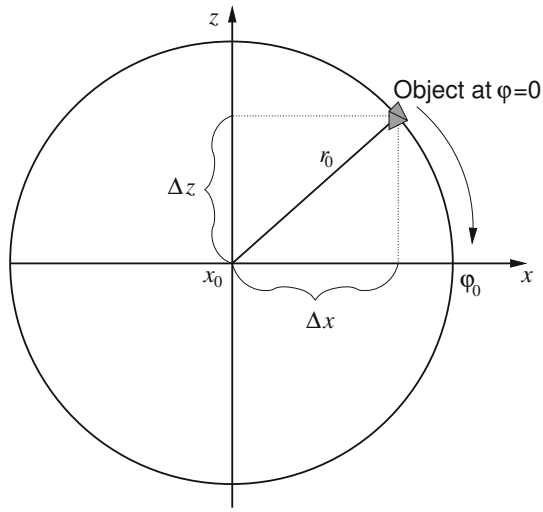


Figure 3.29: Circular movement of an object around the rotation axis ($y$ axis) perpendicular to the $x$ and $z$ axes

the coordinate system according to **Figure 3.29** and must not be mixed with the observations $y_i = f(x_i|\mathbf{a})$ and conditions $x_i$.

The fitting result is almost independent on the use of weights as can be seen in **Figure 3.30**. Since the deviates are relatively homogeneous distributed (**Figure**

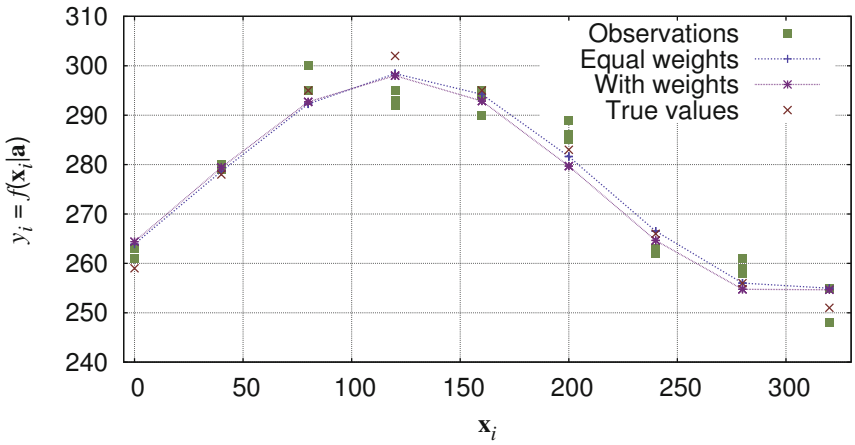


Figure 3.30: Fitting of the circular movement with and without weighting of observations

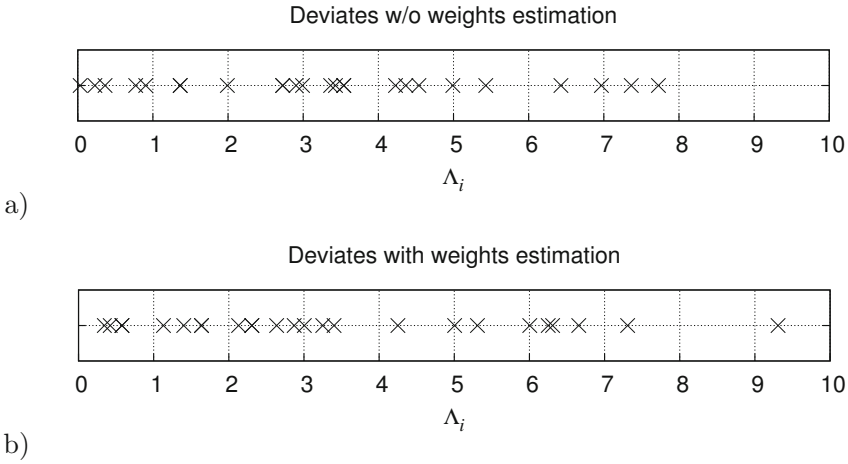


Figure 3.31: Deviates according to the fitting of a cosine; a) without application of weights estimation, b) using the estimation of weights

**3.31**), none of the observations was labelled as outlier. Naturally, fitting with equal weights leads to the best estimated model parameters (**Table 3.13**).

**Figure 3.32** shows the object to be detected at the positions 40 degrees and 200 degrees. The images have been taken at an experimental X-ray station at the European Molecular Biology Laboratory (EMBL) in Hamburg. The object-detection algorithms have been looking for the small polygon-like object in the middle of

Table 3.13: Results of fitting circular movement (example 1)

| **Cosine 1** | $b_1$ | $b_2$ | $b_3$ | Detected outliers |
|---|---|---|---|---|
| True values | 276.1 | 25.15 | 126.4° | 0 |
| Equal weights | **276.3** | 22.19 | **123.9**° | 0 |
| z-score | 276.3 | 22.19 | 123.9° | 0 |
| ClubOD | 276.3 | 22.19 | 123.9° | 0 |
| Estimated weights | 275.7 | **22.32** | 120.3° | 0 |
| Weights + z-score | 275.7 | 22.32 | 120.3° | 0 |
| Weights + ClubOD | 275.7 | 22.32 | 120.3° | 0 |

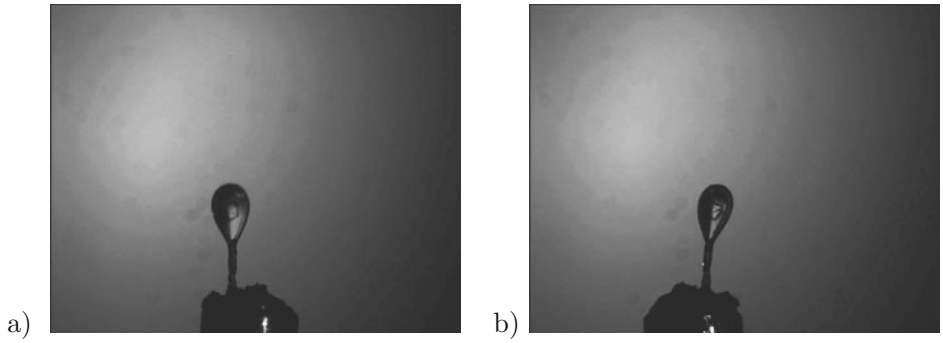

Figure 3.32: Small protein crystal mounted in a rotating nylon loop recorded at a) 40 degrees and b) 200 degrees of rotation. The rotation axis is vertical and the horizontal movement of the crystal is observed.

the loop. This object is a protein crystal with a diameter of approximately 100 microns. It is fixed in the loop by the surface tension of the surrounding liquid. The movement of the crystal must be determined in order to centre the crystal in the X-ray beam. The beam is diffracted by the crystal lattice and the resulting diffraction pattern allows conclusion about the internal structure of the crystal and the protein molecule.

**Example (2)**

**Figure 3.33** shows an example, where the detection of the object was much more uncertain than in the previous example. There are two reason. First, the object shows a rather elongated shape (**Figure 3.34**) making it difficult for the algorithms to agree on a certain point within this object. Secondly, even the true data points, which were derived manually by inspecting the single images, do not

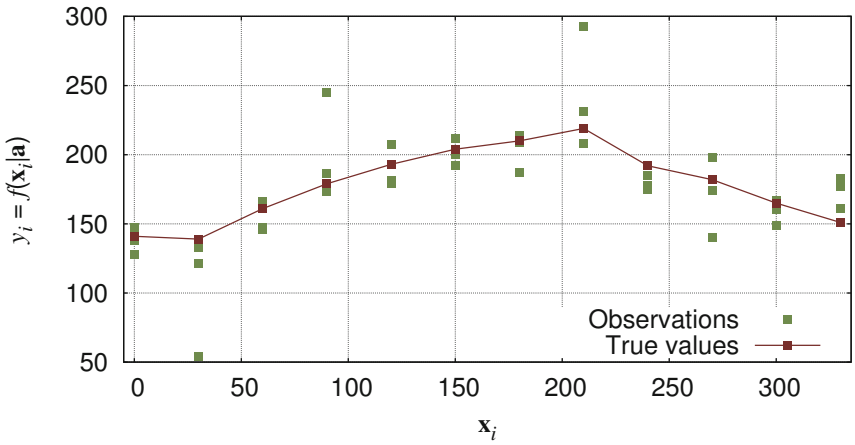


Figure 3.33: Recordings of a circular object movement with high uncertainty. The observations $y_i$ are dependent on the rotation angle $x_i$ (in degrees)

Table 3.14: Results of fitting circular movement (example 2)

| **Sosine 2** | $b_1$ | $b_2$ | $b_3$ | Detected outliers |
|---|---|---|---|---|
| True values | 178.0 | 35.76 | −174.9° | 3 |
| Equal weights | 176.2 | 40.24 | −174.6° | 0 |
| z-score | **178.8** | **35.58** | −178.1° | 1 |
| ClubOD | 174.2 | 31.43 | **−174.9°** | 3 |
| Estimated weights | 171.7 | 34.81 | −174.1° | 0 |
| Weights + z-score | 171.5 | 35.05 | −174.1° | 6 |
| Weights + ClubOD | 171.7 | 34.64 | −174.1° | 3 |
| + weights reset | 174.2 | 31.43 | **−174.9°** | 3 |

lie on a smooth cosine curve. This gives rise to the suspicion that something in the experimental setup was not perfect.

The inspection of the plot in Figure 3.33 by eye suggests at least three observations (at 30, 90, and 210 degrees) as being contaminants. Comparing the found coordinates with the positions inside the corresponding image approves that they do not lie on the crystal. Also the plot of deviates gives the same indication (**Figure 3.35**). The results after outliers removal, however, are ambiguous (**Table 3.14**). Eliminating the three outliers improves only the estimation of the phase shift ($b_3$). Offset $b_1$ and amplitude $b_2$ are estimated best when only the outlier

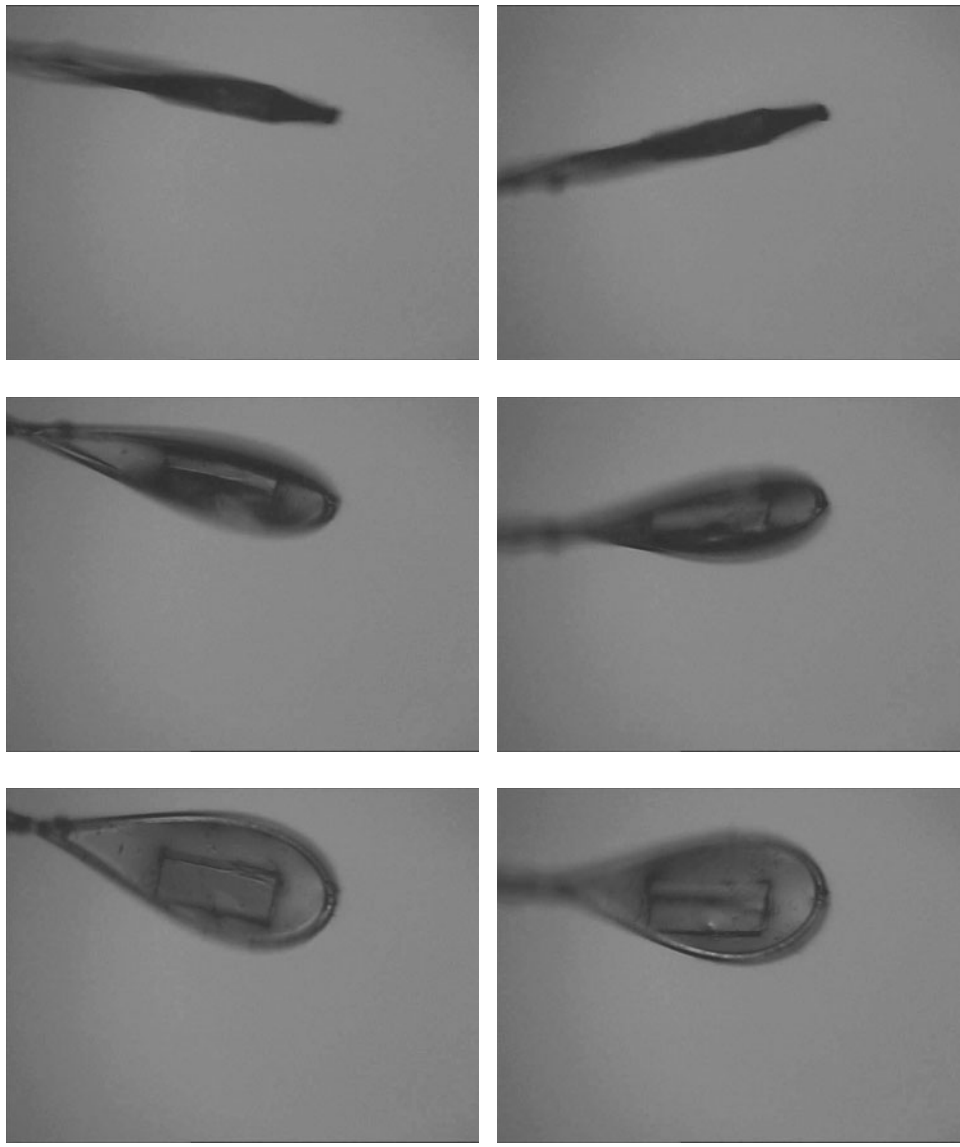

Figure 3.34: Rectangular object to be detected at different rotational positions. The rotation axis is horizontal and the vertical movement of the crystal is observed.

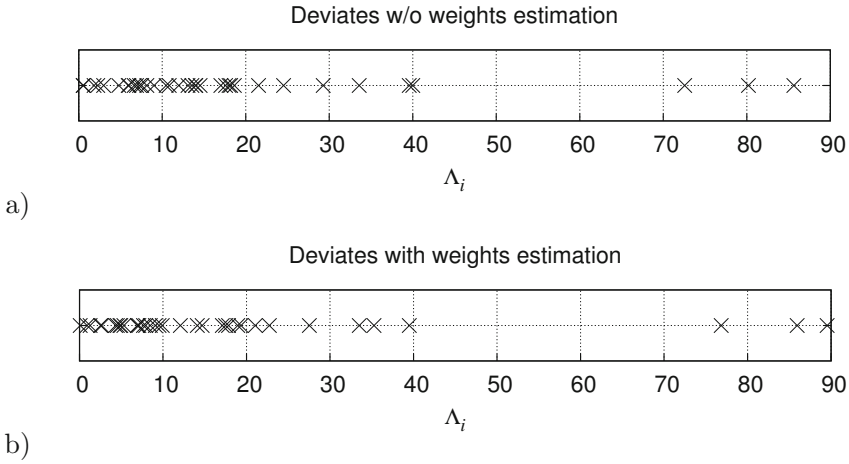


Figure 3.35: Deviates according to the fitting of a cosine (example 2); a) without application of weights estimation, b) using the estimation of weights

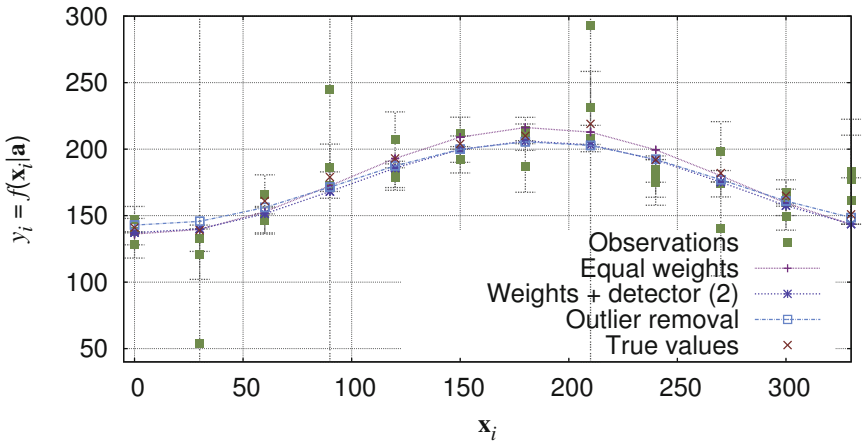


Figure 3.36: Fitting of a cosine function with outlier removal

at 30 degrees is removed and the other two are kept. **Figure 3.36** shows the corresponding plots.

### 3.5.7 Exponential model function

An exponential model function

$$y_i = a_2 \cdot \exp(a_3 \cdot x_i) + \varepsilon_i$$

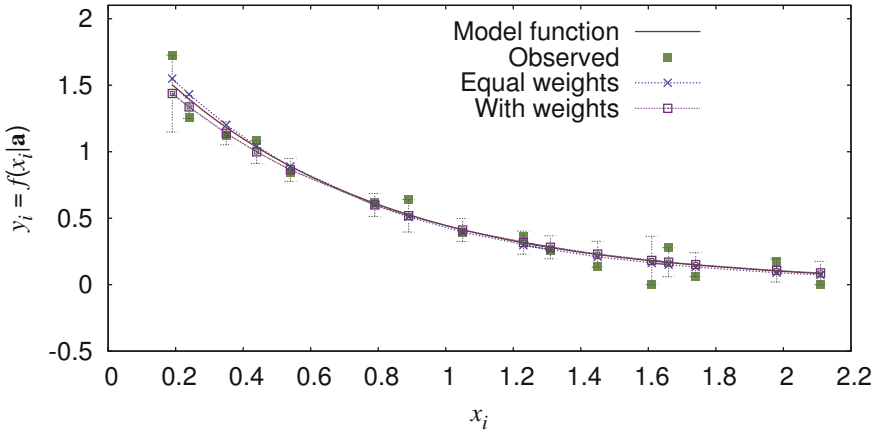


a)

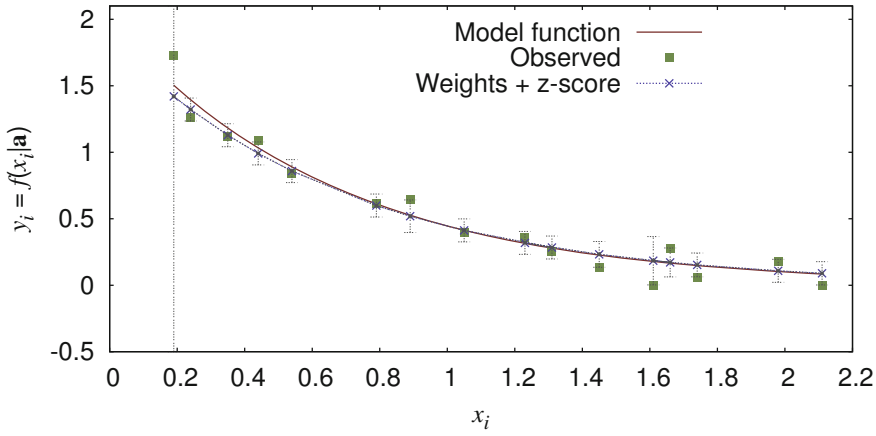


b)

Figure 3.37: Results of fitting an exponential model function; a) with and without weighting of observations, b) weighting and outlier removal

was generated with $a_2 = 2$, $a_3 = -1.5$ and additive Gaussian noise ($\sigma_{\varepsilon_i} = \sigma_\varepsilon = 0.125$). Since this nonlinear function can be linearised according to equation (1.12), there are two approaches in estimating the parameters $a_2$ and $a_3$. First, the data fitting can be performed directly with nonlinear approximation with its drawbacks of estimation of initial parameters and iterative parameter refinement. The result is depicted in **Figure 3.37**. The resulting parameters are listed in **Table 3.15**. Automatic weighting of observations yields worse results compared to the fitting with equal weights for this example data set. Inspecting the plot of

Table 3.15: Results of fitting an exponential function

| **Exponential** | $a_1$ | $a_2$ | Detected outliers |
|---|---|---|---|
| True values | 2.0 | −1.5 | 0 |
| Equal weights | **2.096** | −1.589 | 0 |
| z-score | 2.096 | −1.589 | 0 |
| ClubOD | 2.096 | −1.589 | 0 |
| Estimated weights | 1.895 | **−1.457** | 0 |
| Weights + z-score | 1.866 | −1.437 | 1 |
| Weights + ClubOD | 1.895 | −1.457 | 0 |
| Weights reset | 1.889 | −1.461 | 1 |

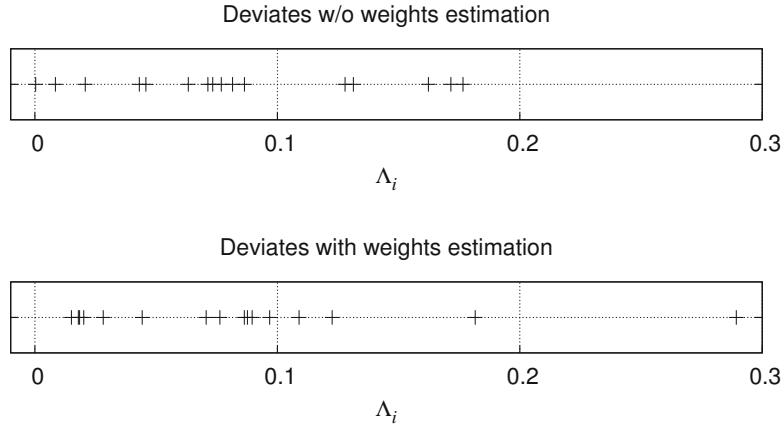


Figure 3.38: Deviates according to the fitting of an exponential function; a) without application of weights estimation, b) using the estimation of weights

deviates (**Figure 3.38**), it becomes clear why the z-score method has declared one observation as contaminant. After weights estimation, the threshold $\lambda_O = \hat{\sigma}_y \cdot \kappa_O$ (eq. 3.17) is equal to 0.209, thus, one observation has a higher deviation.

The linearisation (see Section 1.3) simplifies the fitting distinctly. However, two observations, which are equal to zero, must be remove from the data, because a linearisation is impossible ($\log(0) = -\infty$).

As can be seen in **Table 3.16**, the parameter estimation is better in this particular example compared to the nonlinear approach, also when adapted weights are

Table 3.16: Results of fitting a linearised exponential function

| **Exp. linearised** | $a_1$ | $a_2$ | Detected outliers |
|---|---|---|---|
| True values | 2.0 | −1.5 | 0 |
| Equal weights | **1.996** | −1.512 | (2) |
| z-score | 1.996 | −1.512 | (2) |
| ClubOD | 1.996 | −1.512 | (2) |
| Estimated weights | 1.955 | **−1.508** | (2) |
| Weights + z-score | 1.963 | −1.515 | (2) + 4 |
| Weights + ClubOD | 1.955 | −1.508 | (2) |

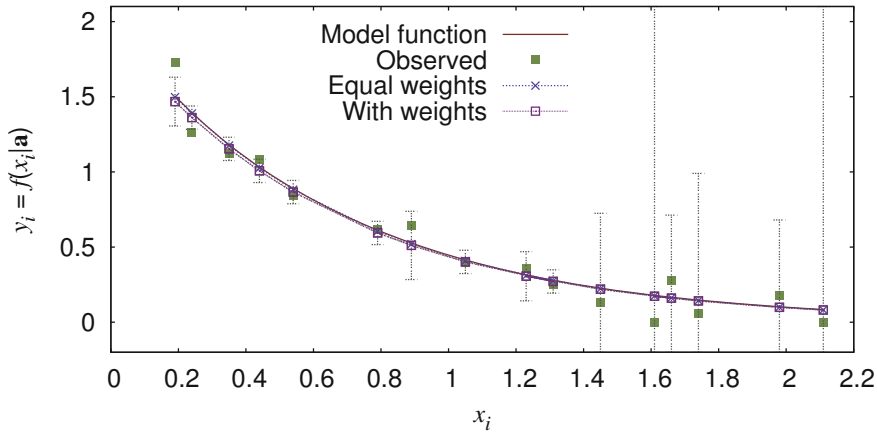


Figure 3.39: Results of fitting an exponential model function with and without weighting of observations using straight line fitting after linearisation

used. Typically, the results after linearisation are less accurate, because it involves logarithmic weighting of the observations. The error bars in **Figure 3.39** reflect that the weights estimation is highly influenced by the linearisation. The errors in large values $y_i$ are suppressed compared to small values $y_i$.

### 3.5.8 Composite Gaussian bell functions

The fitting of two superposed Gaussian bells

$$y = a_1 \cdot \exp\left[(x - a_2)^2 \cdot a_3\right] + a_4 \cdot \exp\left[(x - a_5)^2 \cdot a_6\right]$$

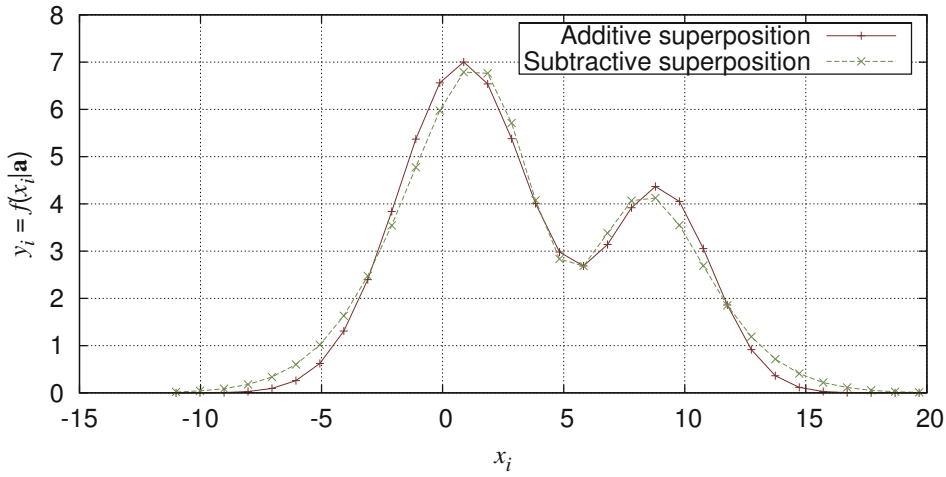


Figure 3.40: Composite Gaussian bell functions with different modes of superposition

can be ambiguous, dependent on whether the amplitudes $a_1$ and $a_4$ have the same sign or not (see also Section 1.5.2). **Figure 3.40** shows two examples with similar curves, but completely different parameters $a_1 \cdots a_6$. Both cases are discussed in the following.

**Example one: additive combination**

The data has been simulated with

$$y_i = 4.3 \cdot \exp\left[(x_i - 9.0)^2 \cdot (-0.11)\right] + 6.7 \cdot \exp\left[(x_i - 0.85)^2 \cdot (-0.069)\right] + \varepsilon_i$$

and $\sigma_{\varepsilon_i} = \sigma_\varepsilon = 0.25$. Dependent on the mode of weights estimation and outlier detection, the data fitting results in different parameter values (**Table 3.17**). and **Figure 3.41** shows the relevant plots. ClubOD misclassifies one observation, since it deviates somewhat stronger (**Figure 3.42**). It can also be seen that the corresponding absolute deviate is not exposed anymore after the application of estimated weights. That is why it is integrated into the bulk of good data points when using ClubOD. The method of standardised residuals, however, mistakes now two observations for contaminants. Surprisingly, the removal of a single outlier has almost no influence on the fitting of the additive data set. The estimated model parameters are identical up to the third decimal position compared to the fitting with equal weights in this case.

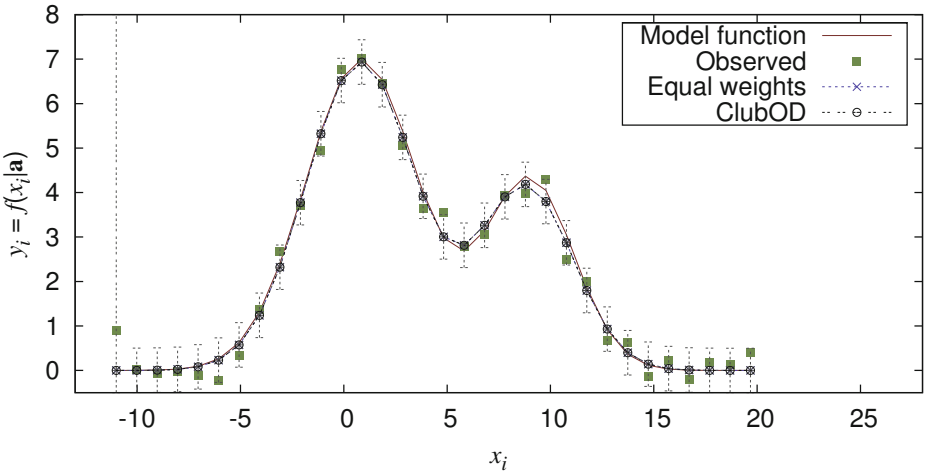


a)

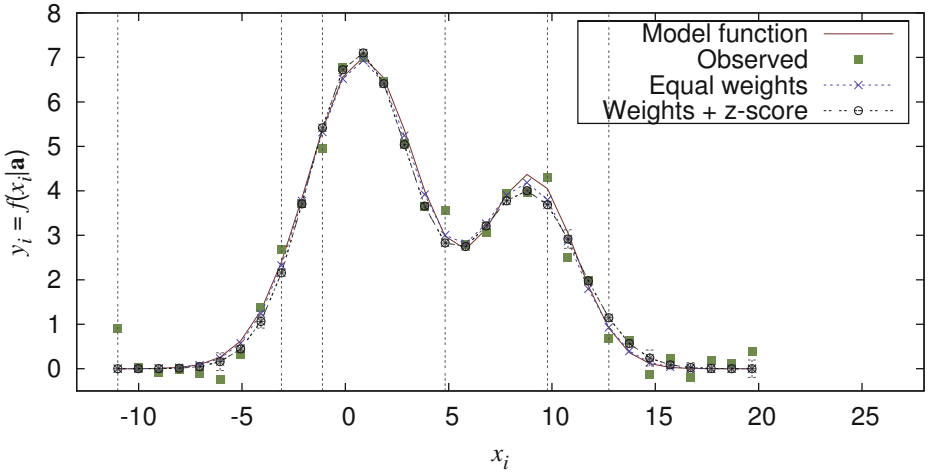


b)

Figure 3.41: Results of fitting two additively combined Gaussian bells ($a_1, a_4 > 0$); a) influence of ClubOD when using equal weights; b) outlier removal after estimation of weights

Table 3.17: Numerical results of fitting two additively combined Gaussian bells

| **Additive Gaussians** | $a_1$ | $a_2$ | $a_3$ | $a_4$ | $a_5$ | $a_6$ | Outl. |
|---|---|---|---|---|---|---|---|
| True values | 4.300 | 9.000 | −0.110 | 6.700 | 0.850 | −0.069 | 0 |
| Equal weights | 4.116 | 8.842 | −0.097 | **6.928** | **0.801** | **−0.072** | 0 |
| z-score | 4.116 | 8.842 | −0.097 | **6.928** | **0.801** | **−0.072** | 0 |
| ClubOD | 4.116 | 8.842 | −0.097 | 6.929 | **0.801** | **−0.072** | 1 |
| Estimated weights | 3.996 | 8.810 | −0.082 | 7.076 | 0.699 | −0.082 | 0 |
| Weights + z-score | 4.001 | 8.814 | −0.082 | 7.079 | 0.699 | −0.082 | 2 |
| Weights + ClubOD | 3.996 | 8.810 | −0.082 | 7.076 | 0.699 | −0.082 | 0 |
| Weights reset (z-score) | **4.176** | **8.865** | **−0.103** | 6.968 | 0.760 | −0.075 | 2 |

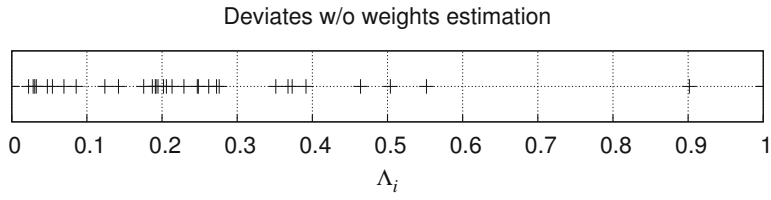


a)

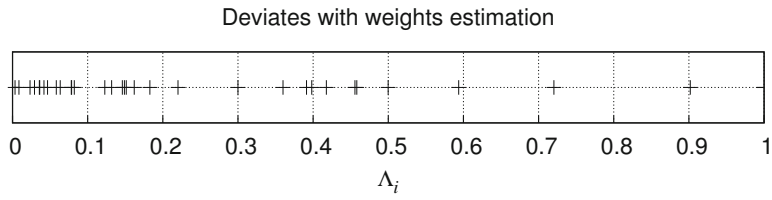


b)

Figure 3.42: Deviates according to the fitting of two additively combined Gaussians; a) without application of weights estimation, b) using the estimation of weights

**Example two: subtractive combination**

The data has been simulated with

$$y_i = 10 \cdot \exp\left[(x_i - 4)^2 \cdot \left(-\frac{1}{36}\right)\right] - 7 \cdot \exp\left[(x_i - 5)^2 \cdot \left(-\frac{1}{8}\right)\right] + \varepsilon_i$$

and $\sigma_{\varepsilon_i} = \sigma_\varepsilon = 0.25$.

In the case of Gaussian bells, which are combined via subtraction, the nonlinear fitting finds not the global but a strong local minimum owing to the misguiding

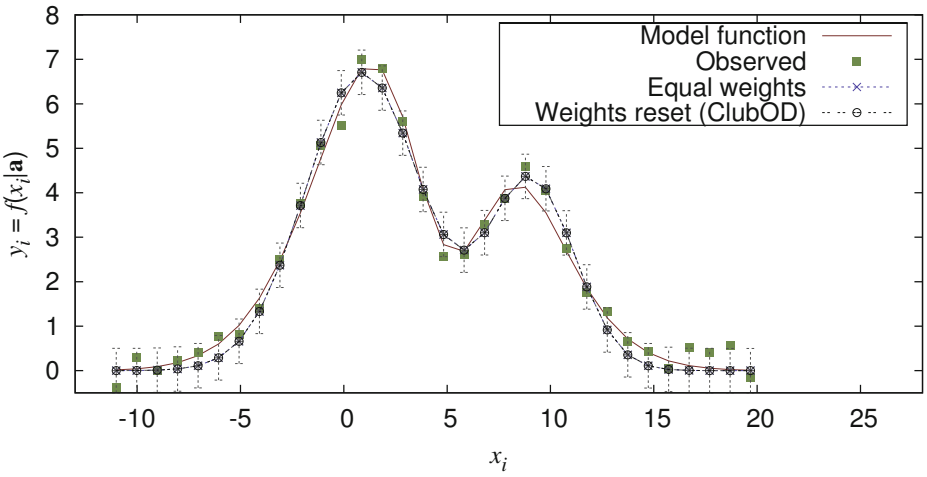


a)

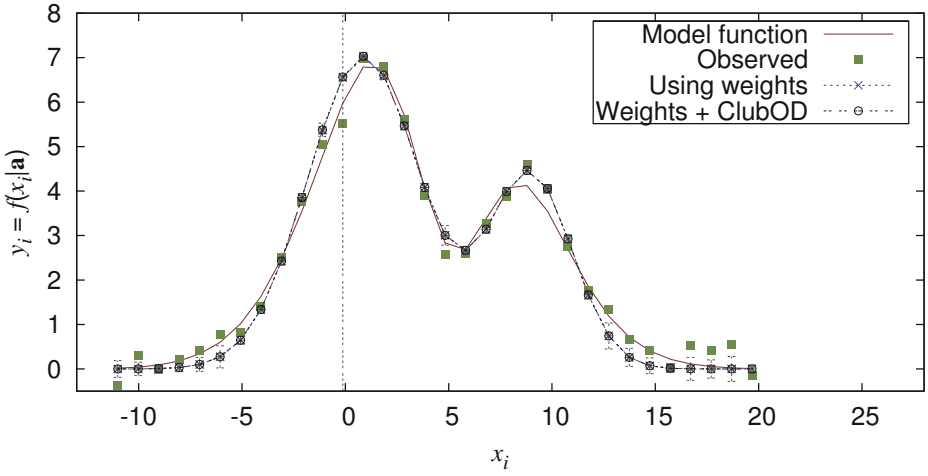


b)

Figure 3.43: Results of fitting two subtractively combined Gaussian bells ($a_1 > 0, a_4 < 0$); a) without weights; b) using weights

initialisation of the model parameters. The procedure guessing the initial parameter values simply assumes an additive composition, i.e. $a_1 > 0$ and $a_4 > 0$, and a corresponding starting point in the parameter space is chosen. The optimisation algorithm is not able to escape this attractive minimum. **Figure 3.43** reveals that the tails of the curve and the peaks are not optimally fitted. It would be possible, in principle, to test both variants (i.e. the additive and the subtractive

Table 3.18: Numerical results of fitting two subtractively combined Gaussian bells

| **Subtractive Gaussians** | $a_1$ | $a_2$ | $a_3$ | $a_4$ | $a_5$ | $a_6$ | Outl. |
|---|---|---|---|---|---|---|---|
| True values | 10.00 | 4.000 | 0.278 | −7.000 | 5.100 | −0.125 | 0 |
| Equal weights | 4.283 | 9.077 | −0.114 | 6.707 | 0.930 | −0.064 | 0 |
| z-score | 4.283 | 9.077 | −0.114 | 6.707 | 0.930 | −0.064 | 0 |
| ClubOD | 4.283 | 9.077 | −0.114 | 6.707 | 0.930 | −0.064 | 0 |
| Estimated weights | 4.373 | 8.960 | −0.124 | 7.012 | 0.892 | −0.067 | 0 |
| Weights + z-score | 4.374 | 8.957 | −0.123 | 7.028 | 0.886 | −0.067 | 1 |
| Weights + ClubOD | 4.374 | 8.957 | −0.123 | 7.028 | 0.886 | −0.067 | 1 |
| + weights reset | 4.299 | 9.019 | −0.109 | 7.008 | 0.847 | −0.069 | 1 |

superposition) in the initial parameter estimation and then to compare the fitting results afterwards. **Table 3.18** lists the numerical results.

The problem of ambiguity, that is, the existence of attractive local maxima, can also occur if Gaussian bells of of similar amplitude and variance are additively superposed. The resulting function would appear as a single Gaussian bell with some degradation.

### 3.5.9 Circle

The use of weights and the assumption of outliers do not make sense in the case of fitting a circle, since the possibly erroneous observations must be stuffed into the fitting framework as conditions, according to equation (1.27)

$$y_i = 0 = (x_{1,i} - a_1)^2 + (x_{2,i} - a_2)^2 - a_3^2 + \varepsilon_i \ ,$$

whereas the 'new' observations are assumed to be correct and equal to zero (see Subsection 1.5.3). Alternatively, the linear version according to equation (1.29) could be applied.

The test data consist of thirty samples of a circle (radius of $a_3 = 10$, centre at $(a_1; a_2) = (15; 15)$) over a range of 240 degrees with randomisation of both $x_{1,i}$ and $x_{2,i}$ (normally distributed with $\sigma_{\varepsilon_i} = \sigma_\varepsilon = 1$). The least-squares approximation calculates a circle at $(a_1, a_2) = (14.9134, 15.4414)$ with a radius of $a_3 = 9.7202$ (see **Figure 3.44**).

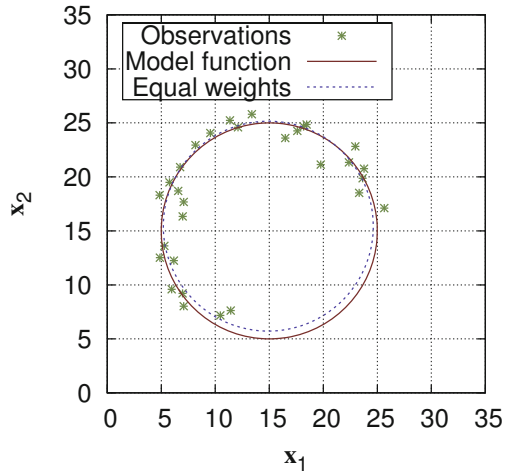


Figure 3.44: Results of fitting a circular object. The model function is $0 = (x_1 - 15)^2 + (x_2 - 15)^2 - 10^2$

### 3.5.10 Comparison of binning and deviate-based weights estimation

So far, only the weights estimator based on deviates has been investigated. This subsection uses a test signal with $N = 500$ samples enabling tests with weights estimation via binning. The chosen model function is

$$f(x|\mathbf{a}) = a_1 + a_2 \cdot x + a_3 \cdot x^2 + \varepsilon$$

with the parameters $a_1 = 10$, $a_2 = 0$ and $a_3 = 15$. The conditions $x_i$ have been randomly chosen and the corresponding function values have been randomised (Gaussian distribution, $\mathcal{N}(0; 1/16)$, see Section 6.1) in order to simulate erroneous observations $y_i$. In addition to this basic noise, a random signal with increasing uncertainty of $\sigma_i = 0.25 + (x_i)^4$ has been added to the signal, as can be seen in **Figure 3.45**a). **Table 3.19** shows the results of the parameter estimation via least squares. The plain fitting, that is, using equal weights, shows a plot close to the correct solution in **Figure 3.45**b), however, the model-parameters estimation can be improved by proper weighting of the observations. While ClubOD detects three outliers in maximum, when the weights are estimated via the conventional technique, the z-score approach cannot cope with the varying uncertainty at all. It relies on the estimation of the standard uncertainty of a Gaussian distribution, while the observations follow another distribution model.

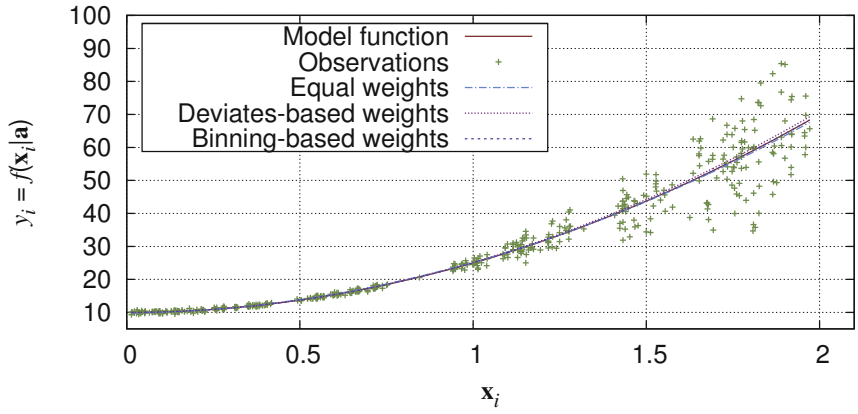


a)

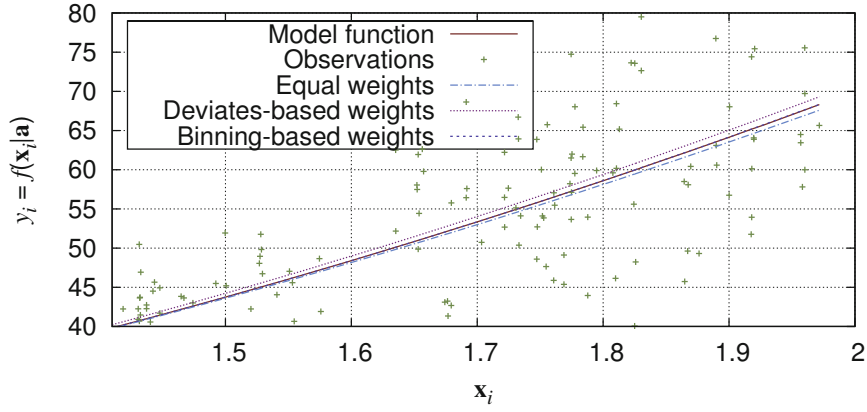


b)

Figure 3.45: Results of fitting polynomial data with and without weights. The model function is $f(\mathbf{x}|\mathbf{a}) = a_1 + a_2 \cdot x + a_3 \cdot x^2$; a) full plot; b) magnified portion

The plots of deviates are giving hints, why the results of outlier detection are so divergent. There is a concentration of small deviates leading to a relatively small estimated standard deviation $\hat{\sigma}_y$. The z-score detector cuts too many data points. Especially after estimating proper weights, most of the 500 observations are relatively close to the modelled curve leading to a small threshold according to equation (3.17). When using conventional estimation of weights, three of the deviates get exposed and ClubOD is able to find them. Best parameter estimates are obtained when the bin-wise uncertainty of the observation is determined. The only difficulty is to assign suitable bins. In the presented example, each bin comprises observations of 50 adjacent conditions.

Table 3.19: Numerical results of fitting a polynomial

| **Polynomial** | $a_1$ | $a_2$ | $a_3$ | Outliers |
|---|---|---|---|---|
| True values | 10.00 | 0.000 | 15.000 | 0 |
| Equal weights | 9.774 | 1.030 | 14.351 | 0 |
| z-score | 9.693 | 1.352 | 14.178 | 8 |
| ClubOD | 9.774 | 1.030 | 14.351 | 0 |
| Estimated weights | 10.007 | −0.248 | 15.379 | 0 |
| Weights + z-score | 10.032 | −0.387 | 15.491 | 96 |
| Weights + ClubOD | 10.008 | −0.256 | 15.385 | 3 |
| + weights reset | 9.911 | 0.305 | 14.905 | 3 |
| Weights via binning | **10.001** | **−0.042** | **15.026** | 0 |
| Binning + z-score | 10.006 | −0.075 | 15.061 | 88 |
| Binning + ClubOD | **10.001** | **−0.042** | **15.026** | 0 |
| Binning reset (z-score) | 9.829 | 0.668 | 14.668 | 88 |

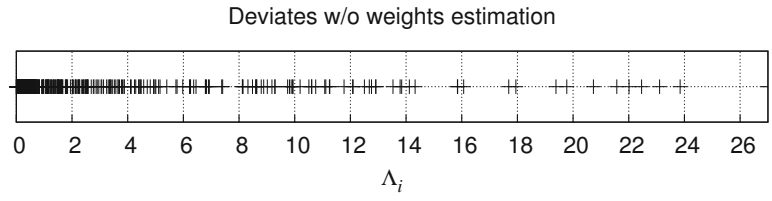


a)

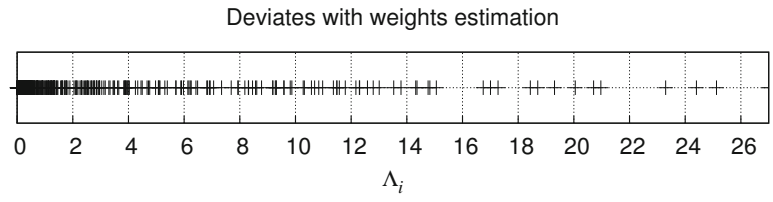


b)

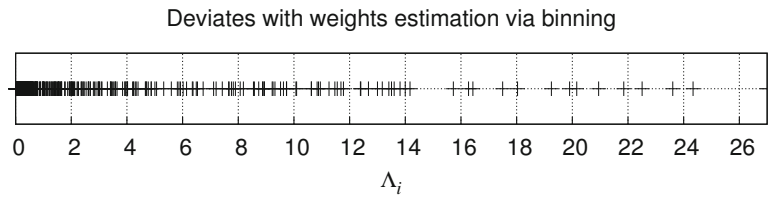


c)

Figure 3.46: Deviates according to the fitting of a polynomial function; a) without application of weights estimation, b) using the estimation of weights, c) weights estimation via binning

## 3.6 Conclusions

In the previous section the influence of different weighting and outlier-detection schemes on the data fitting has been investigated. Although it has not been a comprehensive test, a tendency has been become visible and some conclusions can be drawn about the usefulness of the modules depicted in Figure 3.13. The evaluation is based on the accuracy of the estimated parameter values.

### 3.6.1 Evaluation of weighting

#### Equal weights versus deviates-based weights estimation

The examinations have compared the estimated model parameters in dependence on whether estimated weights have been used for data fitting or not. The application of weights estimation shows a slight advantage, especially in the case of strong outliers, but also when the observations have truly different uncertainties, as in the case of fitting the polynomial. However, the advantage is not so pronounced that the general use of weights can be recommended. This becomes different when the removal of outliers is considered, see below.

#### Comparison of different schemes for weights estimation

Only the example of polynomial fitting with its relative huge number of observations allows an evaluation of the correctness of the weights. **Figure 3.47** shows the estimated weights converted to estimated uncertainties of both weighting schemes in comparison with the true uncertainties used for the generation of the test data. The deviates-based approach somewhat overestimates the uncertainties in the range, where identical weights have been assigned. Then it follows in principle the true uncertainties, however, the uncertainties of observations close to the fitted curve are distinctly underestimated. In contrast, the weights estimation using the binning method is able to compute uncertainties, which are very reasonable owing to the averaging effect. As already mentioned in the beginning of this section, the accuracy of uncertainties for single observations could be improved using a sliding bin or overlapping ones.

### 3.6.2 Comparison of outlier detectors

**Table 3.20** lists the number of outliers found by the z-score and cluster-based method (ClubOD) in dependence on whether weights have been estimated or

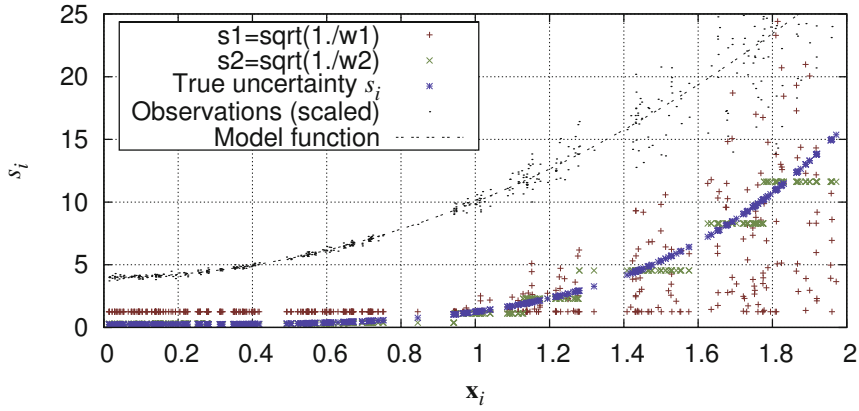


Figure 3.47: Estimated uncertainties $s1_i, s2_i$ for two different weighting schemes compared to the true uncertainty $s_i$. $w_1$ corresponds to deviates-based weighting and $w_2$ to weighting via binning. The observations are superposed for better comparison.

Table 3.20: Summary of outlier detection for thirteen different data sets

| Examples | True number | w/o weigths z-score | w/o weigths ClubOD | With weights z-score | With weights ClubOD |
|---|---|---|---|---|---|
| Constant | 3 | 2 | 3 | 5 | 3 |
| $y^{(0)}$ | 0 | 0 | 0 | 2 | 3 |
| $y^{(1)}$ | 2 | 0 | 0 | 2 | 2 |
| $y^{(2)}$ | 0 | 0 | 0 | 4 | 4 |
| $y^{(3)}$ | 2 | 0 | 0 | 3 | 3 |
| Plane | 9 | 1 | 0 | 12 | 9 |
| Coord. transf. | 18 | 9 | 16 | 17 | 17 |
| Cosine 1 | 0 | 0 | 0 | 0 | 0 |
| Cosine 2 | 3 | 1 | 3 | 6 | 3 |
| Exponential | 0 | 0 | 0 | 1 | 0 |
| Exp. lin. | 0 | 0 | 0 | 4 | 0 |
| Gaussian add. | 0 | 0 | 1 | 2 | 0 |
| Polynomial | 0 | 8 | 0 | 96 | 3 |
| with binning | 0 | - | - | 88 | 0 |
| Total difference | - | 32 | 16 | 202 | 12 |

not. The last row gives a summation of the absolute differences between true and found number of outliers.

The comparison of the columns with and without preceding estimation of weights shows on the one hand that it is sometimes impossible to find outliers if the estimated model-function parameters are far from their optimum. On the other hand, weight estimation can lead to the detection of too many outliers as can be seen in the examples of straight-line regression of $y^{(2)}$. The z-score method reveals its weakness especially in the application to the polynomial function, where much too many outliers have been found. Also in all other examples, the number of outliers found by the z-score approach is never closer to the true number of outliers than the number found by ClubOD.

### 3.6.3 Usefulness of weights

The presented approaches to outlier detection are closely coupled with the estimation of weights as can be concluded from the previous subsection. However, after identification and exclusion of the contaminants, it is possible to forget the weights and to perform a fitting without them, i.e. with ordinary least-squares approximation. The examination of all investigation results leads to the conclusion that it is beneficial indeed in the majority of cases to reset the estimated weights after the contaminants have been deleted from the set of observations. That means, the application of weighted least squares is mainly advantageous when it is accompanied with a suitable outlier-detection scheme. If the data set do not contain outliers or the contaminants have been successfully removed, then equal weights should be used, as long as the true standard uncertainty of the single observations $y_i$ is not known (compare page 47).

## 3.7 Test questions

**3.1** What are the weights good for?

**3.2** What are outliers?

**3.3** What should be the relation between the uncertainty of an observation and its assigned weight?

**3.4** Describe a method for the estimation of proper weights.

**3.5** Under which circumstances should equal weights be used after the removal of outliers?

**3.6** When is the estimation of weights favourable over equal weighting of observations?

**3.7** Which influence do the initially estimated parameters have on the final fitting result?

**3.8** In which cases can the influence of outliers be neglected?

# Chapter 4

# Uncertainty of Results

After fitting the given data in terms of observations $y_i$ using the method of least-squares approximation, the experimenter knows the set of best[1] estimated parameters $\mathbf{a}$ of the utilised model function $f(\mathbf{x}|\mathbf{a})$. This chapter addresses the questions of whether (i) that best solution is adequate and (ii) the hypothesis is correct that the chosen model really represents the phenomena that have been measured in the experiment.

## 4.1 Goodness-of-fit, precision and accuracy

### 4.1.1 Consistence of statistical model and data

Let us first recapitulate the purpose of data fitting. In least-squares approximation, the idea is to minimise the following function

$$\chi^2 = \sum_{i=1}^{N} w_i \cdot [f(\mathbf{x}_i|\mathbf{a}) - y_i]^2 \longrightarrow \text{Min}$$

for an experiment with $N$ observations $y_i$, each measured under certain conditions represented by $\mathbf{x}_i$. The parameter vector $\mathbf{a}$ is the variable to be optimised, while the weights $w_i$ should reflect the reliability of the corresponding observation (see Chapter 3).

Typically, data never exactly fit the chosen model function, regardless of whether the model is the correct one or not. The goodness-of-fit indicates how well a statistical model describes the data. This statistical model comprises both the chosen model function and the assumed deviation of the observations from that function.

[1] "best" means optimised with respect to the chosen minimisation criterion.

T. Strutz, *Data Fitting and Uncertainty*, DOI 10.1007/978-3-8348-9813-5 _4,

The goodness-of-fit is measured via[2]

$$g_{\text{fit}} = \frac{\chi^2}{N_{\text{free}}} = \frac{1}{N_{\text{free}}} \cdot \sum_{i=1}^{N} w_i \cdot [f(\mathbf{x}_i|\mathbf{a}) - y_i]^2 \ , \tag{4.1}$$

where $N_{\text{free}} = N - M$ is the number of degrees of freedom for fitting $N$ data points with $M$ model parameters. A value of $g_{\text{fit}} \approx 1$ is an indicator that the statistical model is consistent with the data. This means that the weights $w_i$ were correctly chosen equal to the reciprocal of the variance of the population from which their corresponding observation $y_i$ was drawn ($w_i = 1/\sigma_i^2$) and that the model function is suitable. Nevertheless, $g_{\text{fit}} \approx 1$ does not rule out the existence of other, possibly more suitable models. If the model function is not appropriate for describing the observations, the deviations will be larger than estimated by the $\sigma_i$s and thus $g_{\text{fit}} > 1$. On the other hand, a goodness-of-fit less than one does not necessarily signal a better fit; instead, it is likely that only the uncertainties $\sigma_i$ are overestimated.

However, as already discussed in the previous chapter, there are many applications without available values for $\sigma_i$, which means the weights have to be determined in a different way. Ideally it is possible to estimate correct relative weights

$$w_i = \frac{k}{\sigma_i^2} \ . \tag{4.2}$$

The goodness-of-fit $g_{\text{fit}}$ is then merely taken to be an estimate of the constant $k$.

### 4.1.2 Sample variance

The variance of the fit (sample variance) is equal to the estimate of the squared standard deviation $\sigma_{\text{y}}^2$ of the data and expressed by

$$\sigma_{\text{y}}^2 = \frac{1}{N_{\text{free}}} \cdot \frac{\sum_{i=1}^{N} w_i \cdot [f(\mathbf{x}_i|\mathbf{a}) - y_i]^2}{\frac{1}{N} \sum_{i=1}^{N} w_i} \ . \tag{4.3}$$

This formula is equivalent to equation (3.10) and it is also related to the goodness-of-fit (eq. 4.1) with additional normalisation of the weights. So it does not include complementary information about the quality of the fitting.

[2] There is no THE goodness-of-fit formula. Different textbooks assign unfortunately sometimes slightly different formulae. The symbol $\chi^2$ points out the tight relation to the so-called $\chi^2$-test (see elsewhere).

At this point, the use of the degrees of freedom $N_{\text{free}} = N - M$ for normalisation in (4.3) and other formulae for the *standard deviation* should be justified. When $N$ is very large compared to the number $M$ of parameters, the difference becomes negligible. Let us consider the straight-line example $y = a_1 \cdot x + a_2$ and let us assume that only $N = 2$ observations are made. It is obvious that it is *always* possible to draw a straight line through these two points. However, the probability that this is the correct line approaches zero and the uncertainty near infinite. Thus the denominator becomes $N_{\text{free}} = N - M = 2 - 2 = 0$ and the estimated deviation infinite as wanted. In general, this is related to the problem of overfitting. Using a model function with enough parameters, the fitting of any data (even noise) is possible. $N_{\text{free}}$ prevents the experimenter to trust in such fits.

A standard deviation is only a measure of *precision*, one which results from random fluctuations of the observations. What the experimenter who collected the data also would like to know is the *accuracy* of the observations to lie in the true range [Bev92].

The difference between accuracy and precision of an experiment is shown in **Figure 4.1**. The accuracy expresses the closeness of observations to true values; it is a measure of correctness of the result (low systematic error). The precision is a measure of how well the observations fit the model function without regarding the true values; it is affected by random errors.

Unfortunately, it is very hard to detect errors of a systematic type and thus to make statements about the accuracy of the result. Systematic errors result from insufficiently calibrated equipment, from dependencies on not considered parameters influencing the measurement (e.g., the temperature etc.), or from bias on the part of the observer.

**Example**:
In an image-processing application, the observer can be a software algorithm for the detection of special objects, for example. The determination of the positions of these objects could be affected by the lighting conditions, introducing a systematic offset. Let us assume the simple case that bright objects have to be separated from a dark background via simple thresholding of the greyvalues and let us further assume that the centre of the object has subsequently to be determined from the remaining object area. If, for instance, the light source is shining from the right side, the object appears darker on the left side, which means the corresponding picture elements might be considered as background owing to the chosen threshold. The derived object centre would automatically be biased to the right.
□□□

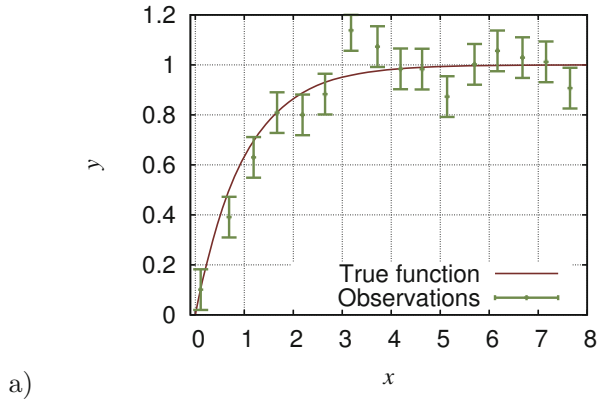


a)

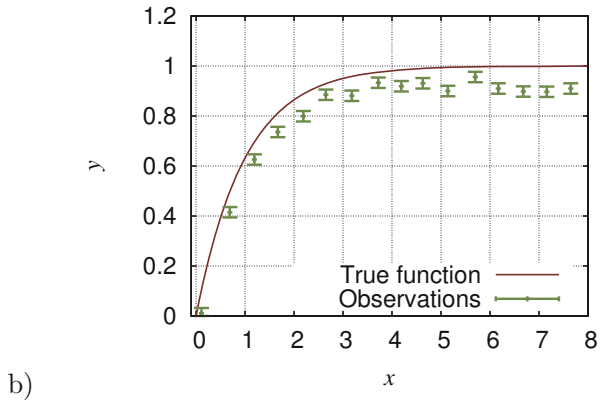


b)

Figure 4.1: Accuracy versus precision: a) accurate observations with low precision, b) precise but inaccurate data

Random errors are typically reduced by simply repeating the experiment to obtain more observations. If the random errors result from instrumental (or algorithmic) uncertainties, they could possibly be reduced by using more advanced instruments or algorithms. It should be noted that it does not make sense in either case to reduce the random error much below the systematic one.

## 4.2 Uncertainty of estimated parameters

In addition to determining the parameters of the model function, one should also make estimates of the uncertainties in those values. These estimates are usually expressed in terms of an *estimated standard deviation* (e.s.d) or *standard uncertainty*.

The standard uncertainty of parameters **a** can be derived directly from equation (2.6). The term

$$\mathbf{C} = \left(\mathbf{J}^{\mathrm{T}}\mathbf{W}\mathbf{J}\right)^{-1} \tag{4.4}$$

is equal to the variance-covariance matrix for all parameters [Rya97] describing how the single parameters are related to each other dependent on the chosen model function. The diagonal element $c_{jj}$ contains the variance of parameter $a_j$. **C** is obviously independent of the actual observations, but influenced by the chosen conditions $x_i$ and the weights $w_i$. If the weights merely represent relative uncertainties of the observations in terms of $w_i = k/\sigma_i^2$, then **C** is commonly multiplied by the goodness-of-fit $g_{\mathrm{fit}}$ (eq. 4.1) [Pri92, Pre92]

$$\sigma_{a_j}^2 = g_{\mathrm{fit}} \cdot c_{jj} \tag{4.5}$$

in order to compensate for the constant factor $k$ (see Section 4.1). The uncertainty $\sigma_{a_j}$ indicates the reliability of the model parameter $a_j$. It is often specified as a percentage of the estimated parameter value. If one or more of the parameters shows a relatively high uncertainty, this might point to an unsuitable model function.

While the diagonal elements of **C** correspond to the variances $\sigma_{a_j}^2$ of the model parameters $a_j$, the off-diagonal elements express the covariances $\sigma_{a_j,a_k}^2$, which could have also negative values.

## 4.3 Uncertainty of data approximation

The purpose of data fitting is not limited to the approximation of the data points. The data model can also be used to predict which values $y$ would most likely be measured if other experimental conditions **x** were chosen. This is known in the literature as *model prediction*. Moreover, we are interested in the uncertainty of this model prediction.

Based on the uncertainty of parameters (eq. 4.5) and utilising the principle of error propagation (eq. 7.13), the uncertainty of the model prediction can be derived as

$$\sigma_f = \sqrt{\sum_j \sigma_{a_j}^2 \cdot \left(\frac{\partial f}{\partial a_j}\right)^2 + 2 \cdot \sum_{j,k} \sigma_{a_j,a_k}^2 \cdot \left(\frac{\partial f}{\partial a_j}\right) \cdot \left(\frac{\partial f}{\partial a_k}\right)} \,.$$

For the example of straight-line fitting

$$f(\mathbf{x}|\mathbf{a}) = a_1 + a_2 \cdot x$$

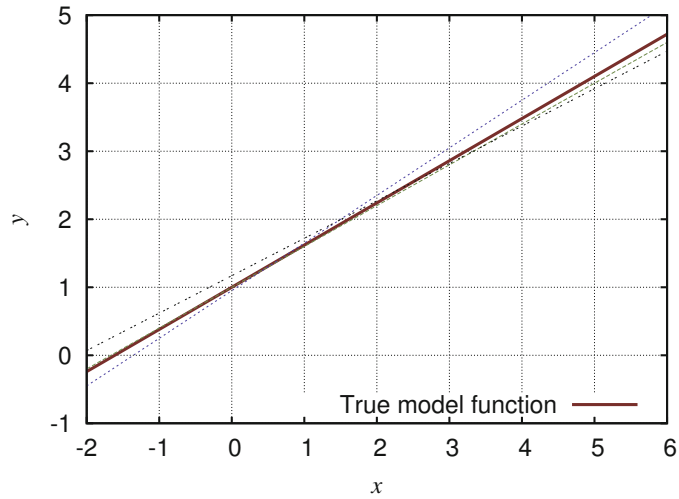


Figure 4.2: Model prediction based on a straight-line approximation. If the estimated model parameters are inaccurate, the prediction of the correct $y$ value becomes more uncertain for a given condition $x$ as $|x|$ increases (examples in green, blue, and black).

we get as derivatives

$$\frac{\partial f}{\partial a_1} = 1 \qquad \frac{\partial f}{\partial a_2} = x$$

and accordingly

$$\sigma_f = \sqrt{\sigma_{a_1}^2 + \sigma_{a_2}^2 \cdot x^2 + 2 \cdot \sigma_{a_1,a_2}^2 \cdot x}$$

as the uncertainty of the modelled function. As you can see, this is a function of the condition $x$ and increases in tendency with higher values of $|x|$. **Figure 4.2** visualizes this effect. The higher $|x|$ is, the more possible approximations deviate from the true model function.

## 4.4 Inspection of plots

Numerical evaluation methods are essential, when the data fitting has to be an automatic process. In case of one-time experiments, it is additionally recommended to have a closer look at least at the plots of residuals $(y_i - f(\mathbf{x}_i|\mathbf{a}))$ and preferably at the plot of the final model function against the observation. The

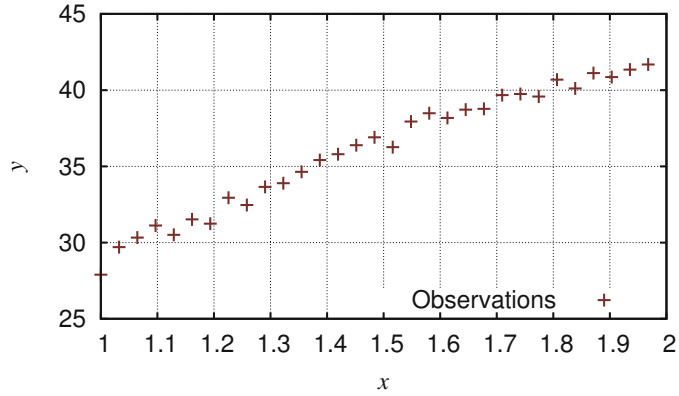


Figure 4.3: Observations of a particular experiment

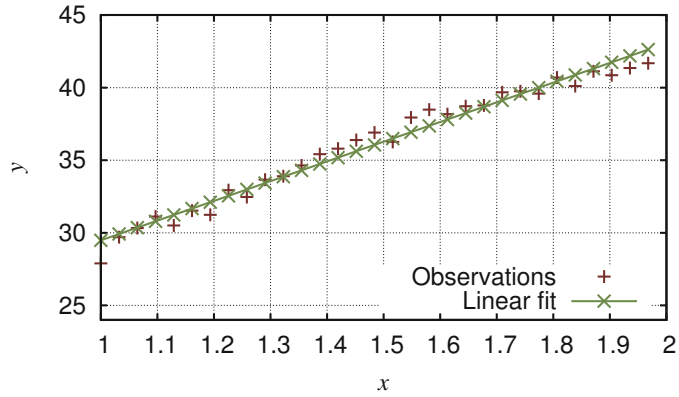


Figure 4.4: Result of data fitting with a straight-line model

latter yields an impression of whether the fitting procedure was successful in general while the former can reveal mismatches between the chosen model function and the true relation between conditions and observations.

**Figure 4.3** shows the outcome of 31 measurements. The relationship between $y$ and $x$ seems to be of a linear nature. Thus,

$$y = f(\mathbf{x}|\mathbf{a}) = a_1 + a_2 \cdot x \tag{4.6}$$

is assumed to describe the system properly. The graph resulting from fitting a straight line is depicted in **Figure 4.4**. At a first glance, the fit seems to be appropriate. An inspection of the deviates, however, reveals that they are

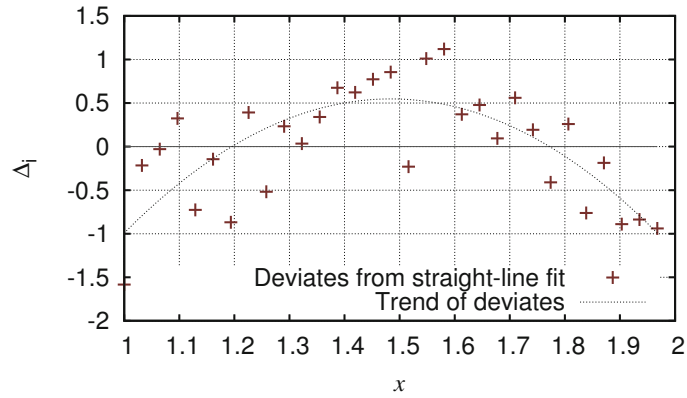


Figure 4.5: Plot of deviates $(y_i - f(\mathbf{x}_i|\mathbf{a}))$

not equally distributed over the range of conditions, but instead show a trend (**Figure 4.5**). This is a strong indication that the chosen model function is not sufficient to describe the process. Either polynomials of higher order or other functions have to be considered.

## 4.5 Example computations

The following brief subsections refer to the results of weighted data fitting reported in the previous chapter. Only three simple model functions are discussed here in detail, since the equations for all other models can be derived accordingly. The problem of model mismatch is then addressed.

### 4.5.1 Constant value

The minimisation problem for a constant value reduces to

$$\chi^2 = \sum_{i=1}^{N} w_i \cdot [f(\mathbf{x}_i|\mathbf{a}) - y_i]^2 = \sum_{i=1}^{N} w_i \cdot [a_1 - y_i]^2 \ .$$

Using the results of Subsection 2.6.1 we get the covariance matrix

$$\mathbf{C} = \left(\mathbf{J}^{\mathrm{T}}\mathbf{W}\mathbf{J}\right)^{-1} = \left(\sum_{i=1}^{N} w_i\right)^{-1} = c_{11} \ ,$$

which is simply a scalar in the current case. The goodness-of-fit is equal to

$$g_{\text{fit}} = \frac{1}{N_{\text{free}}} \cdot \sum_{i=1}^{N} w_i \cdot [a_1 - y_i]^2 \ . \tag{4.7}$$

According to (4.3) and (4.5) the resulting variance of the parameter $a_1$ is therefore

$$\sigma_{a_1}^2 = g_{\text{fit}} \cdot c_{11} = \frac{1}{N_{\text{free}}} \cdot \frac{\sum\limits_{i=1}^{N} w_i \cdot [a_1 - y_i]^2}{\sum\limits_{i=1}^{N} w_i} = \frac{\sigma_{\text{y}}^2}{N} \ .$$

The uncertainty of the determined mean value $a_1$ is thus equal to $\sigma_{a_1} = \sigma_{\text{y}}/\sqrt{N}$. Doubling the number of experiments reduces the uncertainty (the random error) by the factor $1/\sqrt{2}$.

The following table shows the improvement of the data fitting in the example discussed in Subsection 3.5.1 depending on using weights and outlier detection.

| | $\chi^2$ | $g_{\text{fit}}$ | $a_1$ | $\sigma_{a_1}$ | $\sigma_{a_1}[\%]$ | Outliers |
|---|---|---|---|---|---|---|
| Without weights | 247.116 | 5.884 | 9.791 | 0.370 | 3.78 | 0 |
| z-score | 117.805 | 2.945 | 9.829 | 0.268 | 2.73 | 2 |
| ClubOD | 70.000 | 1.795 | 10.000 | 0.212 | 2.12 | 3 |
| Estimated weights | 28.867 | 0.687 | 9.961 | 0.153 | 1.53 | 0 |
| Weights + z-score | 23.857 | 0.645 | 9.942 | 0.149 | 1.50 | 5 |
| Weights + ClubOD | 25.867 | 0.663 | 9.965 | 0.150 | 1.51 | 3 |
| + weights reset | 70.000 | 1.795 | 10.000 | 0.212 | 2.12 | 3 |

The upper half of the table contains results from ordinary least-squares approximation (OLS) with and without the detection of outliers. The detection is performed either using the z-score method (Subsection 3.4.1) or the ClubOD approach (Subsection 3.4.2). The lower half of the table lists results based on weighted least squares.

Which conclusions can be drawn from these values?

- $\chi^2$ is the target of minimisation, so its decreasing value shows at least that the removal of outliers fulfils the optimisation criterion.
- The application of OLS (no weights) implies $w_i = \text{const.} = 1.0$, i.e. a standard uncertainty of $\sigma_i = \sqrt{1/w_i} = \sigma = 1$. This leads to following effects.

  - Introducing weights decreases $\chi^2$ only, if their averaged value is smaller than 1.
  - The value $g_{\text{fit}} = 5.884$ indicates that the uncertainty of the observations is in fact higher than 1, presuming the model function was chosen correctly. After removing the contaminants, of course, the uncertainty decreases and thus the goodness-of-fit as well.

- The application of weights leads to goodness-of-fit values $g_{\text{fit}} < 1$, indicating an overestimation of the uncertainties of the observations, i.e., the weights are too small on average. This is a systematic effect caused by the selected weighting scheme.

- The standard uncertainty of the estimated parameter $a_1$, specified in percent of the parameter value, provides the most reliable information that the fitting process was successful. Of course, the uncertainty decreases if observations with high deviation from the model function are down-weighted or even removed.

### 4.5.2 Straight line

In the straight-line example, we have to determine the uncertainty of two parameters according to the model function

$$y = f(\mathbf{x}|\mathbf{a}) = a_1 + a_2 \cdot x \ .$$

The computation of the covariance matrix becomes a little bit more complex. Following equation (2.16) and applying (5.6) for matrix inversion we get

$$\begin{aligned}
\mathbf{C} &= \left(\mathbf{J}^{\mathrm{T}}\mathbf{W}\mathbf{J}\right)^{-1} = \begin{pmatrix} \sum_{i=1}^{N} w_i & \sum_{i=1}^{N} w_i \cdot x_i \\ \sum_{i=1}^{N} w_i \cdot x_i & \sum_{i=1}^{N} w_i \cdot x_i^2 \end{pmatrix}^{-1} = \begin{pmatrix} c_{11} & c_{12} \\ c_{21} & c_{22} \end{pmatrix} \\
&= \frac{1}{\sum_{i=1}^{N} w_i \cdot \sum_{i=1}^{N} w_i \cdot x_i^2 - \sum_{i=1}^{N} w_i \cdot x_i \cdot \sum_{i=1}^{N} w_i \cdot x_i} \cdot \begin{pmatrix} \sum_{i=1}^{N} w_i \cdot x_i^2 & -\sum_{i=1}^{N} w_i \cdot x_i \\ -\sum_{i=1}^{N} w_i \cdot x_i & \sum_{i=1}^{N} w_i \end{pmatrix} .
\end{aligned}$$

From the matrix structure of $\mathbf{C}$ we can immediately conclude that there are in total four variances or covariances, respectively

$$\begin{pmatrix} \sigma_{a_1}^2 & \sigma_{a_1 a_2}^2 \\ \sigma_{a_2 a_1}^2 & \sigma_{a_2}^2 \end{pmatrix} = g_{\text{fit}} \cdot \begin{pmatrix} c_{11} & c_{12} \\ c_{21} & c_{22} \end{pmatrix} .$$

The influence of the weighting and outlier detection is shown in following tables, where $y^{(0)} \dots y^{(3)}$ refer to the examples discussed in Subsection 3.5.2.

| $y^{(0)}$ | $\chi^2$ | $g_{\text{fit}}$ | $a_1$ | $a_2$ | $\sigma_{a_1}[\%]$ | $\sigma_{a_2}[\%]$ |
|---|---|---|---|---|---|---|
| True values | | | 2.000 | 1.000 | | |
| Without weights | 0.318 | 0.040 | 1.861 | 1.196 | 7.32 | 18.36 |
| z-score | 0.318 | 0.040 | 1.861 | 1.196 | 7.32 | 18.36 |
| ClubOD | 0.318 | 0.040 | 1.861 | 1.196 | 7.32 | 18.36 |
| Estimated weights | 7.539 | 0.942 | 2.000 | 1.111 | 4.62 | 13.19 |
| Weights + z-score | 5.479 | 0.913 | 2.016 | 1.101 | 4.61 | 13.38 |
| Weights + ClubOD | 4.387 | 0.877 | 2.016 | 1.112 | 4.52 | 13.02 |
| + reset (ClubOD) | 0.059 | 0.012 | 2.004 | 1.126 | 4.59 | 13.13 |

| $y^{(1)}$ | $\chi^2$ | $g_{\text{fit}}$ | $a_1$ | $a_2$ | $\sigma_{a_1}[\%]$ | $\sigma_{a_2}[\%]$ |
|---|---|---|---|---|---|---|
| Without weights | 1.857 | 0.232 | 1.939 | 1.379 | 16.97 | 38.48 |
| z-score | 1.857 | 0.232 | 1.939 | 1.379 | 16.97 | 38.48 |
| ClubOD | 1.857 | 0.232 | 1.939 | 1.379 | 16.97 | 38.48 |
| Estimated weights | 6.240 | 0.780 | 1.718 | 1.554 | 7.02 | 13.49 |
| Weights + z-score | 4.218 | 0.703 | 1.712 | 1.546 | 6.73 | 12.99 |
| Weights + ClubOD | 4.218 | 0.703 | 1.712 | 1.546 | 6.73 | 12.99 |
| + weights reset | 0.248 | 0.041 | 1.750 | 1.358 | 9.34 | 19.65 |

| $y^{(2)}$ | $\chi^2$ | $g_{\text{fit}}$ | $a_1$ | $a_2$ | $\sigma_{a_1}[\%]$ | $\sigma_{a_2}[\%]$ |
|---|---|---|---|---|---|---|
| Without weights | 1.932 | 0.242 | 2.436 | −0.109 | 13.78 | 497.10 |
| z-score | 1.932 | 0.242 | 2.436 | −0.109 | 13.78 | 497.10 |
| ClubOD | 1.932 | 0.242 | 2.436 | −0.109 | 13.78 | 497.10 |
| Estimated weights | 4.263 | 0.533 | 2.021 | 1.058 | 2.50 | 10.46 |
| Weights + z-score | 0.221 | 0.055 | 2.015 | 1.084 | 0.81 | 3.39 |
| Weights + ClubOD | 0.221 | 0.055 | 2.015 | 1.084 | 0.81 | 3.39 |
| + weights reset | 0.002 | 0.0004 | 2.015 | 1.084 | 0.81 | 3.39 |

| $y^{(3)}$ | $\chi^2$ | $g_{\text{fit}}$ | $a_1$ | $a_2$ | $\sigma_{a_1}[\%]$ | $\sigma_{a_2}[\%]$ |
|---|---|---|---|---|---|---|
| Without weights | 5.375 | 0.672 | 3.220 | −0.952 | 17.39 | 94.82 |
| z-score | 5.375 | 0.672 | 3.220 | −0.952 | 17.39 | 94.82 |
| ClubOD | 5.375 | 0.672 | 3.220 | −0.952 | 17.39 | 94.82 |
| Estimated weights | 6.269 | 0.784 | 2.220 | 0.460 | 9.90 | 80.21 |
| Weights + z-score | 3.209 | 0.642 | 2.161 | 0.561 | 9.30 | 60.40 |
| Weights + ClubOD | 3.209 | 0.642 | 2.161 | 0.561 | 9.30 | 60.40 |
| + weights reset | 0.440 | 0.088 | 2.150 | 0.677 | 11.83 | 62.16 |

.

The conclusions regarding the values of $\chi^2$, $g_{\text{fit}}$ and $\sigma_{a_j}[\%]$ can be drawn accordingly to the statements in the previous subsection. The uncertainty of the observations is less than one, which is why $\chi^2$ and $g_{\text{fit}}$ become higher after the application of weights estimation in all four cases.

These examples of straight-line regression particularly illustrate the high relation of the standard uncertainty (in percent) of the estimated parameters and their correctness. Values of more than 50% definitely point to untrustworthy parameters or to inadequate model functions, respectively. If outliers are present (and not removed), then typically the chosen model function is not appropriate to represent the observations and high relative standard uncertainties of parameters are observed. Values below 10% indicate parameters with reasonable values, however, the smallest uncertainty must not necessarily point to the parameter value closest to the true one as can be observed for $a_1$ and $a_2$ of $y^{(1)}$ as well as for $a_2$ of $y^{(3)}$, for example.

### 4.5.3 Cosine function

The approximation of the nonlinear model function

$$y = b_1 + b_2 \cdot \cos(x - b_3)$$

based on the observations used in example 2 (Subsection 3.5.6, page 86) leads to the following values:

| Ex. 2 | $\chi^2$ | $g_{\text{fit}}$ | $b_1$ | $b_2$ | $b_3$ | $\sigma_{b_1}$[%] | $\sigma_{b_2}$[%] | $\sigma_{b_3}$[%] |
|---|---|---|---|---|---|---|---|---|
| True values | | | 178.0 | 35.76 | −174.9° | | | |
| Without weights | 28638. | 867.83 | 176.2 | 40.24 | −174.6° | 2.79 | 17.26 | 0.10 |
| z-score | 20637. | 644.94 | 178.8 | 35.58 | −178.1° | 2.40 | 17.21 | 0.10 |
| ClubOD | 8206.7 | 273.56 | 174.2 | 31.43 | −174.9° | 1.65 | 13.03 | 0.07 |
| Estimated weights | 24.566 | 0.744 | 171.7 | 34.81 | −174.1° | 1.04 | 7.21 | 0.04 |
| Weights + z-score | 18.552 | 0.687 | 171.5 | 35.05 | −174.1° | 1.01 | 6.91 | 0.04 |
| Weights + ClubOD | 21.560 | 0.719 | 171.7 | 34.64 | −174.1° | 1.03 | 7.13 | 0.04 |
| + reset (ClubOD) | 8206.7 | 273.56 | 174.2 | 31.43 | −174.9° | 1.65 | 13.03 | 0.07 |

By definition, the uncertainties of the parameters in this fitting example are also smallest when weights are used (and outliers excluded). The standard uncertainty (in percent) of parameter $b_3$ must be interpreted with care, since −174° is equal to 6°, for example.

Comparing the results with and without deletion of mavericks, the advantage of outlier detection becomes obvious in terms of the uncertainties of parameters as well.

### 4.5.4 Model mismatch

#### Example 1

Let us come back to the data set shown in Figures 4.3 – 4.5 on page 111f. The fitting based on a straight-line model

$$y = f(\mathbf{x}|\mathbf{a}) = a_1 + a_2 \cdot x$$

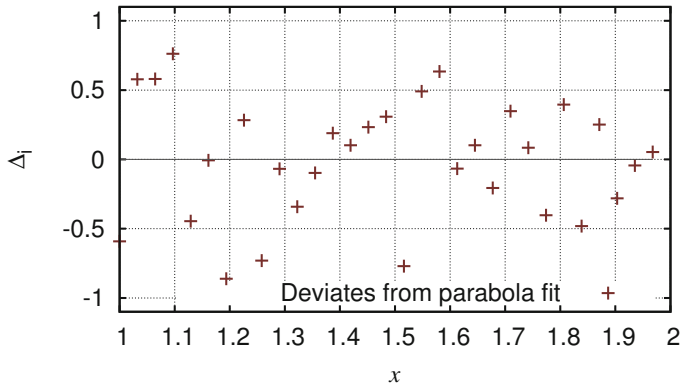


Figure 4.6: Plot of deviates $(y_i - f(\mathbf{x}_i|\mathbf{a}))$ based on the parabola fit

and equal weights leads to the following values

| $\chi^2$ | $g_{\text{fit}}$ | $\sigma_{a_1}[\%]$ | $\sigma_{a_2}[\%]$ |
|---|---|---|---|
| 13.011 | 0.449 | 3.96 | 3.07 |

.

The uncertainty of estimated parameters is reasonably low, leading to the assumption that the chosen model is suitable. The plot of residuals in Figure 4.5, however, gives indication of a model of higher order.

The goodness-of-fit is less than one, i.e., the uncertainty of the observations was over-estimated. One can interpret $g_{\text{fit}}$ as factor $k$ in equation (4.2), and since $w_i = w = 1$ was used, a squared uncertainty of $\sigma^2 = g_{\text{fit}}/w \approx 0.45$ can be derived. Actually, a variance of $\sigma^2 = 0.16$ was used for the generation of data via

$$y_i = f(\mathbf{x}_i|\mathbf{a}) = 10 + 20 \cdot x_i - 1 \cdot x_i^3 + \varepsilon_i \qquad \varepsilon_i \sim \mathcal{N}(0, 0.16) \; .$$

The increased value of the estimated $\sigma^2$ (compared to the true one) is a result of the model mismatch.

Now let us check what happens when a parabola is used instead of a straight line. Applying the model function

$$y = f(\mathbf{x}|\mathbf{a}) = a_1 + a_2 \cdot x + a_3 \cdot x^2$$

the plot of residuals looks more reasonable (**Figure 4.6**). The results of the data-fitting evaluation are

| $\chi^2$ | $g_{\text{fit}}$ | $\sigma_{a_1}[\%]$ | $\sigma_{a_2}[\%]$ | $\sigma_{a_3}[\%]$ |
|---|---|---|---|---|
| 5.602 | 0.200 | 118.26 | 9.73 | 16.43 |

.

The goodness-of-fit has changed to $g_{\text{fit}} = 0.200$, leading to a squared estimated standard deviation of observations of $\sigma^2 = g_{\text{fit}}/w \approx 0.2$, which is already closer to the true value of 0.16. The uncertainties of parameters, however, have increased dramatically.

Using the true third-order model

$$y = f(\mathbf{x}|\mathbf{a}) = a_1 + a_2 \cdot x + a_3 \cdot x^2 + a_4 \cdot x^3$$

things get even worse. The values are

| $\chi^2$ | $g_{\text{fit}}$ | $\sigma_{a_1}[\%]$ | $\sigma_{a_2}[\%]$ | $\sigma_{a_3}[\%]$ | $\sigma_{a_4}[\%]$ |
|---|---|---|---|---|---|
| 5.427 | 0.201 | 93.73 | 385.35 | 170.05 | 107.17 |

.

The estimated model parameters are very uncertain. Although this behaviour seems to be somewhat strange, everything is in accordance with the theory. The reasons become clear when the estimated parameters are compared with the true ones

| | $a_1$ | $a_2$ | $a_3$ | $a_4$ |
|---|---|---|---|---|
| True values | 10.00 | 20.00 | 0.00 | −1.00 |
| Estimated values | 14.17 | 7.24 | 11.25 | −4.01 |

.

The estimated parameters are really far from the true values. The slope change of the curve to be fitted (Figure 4.3) is simply not pronounced enough in comparison with the random error in the data, making it impossible to estimate the parameters with a sufficient accuracy. In addition, the uncertainty of parameters generally increases as the number of parameters increases, while the number of observations is fixed.

**Example 2**

Let us examine another example of model mismatch. Given is a harmonic oscillation with a linear trend according to the model function

$$y_i = a_1 + a_2 \cdot x + a_3 \cdot \cos(x_i - a_4) + \varepsilon_i \qquad \varepsilon_i \sim \mathcal{N}(0, 0.01) \; . \tag{4.8}$$

The data points are slightly disturbed by random errors following a Gaussian distribution with $\sigma = 0.1$. **Figure 4.7** shows the corresponding plot. The model parameters are $a_1 = 6$, $a_2 = 1.5$, $a_3 = 5$, and $a_4 = 0.0873$ $(= 5°)$. The additive noise was generated based on a Gaussian distribution ($\overline{\varepsilon_i} = 0, \sigma = 0.1$). Inspecting the plot could indicate a cubic polynomial, i.e.

$$y = a_1 + a_2 \cdot x + a_3 \cdot x^2 + a_4 \cdot x^3 \; .$$

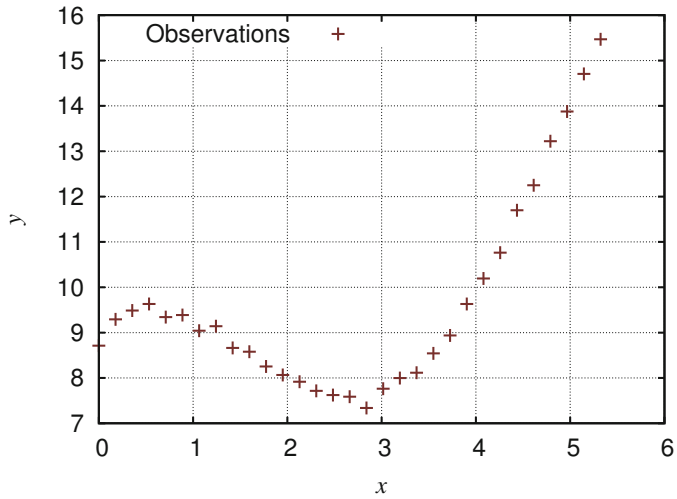


Figure 4.7: Harmonic oscillation with trend

As an alternative, a second-order trigonometric polynomial (see eq. (2.15) in Section 2.5) could be used as model function

$$y = f(x|\mathbf{a}) = a_1 + a_2 \cdot \cos(a_3 x - a_4) + a_5 \cdot \cos(2a_3 x - a_6) \; .$$

Fitting the data points with the true and the presumed polynomial model functions leads to the following numerical results

| | $a_1$ | $a_2$ | $a_3$ | $a_4$ | $a_5$ | $a_6$ |
|---|---|---|---|---|---|---|
| True values | 6.00 | 1.50 | 3.00 | 0.0873 | –– | –– |
| Estimated cosine + trend | 6.01 | 1.49 | 2.92 | 0.0843 | –– | –– |
| Estimated polynomial | 9.44 | −0.026 | −0.660 | 0.170 | –– | –– |
| Trigonometric polynomial | −28.7 | 60.3 | 0.288 | −5.23 | 23.2 | −7.52 |

.

The fitted curve in **Figure 4.8**, corresponding to the polynomial model function, already reveals problems, which become even more visible when the plot of residuals is inspected (**Figure 4.9**). In addition, the uncertainties of the estimated parameters clearly point to a model mismatch, as can be seen in the following table

| $\chi^2$ | $g_{\text{fit}}$ | $\sigma_{a_1}[\%]$ | $\sigma_{a_2}[\%]$ | $\sigma_{a_3}[\%]$ | $\sigma_{a_4}[\%]$ |
|---|---|---|---|---|---|
| 3.272 | 0.121 | 2.36 | 1436.30 | 24.61 | 11.81 |

.

Parameter $a_2$ is completely uncertain; in addition, the values of $a_3$ and $a_4$ seem not to be trustworthy.

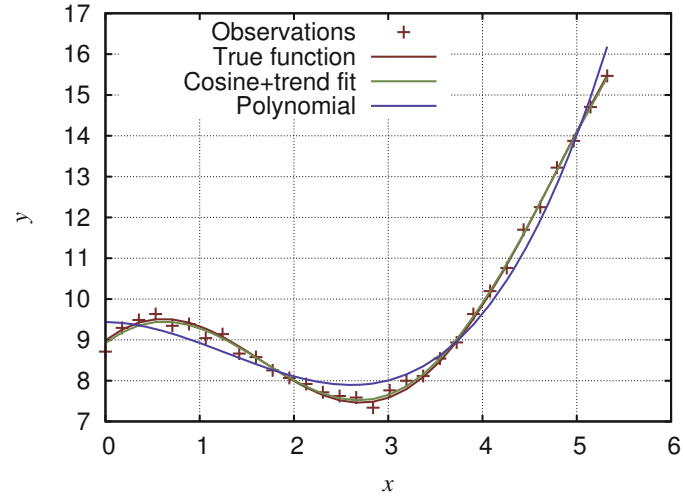


Figure 4.8: Fitting a harmonic oscillation with trend

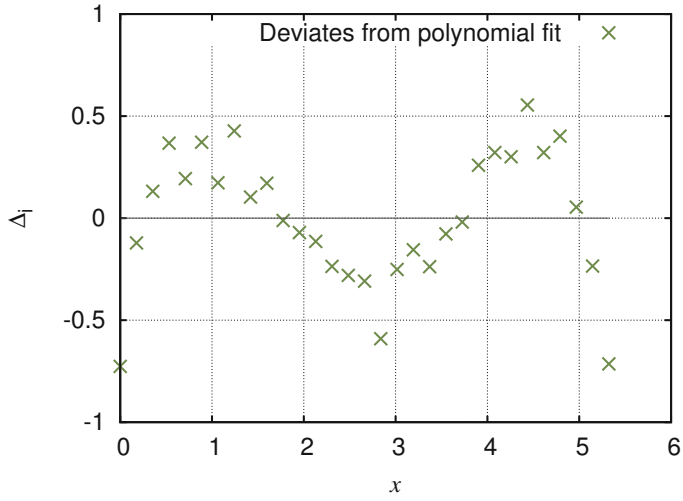


Figure 4.9: Plot of deviates of fitting a harmonic oscillation with trend using a third-order polynomial

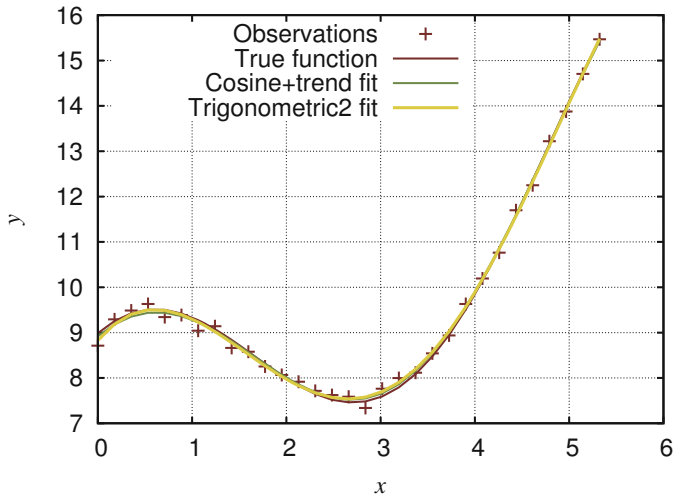


Figure 4.10: Fitting aharmonic oscillation with trend using a second-order trigonometric polynomial

The application of the trigonometric polynomial yields a better fit, mainly because it comprises more model parameters (**Figure 4.10**). The evaluation results are

| $\chi^2$ | $g_{\text{fit}}$ | $\sigma_{a_1}[\%]$ | $\sigma_{a_2}[\%]$ | $\sigma_{a_3}[\%]$ | $\sigma_{a_4}[\%]$ | $\sigma_{a_5}[\%]$ | $\sigma_{a_6}[\%]$ |
|---|---|---|---|---|---|---|---|
| 0.288 | 0.012 | 269.3 | 183.5 | 38.54 | 10.21 | 145.69 | 10.14 |

.

The uncertainties of all parameters are relatively high. Although the uncertainties generally increase with decreasing value of $M/N$ (number of parameters/ number of observations), it can still be concluded that the chosen trigonometric model function is not appropriate.

Fitting using the correct model results to

| $\chi^2$ | $g_{\text{fit}}$ | $\sigma_{a_1}[\%]$ | $\sigma_{a_2}[\%]$ | $\sigma_{a_3}[\%]$ | $\sigma_{a_4}[\%]$ |
|---|---|---|---|---|---|
| 0.332 | 0.012 | 1.28 | 1.86 | 1.40 | 21.27 |

.

Here, only the phase shift ($a_4$) seems to be somewhat uncertain. This, however, is rather typical in fitting oscillations, especially because of the duality $\cos(\alpha) = \cos(2\pi - \alpha)$.

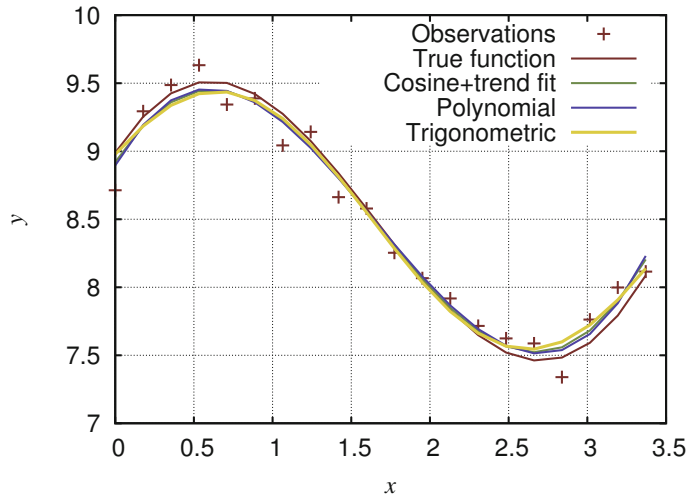


Figure 4.11: Fitting a harmonic oscillation with trend, limited range of conditions

**Example 3**

Unfortunately, the indication of model mismatch is not always such obvious as in Example 2. Let us take the same data points from the previous example, but using a more narrow range of conditions (**Figure 4.11**). The range is now cut at about $x = 3.37$ decreasing the influence of the trend (parameter $a_2$ in eq. 4.8). The estimated parameters changes to

| | $a_1$ | $a_2$ | $a_3$ | $a_4$ |
|---|---|---|---|---|
| True values | 6.00 | 1.50 | 3.00 | 0.0873 |
| Estimated cosine + trend | 5.95 | 1.54 | 2.98 | 0.0747 |
| Estimated polynomial | 8.90 | 2.034 | −2.073 | 0.419 |
| Trigonometric 1st order | 8.49 | 0.948 | 1.591 | 1.033 |

and their uncertainties to

| | $\chi^2$ | $g_{\text{fit}}$ | $\sigma_{a_1}[\%]$ | $\sigma_{a_2}[\%]$ | $\sigma_{a_3}$ | $\sigma_{a_4}[\%]$ |
|---|---|---|---|---|---|---|
| Cosine + trend | 0.242 | 0.017 | 5.26 | 11.87 | 8.43 | 35.49 |
| 3rd order polynomial | 0.255 | 0.016 | 1.06 | 12.27 | 8.42 | 8.12 |
| Trigonometric 1st order | 0.324 | 0.142 | 0.38 | 4.71 | 3.32 | 10.19 |

.

Although the estimated parameters of the correct model remain nearly the same, its advantage over the polynomial approaches has vanished. This is also reflected

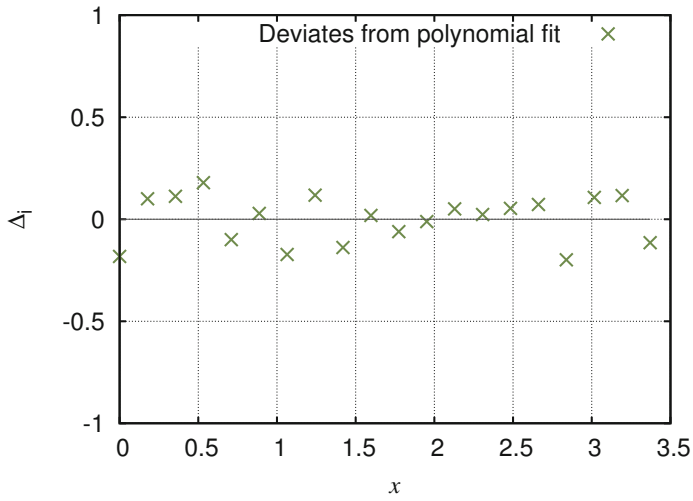


Figure 4.12: Plot of deviates of fitting a harmonic oscillation with trend using a third-order polynomial (limited range of conditions)

in the fitted curves (Figure 4.11). The plot of residual is not suspicious any more, either (**Figure 4.12**).

The results can be summarised in two statements

- It is possible to accurately fit data points stemming from an unknown model by a polynomial or trigonometric polynomial of adequate order, presuming the range of conditions is sufficiently narrow compared to that model order.
- The wider the range of condition, under which the observations are taken, the more reliably the test of model mismatch can be done.

## 4.6 Test questions

**4.1** The goodness-of-fit indicates the consistency of the model function and data only if a certain prerequisite is fulfilled. What is the prerequisite?

**4.2** Explain the difference between precision and accuracy.

**4.3** Explain the difference between systematic and random errors?

**4.4** How does the goodness-of-fit influence the standard uncertainty of the estimated model parameters?

**4.5** On what does the uncertainty of model prediction depend?

**4.6** What does the uncertainty of estimated model parameters tell us?

**4.7** How can model mismatch be detected?

# Part II

# Mathematics, Optimisation Methods, and Add ons

# Chapter 5

# Matrix Algebra

This chapter briefly repeats basics and algorithms of linear algebra required for the understanding of the least-squares equations used in the previous chapters. For readers without any knowledge in linear algebra, we recommend to consult in addition textbooks about this topic as for instance "Linear algebra and its applications" by G. Strang [Str88].

## 5.1 Basics

A *matrix* is a rectangular array of numbers arranged in rows and columns. The elements of a matrix are referred using coordinates $i$ and $j$. $a_{ij}$ is the element in the $i$th row and the $j$th column of matrix $\mathbf{A}$. The number of rows is denoted by $N$, the number of columns by $M$

$$\mathbf{A} = \begin{pmatrix} a_{11} & a_{12} & \cdots & a_{1j} & \cdots & a_{1M} \\ a_{21} & a_{22} & \cdots & a_{2j} & \cdots & a_{2M} \\ \vdots & \vdots & \ddots & \cdots & \cdots & \vdots \\ a_{i1} & a_{i2} & \vdots & a_{ij} & \cdots & a_{iM} \\ \vdots & \vdots & \vdots & \vdots & \ddots & \vdots \\ a_{N1} & a_{N2} & \cdots & a_{Nj} & \cdots & a_{NM} \end{pmatrix}.$$

Matrices with the same number of rows and columns are *square*. If $a_{ij} = 0$ for all $i \neq j$, $\mathbf{A}$ is *diagonal*. Matrix $\mathbf{B}$ with $b_{ij} = a_{ji}$ for all $i$ and $j$ is called the *transpose* of $\mathbf{A}$ or $\mathbf{B} = \mathbf{A}^{\mathrm{T}}$. In the case of $a_{ij} = a_{ji}$, i.e. $\mathbf{A} = \mathbf{A}^{\mathrm{T}}$, $\mathbf{A}$ is called *symmetric*.

**Examples**:

$$\text{square matrix:} \quad \mathbf{A} = \begin{pmatrix} 1 & 3 & 4 \\ 2 & 2 & 1 \\ 5 & 7 & 3 \end{pmatrix}$$

$$\text{non-square matrix:} \quad \mathbf{A} = \begin{pmatrix} 6 & 3 & 4 \\ 2 & 8 & 1 \end{pmatrix}$$

T. Strutz, *Data Fitting and Uncertainty*, DOI 10.1007/978-3-8348-9813-5 _5,

$$\text{diagonal matrix:} \quad \mathbf{A} = \begin{pmatrix} 1 & 0 & 0 \\ 0 & 2 & 0 \\ 0 & 0 & 3 \end{pmatrix}$$

$$\text{matrix and its transpose:} \quad \mathbf{A} = \begin{pmatrix} 1 & 2 & 3 & 4 \\ 5 & 6 & 7 & 8 \end{pmatrix} \quad \mathbf{A}^{\mathrm{T}} = \begin{pmatrix} 1 & 5 \\ 2 & 6 \\ 3 & 7 \\ 4 & 8 \end{pmatrix}$$

$$\text{symmetric matrix:} \quad \mathbf{A} = \mathbf{A}^{\mathrm{T}} = \begin{pmatrix} 1 & 2 & 3 \\ 2 & 4 & 5 \\ 3 & 5 & 6 \end{pmatrix}$$

□□□

If the number of rows $N$ is equal to one, the matrix is reduced to a *row vector* $\mathbf{a} = (a_1\ a_2\ \ldots\ a_M)$. When, in contrast, the number of columns $M$ is equal to one, the matrix is called *column vector* $\mathbf{a} = (a_1\ a_2\ \ldots\ a_N)^{\mathrm{T}}$.

**Examples**:

$$\text{row vector:} \quad \mathbf{a} = \begin{pmatrix} 1 & 3 & 4 & 7 \end{pmatrix} \qquad \text{column vector} \quad \mathbf{b} = \mathbf{a}^{\mathrm{T}} = \begin{pmatrix} 1 \\ 3 \\ 4 \\ 7 \end{pmatrix}$$

□□□

A square matrix, whose diagonal elements ($i = j$) are equal to one and whose off-diagonal elements ($i \neq j$) are equal to zero, is an *identity matrix* (sometimes also called *unity matrix*), denoted by $\mathbf{I}$ with the property $\mathbf{A} \cdot \mathbf{I} = \mathbf{A}$.

**Example**: identity matrix

$$\mathbf{I} = \begin{pmatrix} 1 & 0 & \cdots & 0 & 0 \\ 0 & 1 & \cdots & 0 & 0 \\ \vdots & \vdots & \ddots & \vdots & \vdots \\ 0 & 0 & \cdots & 1 & 0 \\ 0 & 0 & \cdots & 0 & 1 \end{pmatrix}$$

□□□

A system of linear equations like

$$\begin{aligned}
a_{11}x_1 + a_{12}x_2 + \cdots + a_{1j}x_j + \cdots + a_{1M}x_M &= y_1 \\
a_{21}x_1 + a_{22}x_2 + \cdots + a_{2j}x_j + \cdots + a_{2M}x_M &= y_2 \\
&\vdots \\
a_{i1}x_1 + a_{i2}x_2 + \cdots + a_{ij}x_j + \cdots + a_{iM}x_M &= y_i \\
&\vdots \\
a_{N1}x_1 + a_{N2}x_2 + \cdots + a_{Nj}x_j + \cdots + a_{NM}x_M &= y_N
\end{aligned}$$

can be easily written as

$$\mathbf{A} \cdot \mathbf{x} = \mathbf{y} \ ,$$

that is,

$$\begin{pmatrix} a_{11} & \cdots & a_{1M} \\ a_{21} & \cdots & a_{2M} \\ \vdots & \cdots & \vdots \\ a_{N1} & \cdots & a_{NM} \end{pmatrix} \cdot \begin{pmatrix} x_1 \\ \vdots \\ x_M \end{pmatrix} = \begin{pmatrix} y_1 \\ y_2 \\ \vdots \\ y_N \end{pmatrix} \ ,$$

where $\mathbf{x}$ and $\mathbf{y}$ are column vectors with $M$ and $N$ elements, respectively.

When $\mathbf{A}$ is a $N \times M$ matrix and $\mathbf{B}$ of size $M \times K$, then the $N \times K$ elements of the product $\mathbf{C}$ are computed according

$$\mathbf{C} = \mathbf{AB} \quad \longrightarrow \quad c_{ik} = \sum_{j=1}^{M} a_{ij} \cdot b_{jk} \ ,$$

thus, $c_{ik}$ is the inner product of the $i$th row of $\mathbf{A}$ and the $k$th column of $\mathbf{B}$. The number of columns in $\mathbf{A}$ must be equal to the number of rows of $\mathbf{B}$.

**Example**: matrix multiplication

$$\mathbf{A} = \begin{pmatrix} 1 & 1 & 2 \\ 2 & 2 & 1 \end{pmatrix} \qquad \mathbf{B} = \begin{pmatrix} 0 & 1 \\ 2 & 4 \\ 1 & 1 \end{pmatrix}$$

$$\mathbf{A} \cdot \mathbf{B} = \begin{pmatrix} 4 & 7 \\ 5 & 11 \end{pmatrix} \qquad \mathbf{B} \cdot \mathbf{A} = \begin{pmatrix} 2 & 2 & 1 \\ 10 & 10 & 8 \\ 3 & 3 & 3 \end{pmatrix}$$

□□□

The product of two matrices is in general dependent on their order, thus $\mathbf{AB} \neq \mathbf{BA}$.

**Example**: matrix multiplication

$$\mathbf{A} = \begin{pmatrix} 1 & 1 & 2 \\ 2 & 2 & 1 \\ 1 & 3 & 3 \end{pmatrix} \qquad \mathbf{B} = \begin{pmatrix} 0 & 0 & 1 \\ 2 & 4 & 0 \\ 1 & 1 & 2 \end{pmatrix}$$

$$\mathbf{A} \cdot \mathbf{B} = \begin{pmatrix} 4 & 6 & 5 \\ 5 & 9 & 4 \\ 9 & 15 & 7 \end{pmatrix} \qquad \mathbf{B} \cdot \mathbf{A} = \begin{pmatrix} 1 & 3 & 3 \\ 10 & 10 & 8 \\ 5 & 9 & 9 \end{pmatrix}$$

□□□

In addition, the multiplication is associative, i.e.,

$$(\mathbf{AB})\mathbf{C} = \mathbf{A}(\mathbf{BC}) \; . \tag{5.1}$$

Further, $(\mathbf{AB})^{\mathrm{T}} = \mathbf{B}^{\mathrm{T}}\mathbf{A}^{\mathrm{T}}$ holds.

**Example**:

$$\mathbf{A} = \begin{pmatrix} 1 & 3 \\ 2 & 2 \end{pmatrix} \qquad \mathbf{B} = \begin{pmatrix} 0 & 1 \\ 6 & 5 \end{pmatrix}$$

$$(\mathbf{A} \cdot \mathbf{B})^{\mathrm{T}} = \begin{pmatrix} 18 & 12 \\ 16 & 12 \end{pmatrix}$$

$$\mathbf{B}^{\mathrm{T}} \cdot \mathbf{A}^{\mathrm{T}} = \begin{pmatrix} 0 & 6 \\ 1 & 5 \end{pmatrix} \cdot \begin{pmatrix} 1 & 2 \\ 3 & 2 \end{pmatrix} = \begin{pmatrix} 18 & 12 \\ 16 & 12 \end{pmatrix}$$

□□□

If the determinant[1] $\det(\mathbf{A})$ of a square matrix $\mathbf{A}$ is equal to zero, then $\mathbf{A}$ is *singular* and no inverse of $\mathbf{A}$ exists, otherwise $\mathbf{A}$ is *nonsingular* and there is an *inverse* matrix $\mathbf{A}^{-1}$, such that $\mathbf{A}\mathbf{A}^{-1} = \mathbf{A}^{-1}\mathbf{A} = \mathbf{I}$.

[1] see Section 5.2

## 5.2 Determinants

The *determinant* of a square $N \times N$ matrix $\mathbf{A}_N$

$$\det(\mathbf{A}_N) = \begin{vmatrix} a_{11} & \cdots & a_{1N} \\ a_{21} & \cdots & a_{2N} \\ \vdots & \ddots & \vdots \\ a_{N1} & \cdots & a_{NN} \end{vmatrix} \tag{5.2}$$

is a scalar value. The calculation of determinants of second and third order, i.e. of $2 \times 2$ and $3 \times 3$ matrices, is rather simple

$$\det(\mathbf{A}_2) = \begin{vmatrix} a_{11} & a_{12} \\ a_{21} & a_{22} \end{vmatrix} = a_{11} \cdot a_{22} - a_{12} \cdot a_{21} \tag{5.3}$$

and

$$\det(\mathbf{A}_3) = \begin{vmatrix} a_{11} & a_{12} & a_{13} \\ a_{21} & a_{22} & a_{23} \\ a_{31} & a_{32} & a_{33} \end{vmatrix} = \begin{array}{l} a_{11}a_{22}a_{33} + a_{12}a_{23}a_{31} + a_{13}a_{21}a_{32} - \\ (a_{13}a_{22}a_{31} + a_{11}a_{23}a_{32} + a_{12}a_{21}a_{33}) \end{array} . \tag{5.4}$$

For determinants of higher order, *cofactors* $A^{jk}$ of $\mathbf{A}$ have to be introduced. Cofactors are defined as $(-1)^{j+k}$ times the *minor* $M^{jk}$ of $\mathbf{A}$. The minor $M^{jk}$ is in turn the determinant of a subset of $\mathbf{A}$ given by cancelling all elements of the $j$th row and the $k$th column.

**Example**:
The cofactor $A^{23}$ of a $3 \times 3$ matrix $\mathbf{A}$ is computed as follows.

At first the second row and the third column are deleted.

$$\mathbf{A} = \begin{pmatrix} a_{11} & a_{12} & a_{13} \\ a_{21} & a_{22} & a_{23} \\ a_{31} & a_{32} & a_{33} \end{pmatrix} \longrightarrow \begin{pmatrix} a_{11} & a_{12} & | \\ -- & -- & | \\ a_{31} & a_{32} & | \end{pmatrix}$$

The determinant of the remaining submatrix leads to the minor

$$M^{23} = \begin{vmatrix} a_{11} & a_{12} \\ a_{31} & a_{32} \end{vmatrix} = a_{11} \cdot a_{32} - a_{12} \cdot a_{31}$$

and, choosing the right sign, the cofacter can be derived as

$$A^{23} = (-1)^{2+3} \cdot M^{23} = -(a_{11} \cdot a_{32} - a_{12} \cdot a_{31}) .$$

□□□

Then, the determinant of arbitrary order is defined by a recursive process which is either an expansion along the $j$th column

$$\det(\mathbf{A}_N) = a_{1j} \cdot A^{1j} + a_{2j} \cdot A^{2j} + \ldots + a_{Nj} \cdot A^{Nj}$$

or an expansion along the $i$th row

$$\det(\mathbf{A}_N) = a_{i1} \cdot A^{i1} + a_{i2} \cdot A^{i2} + \ldots + a_{iN} \cdot A^{iN} \ .$$

Determinants equal to zero indicate the singularity of the corresponding matrix, as will become obvious in Subsection 5.3.1, equation (5.5). Nearly singular matrices have a very small determinant. A matrix is singular, for example, if one of its columns is equal to the multiple of another column.

**Example**:

$$\mathbf{A} = \begin{pmatrix} a_{11} & a_{12} & c \cdot a_{11} \\ a_{21} & a_{22} & c \cdot a_{21} \\ a_{31} & a_{32} & c \cdot a_{31} \end{pmatrix} \qquad \text{with } c = \text{const.}$$

The determinant is according to equation (5.4) equal to

$$\begin{aligned} \det(\mathbf{A}) &= a_{11}a_{22}ca_{31} + a_{12}ca_{21}a_{31} + ca_{11}a_{21}a_{32} - \\ &\quad (ca_{11}a_{22}a_{31} + a_{12}a_{21}ca_{31} + a_{11}ca_{21}a_{32}) \\ &= c \cdot (a_{11}a_{22}a_{31} + a_{12}a_{21}a_{31} + a_{11}a_{21}a_{32}) - \\ &\quad c \cdot (a_{11}a_{22}a_{31} + a_{12}a_{21}a_{31} + a_{11}a_{21}a_{32}) \\ &= 0 \ . \end{aligned}$$

□□□

The same holds true if one of the rows is a multiple of another row, as can be easily verified. However, this is not the sole reason of having a determinant equal to zero, as the following example shows

$$\mathbf{A} = \begin{pmatrix} 2 & 1 & 3 \\ 1 & 4 & 1 \\ 3 & 5 & 4 \end{pmatrix} \ .$$

In this case, the rows are not linearly independent of each other. The sum of the first two rows is equal to the third row.

## 5.3 Numerical solutions for matrix inversion

Solving least-squares problems using computer programs requires numerical solutions. The inversion of the square matrix $\mathbf{N} = \mathbf{J}^{\mathrm{T}}\mathbf{W}\mathbf{J}$ in equations (2.6) or (2.10) is the only problematical operation. There are different methods to invert matrices; four of them will be explained in the following.

### 5.3.1 Cofactor-matrix method

The cofactor-matrix approach is a basic method for inversion of square matrices, but should be used only for small matrices for different reasons.

Using the determinant $\det(\mathbf{A})$ and cofactors $A^{jk}$ (see Section 5.2), the inverse matrix $\mathbf{A}^{-1}$ of $\mathbf{A}$ with the property $\mathbf{A}^{-1} \cdot \mathbf{A} = \mathbf{A} \cdot \mathbf{A}^{-1} = \mathbf{I}$ is defined by

$$\mathbf{A}^{-1} = \frac{1}{\det(\mathbf{A})} \cdot \begin{pmatrix} A^{11} & A^{21} & \cdots & A^{M1} \\ A^{12} & A^{22} & \cdots & A^{M2} \\ \vdots & \vdots & \cdots & \vdots \\ A^{1M} & A^{2M} & \cdots & A^{MM} \end{pmatrix} . \tag{5.5}$$

Thus the inverses of a $2 \times 2$ matrix $\mathbf{A}_2$ and a $3 \times 3$ matrix $\mathbf{A}_3$ are

$$(\mathbf{A}_2)^{-1} = \frac{1}{a_{11} \cdot a_{22} - a_{12} \cdot a_{21}} \cdot \begin{pmatrix} a_{22} & -a_{12} \\ -a_{21} & a_{11} \end{pmatrix} \tag{5.6}$$

and

$$(\mathbf{A}_3)^{-1} = \frac{1}{\det(\mathbf{A}_3)} \cdot \begin{pmatrix} (a_{22}a_{33} - a_{23}a_{32}) & -(a_{21}a_{33} - a_{23}a_{31}) & (a_{21}a_{32} - a_{22}a_{31}) \\ -(a_{12}a_{33} - a_{13}a_{32}) & (a_{11}a_{33} - a_{13}a_{31}) & -(a_{11}a_{32} - a_{12}a_{31}) \\ (a_{12}a_{23} - a_{13}a_{22}) & -(a_{11}a_{23} - a_{13}a_{21}) & (a_{11}a_{22} - a_{12}a_{21}) \end{pmatrix} . \tag{5.7}$$

The recursive development of determinants of higher order is disadvantageous in computational solutions and can be source of accumulation of round-off errors. That is why the cofactor method should not be used for matrices larger than $3 \times 3$.

The precomputed inverse of a $4 \times 4$ matrix $\mathbf{A}_4$ is

$$(\mathbf{A}_4)^{-1} = \frac{1}{\delta} \cdot \begin{pmatrix} \alpha_{11} & \alpha_{12} & \alpha_{13} & \alpha_{14} \\ \alpha_{21} & \alpha_{22} & \alpha_{23} & \alpha_{24} \\ \alpha_{31} & \alpha_{32} & \alpha_{33} & \alpha_{34} \\ \alpha_{41} & \alpha_{42} & \alpha_{43} & \alpha_{44} \end{pmatrix} \tag{5.8}$$

with

$$\begin{aligned}\delta \;=\;& a_{11}a_{22}a_{33}a_{44} - a_{11}a_{22}a_{34}a_{43} - a_{11}a_{32}a_{23}a_{44} + a_{11}a_{32}a_{24}a_{43} + \\ & a_{11}a_{42}a_{23}a_{34} - a_{11}a_{42}a_{24}a_{33} - a_{21}a_{12}a_{33}a_{44} + a_{21}a_{12}a_{34}a_{43} + \\ & a_{21}a_{32}a_{13}a_{44} - a_{21}a_{32}a_{14}a_{43} - a_{21}a_{42}a_{13}a_{34} + a_{21}a_{42}a_{14}a_{33} + \\ & a_{31}a_{12}a_{23}a_{44} - a_{31}a_{12}a_{24}a_{43} - a_{31}a_{22}a_{13}a_{44} + a_{31}a_{22}a_{14}a_{43} + \\ & a_{31}a_{42}a_{13}a_{24} - a_{31}a_{42}a_{14}a_{23} - a_{41}a_{12}a_{23}a_{34} + a_{41}a_{12}a_{24}a_{33} + \\ & a_{41}a_{22}a_{13}a_{34} - a_{41}a_{22}a_{14}a_{33} - a_{41}a_{32}a_{13}a_{24} + a_{41}a_{32}a_{14}a_{23}\end{aligned}$$

$$\begin{aligned}\alpha_{11} &= a_{22}\cdot(a_{33}a_{44} - a_{34}a_{43}) - a_{32}\cdot(a_{23}a_{44} - a_{24}a_{43}) + a_{42}\cdot(a_{23}a_{34} - a_{24}a_{33}) \\ \alpha_{12} &= -a_{12}\cdot(a_{33}a_{44} - a_{34}a_{43}) + a_{32}\cdot(a_{13}a_{44} - a_{14}a_{43}) - a_{42}\cdot(a_{13}a_{34} - a_{14}a_{33}) \\ \alpha_{13} &= a_{12}\cdot(a_{23}a_{44} - a_{24}a_{43}) - a_{22}\cdot(a_{13}a_{44} - a_{14}a_{43}) + a_{42}\cdot(a_{13}a_{24} - a_{14}a_{23}) \\ \alpha_{14} &= -a_{12}\cdot(a_{23}a_{34} - a_{24}a_{33}) + a_{22}\cdot(a_{13}a_{34} - a_{14}a_{33}) - a_{32}\cdot(a_{13}a_{24} - a_{14}a_{23})\end{aligned}$$

$$\begin{aligned}\alpha_{21} &= -a_{21}\cdot(a_{33}a_{44} - a_{34}a_{43}) + a_{31}\cdot(a_{23}a_{44} - a_{24}a_{43}) - a_{41}\cdot(a_{23}a_{34} - a_{24}a_{33}) \\ \alpha_{22} &= a_{11}\cdot(a_{33}a_{44} - a_{34}a_{43}) - a_{31}\cdot(a_{13}a_{44} - a_{14}a_{43}) + a_{41}\cdot(a_{13}a_{34} - a_{14}a_{33}) \\ \alpha_{23} &= -a_{11}\cdot(a_{23}a_{44} - a_{24}a_{43}) + a_{21}\cdot(a_{13}a_{44} - a_{14}a_{43}) - a_{41}\cdot(a_{13}a_{24} - a_{14}a_{23}) \\ \alpha_{24} &= a_{11}\cdot(a_{23}a_{34} - a_{24}a_{33}) - a_{21}\cdot(a_{13}a_{34} - a_{14}a_{33}) + a_{31}\cdot(a_{13}a_{24} - a_{14}a_{23})\end{aligned}$$

$$\begin{aligned}\alpha_{31} &= a_{21}\cdot(a_{32}a_{44} - a_{34}a_{42}) - a_{31}\cdot(a_{22}a_{44} - a_{24}a_{42}) + a_{41}\cdot(a_{22}a_{34} - a_{24}a_{32}) \\ \alpha_{32} &= -a_{11}\cdot(a_{32}a_{44} - a_{34}a_{42}) + a_{31}\cdot(a_{12}a_{44} - a_{14}a_{42}) - a_{41}\cdot(a_{12}a_{34} - a_{14}a_{32}) \\ \alpha_{33} &= a_{11}\cdot(a_{22}a_{44} - a_{24}a_{42}) - a_{21}\cdot(a_{12}a_{44} - a_{14}a_{42}) + a_{41}\cdot(a_{12}a_{24} - a_{14}a_{22}) \\ \alpha_{34} &= -a_{11}\cdot(a_{22}a_{34} - a_{24}a_{32}) + a_{21}\cdot(a_{12}a_{34} - a_{14}a_{32}) - a_{31}\cdot(a_{12}a_{24} - a_{14}a_{22})\end{aligned}$$

$$\begin{aligned}\alpha_{41} &= -a_{21}\cdot(a_{32}a_{43} - a_{33}a_{42}) + a_{31}\cdot(a_{22}a_{43} - a_{23}a_{42}) - a_{41}\cdot(a_{22}a_{33} - a_{23}a_{32}) \\ \alpha_{42} &= a_{11}\cdot(a_{32}a_{43} - a_{33}a_{42}) - a_{31}\cdot(a_{12}a_{43} - a_{13}a_{42}) + a_{41}\cdot(a_{12}a_{33} - a_{13}a_{32}) \\ \alpha_{43} &= -a_{11}\cdot(a_{22}a_{43} - a_{23}a_{42}) + a_{21}\cdot(a_{12}a_{43} - a_{13}a_{42}) - a_{41}\cdot(a_{12}a_{23} - a_{13}a_{22}) \\ \alpha_{44} &= a_{11}\cdot(a_{22}a_{33} - a_{23}a_{32}) - a_{21}\cdot(a_{12}a_{33} - a_{13}a_{32}) + a_{31}\cdot(a_{12}a_{23} - a_{13}a_{22})\end{aligned}$$

### 5.3.2 Inversion via Gauss-Jordan elimination

The Gauss-Jordan elimination[2] is a version of the Gauss elimination[3] that produces not a upper triangular matrix but a diagonal one. It can be straightforwardly used for the inversion of square matrices.

[2] named after Carl-Friedrich Gauss (1777 – 1855) and Wilhelm Jordan (1842 – 1899)
[3] see, for instance, reference [Str88]

The basic idea is to augment the matrix with an identity matrix of proper size.

$$\mathbf{A} = \begin{pmatrix} a_{11} & a_{12} & a_{13} \\ a_{21} & a_{22} & a_{23} \\ a_{31} & a_{32} & a_{33} \end{pmatrix} \quad \Longrightarrow \quad [\mathbf{AI}] = \left(\begin{array}{ccc|ccc} a_{11} & a_{12} & a_{13} & 1 & 0 & 0 \\ a_{21} & a_{22} & a_{23} & 0 & 1 & 0 \\ a_{31} & a_{32} & a_{33} & 0 & 0 & 1 \end{array}\right)$$

This new matrix has to be modified in order to find a form

$$[\mathbf{IB}] \quad \text{with} \quad \mathbf{A}^{-1} = \mathbf{B}$$

The processing steps are as follows

1. Select the first column from the left, which has at least one non-zero element.
2. If the top element of the selected column equal to zero, then exchange the first row with another one that does not contain a zero element in this column. The desired elements on the diagonal are the *pivot*s and the exchange of rows is called *pivoting*.
3. Divide the first row by the top element of the selected column.
4. Multiples of the first row must be subtracted from all remaining rows in order to produce zeros at the first position of all rows.
5. Reduce the matrix by deleting the first row and the first column.
6. Repeat steps 1 to 5 until the entire matrix is triangular.
7. Do the same procedure in order to produce a diagonal (identity) matrix.

**Example**:

$$\mathbf{A} = \begin{pmatrix} 0 & 1 & 2 \\ 2 & 2 & 1 \\ 2 & 1 & 0 \end{pmatrix} \quad \Longrightarrow \quad [\mathbf{AI}] = \left(\begin{array}{ccc|ccc} 0 & 1 & 2 & 1 & 0 & 0 \\ 2 & 2 & 1 & 0 & 1 & 0 \\ 2 & 1 & 0 & 0 & 0 & 1 \end{array}\right)$$

The first column has non-zero elements, but the top element is zero. Therefore, the first two rows must exchanged (pivoting)

$$\left(\begin{array}{ccc|ccc} 2 & 2 & 1 & 0 & 1 & 0 \\ 0 & 1 & 2 & 1 & 0 & 0 \\ 2 & 1 & 0 & 0 & 0 & 1 \end{array}\right) .$$

Then, we divide the first row by its most-left element

$$\left(\begin{array}{ccc|ccc} 1 & 1 & 1/2 & 0 & 1/2 & 0 \\ 0 & 1 & 2 & 1 & 0 & 0 \\ 2 & 1 & 0 & 0 & 0 & 1 \end{array}\right) .$$

The second row already looks okay, but we have to subtract the first row two times from the third row

$$\left(\begin{array}{ccc|ccc} 1 & 1 & 1/2 & 0 & 1/2 & 0 \\ 0 & 1 & 2 & 1 & 0 & 0 \\ 0 & -1 & -1 & 0 & -1 & 1 \end{array}\right) .$$

Subtract second row multiplied with -1 from third row

$$\left(\begin{array}{ccc|ccc} 1 & 1 & 1/2 & 0 & 1/2 & 0 \\ 0 & 1 & 2 & 1 & 0 & 0 \\ 0 & 0 & 1 & 1 & -1 & 1 \end{array}\right) .$$

Subtract third row two times from second row. Subtract third row, times 1/2, from first row

$$\left(\begin{array}{ccc|ccc} 1 & 1 & 0 & -1/2 & 1 & -1/2 \\ 0 & 1 & 0 & -1 & 2 & -2 \\ 0 & 0 & 1 & 1 & -1 & 1 \end{array}\right) .$$

Subtract second from first row

$$\left(\begin{array}{ccc|ccc} 1 & 0 & 0 & 1/2 & -1 & 3/2 \\ 0 & 1 & 0 & -1 & 2 & -2 \\ 0 & 0 & 1 & 1 & -1 & 1 \end{array}\right) = [\mathbf{I}\mathbf{A}^{-1}] .$$

The result is

$$\mathbf{A}^{-1} = \frac{1}{2} \cdot \begin{pmatrix} 1 & -2 & 3 \\ -2 & 4 & -4 \\ 2 & -2 & 2 \end{pmatrix} = \frac{1}{\det(\mathbf{A})} \cdot \begin{pmatrix} -1 & 2 & -3 \\ 2 & -4 & 4 \\ -2 & 2 & -2 \end{pmatrix} .$$

□□□

### 5.3.3 Inversion via LU decomposition

#### Basic Idea

The idea of the LU approach is to split a square matrix $\mathbf{A}$ into two triangular matrices $\mathbf{L}$ and $\mathbf{U}$ such that

$$\mathbf{A} = \mathbf{L} \cdot \mathbf{U} \tag{5.9}$$

in which $\mathbf{L}$ is *lower triangular* and $\mathbf{U}$ is *upper triangular*

$$\mathbf{L} = \begin{pmatrix} \lambda_{11} & 0 & \cdots & 0 \\ \lambda_{21} & \lambda_{22} & \cdots & 0 \\ \vdots & \vdots & \ddots & \vdots \\ \lambda_{M1} & \lambda_{M2} & \cdots & \lambda_{MM} \end{pmatrix} \qquad \mathbf{U} = \begin{pmatrix} \upsilon_{11} & \upsilon_{12} & \cdots & \upsilon_{1M} \\ 0 & \upsilon_{22} & \cdots & \upsilon_{2M} \\ \vdots & \vdots & \ddots & \vdots \\ 0 & 0 & \cdots & \upsilon_{MM} \end{pmatrix} \tag{5.10}$$

with typically $\lambda_{jj} = 1$.

What is the advantage of this triangular representation? Let us consider again the case of a linear equation system

$$\mathbf{A} \cdot \mathbf{x} = \mathbf{y} \,, \tag{5.11}$$

where the result for $\mathbf{x}$ has to be found via matrix inversion

$$\mathbf{x} = \mathbf{A}^{-1} \cdot \mathbf{y} \,.$$

Using the LU decomposition we write instead

$$\mathbf{A} \cdot \mathbf{x} = (\mathbf{L} \cdot \mathbf{U}) \cdot \mathbf{x} = \mathbf{L} \cdot (\mathbf{U} \cdot \mathbf{x}) = \mathbf{L} \cdot \mathbf{u} = \mathbf{y} \tag{5.12}$$

in order to find a solution for $\mathbf{u}$ first. In a second step, $\mathbf{U} \cdot \mathbf{x} = \mathbf{u}$ has to be solved. Both cases can benefit from the properties of the triangular matrices as follows. Based on

$$\mathbf{L} \cdot \mathbf{u} = \begin{pmatrix} \lambda_{11} & 0 & \cdots & 0 \\ \lambda_{21} & \lambda_{22} & \cdots & 0 \\ \vdots & \vdots & \ddots & \vdots \\ \lambda_{M1} & \lambda_{M2} & \cdots & \lambda_{MM} \end{pmatrix} \cdot \begin{pmatrix} u_1 \\ u_2 \\ \vdots \\ u_M \end{pmatrix} = \begin{pmatrix} y_1 \\ y_2 \\ \vdots \\ y_M \end{pmatrix} \,, \tag{5.13}$$

the first element of $\mathbf{u}$ is simply

$$u_1 = \frac{y_1}{\lambda_{11}} \,,$$

the second element is computed via

$$\lambda_{21} \cdot u_1 + \lambda_{22} \cdot u_2 = y_2 \quad \rightsquigarrow \quad u_2 = \frac{y_2 - \lambda_{21} \cdot u_1}{\lambda_{22}} \,,$$

the third one by

$$\lambda_{31} \cdot u_1 + \lambda_{32} \cdot u_2 + \lambda_{33} \cdot u_3 = y_3 \quad \rightsquigarrow \quad u_3 = \frac{y_3 - \lambda_{21} \cdot u_1 - \lambda_{32} \cdot u_2}{\lambda_{33}} \,,$$

and so on and so forth. The general formula is

$$u_i = \frac{1}{\lambda_{ii}} \cdot \left[ y_i - \sum_{j=1}^{i-1} \lambda_{ij} \cdot u_j \right] \qquad i = 2, 3, \ldots, M \; . \tag{5.14}$$

As soon as $\mathbf{u}$ is known, equation

$$\mathbf{U} \cdot \mathbf{x} = \begin{pmatrix} \upsilon_{11} & \upsilon_{12} & \cdots & \upsilon_{1M} \\ 0 & \upsilon_{22} & \cdots & \upsilon_{2M} \\ \vdots & \vdots & \ddots & \vdots \\ 0 & 0 & \cdots & \upsilon_{MM} \end{pmatrix} \cdot \begin{pmatrix} x_1 \\ x_2 \\ \vdots \\ x_M \end{pmatrix} = \begin{pmatrix} u_1 \\ u_2 \\ \vdots \\ u_M \end{pmatrix} \tag{5.15}$$

is also solvable using the same procedure with the single difference that the last element $x_M$ is calculated first via

$$\upsilon_{MM} \cdot x_M = u_M \quad \rightsquigarrow \quad x_M = \frac{u_M}{\upsilon_{MM}} \; ,$$

the next element via

$$\begin{aligned} \upsilon_{M-1,M-1} \cdot x_{M-1} + \upsilon_{M-1,M} \cdot x_M &= u_{M-1} \\ \rightsquigarrow \quad x_{M-1} &= \frac{u_{M-1} - \upsilon_{M-1,M} \cdot x_M}{\upsilon_{M-1,M-1}} \; , \end{aligned}$$

or in general

$$x_i = \frac{1}{\upsilon_{ii}} \cdot \left[ u_i - \sum_{j=i+1}^{M} \upsilon_{ij} \cdot x_j \right] \qquad i = 2, 3, \ldots, M \; .$$

In principle, the inverse of $\mathbf{A}$ is not required to solve (5.11), since $\mathbf{x}$ results from equations (5.13) and (5.15). However, given the LU decomposition of $\mathbf{A}$, its inverse can be computed column by column. Using a vector $\mathbf{y}$ with all elements equal to zero apart from $y_i = 1$, the resulting vector $\mathbf{x}$ contains the $i$th column of $\mathbf{A}^{-1}$. This is explained below using a concrete example.

The decomposition of $\mathbf{A}$ into $\mathbf{L}$ and $\mathbf{U}$ is performed via the Gaussian elimination method (see [Str88], for instance) or Crout's algorithm (see [Pre92]).

**Example for LU decomposition**

The LU decomposition of $\mathbf{A}$ is computed in an iterative fashion. Let us define $\mathbf{A}^{(0)} = \mathbf{A}$ with

$$\mathbf{A} = \begin{pmatrix} 1 & 5 & 3 & 2 \\ 4 & 2 & 3 & 2 \\ 2 & 3 & 4 & 1 \\ 3 & 0 & 1 & 2 \end{pmatrix} .$$

The matrix elements below the main diagonal in the $n$-th column ($n = 1, 2, \ldots, N-1$) of $\mathbf{A}^{(n-1)}$ are eliminated by adding the $n$-th row multiplied by

$$b_{i,n} = -\frac{a_{i,n}^{(n-1)}}{a_{n,n}^{(n-1)}} \qquad a_{n,n}^{(n-1)} \neq 0$$

to the $i$-th row of this matrix for $i = n+1, 2, \ldots, N$. Please note that $(n-1)$ is not an exponent but indicates the matrix $\mathbf{A}^{(n-1)}$ at the iteration number $n-1$. In case that the element $a_{n,n}^{(n-1)}$ is zero, the $n$-th row must be interchanged with another row below before continuing. This corresponds to the procedure described in Subsection 5.3.2, steps 1.– 6.

For $n = 1$, the factors are

$$b_{2,1} = -\frac{a_{2,1}^{(0)}}{a_{1,1}^{(0)}} = -\frac{4}{1} \qquad b_{3,1} = -\frac{a_{3,1}^{(0)}}{a_{1,1}^{(0)}} = -\frac{2}{1} \qquad b_{4,1} = -\frac{a_{4,1}^{(0)}}{a_{1,1}^{(0)}} = -\frac{3}{1}$$

and the operations result in matrix

$$\mathbf{A}^{(1)} = \begin{pmatrix} 1 & 5 & 3 & 2 \\ 0 & -18 & -9 & -6 \\ 0 & -7 & -2 & -3 \\ 0 & -15 & -8 & -4 \end{pmatrix} .$$

This operation is equal to

$$\mathbf{A}^{(n)} = \mathbf{B}_n \cdot \mathbf{A}^{(n-1)}$$

with

$$\mathbf{B}_n = \begin{pmatrix} 1 & \cdots & 0 & \cdots & 0 \\ & \ddots & 0 & & 0 \\ & 0 & 1 & & \vdots \\ & 0 & b_{n+1,n} & \ddots & 0 \\ & 0 & \vdots & 0 & \ddots & \vdots \\ & 0 & b_{N,n} & 0 & & 1 \end{pmatrix} .$$

Using the example matrix, we have

$$\begin{aligned}\mathbf{A}^{(1)} = \mathbf{B}_1 \cdot \mathbf{A}^{(0)} &= \begin{pmatrix} 1 & 0 & 0 & 0 \\ -4 & 1 & 0 & 0 \\ -2 & 0 & 1 & 0 \\ -3 & 0 & 0 & 1 \end{pmatrix} \cdot \begin{pmatrix} 1 & 5 & 3 & 2 \\ 4 & 2 & 3 & 2 \\ 2 & 3 & 4 & 1 \\ 3 & 0 & 1 & 2 \end{pmatrix} \\ &= \begin{pmatrix} 1 & 5 & 3 & 2 \\ 0 & -18 & -9 & -6 \\ 0 & -7 & -2 & -3 \\ 0 & -15 & -8 & -4 \end{pmatrix}.\end{aligned}$$

The next iteration $n = 2$ yields

$$b_{3,2} = -\frac{a^{(1)}_{3,2}}{a^{(1)}_{2,2}} = -\frac{-7}{-18} = -\frac{7}{18} \qquad b_{4,2} = -\frac{a^{(1)}_{4,2}}{a^{(1)}_{2,2}} = -\frac{-15}{-18} = -\frac{15}{18}$$

and

$$\begin{aligned}\mathbf{A}^{(2)} = \mathbf{B}_2 \cdot \mathbf{A}^{(1)} &= \begin{pmatrix} 1 & 0 & 0 & 0 \\ 0 & 1 & 0 & 0 \\ 0 & -7/18 & 1 & 0 \\ 0 & -15/18 & 0 & 1 \end{pmatrix} \cdot \begin{pmatrix} 1 & 5 & 3 & 2 \\ 0 & -18 & -9 & -6 \\ 0 & -7 & -2 & -3 \\ 0 & -15 & -8 & -4 \end{pmatrix} \\ &= \begin{pmatrix} 1 & 5 & 3 & 2 \\ 0 & -18 & -9 & -6 \\ 0 & 0 & 3/2 & -2/3 \\ 0 & 0 & -1/2 & 1 \end{pmatrix}.\end{aligned}$$

The third and last iteration reads as

$$b_{4,3} = -\frac{a^{(2)}_{4,3}}{a^{(2)}_{3,3}} = -\frac{-1/2}{3/2} = \frac{1}{3}$$

and

$$\begin{aligned}\mathbf{A}^{(3)} = \mathbf{B}_3 \cdot \mathbf{A}^{(2)} &= \begin{pmatrix} 1 & 0 & 0 & 0 \\ 0 & 1 & 0 & 0 \\ 0 & 0 & 1 & 0 \\ 0 & 0 & 1/3 & 1 \end{pmatrix} \cdot \begin{pmatrix} 1 & 5 & 3 & 2 \\ 0 & -18 & -9 & -6 \\ 0 & 0 & 3/2 & -2/3 \\ 0 & 0 & -1/2 & 1 \end{pmatrix} \\ &= \underline{\underline{\begin{pmatrix} 1 & 5 & 3 & 2 \\ 0 & -18 & -9 & -6 \\ 0 & 0 & 3/2 & -2/3 \\ 0 & 0 & 0 & 7/9 \end{pmatrix}}}.\end{aligned}$$

The final upper triangular matrix $\mathbf{A}^{(N-1)}$ is equal to $\mathbf{U}$ from equation (5.9).

The lower triangular matrix $\mathbf{L}$ can be determined based on the given matrix $\mathbf{A}$ and the corresponding upper triangular matrix $\mathbf{U}$ via

$$\mathbf{A} = \mathbf{L} \cdot \mathbf{U}$$

$$\begin{pmatrix} 1 & 5 & 3 & 2 \\ 4 & 2 & 3 & 2 \\ 2 & 3 & 4 & 1 \\ 3 & 0 & 1 & 2 \end{pmatrix} = \begin{pmatrix} \lambda_{11} & 0 & 0 & 0 \\ \lambda_{21} & \lambda_{22} & 0 & 0 \\ \lambda_{31} & \lambda_{32} & \lambda_{33} & 0 \\ \lambda_{41} & \lambda_{42} & \lambda_{43} & \lambda_{44} \end{pmatrix} \cdot \begin{pmatrix} 1 & 5 & 3 & 2 \\ 0 & -18 & -9 & -6 \\ 0 & 0 & 3/2 & -2/3 \\ 0 & 0 & 0 & 7/9 \end{pmatrix}$$

$$\begin{aligned} a_{i1} &= \lambda_{i1} \cdot \upsilon_{11} \quad \rightsquigarrow \quad \lambda_{i1} = \frac{a_{i1}}{\upsilon_{11}} \\ a_{i2} &= \lambda_{i1} \cdot \upsilon_{12} + \lambda_{i2} \cdot \upsilon_{22} \quad \rightsquigarrow \quad \lambda_{i2} = \frac{a_{i2} - \lambda_{i1} \cdot \upsilon_{12}}{\upsilon_{22}} \\ a_{i3} &= \lambda_{i1} \cdot \upsilon_{13} + \lambda_{i2} \cdot \upsilon_{23} + \lambda_{i3} \cdot \upsilon_{33} \\ &\rightsquigarrow \quad \lambda_{i3} = \frac{a_{i3} - (\lambda_{i1} \cdot \upsilon_{13} + \lambda_{i2} \cdot \upsilon_{23})}{\upsilon_{33}} \end{aligned}$$

or in general

$$\lambda_{ij} = \frac{1}{\upsilon_{jj}} \cdot \left[ a_{ij} - \sum_{k=1}^{j-1} \lambda_{ik} \cdot \upsilon_{k,j} \right] \qquad i \geq j \tag{5.16}$$

leading to

$$\mathbf{L} = \begin{pmatrix} \lambda_{11} & 0 & 0 & 0 \\ \lambda_{21} & \lambda_{22} & 0 & 0 \\ \lambda_{31} & \lambda_{32} & \lambda_{33} & 0 \\ \lambda_{41} & \lambda_{42} & \lambda_{43} & \lambda_{44} \end{pmatrix} = \underline{\underline{\begin{pmatrix} 1 & 0 & 0 & 0 \\ 4 & 1 & 0 & 0 \\ 2 & 7/18 & 1 & 0 \\ 3 & 5/6 & -1/3 & 1 \end{pmatrix}}} .$$

The LU decomposition of $\mathbf{A}$ is finally

$$\begin{aligned} \mathbf{A} &= \begin{pmatrix} 1 & 5 & 3 & 2 \\ 4 & 2 & 3 & 2 \\ 2 & 3 & 4 & 1 \\ 3 & 0 & 1 & 2 \end{pmatrix} \\ &= \begin{pmatrix} 1 & 0 & 0 & 0 \\ 4 & 1 & 0 & 0 \\ 2 & 7/18 & 1 & 0 \\ 3 & 5/6 & -1/3 & 1 \end{pmatrix} \cdot \begin{pmatrix} 1 & 5 & 3 & 2 \\ 0 & -18 & -9 & -6 \\ 0 & 0 & 3/2 & -2/3 \\ 0 & 0 & 0 & 7/9 \end{pmatrix} . \end{aligned}$$

**Example for matrix inversion via LU decomposition**

Based on the LU decomposition example from previous Subsection

$$\mathbf{A} = \mathbf{L} \cdot \mathbf{U}$$

$$\begin{pmatrix} 1 & 5 & 3 & 2 \\ 4 & 2 & 3 & 2 \\ 2 & 3 & 4 & 1 \\ 3 & 0 & 1 & 2 \end{pmatrix} = \begin{pmatrix} 1 & 0 & 0 & 0 \\ 4 & 1 & 0 & 0 \\ 2 & 7/18 & 1 & 0 \\ 3 & 5/6 & -1/3 & 1 \end{pmatrix} \cdot \begin{pmatrix} 1 & 5 & 3 & 2 \\ 0 & -18 & -9 & -6 \\ 0 & 0 & 3/2 & -2/3 \\ 0 & 0 & 0 & 7/9 \end{pmatrix},$$

the inverse matrix $\mathbf{A}^{-1}$ has to be determined via equations (5.12), (5.13) and (5.15).

The determination $i$-th column of $\mathbf{A}^{-1}$ is based on a vector $\mathbf{y}$ with all elements equal to zero apart from $y_i = 1$. Here, only the first column of $\mathbf{A}^{-1}$ shall be computed.

Based on

$$\mathbf{L} \cdot \mathbf{u} = \mathbf{y} \tag{5.17}$$

$$\begin{pmatrix} 1 & 0 & 0 & 0 \\ 4 & 1 & 0 & 0 \\ 2 & 7/18 & 1 & 0 \\ 3 & 5/6 & -1/3 & 1 \end{pmatrix} \cdot \begin{pmatrix} u_1 \\ u_2 \\ u_3 \\ u_4 \end{pmatrix} = \begin{pmatrix} 1 \\ 0 \\ 0 \\ 0 \end{pmatrix}, \tag{5.18}$$

the vector $\mathbf{u}$ has firstly to be determined via eq. (5.14) leading to

$$\mathbf{u} = \begin{pmatrix} 1 & -4 & -4/9 & 5/27 \end{pmatrix}^{\mathrm{T}}.$$

Now $\mathbf{x}$, i.e. the first column of $\mathbf{A}^{-1}$, can be computed

$$\mathbf{U} \cdot \mathbf{x} = \mathbf{u}$$

$$\begin{pmatrix} 1 & 5 & 3 & 2 \\ 0 & -18 & -9 & -6 \\ 0 & 0 & 3/2 & -2/3 \\ 0 & 0 & 0 & 7/9 \end{pmatrix} \cdot \begin{pmatrix} x_1 \\ x_2 \\ x_3 \\ x_4 \end{pmatrix} = \begin{pmatrix} 1 \\ -4 \\ -4/9 \\ 5/27 \end{pmatrix},$$

leading to

$$\mathbf{x} = (a_{i1}) = \begin{pmatrix} -2/21 & 5/21 & -4/21 & 5/21 \end{pmatrix}^{\mathrm{T}}.$$

All other columns of $\mathbf{A}^{-1}$ are derived in the same manner, however, with shifted positions of the value of 1 in $\mathbf{y}$ of equation (5.18)

$$\mathbf{A}^{-1} = \frac{1}{21} \cdot \begin{pmatrix} -2 & 23 & -12 & -15 \\ 5 & 16 & -12 & -15 \\ -4 & -17 & 18 & 12 \\ 5 & -26 & 9 & 27 \end{pmatrix} .$$

**Determinant computation via LU decomposition**

The determinant of matrix $\mathbf{A}$ can be easily computed using the LU decomposition of $\mathbf{A}$. In general, if $\mathbf{A} = \mathbf{B} \cdot \mathbf{C}$ then $\det(\mathbf{A}) = \det(\mathbf{B}) \cdot \det(\mathbf{C})$. As the determinant of a triangular matrix is simply the product of its elements on the main diagonal,

$$\det(\mathbf{A}) = \det(\mathbf{L}) \cdot \det(\mathbf{U}) = 1 \cdot \det(\mathbf{U}) = \prod_{i=1}^{M} v_{ii}$$

holds with $v_{ii}$ according to equation (5.10).

### 5.3.4 Inversion by singular value decomposition (SVD)

The method of singular value decomposition enables the direct inversion even of non-square matrices. Each rectangular $N \times M$ matrix can be decomposed into a $N \times M$ matrix $\mathbf{U}$, a diagonal matrix $\mathbf{S}$ containing the so-called singular values, and a $M \times M$ matrix $\mathbf{V}$

$$\begin{pmatrix} \\ \mathbf{A} \\ \\ \end{pmatrix} = \begin{pmatrix} \\ \mathbf{U} \\ \\ \end{pmatrix} \cdot \begin{pmatrix} \\ \mathbf{S} \\ \\ \end{pmatrix} \cdot \begin{pmatrix} \\ \mathbf{V}^{\mathrm{T}} \\ \\ \end{pmatrix} \tag{5.19}$$

with

$$\mathbf{S} = \begin{pmatrix} s_1 & & & \\ & s_2 & & \\ & & \ddots & \\ & & & s_M \end{pmatrix} . \tag{5.20}$$

A value of $s_j = 0$ indicates a singular matrix $\mathbf{A}$, while one or more very small values of $s_j$ signal indicate a nearly singular matrix.

The matrix $\mathbf{U}$ is orthogonal in its columns, i.e.,

$$\sum_{i=1}^{N} u_{i,j} \cdot u_{i,k} = \begin{cases} 0 & \text{for} \quad j \neq k \\ C & \text{for} \quad j = k \end{cases} \qquad j,k = 1,\ldots,M \; . \tag{5.21}$$

such that $\mathbf{U}^{\mathrm{T}} \cdot \mathbf{U} = \mathbf{I}$ holds. $\mathbf{V}$ is a square matrix with orthogonality in both, columns and rows; its inverse is identical to its transpose $\mathbf{V}^{\mathrm{T}} \cdot \mathbf{V} = \mathbf{I} = \mathbf{V} \cdot \mathbf{V}^{\mathrm{T}}$.

Using these properties, the solution of the equation system is straightforward

$$\begin{aligned} \mathbf{A} \cdot \mathbf{x} &= \mathbf{y} \\ \mathbf{U} \cdot \mathbf{S} \cdot \mathbf{V}^{\mathrm{T}} \cdot \mathbf{x} &= \mathbf{y} \\ \mathbf{S} \cdot \mathbf{V}^{\mathrm{T}} \cdot \mathbf{x} &= \mathbf{U}^{\mathrm{T}} \cdot \mathbf{y} \\ \mathbf{V}^{\mathrm{T}} \cdot \mathbf{x} &= \mathbf{S}^{-1} \cdot \mathbf{U}^{\mathrm{T}} \cdot \mathbf{y} \\ \mathbf{x} &= \mathbf{V} \cdot \mathbf{S}^{-1} \cdot \mathbf{U}^{\mathrm{T}} \cdot \mathbf{y} \; . \end{aligned}$$

The inverse of a diagonal matrix is another diagonal with its reciprocal values as elements

$$\mathbf{S}^{-1} = \begin{pmatrix} 1/s_1 & & & \\ & 1/s_2 & & \\ & & \ddots & \\ & & & 1/s_M \end{pmatrix} \; .$$

Finally we get

$$\mathbf{A}^{-1} = \left(\mathbf{U} \cdot \mathbf{S} \cdot \mathbf{V}^{\mathrm{T}}\right)^{-1} = \mathbf{V} \cdot \mathbf{S}^{-1} \cdot \mathbf{U}^{\mathrm{T}} \; , \tag{5.22}$$

that is,

$$\begin{pmatrix} \quad \mathbf{A}^{-1} \quad \end{pmatrix} = \begin{pmatrix} \quad \mathbf{V} \quad \end{pmatrix} \cdot \begin{pmatrix} \quad \mathbf{S}^{-1} \quad \end{pmatrix} \cdot \begin{pmatrix} \quad \mathbf{U}^{\mathrm{T}} \quad \end{pmatrix} \tag{5.23}$$

as the inverse of an arbitrarily shaped matrix $\mathbf{A}$.

The singular value decomposition is described for instance in [Bjo96, Law95].

## 5.4 Test questions

**5.1** To which row of a matrix does the element $a_{43}$ belong?

**5.2** What are the properties of a diagonal matrix?

**5.3** The elements of matrix $\mathbf{B}$ have following property: $b_{ij} = b_{ji}$. To which special group of matrices does $\mathbf{B}$ belong?

**5.4** What is a column vector?

**5.5** How is the matrix $\mathbf{I}$ called?

**5.6** Which of the following statements is true: $\mathbf{C} \cdot \mathbf{D} = \mathbf{D} \cdot \mathbf{C}$ or $\mathbf{C} \cdot \mathbf{B} \neq \mathbf{B} \cdot \mathbf{C}$?

**5.7** If $\mathbf{D}$ and $\mathbf{E}$ have to be multiplied, which requirement has to be fulfilled?

**5.8** How can the singularity of a matrix be tested?

**5.9** What is the result of $\mathbf{D}\mathbf{D}^{-1}$?

**5.10** How can the determinant of a $3 \times 3$ matrix easily be computed?

**5.11** Explain the matrix inversion using the cofactor-matrix method.

**5.12** What is the principle idea of matrix inversion via LU decomposition?

**5.13** Compute the inverse of

$$\mathbf{A} = \begin{pmatrix} 2 & 1 & 1 & 1 \\ 1 & 4 & 1 & 3 \\ 2 & 2 & 1 & 3 \\ 3 & 12 & 4 & 2 \end{pmatrix}$$

via
- Gauss-Jordan elimination
- LU decomposition.

**5.14** How is the singular value decomposition defined?

# Chapter 6

# The Idea behind Least Squares

## 6.1 Normal distribution

The *normal distribution* or *Gaussian distribution* of continuous values plays a fundamental role for the principle of least-squares approximation, as will be shown in the next section. Many random numbers are distributed normally in real life, i.e., they follow a probability density function given by

$$f(x) = \frac{1}{\sigma\sqrt{2\pi}} \cdot \exp\left\{-\frac{1}{2} \cdot \left[\frac{x-\mu}{\sigma}\right]^2\right\} \qquad -\infty < x < \infty \,. \tag{6.1}$$

with

$$\int_{-\infty}^{\infty} f(x)\, dx = 1 \,. \tag{6.2}$$

**Figure 6.1** depicts the graph of the normal distribution. Because of its characteristic shape, it is also called a *Gaussian bell curve*. The distribution is determined by two parameters, namely the mean (or expectation) value $\mu$ and the standard deviation $\sigma$ of the variable $x$. The notation is typically $x \sim \mathcal{N}(\mu; \sigma^2)$. The mean value defines the position of the curve's peak; the parameter $\sigma$ influences the width of the distribution, as well as the maximum of the distribution, as can be seen in **Figure 6.2**. The area below the graph of the Gaussian bell is equal to one, due to the normalisation factor $1/(\sigma\sqrt{2\pi})$ in eq. (6.1). 68.26 percent of the area lies within the range of $\mu - \sigma < x < \mu + \sigma$, i.e., approximately 68 out of 100 random numbers drawn from a Gaussian distribution deviate not more than the standard deviation. 95.44% of all random values are located within the limits of $\pm 2\sigma$. Only 0.27% of all normal distributed values are outside the range of $\mu - 3\sigma < x < \mu + 3\sigma$. That means values of $x$ deviating more than $3\sigma$ from the mean $\mu$ are very unlikely, but of course not impossible.

T. Strutz, *Data Fitting and Uncertainty*, DOI 10.1007/978-3-8348-9813-5 _6,

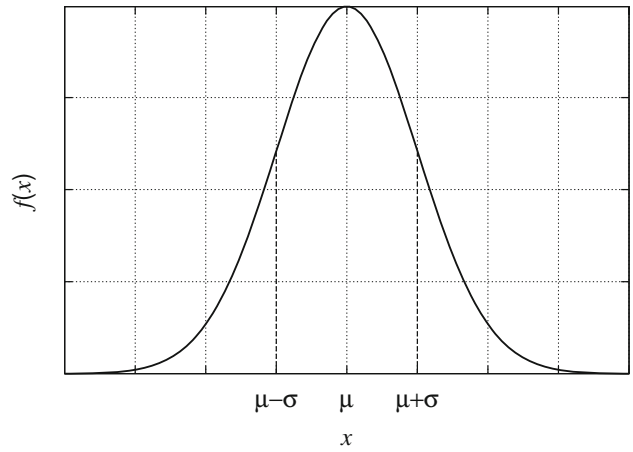


Figure 6.1: Probability density function of the normally distributed variable $x$

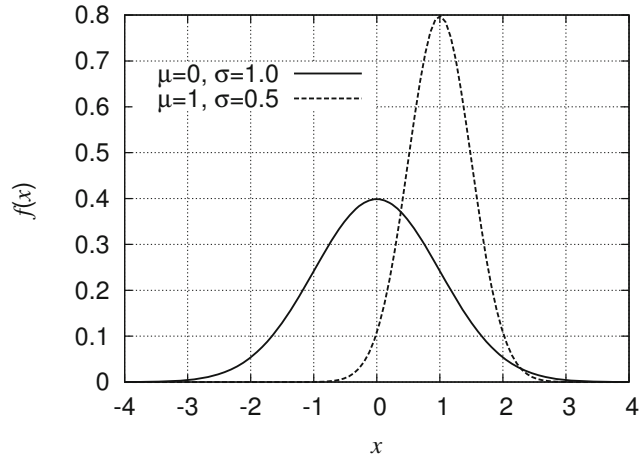


Figure 6.2: Normal probability density function in dependence of its parameters $\mu$ and $\sigma$

## 6.2 Maximum likelihood principle

The method of least squares can be considered as a special case of the more general *method of maximum likelihood* ([Bev92, Gel68, Tay97]).

Given an experiment with the functional connection

$$y = f(\mathbf{x}|\mathbf{a}) \,,$$

for a certain vector of conditions $\mathbf{x}_i$ and a model-parameter vector $\mathbf{a}$, the experimental outcome might be $y_i$. It is assumed that the individual observation $y_i$ is drawn from a Gaussian distribution (see previous section) with mean equal to $f(\mathbf{x}_i|\mathbf{a})$ and a standard deviation $\sigma_i$, i.e., the errors $(f(\mathbf{x}_i|\mathbf{a}) - y_i)$ are expected to be distributed normally. Instead of asking about the probability that a particular vector of parameters $\mathbf{a}$ is correct, we have to consider the probability that the observation $y_i$ could have occurred for the given set of parameters. Thus, according to eq.(6.1), the probability $P_i$ for making the single measurement $y_i$ is

$$P_i = P_{y_i|\mathbf{a}} = \frac{1}{\sigma_i\sqrt{2\pi}} \cdot \exp\left\{-\frac{1}{2}\cdot\left[\frac{f(\mathbf{x}_i|\mathbf{a}) - y_i}{\sigma_i}\right]^2\right\} \,. \tag{6.3}$$

Performing the experiment $N$ times and assuming that the single observations are not influenced by others, i.e., the data can be assumed to be uncorrelated, the measurement probability dependent on chosen model parameters $\mathbf{a}$ is the product of the probabilities of each single observation

$$\begin{aligned} P|_{\mathbf{a}} &= \prod_{i=1}^{N} P_i = \prod_{i=1}^{N}\left(\frac{1}{\sigma_i\sqrt{2\pi}}\right) \cdot \exp\left\{-\frac{1}{2}\cdot\sum_{i=1}^{N}\left[\frac{f(\mathbf{x}_i|\mathbf{a}) - y_i}{\sigma_i}\right]^2\right\} \\ &= \prod_{i=1}^{N}\left(\frac{1}{\sigma_i\sqrt{2\pi}}\right) \cdot \exp\left\{-\chi^2\left(\mathbf{a}\right)\right\} \,. \end{aligned}$$

The product of the exponentials is expressed by the sum of the arguments. Since $P|_{\mathbf{a}}$ has to be maximised, the best choice of the parameter vector $\mathbf{a}$ is given when $\chi^2(\mathbf{a})$ is minimised

$$\chi^2\left(\mathbf{a}\right) = \frac{1}{2}\cdot\sum_{i=1}^{N}\left[\frac{f(\mathbf{x}_i|\mathbf{a}) - y_i}{\sigma_i}\right]^2 \,. \tag{6.4}$$

In contrast to equation (2.2) on page 25, an additional factor of 1/2 is used for convenience in the following. It has no influence on the fitting procedure. The factors $1/\sigma_i^2$ act as weights in order to adjust the influence of single observations according to their importance.

This derivation is based on the initial assumption that the measurement errors follow a Gaussian (normal) distribution. "Taken too literally, this requirement would practically eliminate least squares as a method of computation; for in

nearly every set of measurements there is presumably a certain amount of systematic or constant error" [Bir32] or the random error follows divergent (non-Gaussian) distributions. Nevertheless, the least-squares approach is a handy tool that yields sufficient model parameters in the majority of cases, especially if proper weighting and outlier detection is used as described in Chapter 3.

In applications with more than one observation per measurement, a vector $\mathbf{y}$ must be used instead of a scalar $y$ and the probability in equation (6.3) has to be calculated based on a multidimensional Gaussian function accordingly.

## 6.3 Fitting of linear model functions

The principle formula for solving linear data fitting problems in data fitting was given in Section 2.4 (eqs. 2.10 and 2.11) with

$$\mathbf{a} = \left(\mathbf{J}^{\mathrm{T}} \cdot \mathbf{W} \cdot \mathbf{J}\right)^{-1} \cdot \mathbf{J}^{\mathrm{T}} \cdot \mathbf{W} \cdot \mathbf{y} \,, \tag{6.5}$$

i.e., the optimal parameter vector $\mathbf{a}$ is dependent on the Jacobian matrix $\mathbf{J}$ (see pages 28ff), the matrix of weights $\mathbf{W}$, and the vector of observations $\mathbf{y}$.

It had become apparent at closer inspection that the problem, ignoring the weights, can be expressed simply by the multiplication of the Jacobian matrix with the vector of parameters resulting to the set of observations $\mathbf{y}$ (eq. (2.12))

$$\mathbf{y} = f(\mathbf{x}|\mathbf{a}) = \mathbf{J} \cdot \mathbf{a} \,.$$

The solution for $\mathbf{a}$ is obviously

$$\mathbf{a} = \mathbf{J}^{-1} \cdot \mathbf{y} \,.$$

The following subsections deal with the inversion of the Jacobian matrix $\mathbf{J}$.

### 6.3.1 Standard approach

Since the Jacobian matrix $\mathbf{J}$ is not a square matrix, $\mathbf{J}^{-1}$ is mostly written as $\mathbf{J}^{+}$ and called *pseudoinverse*, *generalised inverse*, or Moore-Penrose inverse [Wei98].

Where equation (6.5) does comes from? In order to make the matrices square, both sides of the equation are multiplied by the transpose of $\mathbf{J}$

$$\begin{aligned} \mathbf{J} \cdot \mathbf{a} &= \mathbf{y} \\ \mathbf{J}^{\mathrm{T}} \cdot \mathbf{J} \cdot \mathbf{a} &= \mathbf{J}^{\mathrm{T}} \cdot \mathbf{y} \,. \end{aligned} \tag{6.6}$$

On the left side of the equation, the term $\mathbf{J}^{\mathrm{T}} \cdot \mathbf{J}$ has to be removed in order to get a result for $\mathbf{a}$. This is performed through multiplication with the corresponding inverse expression yielding the formula for solving linear data fitting by ordinary least squares

$$\mathbf{a} = (\mathbf{J}^{\mathrm{T}} \cdot \mathbf{J})^{-1} \cdot \mathbf{J}^{\mathrm{T}} \cdot \mathbf{y} \; . \tag{6.7}$$

Since $\mathbf{J}^{\mathrm{T}} \cdot \mathbf{J}$ is a square matrix, its inversion is straightforward (see Section 5.3). The pseudo-inverse of $\mathbf{J}$ is obviously equal to $(\mathbf{J}^{\mathrm{T}} \cdot \mathbf{J})^{-1} \cdot \mathbf{J}^{\mathrm{T}}$.

Now, the weights $w_i$, i.e. the standard uncertainties of the single observations, have to be incorporated. According to the maximum-likelihood principle (eq. 6.4), both, $f(\mathbf{x}_i|\mathbf{a})$ and $y_i$, are divided by the standard deviation $\sigma_i$ . Since $w_i = 1/\sigma_i^2$, (eq. 2.5 on page 47), equation (6.6) changes to

$$\mathbf{J}' \cdot \mathbf{a} \;\; = \;\; \mathbf{y}' \tag{6.8}$$

with

$$\mathbf{J}' = \mathbf{\Sigma} \cdot \mathbf{J} \qquad \mathbf{y}' = \mathbf{\Sigma} \cdot \mathbf{y}$$

and

$$\mathbf{\Sigma} = \begin{pmatrix} \sqrt{w_1} & 0 & 0 & \cdots & 0 \\ 0 & \sqrt{w_2} & 0 & \cdots & 0 \\ 0 & 0 & \ddots & \cdots & \vdots \\ \vdots & \vdots & \vdots & \ddots & 0 \\ 0 & 0 & \cdots & 0 & \sqrt{w_N} \end{pmatrix} = \begin{pmatrix} 1/\sigma_1 & 0 & 0 & \cdots & 0 \\ 0 & 1/\sigma_2 & 0 & \cdots & 0 \\ 0 & 0 & \ddots & \cdots & \vdots \\ \vdots & \vdots & \vdots & \ddots & 0 \\ 0 & 0 & \cdots & 0 & 1/\sigma_N \end{pmatrix} .$$

$\mathbf{J}'$ is also called a *design matrix*. Substituting $\mathbf{J}$ with $\mathbf{J}'$ and $\mathbf{y}$ with $\mathbf{y}'$ in equation (6.7), the parameter vector is computed as

$$\begin{aligned} \mathbf{a} &= (\mathbf{J}'^{\mathrm{T}} \cdot \mathbf{J}')^{-1} \cdot (\mathbf{J}')^{\mathrm{T}} \cdot \mathbf{y}' \\ &= \left((\mathbf{\Sigma} \cdot \mathbf{J})^{\mathrm{T}} \cdot \mathbf{\Sigma} \cdot \mathbf{J}\right)^{-1} \cdot (\mathbf{\Sigma} \cdot \mathbf{J})^{\mathrm{T}} \cdot \mathbf{\Sigma} \cdot \mathbf{y} \\ &= \left(\mathbf{J}^{\mathrm{T}} \cdot \mathbf{\Sigma}^{\mathrm{T}} \cdot \mathbf{\Sigma} \cdot \mathbf{J}\right)^{-1} \cdot \mathbf{J}^{\mathrm{T}} \cdot \mathbf{\Sigma}^{\mathrm{T}} \cdot \mathbf{\Sigma} \cdot \mathbf{y} \\ &= \left(\mathbf{J}^{\mathrm{T}} \cdot \mathbf{W} \cdot \mathbf{J}\right)^{-1} \cdot \mathbf{J}^{\mathrm{T}} \cdot \mathbf{W} \cdot \mathbf{y} \; , \end{aligned} \tag{6.9}$$

which is identical to formula (6.5).

### 6.3.2 Solution using singular value decomposition (SVD)

Using the technique of *singular value decomposition* (see Subsection 5.3.4) non-squared matrices can also be inverted directly. Therefore, we can write, based on eq. (6.8)

$$\begin{aligned} \mathbf{a} &= \left(\mathbf{J}'\right)^{-1} \cdot \mathbf{y}' \\ &= \left(\mathbf{\Sigma} \cdot \mathbf{J}\right)^{-1} \cdot \mathbf{\Sigma} \cdot \mathbf{y} \; . \end{aligned}$$

The term $\mathbf{\Sigma} \cdot \mathbf{J}$ is decomposed into $\mathbf{U} \cdot \mathbf{S} \cdot \mathbf{V}^{\mathrm{T}}$ (compare eq. (5.19))

$$\mathbf{a} = \left(\mathbf{U} \cdot \mathbf{S} \cdot \mathbf{V}^{\mathrm{T}}\right)^{-1} \cdot \mathbf{\Sigma} \cdot \mathbf{y} \; . \tag{6.10}$$

Since $\left(\mathbf{U} \cdot \mathbf{S} \cdot \mathbf{V}^{\mathrm{T}}\right)^{-1} = \mathbf{V} \cdot \mathbf{S}^{-1} \cdot \mathbf{U}^{\mathrm{T}}$ (see equation 5.22 on page 144), the weighted linear fitting problem can be solved now via

$$\mathbf{a} = \mathbf{V} \cdot \begin{pmatrix} 1/s_1 & & & \\ & 1/s_2 & & \\ & & \ddots & \\ & & & 1/s_M \end{pmatrix} \cdot \mathbf{U}^{\mathrm{T}} \cdot \mathbf{\Sigma} \cdot \begin{pmatrix} y_1 \\ y_2 \\ \vdots \\ y_N \end{pmatrix} \; . \tag{6.11}$$

As the reciprocal singular values are required, the values of $s_j$ have to be checked in advance. If $s_j$ is very close to zero, then matrix $\mathbf{\Sigma} \cdot \mathbf{J}$ is nearly singular and its inversion becomes obviously critical. The value $1/s_j$ should be set to zero.

[Pre92] recommends SVD as the method of choice for solving most linear least-squares tasks, since it can deal with problematic, e.g. singular or nearly singular matrices.

Compared to the solution via equation (6.7), where the normal matrix $\mathbf{J}^{\mathrm{T}} \cdot \mathbf{W} \cdot \mathbf{J}$ must be inverted, equation (6.7) merely requires the decomposition of $\mathbf{\Sigma} \cdot \mathbf{J}$. This increases the numerical stability. Least-squares approximation based on polynomials of high order, for example, can lead to ill-conditioned matrices, which cannot be processed accurately with (6.9). Subsection B.7 provides some examples.

#### Uncertainty of parameters

One minor disadvantage in using SVD is the missing covariance matrix $\mathbf{C} = (\mathbf{J}^{\mathrm{T}} \cdot \mathbf{W} \cdot \mathbf{J})^{-1}$ of the model parameters (eq. 4.4 on page 109). Thus, the uncertainties of the estimated parameters have to be determined differently from what was

shown in Section 4.2. Instead, the properties of $\mathbf{V}$ are exploited. The covariance matrix is computed based on the matrices $\mathbf{V}$ and $\mathbf{S}$

$$\begin{aligned}\mathbf{C} &= \mathbf{V}\mathbf{S}^{-1} \cdot \left(\mathbf{V}\mathbf{S}^{-1}\right)^{\mathrm{T}} = \mathbf{V}\mathbf{S}^{-1} \cdot \left(\mathbf{S}^{-1}\right)^{\mathrm{T}} \mathbf{V}^{\mathrm{T}} \\ &= \mathbf{V}\mathbf{S}^{-2}\mathbf{V}^{\mathrm{T}} \end{aligned} \tag{6.12}$$

and the variances of the estimated parameters $a_j$ can be derived via

$$\sigma_{a_j}^2 = g_{\mathrm{fit}} \cdot c_{jj}$$

as in the standard approach.

### 6.3.3 Scaling of conditions

The numerical stability of the matrix inversion in equations (6.7) and (6.10) depends, among other things, on the dynamic range of the matrix elements. If the matrix contains very small and very large elements, the CPU precision might not be sufficient to allow a correct inversion. Polynomial functions like

$$y_i = f(\mathbf{x}_i|\mathbf{a}) = a_1 + \sum_{j=2}^{M} a_j \cdot x_i^{j-1} + \varepsilon_i \qquad i = 1, 2, \ldots, N \tag{6.13}$$

are typical examples in which the elements of the Jacobian matrix

$$\mathbf{J} = \begin{pmatrix} 1 & x_1 & x_1^2 & \cdots & x_1^{M-1} \\ 1 & x_2 & x_2^2 & \cdots & x_2^{M-1} \\ \vdots & \vdots & \vdots & \cdots & \vdots \\ 1 & x_N & x_N^2 & \cdots & x_N^{M-1} \end{pmatrix},$$

show a high dynamic range, dependent on the order $M-1$ of the polynomial. The range becomes even larger when computing the normal matrix $\mathbf{J}^{\mathrm{T}} \cdot \mathbf{J}$. If, for example, $x_1 = 10$, then the entries of the first row of $\mathbf{J}$ are $(1, 10, 100, 1000, 10000, \ldots)$.

In order to avoid this exponential increase of values, it would be desired to keep the conditions in the range $[-1, 1]$. Let us assume that $\tilde{x} = \max_i(|x_i|)$ is the maximum absolute condition value. Then we can re-formulate equation (6.13) as

$$\begin{aligned} y_i &= f(\mathbf{x}_i|\mathbf{a}) = a_1 + \sum_{j=2}^{M} (a_j \cdot \tilde{x}^{j-1}) \cdot \left(\frac{x_i}{\tilde{x}}\right)^{j-1} + \varepsilon_i \\ &= f(\mathbf{x}_i|\mathbf{a}) = b_1 + \sum_{j=2}^{M} b_j \cdot (x_i')^{j-1} + \varepsilon_i \quad \text{with} \quad a_j = \frac{b_j}{\tilde{x}^{j-1}},\ x_i' = \frac{x_i}{\tilde{x}}\ . \end{aligned}$$

The values $x_i'$ are within the range of $[-1, 1]$ and the matrix inversion should be more stable. The true model parameters $a_j$ must be derived from the intermediate values $b_j$.

Other model functions can be treated in the same manner, as long as each $x$ is multiplicatively combined with one model parameter. Subsection B.7.1 demonstrates the effectiveness of this normalisation technique.

## 6.4 Fitting of nonlinear model functions

### 6.4.1 Error-surface approximation

As already described in Chapter 2, the fitting of models that are nonlinear for at least one model parameter has to be performed iteratively. The set of $M$ parameters in $\mathbf{a}$ spans an $M$-dimensional space. Each point in this space is characterised by a corresponding value of $\chi^2(\mathbf{a})$ according to equation (6.4). The entity of all points in that space is called the *hyper-surface* (see also Section 2.1). Starting from an initial position $\mathbf{a}$, the fitting algorithm is expected to walk towards the global minimum of $\chi^2(\mathbf{a})$.

In order to determine the right direction, the principle of expansion by Taylor series [Gel68] is used. Any function $f(x)$ that is defined in the vicinity of $f(x_0)$ and has infinite continuous derivatives $f^{(\nu)}(x)$ can be expanded in the following fashion

$$f(x) = \sum_{\nu=0}^{\infty} \frac{f^{(\nu)}(x_0)}{\nu!} \cdot (x - x_0)^{\nu}$$

or, when expressing $x$ as sum of the point $x_0$ and an offset $h$ by $x = x_0 + h$,

$$f(x_0 + h) = \sum_{\nu=0}^{\infty} \frac{f^{(\nu)}(x_0)}{\nu!} \cdot h^{\nu} \; .$$

For small offsets $h$, the first three terms including the first and second derivative of $f(x)$ at $x_0$ provide a fairly good approximation

$$f(x_0 + h) \simeq f(x_0) + \frac{f^{'}(x_0)}{1!} \cdot h + \frac{f^{''}(x_0)}{2!} \cdot h^2 \; . \tag{6.14}$$

Now let us analyse how this approximation can be utilised to determine the steps on the hyper-surface, i.e. the improvement of the parameter vector $\mathbf{a}$.

### 6.4.2 Gauss-Newton method

The Gauss-Newton method is an approach for finding the minimum in an one- or multi-dimensional signal. With respect to data fitting via least squares, the average quadratic error between the observations and the model function has to be minimised, i.e., the minimum of the hyper-surface $\chi^2(\mathbf{a})$ has to be found. This is achieved by approximating the target function by a Taylor series of second order.

The parameter vector $\mathbf{a} = (a_1\ a_2\ \ldots\ a_j\ \ldots\ a_M)^{\mathrm{T}}$ determines the dimensionality of the minimisation problem. The variables from equation (6.14) must be substituted as follows. The independent variable we are looking for is $\mathbf{a}$, thus

$$x_0 \longrightarrow \mathbf{a}$$

and the corresponding step size is

$$h \longrightarrow \boldsymbol{\Delta}\mathbf{a}\ .$$

The function that has to be approximated via Taylor series is

$$f(x_0) \longrightarrow \chi^2(\mathbf{a})$$

and its derivatives are

$$f^{'}(x_0) \longrightarrow \frac{\partial \chi^2(\mathbf{a})}{\partial \mathbf{a}} = \sum_{j=1}^{M} \frac{\partial \chi^2(\mathbf{a})}{\partial a_j}$$

and

$$f^{''}(x_0) \longrightarrow \frac{\partial^2 \chi^2(\mathbf{a})}{\partial \mathbf{a}^2} = \sum_{j=1}^{M}\sum_{k=1}^{M} \frac{\partial^2 \chi^2(\mathbf{a})}{\partial a_j \partial a_k}\ .$$

Corresponding to equation (6.14), this leads to an approximation of the error surface at the new position $\mathbf{a} + \boldsymbol{\Delta}\mathbf{a}$

$$\begin{aligned} \chi^2(\mathbf{a}+\boldsymbol{\Delta}\mathbf{a}) &\simeq \chi^2(\mathbf{a}) + \sum_{j=1}^{M} \frac{\partial \chi^2(\mathbf{a})}{\partial a_j} \cdot \Delta a_j + \frac{1}{2} \cdot \sum_{j=1}^{M}\sum_{k=1}^{M} \frac{\partial^2 \chi^2(\mathbf{a})}{\partial a_j \partial a_k} \cdot \Delta a_j \cdot \Delta a_k \\ &\simeq F(\mathbf{a}+\boldsymbol{\Delta}\mathbf{a})\ . \end{aligned}$$

Using matrices, this reads as

$$F(\mathbf{a}+\boldsymbol{\Delta}\mathbf{a}) = \chi^2(\mathbf{a}) + (\boldsymbol{\Delta}\mathbf{a})^{\mathrm{T}} \cdot \mathbf{g} + \frac{1}{2} \cdot (\boldsymbol{\Delta}\mathbf{a})^{\mathrm{T}} \cdot \mathbf{H} \cdot \boldsymbol{\Delta}\mathbf{a} \tag{6.15}$$

with a gradient vector

$$\mathbf{g} = \left( \frac{\partial \chi^2(\mathbf{a})}{\partial a_1} \quad \frac{\partial \chi^2(\mathbf{a})}{\partial a_2} \quad \dots \quad \frac{\partial \chi^2(\mathbf{a})}{\partial a_M} \right)^{\mathrm{T}} . \tag{6.16}$$

The elements $g_j$ of $\mathbf{g}$ are, using the equation (6.4) for $\chi^2$ and $w_i = 1/\sigma_i^2$, equal to

$$g_j = \frac{\partial \chi^2(\mathbf{a})}{\partial a_j} = \sum_{i=1}^{N} w_i \cdot \frac{\partial f(\mathbf{x}_i|\mathbf{a})}{\partial a_j} \cdot [f(\mathbf{x}_i|\mathbf{a}) - y_i] \ . \tag{6.17}$$

$\mathbf{H}$ in eq.(6.15) is the so-called *Hessian* matrix[1]

$$\mathbf{H} = \begin{pmatrix} \frac{\partial^2 \chi^2(\mathbf{a})}{\partial a_1 \partial a_1} & \frac{\partial^2 \chi^2(\mathbf{a})}{\partial a_1 \partial a_2} & \dots & \frac{\partial^2 \chi^2(\mathbf{a})}{\partial a_1 \partial a_M} \\ \frac{\partial^2 \chi^2(\mathbf{a})}{\partial a_2 \partial a_1} & \frac{\partial^2 \chi^2(\mathbf{a})}{\partial a_2 \partial a_2} & \dots & \frac{\partial^2 \chi^2(\mathbf{a})}{\partial a_2 \partial a_M} \\ \vdots & \vdots & \ddots & \vdots \\ \frac{\partial^2 \chi^2(\mathbf{a})}{\partial a_M \partial a_1} & \frac{\partial^2 \chi^2(\mathbf{a})}{\partial a_M \partial a_2} & \dots & \frac{\partial^2 \chi^2(\mathbf{a})}{\partial a_M \partial a_M} \end{pmatrix} . \tag{6.18}$$

The elements of $\mathbf{H}$ are computed using the product rule for derivations $(u \cdot v)' = u' \cdot v + u \cdot v'$

$$\begin{aligned} H_{jk} &= \frac{\partial^2 \chi^2(\mathbf{a})}{\partial a_j \partial a_k} = \frac{\partial g_j}{\partial a_k} \\ &= \sum_{i=1}^{N} w_i \cdot \left[ \frac{\partial^2 f(\mathbf{x}_i|\mathbf{a})}{\partial a_j \partial a_k} \cdot [f(\mathbf{x}_i|\mathbf{a}) - y_i] + \frac{\partial f(\mathbf{x}_i|\mathbf{a})}{\partial a_j} \cdot \frac{\partial f(\mathbf{x}_i|\mathbf{a})}{\partial a_k} \right] \\ &= \sum_{i=1}^{N} w_i \cdot \frac{\partial^2 f(\mathbf{x}_i|\mathbf{a})}{\partial a_j \partial a_k} \cdot [f(\mathbf{x}_i|\mathbf{a}) - y_i] + \sum_{i=1}^{N} w_i \cdot \frac{\partial f(\mathbf{x}_i|\mathbf{a})}{\partial a_j} \cdot \frac{\partial f(\mathbf{x}_i|\mathbf{a})}{\partial a_k} \ . \end{aligned} \tag{6.19}$$

In order to minimise $\chi^2(\mathbf{a}+\boldsymbol{\Delta}\mathbf{a}) \simeq F(\mathbf{a}+\boldsymbol{\Delta}\mathbf{a})$, we have to look for a point where the gradient of $F(\mathbf{a}+\boldsymbol{\Delta}\mathbf{a})$ (eq. (6.15)) is zero

$$\frac{d\, F(\mathbf{a}+\boldsymbol{\Delta}\mathbf{a})}{d\, (\boldsymbol{\Delta}\mathbf{a})^{\mathrm{T}}} = F'(\mathbf{a}+\boldsymbol{\Delta}\mathbf{a}) = \mathbf{g} + \mathbf{H} \cdot \boldsymbol{\Delta}\mathbf{a} = 0$$

[1] named after the German mathematician Ludwig Otto Hesse (1811-1874)

with the result of

$$\mathbf{\Delta a} = -\mathbf{H}^{-1} \cdot \mathbf{g} \,. \tag{6.20}$$

Voilá! The step $\mathbf{\Delta a}$ can be computed. However, compared to (2.6), equation (6.20) seems to be very different. Let us take a closer look at the elements of $\mathbf{g}$ and $\mathbf{H}$ (eqs. 6.17 and 6.20). It turns out that

$$\mathbf{g} = -\mathbf{J}^{\mathrm{T}} \cdot \mathbf{W} \cdot \mathbf{r} \qquad \text{and} \qquad \mathbf{H} = \mathbf{Q} + \mathbf{J}^{\mathrm{T}} \cdot \mathbf{W} \cdot \mathbf{J} \tag{6.21}$$

with $\mathbf{J}$, $\mathbf{r}$, and $\mathbf{W}$, already defined in equations (2.3), (2.4), and (2.5), respectively

$$\mathbf{J} = \begin{pmatrix} \dfrac{\partial f(\mathbf{x}_1|\mathbf{a})}{\partial a_1} & \dfrac{\partial f(\mathbf{x}_1|\mathbf{a})}{\partial a_2} & \cdots & \dfrac{\partial f(\mathbf{x}_1|\mathbf{a})}{\partial a_M} \\ \dfrac{\partial f(\mathbf{x}_2|\mathbf{a})}{\partial a_1} & \dfrac{\partial f(\mathbf{x}_2|\mathbf{a})}{\partial a_2} & \cdots & \dfrac{\partial f(\mathbf{x}_2|\mathbf{a})}{\partial a_M} \\ \vdots & \vdots & \ddots & \vdots \\ \dfrac{\partial f(\mathbf{x}_N|\mathbf{a})}{\partial a_1} & \dfrac{\partial f(\mathbf{x}_N|\mathbf{a})}{\partial a_2} & \cdots & \dfrac{\partial f(\mathbf{x}_N|\mathbf{a})}{\partial a_M} \end{pmatrix},$$

$$\mathbf{r} = \begin{pmatrix} y_1 - f(\mathbf{x}_1|\mathbf{a}) \\ y_2 - f(\mathbf{x}_2|\mathbf{a}) \\ y_3 - f(\mathbf{x}_3|\mathbf{a}) \\ \vdots \\ y_N - f(\mathbf{x}_N|\mathbf{a}) \end{pmatrix},$$

and

$$\mathbf{W} = \begin{pmatrix} w_1 & 0 & 0 & \cdots & 0 \\ 0 & w_2 & 0 & \cdots & 0 \\ 0 & 0 & \ddots & \cdots & \vdots \\ \vdots & \vdots & \vdots & \ddots & 0 \\ 0 & 0 & \cdots & 0 & w_N \end{pmatrix}.$$

The term $\mathbf{Q}$ contains the second-order derivatives in equation (6.20), which are ignored in many texts – on the one hand because it is zero for linear problems, and on the other hand because the multiplying term $[f(\mathbf{x}_i|\mathbf{a}) - y_i]$ in equation (6.20) is merely a random measurement error of each point. This error can be either positive or negative as soon as $\mathbf{a}$ is close to its optimum. If the multiplying

term is uncorrelated with the second derivative of $f(\mathbf{x}_i|\mathbf{a})$, then these terms tend to cancel each other out when summed over $i$ [Pre92] and we get

$$\boldsymbol{\Delta}\mathbf{a} = \left(\mathbf{J}^{\mathrm{T}} \cdot \mathbf{W} \cdot \mathbf{J}\right)^{-1} \cdot \mathbf{J}^{\mathrm{T}} \cdot \mathbf{W} \cdot \mathbf{r} \,. \tag{6.22}$$

This procedure of minimisation is called the *Gauss-Newton method*. Fast convergence to the closest minimum is its main advantage. The success of finding the minimum, however, depends on the curvature of the target function. Without special treatment, the algorithm gets stuck in saddle points and also can walk in the wrong direction (see Subsection 6.4.5).

### 6.4.3 Gradient-descent method

Although the Gauss-Newton method is quite efficient, it is possible that it does not convert to the desired minimum. Especially when the initial estimation of parameter vector $\mathbf{a} = (a_1\ a_2\ \ldots\ a_j\ \ldots\ a_M)^{\mathrm{T}}$ is not close enough to the target point, the approximation using limited Taylor series can affect the procedure adversely, in terms of too large update steps $\boldsymbol{\Delta}\mathbf{a}$ or wrong directions. In these cases, it is preferable to walk strictly downhill using a *gradient-descent method*.

Utilising the expansion by a Taylor series with use of the first derivatives only (see equations (6.14) and (6.15)), it can be stated

$$\begin{aligned} \chi^2(\mathbf{a}+\boldsymbol{\Delta}\mathbf{a}) &\simeq \chi^2(\mathbf{a}) + (\boldsymbol{\Delta}\mathbf{a})^{\mathrm{T}} \cdot \mathbf{g} \\ &\simeq \chi^2(\mathbf{a}) + \mathbf{g}^{\mathrm{T}} \cdot \boldsymbol{\Delta}\mathbf{a} \end{aligned} \tag{6.23}$$

with $\mathbf{g}$ defined by (6.16).

In order to decrease $\chi^2(\mathbf{a})$, $\mathbf{g}^{\mathrm{T}} \cdot \boldsymbol{\Delta}\mathbf{a}$ must be obviously less than zero, say

$$\mathbf{g}^{\mathrm{T}} \cdot \boldsymbol{\Delta}\mathbf{a} = -\beta \qquad \beta > 0$$

leading to

$$\begin{aligned} \mathbf{g} \cdot \mathbf{g}^{\mathrm{T}} \cdot \boldsymbol{\Delta}\mathbf{a} &= -\mathbf{g} \cdot \beta \\ \boldsymbol{\Delta}\mathbf{a} &= -\frac{\beta}{||\mathbf{g}||^2} \cdot \mathbf{g} \\ &= -\gamma \cdot \frac{\mathbf{g}}{||\mathbf{g}||} \qquad (6.24) \\ &= -\alpha \cdot \mathbf{g} \,. \qquad (6.25) \end{aligned}$$

The factor $\gamma$ determines the step width and $\mathbf{g}$ only controls the direction of move, due to the normalisation with the norm of the gradient vector.

This method is rather stable when the current position in the parameter space is far from the final solution. However, it is difficult to estimate $\gamma$ and its value has to be kept relatively small. Close to the target minimum, the steepest-descent method becomes unfavourable. Without the normalisation by $||\mathbf{g}||$ (eq. 6.25), the convergence process would slow down due to the very small gradients in this region; in addition, saddle points would be a barrier for the gradient descent. When applying the normalisation as in eq. (6.24), the value of $\gamma$ must be lowered as soon as the position of the minimum has passed over and the algorithm starts to oscillate. That is why the Gauss-Newton approach should be used in the vicinity of the minimum instead (see next the two subsections).

### 6.4.4 Levenberg-Marquardt method

The *Levenberg-Marquardt method* combines the advantages of the gradient-descent and Gauss-Newton methods, introducing a damping factor $\mu$ [Lev44, Mar63]. This factor modifies equation (6.22) to

$$\boldsymbol{\Delta}\mathbf{a} = \left(\mathbf{J}^{\mathrm{T}} \cdot \mathbf{W} \cdot \mathbf{J} + \mu \cdot \mathbf{I}\right)^{-1} \cdot \mathbf{J}^{\mathrm{T}} \cdot \mathbf{W} \cdot \mathbf{r} \ . \tag{6.26}$$

Positive values of $\mu$ guarantee that $\boldsymbol{\Delta}\mathbf{a}$ is a descent direction. For large $\mu$, the introduced term $\mu \cdot \mathbf{I}$ becomes dominant and the solution is

$$\boldsymbol{\Delta}\mathbf{a} = \frac{1}{\mu} \cdot \mathbf{J}^{\mathrm{T}} \cdot \mathbf{W} \cdot \mathbf{r} = -\frac{1}{\mu} \cdot \mathbf{g} \ ,$$

which corresponds to the gradient-descent method (6.23), (6.25). Very small values of $\mu$ force steps similar to the Gauss-Newton method, supporting final convergence at the global minimum [Mad04].

The adaptation of $\mu$ is as follows. Let $\mathbf{N} = \mathbf{J}^{\mathrm{T}} \cdot \mathbf{W} \cdot \mathbf{J}$. Starting with a very small value, say $\mu$ equal to 0.001 times the maximum of all diagonal elements of $\mathbf{N}$ ($\mu = 0.001 \cdot \max_j(N_{jj})$), the decrease (or increase) of $\chi^2(\mathbf{a})$ is observed. When $\chi^2(\mathbf{a} + \boldsymbol{\Delta}\mathbf{a}) < \chi^2(\mathbf{a})$, the algorithm is on the right path. The position in the parameter space has to be updated via $\mathbf{a} \leftarrow \mathbf{a} + \boldsymbol{\Delta}\mathbf{a}$ and $\mu$ can be decreased. Otherwise, the gradient descent seems to be more suitable; the update step is skipped and $\mu$ increased by a substantial factor. The choice of $\mu$ could be also linked directly to the conformance between the predicted value of $\chi^2$ (based on the Taylor expansion) and the real $\chi^2$ after the update step ([Mad04]).

### 6.4.5 Example of finding the minimum

Let us assume the one-dimensional error-surface is described by

$$\chi^2(a) = a^4 - 3 \cdot a^3 + 10 \ . \tag{6.27}$$

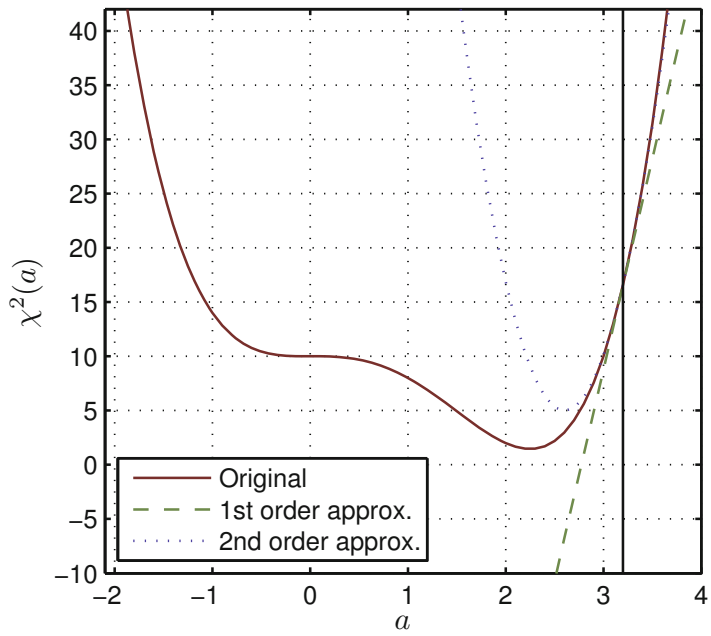


Figure 6.3: Approximation of a curve using Taylor expansion. The vertical line indicates the operating point $a_0 = 3.2$.

Using the Taylor expansion (see also Subsection 6.4.1) we can approximate this function around a certain (initial) point $a_0$ with arbitrary accuracy. The zero-order approximation would simply be a constant

$$\chi^2(a_0 + \Delta a) \quad \approx \quad \chi^2(a_0) \; . \tag{6.28}$$

Approximations of the first and second order correspond to a straight line and a parabola, respectively

$$\chi^2(a_0 + \Delta a) \quad \approx \quad \chi^2(a_0) + \frac{\partial \chi^2(a_0)}{\partial a} \cdot \Delta a \tag{6.29}$$

and

$$\chi^2(a_0 + \Delta a) \quad \approx \quad \chi^2(a_0) + \frac{\partial \chi^2(a_0)}{\partial a} \cdot \Delta a + \frac{1}{2} \cdot \frac{\partial^2 \chi^2(a_0)}{\partial^2 a} \cdot (\Delta a)^2 \; . \tag{6.30}$$

**Figure 6.3** shows the error-surface example $\chi^2(a)$ (solid line) and its approximated versions $\chi^2(a_0 + \Delta a)$ for $a_0 = 3.2$. As can be seen, the approximated versions touch the original function at $(a_0; \chi^2(a_0))$ and slightly diverge with increasing distance from this position.

Two things can be derived from this plot. First, the parabola approximation is, in accordance with the theory of Taylor series, more accurate than the straight-line approximation. Secondly, the parabola shows a turning point, which can assist in searching for the minimum of $\chi^2(a)$. This is exactly what the Gauss-Newton method is doing. It takes the second-order approximation, determines the turning point, and assumes that the turning point is closer to the desired minimum position than the current operating point $a_0$. Then, the new position is taken as operating point and so on until the operating point and turning point of the parabola are identical.

In application to the example function (6.27), we have

$$\begin{aligned} \chi^2(a_0 + \Delta a) &\approx \chi^2(a_0) + \frac{\partial \chi^2(a_0)}{\partial a} \cdot \Delta a + \frac{1}{2} \cdot \frac{\partial^2 \chi^2(a_0)}{\partial^2 a} \cdot (\Delta a)^2 \\ \chi^2(a_0 + \Delta a) &\approx (a_0^4 - 3 \cdot a_0^3 + 10) + (4 \cdot a_0^3 - 9 \cdot a_0^2) \cdot \Delta a \\ &\quad + \frac{1}{2} \cdot (12 \cdot a_0^2 - 18 \cdot a_0) \cdot (\Delta a)^2 \, . \end{aligned} \tag{6.31}$$

The course of the Gauss-Newton method results in a series of operating points. **Figure 6.4** shows the progress of convergence. Six iterations are sufficient in this example.

The first-order approximation corresponds to the gradient-descent method. If the gradient of the first-order approximation is positive, then the value of $a_0$ must be decreased; if the gradient is negative, $a_0$ must be increased in order to walk towards the minimum. The minimum is reached when the gradient is zero.

As already pointed out in Subsection 2.3, the choice of the initial operation point $a_0$ is a crucial task in nonlinear data fitting. **Figure 6.5** illustrates what happens if the operation point (the model parameter) is initialised with $a_0 = -1.5$ and the Gauss-Newton method is applied. Now, 25 iterations are required, however, the algorithm fails to reach the global minimum and converges instead at the saddle point. It also can be concluded from the iteration numbers that the convergence process slows down in the vicinity of the saddle point. The incremental steps $\Delta a$ become very small. This problem could only be solved using a momentum that pushes the algorithm a little bit beyond the critical position.

Let us assume that the initialisation is slightly more accurate and that the starting point is $a_0 = 1.2$ (**Figure 6.6**). What happens? Since the curvature of the original function is different, the turning point of the parabola becomes a maximum instead of a minimum. The Gauss-Newton method accordingly walks in the wrong direction, increasing the value of $\chi^2(a)$.

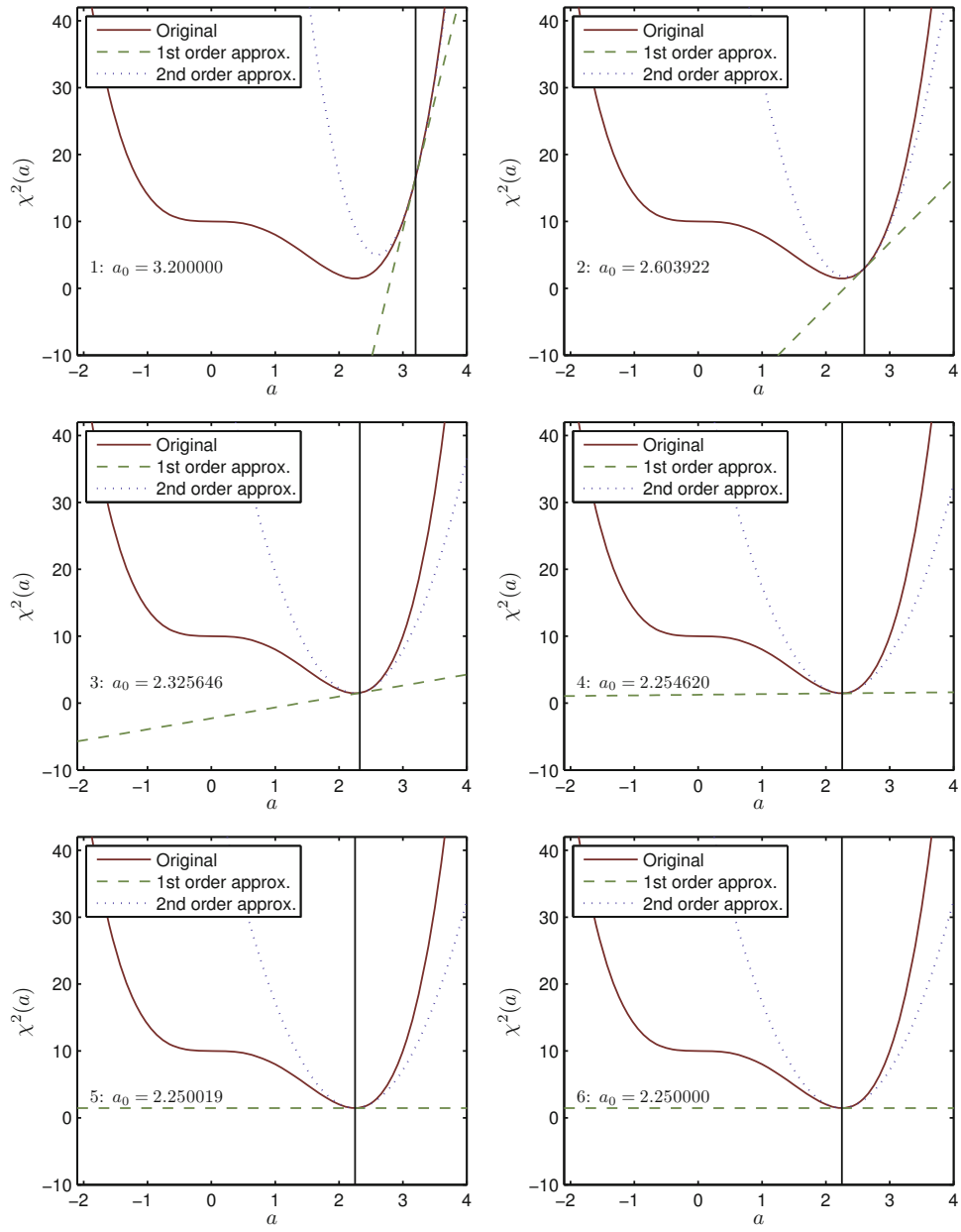


Figure 6.4: Searching the global minimum using the Gauss-Newton method. The initial starting point is $a_0 = 3.2$.

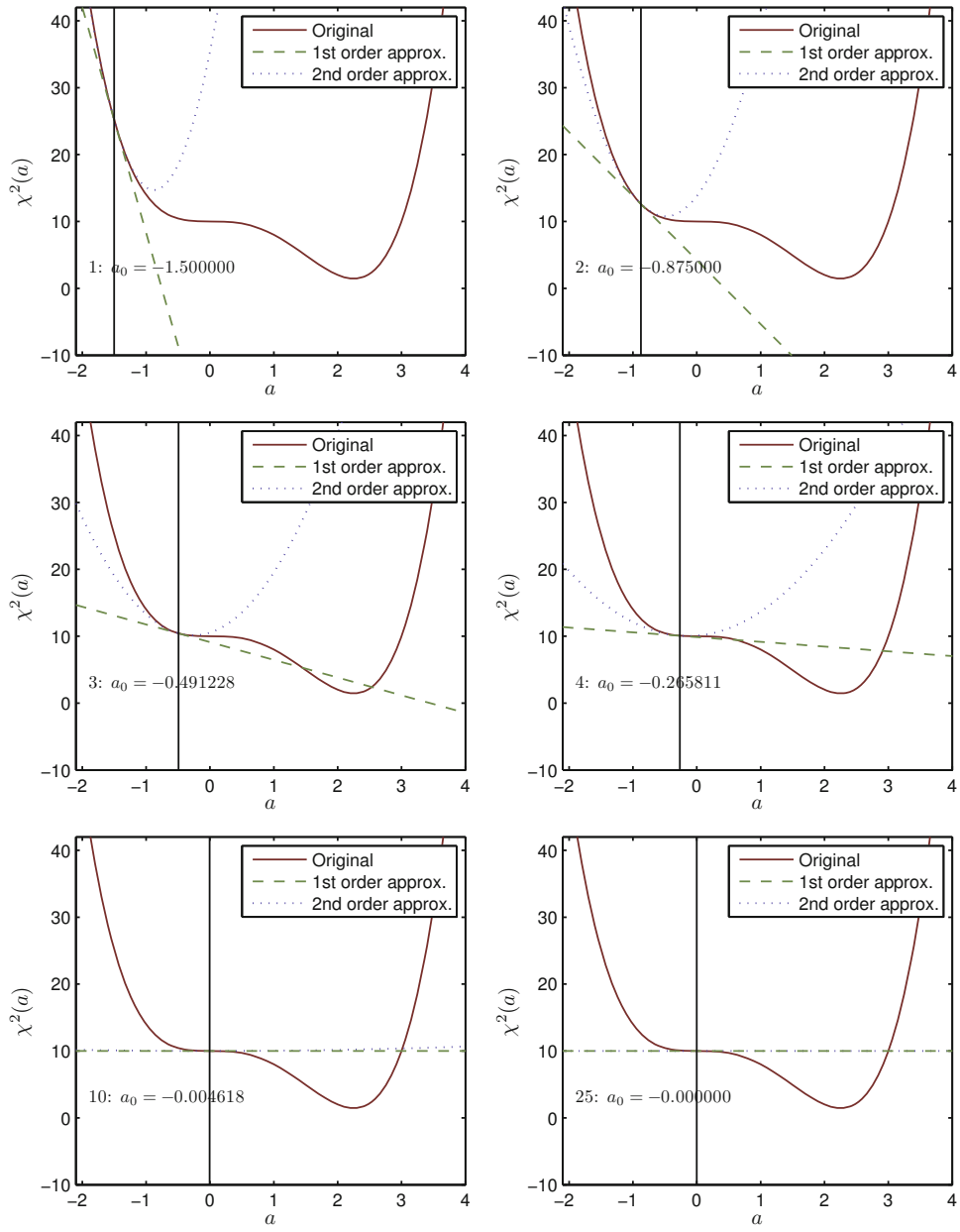


Figure 6.5: Searching the global minimum using the Gauss-Newton method. The initial starting point is $a_0 = -1.5$.

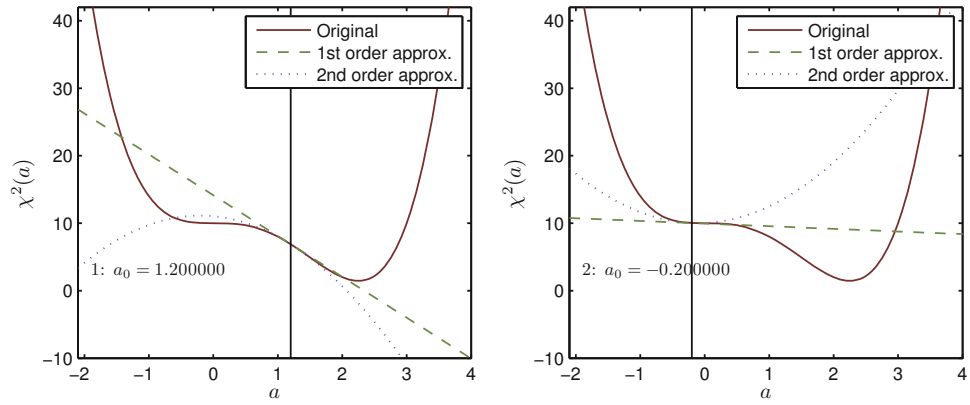


Figure 6.6: Searching the global minimum using the Gauss-Newton method. The initial starting point is $a_0 = 1.2$.

This is exactly the reason why the Levenberg-Marquardt method should be used instead the plain Gauss-Newton approach. The parabola enables more exact steps in most cases. However, it can also misguide the minimisation process, whereas the gradient (first-order approximation) always points to the minimum (**Figure 6.6**, left plot). As soon as the value of $\chi^2(a)$ increases, the minimisation procedure must therefore omit this step and increase the influence of the gradient-descent method, forcing the process to walk strictly downhill.

Since the gradient-descent method always guides the minimisation process in the right direction, why not use it in general? There are at least two reasons. First, it is difficult to determine a proper step size $\Delta a$. It has to be kept relatively small. Secondly, when the vicinity of the minimum is reached, the method will jump over this minimum, regardless how small the step size is, and the algorithm runs into oscillation. In order to overcome these problems, the gradient descent must, firstly, be combined with simulated annealing in terms of starting with a larger step size, which then is decreased as long as the oscillation persists. Secondly, the step size could be increased as long as the algorithm walks in same direction, in order to speed up the convergence if the initial step size was to small. And thirdly, the step size should be independent of the absolute value of the actual gradient. The latter helps to escape long valleys or saddle points. For the tests with the error surface defined by (6.27), the following rule is used

$$\mathbf{\Delta a} = \begin{cases} 0 & \text{if} \quad |g| < 10^{-15} \\ -\beta \cdot \dfrac{g}{|g|} & \text{otherwise} \end{cases} \qquad \text{with} \quad g = \frac{\partial \chi^2(a_0)}{\partial a} \,. \tag{6.32}$$

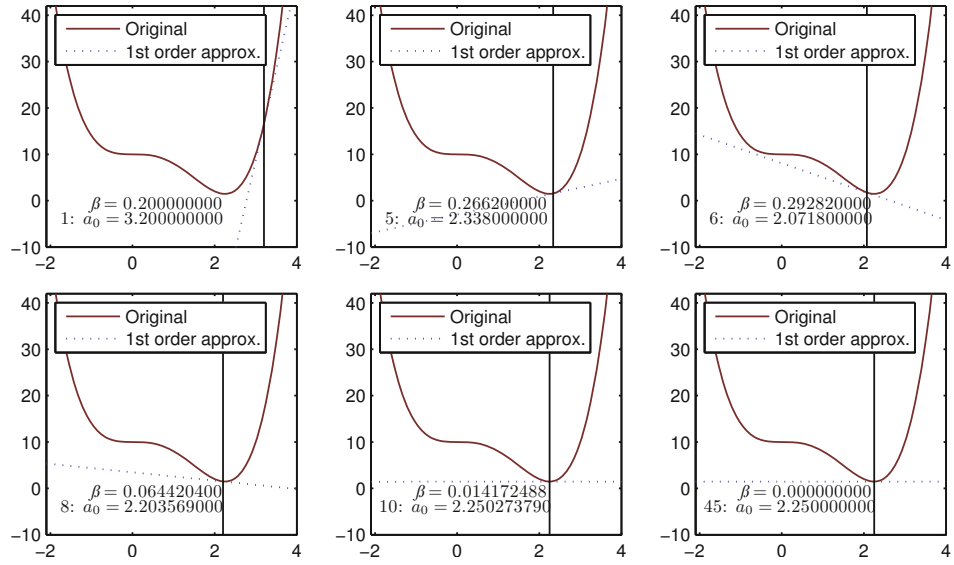


Figure 6.7: Searching the global minimum using the gradient-descent method. The initial starting point is $a_0 = 3.2$. The value of $\beta$ corresponds in equation (6.32).

The normalisation with the absolute value of the gradient avoids convergence at saddle points. The value of $\beta$ is initially set to 0.2 in this example and is increased by 10% after each successful iteration. As soon as the operating point has passed the minimum and the walking direction is reversed, $\beta$ is divided by 5 and only 25% of the computed step size is applied, in order to damp the oscillation. The procedure of decreasing the modifications from cycle to cycle is also called *simulated annealing*. **Figure 6.7** shows the result with an initial operation point $a_0 = 3.2$. The entire process of convergence takes 45 iterations, while the Gauss-Newton method was ready after only six. One can conclude from the plots that major efforts (iterations 10 ... 45) are required to finally approach the target.

We should also test the course of convergence when starting at $a_0 = -1.5$ (**Figure 6.8**). Since the gradient is normalised by its absolute value (eq. 6.32), the step size is only defined by $\beta$ and increases consistently, speeding up the process of walking towards the minimum. For the same reason, the saddle point is easily passed over (iterations 6 to 8) and the operation point moves steadily until the minimum is also passed (iteration 13). Then, again, oscillation starts with decreasing values of $\beta$, i.e. decreasing step sizes. The majority of iterations is spent reaching the

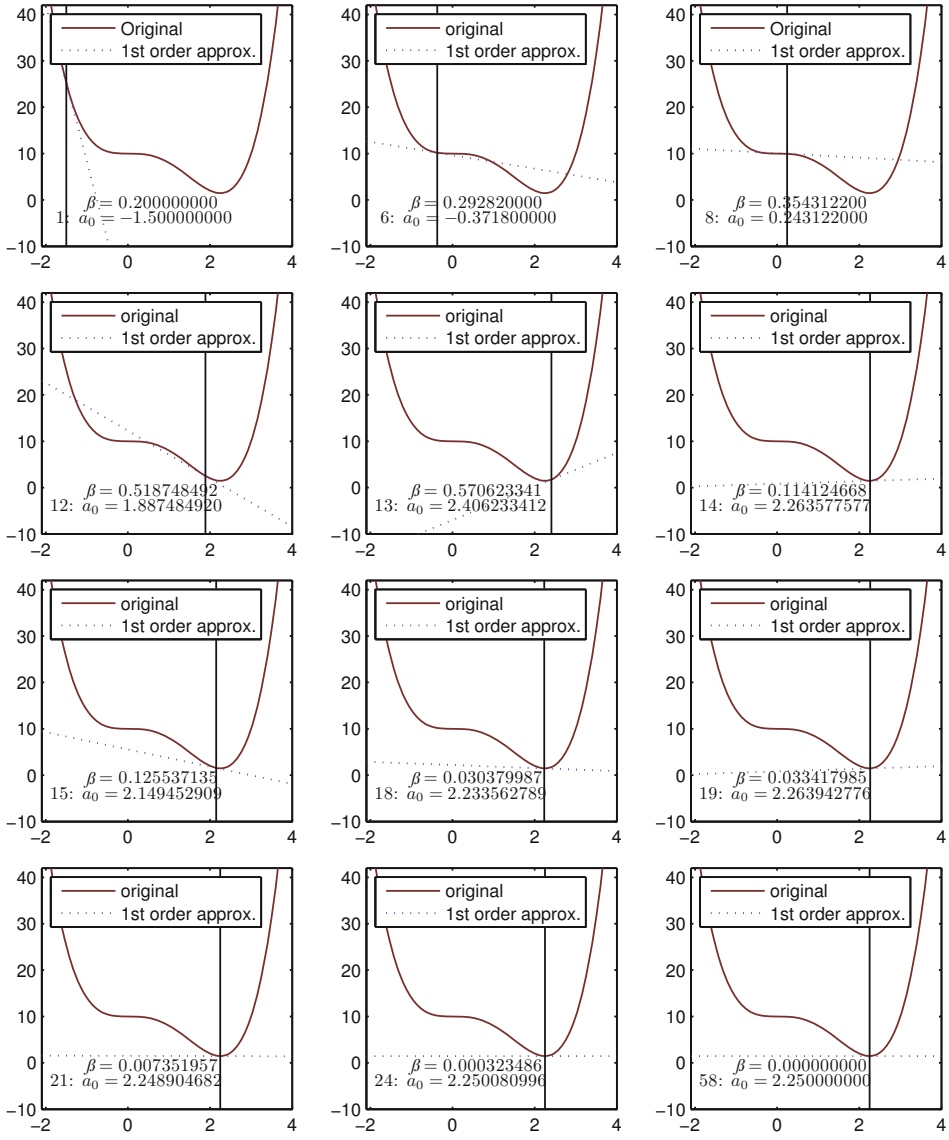


Figure 6.8: Searching the global minimum using the gradient-descent method. The initial starting point is $a_0 = -1.5$. The value of $\beta$ corresponds to equation (6.32).

equilibrium. This underlines that the gradient-descent approach is helpful to a certain extent, however, convergence is achieved much faster when using the Gauss-Newton method.

## 6.5 Test questions

**6.1** What are the parameters of the Gaussian distribution and how do they influence its characteristics?

**6.2** How are the least-squares method and the maximum-likelihood principle related to each other?

**6.3** How can the SVD be used to fit linear models?

**6.4** What is an error surface?

**6.5** Give the definition of the expansion of an arbitrary function by Taylor series.

**6.6** How many derivations are used in the Gaussian-Newton method for minimisation problems?

**6.7** What is a Hessian matrix?

**6.8** How can the Hessian matrix be approximated?

**6.9** Explain the gradient-descent method.

**6.10** What is the principle of the Levenberg-Marquardt method?

**6.11** Discuss the advantages and disadvantages of the Gauss-Newton method based on an arbitrary example.

**6.12** Discuss the advantages and disadvantages of the gradient-descent method based on an arbitrary example.

# Chapter 7

# Supplemental Tools and Methods

## 7.1 Alternative parameter estimation

Besides the least-squares methods explained in this book so far, there is a variety of alternatives for optimisation (see for instance [Pre92]), which might be favourable for particular problems. Three examples are briefly discussed in this section to give the reader an overview.

### 7.1.1 Recursive adaptation of parameters

Let us consider the case that the model parameters of a given linear system are not constant but vary slightly over $n$ (e.g. over time or any other condition). Obviously, there is no optimal set of parameters, but it has to be estimated on the fly. This problem occurs for instance in applications with prediction of signals. The typical task of prediction is to forecast a signal value $x[n]$ (or more abstract: a symbol) from previous ones. The estimated value of $x[n]$ is denoted with $\hat{x}[n]$ (compare eq.(1.23))

$$\hat{x}[n] = f(\mathbf{x}_n|\mathbf{a}) = a_1 \cdot x[n-1] + a_2 \cdot x[n-2] + a_3 \cdot x[n-3] + \dots \ .$$

Signal values, which have already been processed, serve as vector of conditions $\mathbf{x}_n$, which is itself dependent on $n$. Here, $x[n]$ has to be interpreted as a certain value of a time-discrete signal $\{x[n]\}$.

Given a set of initial parameters, their step-by-step update could be achieved dependent on the prediction error $e[n]$, the observation $y = x[n]$ and the current parameter value $a_j[n]$

$$a_j[n+1] = a_j[n] + \mu \cdot x[n-j] \cdot e[n] \qquad \text{with} \qquad e[n] = x[n] - \hat{x}[n] \ .$$

$\mu$ determines the speed of adaptation. In some contexts, it is also called the *learning rate*. Its optimal value is dependent on both the speed of changes of

T. Strutz, *Data Fitting and Uncertainty*, DOI 10.1007/978-3-8348-9813-5 _7,

signal properties and the values of the signal themselves. In the case of a too large value of $\mu$, oscillation could happen. A rule of thumb recommends $0 < \mu < 1/\sigma_x^2$, however, the choice should be made carefully.

### 7.1.2 Iterative gradient descent

This method of best parameter determination utilises similar ideas as the gradient-descent method discussed in Subsection 6.4.3. Knowing the error hyper-surface $\chi^2(\mathbf{a})$ and a set of initial parameters, it is possible to slightly vary the elements $a_j$ of $\mathbf{a}$ one after each other in order to determine the direction of descent without implicitly knowing the gradient itself

$$a_j[n+1] = \begin{cases} a_j[n]+\Delta a_j & \text{if} \quad \chi^2[\mathbf{a}(n)+\Delta] \leq \min\left(\chi^2[\mathbf{a}(n)], \chi^2[\mathbf{a}(n)-\Delta]\right) \\ a_j[n]-\Delta a_j & \text{if} \quad \chi^2[\mathbf{a}(n)-\Delta] \leq \min\left(\chi^2[\mathbf{a}(n)], \chi^2[\mathbf{a}(n)+\Delta]\right) \\ a_j[n] & \text{otherwise} \end{cases} .$$

In words: for each parameter $a_j$, the algorithm is testing the steps in both directions and takes the one in downhill direction or stays at its position, respectively, if the position corresponds to a saddle point or a minimum. Unfortunately, the optimal step sizes $\Delta a_j$ are not known in advance and have to be kept relatively small. The convergence to the desired parameter values can take many iterations in unfortunate cases. Besides of this, at each iteration both, $\chi^2[\mathbf{a}(n) + \Delta]$ and $\chi^2[\mathbf{a}(n) - \Delta]$, have to be evaluated. On the other hand, nonlinear systems are also supported and arbitrary hyper-surfaces $\chi^2(\mathbf{a})$ are tractable, enabling even the principle of total-least-squares fitting, when the shortest distance between the measured point $(y_i; \mathbf{x}_i)$ and the model function $(f(\mathbf{x}_i^{\mathrm{TLS}}|\mathbf{a}), \mathbf{x}_i^{\mathrm{TLS}})$ is evaluated instead of the simple difference $y_i - f(\mathbf{x}_i|\mathbf{a})$ (see Figure 7.3 in Section 7.6).

The choice of $\Delta a_j$ can be combined with the method of simulated annealing, i.e. using high absolute step values in the beginning in order to escape local minima and then slowly decreasing the step sizes for each iteration. An alternation between positive and negative steps is an indication of oscillation and the corresponding step sizes must be shortened.

### 7.1.3 Evolutionary approach

The optimisation of model parameters can also be regarded as an evolutionary process. All parameters $a_j$ are considered as genes, which are subject of mutation, selection, and cross-over. Mutations can be introduced via randomisation. An entire population of $K$ randomised parameter vectors $\mathbf{a}_k$ $(k = 1, 2, \ldots, K)$ has

to be generated. A certain percentage of those vectors yielding the best fits, i.e. smallest values of $\chi^2(\mathbf{a}_k)$, is selected for further investigations. By chance, single elements $a_j$ of different $\mathbf{a}_k$ are exchanged (cross-over). These steps are iterated until convergence. Excluding the cross-over step, this method is also known as Metropolis' algorithm.

Obviously, this approach is rather computational expensive. Besides of this, the success is sensitive to the chosen options, that is, strength of randomisation in mutation and cross-over, total size of the population, portion of surviving individuals (parameter vectors $\mathbf{a}_k$), etc.

Of course, evolutionary approaches may also be combined with the method of simulated annealing.

## 7.2 Chauvenet's criterion for outlier detection

Given a model function $f(\mathbf{x}|\mathbf{a})$ and observations $y_i$, Chauvenet's criterion [Cha71] for outlier detection examines the deviates

$$\Delta_i = y_i - f(\mathbf{x}_i|\hat{\mathbf{a}}) = y_i - \hat{y}_i \ ,$$

wherein $y_i$ denotes the measurements observed under the conditions $\mathbf{x}$ and $\hat{y}_i$ denotes their estimates based on fitting a model function $f(\mathbf{x}|\hat{\mathbf{a}})$ with the estimated parameter vector $\hat{\mathbf{a}} = (a_1\ a_2\ \ldots\ a_M)$.

It is assumed that the values of the deviates are normally distributed with a mean value of zero and a deviation of $\sigma_\mathrm{y}$

$$f(\Delta) = \frac{1}{\sqrt{2\pi}\cdot\sigma_\mathrm{y}} \cdot \exp\left[-0.5 \cdot \left(\frac{\Delta}{\sigma_\mathrm{y}}\right)^2\right] \tag{7.1}$$

with

$$\int_{-\infty}^{+\infty} f(\Delta)\, d\Delta = 1 \ . \tag{7.2}$$

The standard uncertainty $\sigma_\mathrm{y}$ under consideration of $N$ observations $y_i$ and using $M$ model parameters is

$$\sigma = \sigma_\mathrm{y} = \sqrt{\frac{1}{N-M} \cdot \sum_{i=1}^{N} [y_i - f(\mathbf{x}_i|\hat{\mathbf{a}})]^2} \ . \tag{7.3}$$

As already pointed out in Section 6.1, the majority of all observations drawn from a normal distribution are not more distant to the mean than a certain multiple of its standard deviation. Chauvenet's criterion utilises this fact and investigates how likely a value with a certain distance to the mean might occur.

The a priori probability $P_{\text{in}}$ that all deviates are inside the range of $-\kappa \cdot \sigma \leq \Delta \leq \kappa \cdot \sigma$ is given by

$$\begin{aligned} P_{\text{in}} &= \int_{-\kappa\cdot\sigma}^{+\kappa\cdot\sigma} \frac{1}{\sqrt{2\pi}\cdot\sigma} \cdot \exp\left[-0.5 \cdot \left(\frac{\Delta}{\sigma}\right)^2\right] d\Delta \\ &= 2 \cdot \int_{0}^{\kappa\cdot\sigma} \frac{1}{\sqrt{2\pi}\cdot\sigma} \cdot \exp\left[-0.5 \cdot \left(\frac{\Delta}{\sigma}\right)^2\right] d\Delta \\ &= 2 \cdot \left[\frac{1}{\sqrt{2\pi}\cdot\sigma} \cdot \sqrt{\frac{\pi}{2}} \cdot \sigma \cdot \text{erf}\left(\frac{\Delta}{\sqrt{2}\cdot\sigma}\right)\right]_0^{\kappa\cdot\sigma} = \text{erf}\left(\frac{\kappa}{\sqrt{2}}\right). \end{aligned} \tag{7.4}$$

$P_{\text{out}} = 1 - P_{\text{in}}$ is related to all possible values of $\Delta$ outside the range defined by $\kappa$

$$P_{\text{out}} = 1 - \text{erf}\left(\frac{\kappa}{\sqrt{2}}\right)$$

(see **Figure 7.1** a and b).

The question is how likely a deviate outside this range can occur, when a certain number $N$ of measurements are made. Scaled to the number of observations $N$, $\nu_0 = N \cdot P_{\text{out}}$ expresses the averaged number of deviates outside $-\kappa\cdot\sigma \leq \Delta \leq \kappa\cdot\sigma$.

Since we are interested in the threshold $\kappa \cdot \sigma$ separating the good observations from the contaminants, $\kappa$ must be expressed dependent on $N$ and $\nu_0$. It is

$$\begin{aligned} \kappa &= \sqrt{2} \cdot [\text{inverf}\,(1 - P_{\text{out}})] \\ &= \sqrt{2} \cdot \left[\text{inverf}\left(1 - \frac{\nu_0}{N}\right)\right]. \end{aligned} \tag{7.5}$$

Using $\nu_0$, the threshold can be adjusted to the wanted sensitivity.

Chauvenet's criterion is one of the first attempts to identify contaminants and was used from the beginning also by other scientist (e.g. [Wri84]). It yields a quite plain and logical measure for outlier detection. Chauvenet had proposed a portion of $\nu_0 = 0.5$. This, however, would imply 0.5 outliers per data set on average. In practice, the outliers would not be evenly distributed over all possible

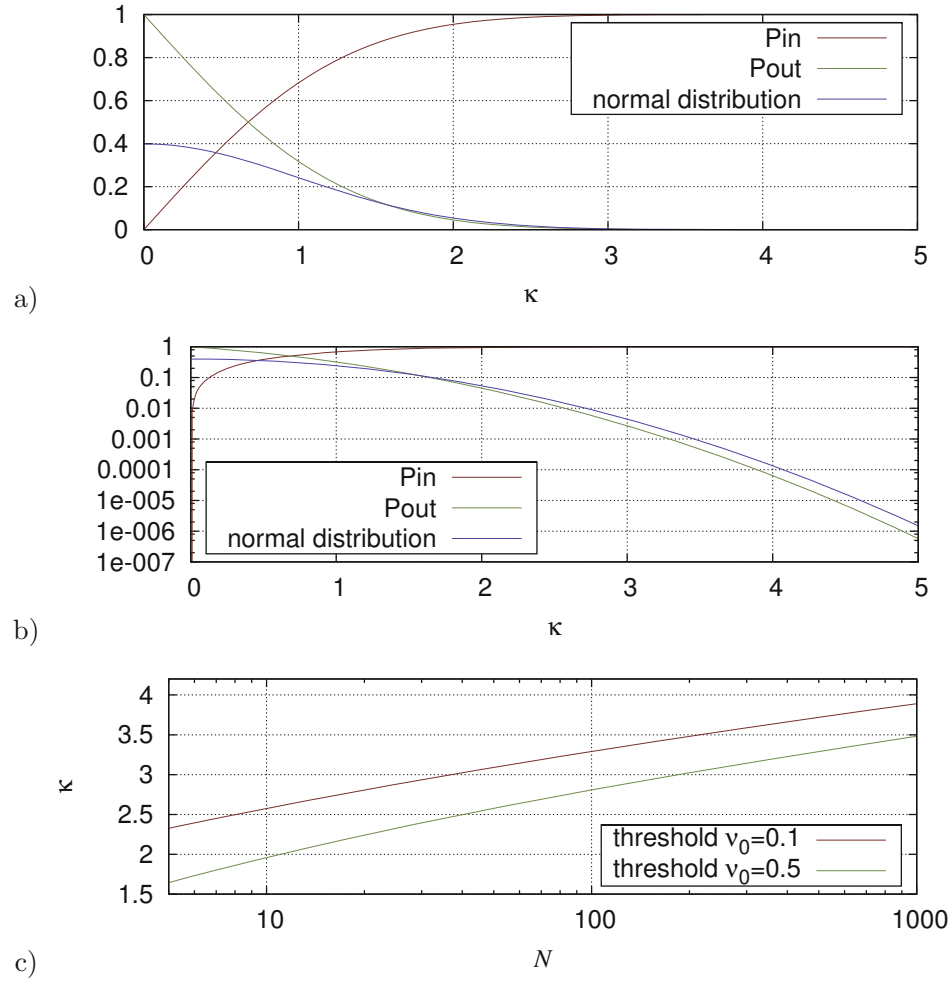


Figure 7.1: Chauvenet's criterion; a) a priori probability $P_{\text{in}}$ that all deviates are inside the range of $-\kappa \cdot \sigma \leq \Delta \leq \kappa \cdot \sigma$; b) same as a) with logarithmic scale on y-axis; c) parameter $\kappa$ for outlier detection as function of the number of observations

data sets. Less then fifty percent of all data sets would be declared containing outliers, but some would contain more than a single one. The value $\nu_0 = 0.5$ is obviously much too high. In principle, it is up to the implementer to choose another value $\nu_0$. In order to tighten the limits for outliers, a lower value $\nu_0$ should be used (**Figure 7.1** c). In many applications, $\kappa$ is simply set to a value of about 3.

In the context of regression analysis, a variety of approaches to outlier detection exists, mostly tailored to the distribution of the observations or assumptions of the estimated number of possible contaminants [Bar94, Car88, Ham86]. Some scientists believe that observations should never be rejected without reliable evidence that the measurement in question is incorrect. Barnett and Lewis [Bar94] even call Chauvenet's criterion as "primitive", "unreasonable", "misguided" and "having evident short comings". The major weakness lies in the estimation of $\sigma_y$ (7.3). Enough data must be available to have considerable confidence in $\sigma_y$. Besides of this, the assumption of normal distributed deviates is not always fulfilled. However, dealing with computational measurements for instance, it is nevertheless a suitable method for outlier detection. For a more detailed discussion see, for instance, [Tay97].

## 7.3 Propagation of errors

In addition to the statements about uncertainties in Chapter 4, it might be of interest what the error is of a dependent variable $z = f(y_1, \ldots, y_j, \ldots, y_M)$ when the uncertainties of the measured variables $y_j$ are known. This is achieved by propagation of the errors of all $y_j$.

Let us start with the simplified case that the error $\Delta\mathbf{y} = (\Delta y_1\ \Delta y_2\ \ldots\ \Delta y_M)$ is assumed to be known in order to derive the error in $z = f(\mathbf{y})$. This assumption will be dropped later on and the uncertainty in $z$ will be derived.

The expansion into a Taylor series can be used to express $f(y)$ as linear superposition of power functions [Gel68]

$$\begin{aligned} f(y) &= \sum_{\nu=0}^{\infty} \frac{f^{(\nu)}(y_0)}{\nu!} \cdot (y - y_0)^{\nu} \\ &= f(y_0) + \frac{f^{(1)}(y_0)}{1} \cdot (y - y_0) + \frac{f^{(2)}(y_0)}{2} \cdot (y - y_0)^2 + \\ &\qquad \frac{f^{(3)}(y_0)}{6} \cdot (y - y_0)^3 + \ldots \end{aligned}$$

for any function $f(y)$ which is defined in the vicinity of $f(y_0)$ and has infinite continuous derivatives $f^{(\nu)}(y)$. Let the known error in $y$ be $\Delta y = y - y_0$. Then an approximation with only the first derivative $f'(y) = f^{(1)}(y)$ expands $f(y)$ around $y_0$

$$f(y) \simeq f(y_0) + f'(y_0) \cdot (y - y_0) = f(y_0) + f'(y_0) \cdot \Delta y$$

For higher dimensional functions $\mathbf{y} = (y_1 \cdots y_j \cdots y_M)$ this yields

$$f(\mathbf{y}) \simeq f(\mathbf{y}_0) + \sum_{j=1}^{M} \frac{\partial f(\mathbf{y}_0)}{\partial y_j} \cdot \Delta y_j$$

or

$$\Delta f(\mathbf{y}) = f(\mathbf{y}) - f(\mathbf{y}_0) \simeq \sum_{j=1}^{M} \frac{\partial f(\mathbf{y}_0)}{\partial y_j} \cdot \Delta y_j \; . \tag{7.6}$$

Let us consider the example of Ohm's law

$$R = U/I \; .$$

In an experiment, the voltage $U$ and the current $I$ are measured in order to get some information about the resistor $R$. The errors might be $\Delta U = U - U_0$ and $\Delta I = I - I_0$. Equation (7.6) reads now as follows

$$\Delta R \simeq \Delta U \cdot \left.\frac{\partial R}{\partial U}\right|_{U_0,I_0} + \Delta I \cdot \left.\frac{\partial R}{\partial I}\right|_{U_0,I_0} = \Delta U \cdot \frac{1}{I_0} + \Delta I \cdot \frac{U_0}{I_0^2}$$

with $\Delta R$ as error in $R$.

Unfortunately, the errors in $\mathbf{y}$ are typically not known, but only their distributions, for instance in terms of the standard uncertainty. Hence, we have to find another description of the error propagation. Let us assume that the most probable value for $z$ is given by

$$\overline{z} = f(\overline{y}_1, \ldots, \overline{y}_j, \ldots, \overline{y}_M)$$

then the uncertainty in the resulting value $z$ is found by considering individual observations $y_{j,1}$, $y_{j,2}$, ...

$$z_i = f(y_{1,i}, \ldots, y_{j,i}, \ldots, y_{M,i}) \; .$$

where $y_{j,i}$ is the $i$th instance of the $j$th element of $\mathbf{y}$. The estimated variance of $z$ is

$$\sigma_z^2 = \frac{1}{N-1}\sum_{i=1}^{N}(z_i - \overline{z})^2 \,. \tag{7.7}$$

Analog to equation (7.6), we can express the deviates $z_i - \overline{z}$, i.e. the simple errors, by [Bev92]

$$z_i - \overline{z} \simeq \sum_{j=1}^{M} \frac{\partial f(\mathbf{y}_0)}{\partial y_j} \cdot (y_{j,i} - \overline{y}_j) \tag{7.8}$$

The combination of equations (7.7) and (7.8) yields

$$\begin{aligned}
\sigma_z^2 &\simeq \frac{1}{N-1}\sum_{i=1}^{N}\left[\sum_{j=1}^{M}\frac{\partial f(\mathbf{y}_0)}{\partial y_j}\cdot(y_{j,i}-\overline{y}_j)\right]^2 \\
&\simeq \frac{1}{N-1}\sum_{i=1}^{N}\left[\frac{\partial f(\mathbf{y}_0)}{\partial y_1}\cdot(y_{1,i}-\overline{y}_1) + \frac{\partial f(\mathbf{y}_0)}{\partial y_2}\cdot(y_{2,i}-\overline{y}_2) + \cdots\right]^2 \\
&\simeq \frac{1}{N-1}\sum_{i=1}^{N}\left[\left(\frac{\partial f(\mathbf{y}_0)}{\partial y_1}\right)^2\cdot(y_{1,i}-\overline{y}_1)^2 + \left(\frac{\partial f(\mathbf{y}_0)}{\partial y_2}\right)^2\cdot(y_{2,i}-\overline{y}_2)^2 + \right. \\
&\qquad \left. 2\cdot\frac{\partial f(\mathbf{y}_0)}{\partial y_1}\cdot\frac{\partial f(\mathbf{y}_0)}{\partial y_2}\cdot(y_{1,i}-\overline{y}_1)\cdot(y_{2,i}-\overline{y}_2) + \cdots\right]
\end{aligned} \tag{7.9}$$

A reordering of the terms results to

$$\begin{aligned}
\sigma_z^2 \simeq\ & \left(\frac{\partial f(\mathbf{y}_0)}{\partial y_1}\right)^2\cdot\frac{1}{N-1}\sum_{i=1}^{N}(y_{1,i}-\overline{y}_1)^2 + \\
& \left(\frac{\partial f(\mathbf{y}_0)}{\partial y_2}\right)^2\cdot\frac{1}{N-1}\sum_{i=1}^{N}(y_{2,i}-\overline{y}_2)^2 + \cdots + \\
& 2\cdot\frac{\partial f(\mathbf{y}_0)}{\partial y_1}\cdot\frac{\partial f(\mathbf{y}_0)}{\partial y_2}\cdot\frac{1}{N-1}\sum_{i=1}^{N}(y_{1,i}-\overline{y}_1)\cdot(y_{2,i}-\overline{y}_2) + \cdots
\end{aligned} \tag{7.10}$$

It becomes apparent that the first two sums express the variances of $y_1$ and $y_2$, respectively

$$\sigma_{y_1}^2 = \frac{1}{N-1}\sum_{i=1}^{N}(y_{1,i}-\overline{y}_1)^2 \qquad \sigma_{y_2}^2 = \frac{1}{N-1}\sum_{i=1}^{N}(y_{2,i}-\overline{y}_2)^2 \,, \tag{7.11}$$

whereas the third sum corresponds to the covariance of $y_1$ and $y_2$

$$\sigma^2_{y_1,y_2} = \frac{1}{N-1}\sum_{i=1}^{N}(y_{1,i} - \overline{y}_1)\cdot(y_{2,i} - \overline{y}_2) \tag{7.12}$$

Hence, we can write (7.10) as

$$\begin{aligned}\sigma_z^2 \;\simeq\; & \left(\frac{\partial f(\mathbf{y}_0)}{\partial y_1}\right)^2 \cdot \sigma^2_{y_1} + \left(\frac{\partial f(\mathbf{y}_0)}{\partial y_2}\right)^2 \cdot \sigma^2_{y_2} + \cdots \\ & + 2\frac{\partial f(\mathbf{y}_0)}{\partial y_1}\frac{\partial f(\mathbf{y}_0)}{\partial y_2}\cdot\sigma^2_{y_1,y_2} + \cdots \end{aligned} \tag{7.13}$$

what is called *error propagation equation*. In case of uncorrelated deviates $(y_{1,i} - \overline{y}_1)$ and $(y_{2,i} - \overline{y}_2)$, the contribution of the sum in (7.12) will be positive or negative in equal parts, that is, they average out for large $N$ and the covariance vanishes leading to the simplified formula

$$\sigma_z^2 \approx \left(\frac{\partial f(\mathbf{y}_0)}{\partial y_1}\right)^2 \cdot \sigma^2_{y_1} + \left(\frac{\partial f(\mathbf{y}_0)}{\partial y_2}\right)^2 \cdot \sigma^2_{y_2} + \cdots \,. \tag{7.14}$$

Regarding the aforementioned example of Ohm's law $R = U/I$, the variance in $R$ is

$$\sigma^2_{\mathrm{R}} \approx \left(\frac{1}{I_0}\right)^2 \cdot \sigma^2_{\mathrm{U}} + \left(\frac{U_0}{I_0^2}\right)^2 \cdot \sigma^2_{\mathrm{I}} \,.$$

## 7.4 Manual calculation of linear least squares

The general solution given in equation (2.10)

$$\mathbf{a} = \left(\mathbf{J}^{\mathrm{T}}\cdot\mathbf{W}\cdot\mathbf{J}\right)^{-1}\cdot\mathbf{J}^{\mathrm{T}}\cdot\mathbf{W}\cdot\mathbf{y}$$

results to optimal parameters for all linear minimisation problems in terms of least squares. In general, the model parameters can also be calculated 'by hand'. This is the initially used technique in the early years of least-squares history and exemplified in the following for the fitting of a straight line (see also Subsection 1.4.2) with the model function

$$y = f(\mathbf{x}|\mathbf{a}) = a_1 + a_2\cdot x \,.$$

The setup with respect to the minimisation task is the same as before

$$\chi^2 = \sum_{i=1}^{N} w_i\cdot[f(\mathbf{x}_i|\mathbf{a}) - y_i]^2 = \sum_{i=1}^{N} w_i\cdot[(a_1 + a_2\cdot x_i) - y_i]^2 \longrightarrow \mathrm{Min} \,.$$

Minima are characterised by gradients equal to zero, thus we solve at first the square operator

$$\begin{aligned}\chi^2 &= \sum_{i=1}^{N} w_i \cdot \left[(a_1 + a_2 \cdot x_i)^2 - 2(a_1 + a_2 \cdot x_i)y_i + y_i^2\right] \\ &= \sum_{i=1}^{N} w_i \cdot \left[(a_1^2 + 2a_1a_2x_i + a_2^2x_i^2) - 2a_1y_i - 2a_2x_iy_i + y_i^2\right]\end{aligned}$$

and set the partial derivatives to zero

$$\begin{aligned}\frac{\partial\chi^2}{\partial a_1} &= \sum_{i=1}^{N} w_i \cdot [2a_1 + 2a_2x_i - 2y_i] &= 0 \\ \frac{\partial\chi^2}{\partial a_2} &= \sum_{i=1}^{N} w_i \cdot \left[2a_1x_i + 2a_2x_i^2 - 2x_iy_i\right] &= 0\,.\end{aligned}$$

Separate summation yields

$$\begin{aligned}\sum_{i=1}^{N} w_i \cdot a_1 + \sum_{i=1}^{N} w_i \cdot a_2x_i - \sum_{i=1}^{N} w_i \cdot y_i &= 0 \\ \sum_{i=1}^{N} w_i \cdot a_1x_i + \sum_{i=1}^{N} w_i \cdot a_2x_i^2 - \sum_{i=1}^{N} w_i \cdot x_iy_i &= 0\,.\end{aligned}$$

Now, the terms containing elements from **a** have to be separated from others

$$\begin{aligned}a_1 \sum_{i=1}^{N} w_i + a_2 \sum_{i=1}^{N} w_i \cdot x_i &= \sum_{i=1}^{N} w_i \cdot y_i \\ a_1 \sum_{i=1}^{N} w_i \cdot x_i + a_2 \sum_{i=1}^{N} w_i \cdot x_i^2 &= \sum_{i=1}^{N} w_i \cdot x_iy_i\,.\end{aligned}$$

Using matrices we can write

$$\begin{pmatrix} \sum_{i=1}^{N} w_i & \sum_{i=1}^{N} w_ix_i \\ \sum_{i=1}^{N} w_ix_i & \sum_{i=1}^{N} w_ix_i^2 \end{pmatrix} \cdot \begin{pmatrix} a_1 \\ a_2 \end{pmatrix} = \begin{pmatrix} \sum_{i=1}^{N} w_iy_i \\ \sum_{i=1}^{N} w_ix_iy_i \end{pmatrix}$$

and the solution for **a** is obviously

$$\begin{pmatrix} a_1 \\ a_2 \end{pmatrix} = \begin{pmatrix} \sum_{i=1}^{N} w_i & \sum_{i=1}^{N} w_ix_i \\ \sum_{i=1}^{N} w_ix_i & \sum_{i=1}^{N} w_ix_i^2 \end{pmatrix}^{-1} \cdot \begin{pmatrix} \sum_{i=1}^{N} w_iy_i \\ \sum_{i=1}^{N} w_ix_iy_i \end{pmatrix}\,. \tag{7.15}$$

Not surprisingly, this is exact the same result as in equation (2.16). Using the shortcuts

$$S \equiv \sum_{i=1}^{N} w_i \ , \qquad S_{\mathrm{x}} \equiv \sum_{i=1}^{N} w_i x_i \ , \qquad S_{\mathrm{xx}} \equiv \sum_{i=1}^{N} w_i x_i^2 \ ,$$
$$S_{\mathrm{y}} \equiv \sum_{i=1}^{N} w_i y_i \ , \qquad S_{\mathrm{xy}} \equiv \sum_{i=1}^{N} w_i x_i y_i$$

and applying equation (5.6) for matrix inversion result to

$$\mathbf{a} \ = \ \frac{1}{S \cdot S_{\mathrm{xx}} - (S_{\mathrm{x}})^2} \begin{pmatrix} S_{\mathrm{xx}} & -S_{\mathrm{x}} \\ -S_{\mathrm{x}} & S \end{pmatrix} \begin{pmatrix} S_{\mathrm{y}} \\ S_{\mathrm{xy}} \end{pmatrix} \ . \tag{7.16}$$

i.e., the single parameters can be calculated as follows

$$\begin{aligned} a_1 &= \frac{S_{\mathrm{xx}} \cdot S_{\mathrm{y}} - S_{\mathrm{x}} \cdot S_{\mathrm{xy}}}{S \cdot S_{\mathrm{xx}} - (S_{\mathrm{x}})^2} \\ a_2 &= \frac{S \cdot S_{\mathrm{xy}} - S_{\mathrm{x}} S_{\mathrm{y}}}{S \cdot S_{\mathrm{xx}} - (S_{\mathrm{x}})^2} \ . \end{aligned}$$

The second derivatives have not to be check for the discrimination between maxima and minima. The found extremum is always a minimum because of $w_i \geq 0$, $[f(\mathbf{x}|\mathbf{a}) - y]^2 \geq 0$ and the typical shape of a parabola.

The first two factors of (7.16) are equal to the covariance matrix which can be used for the evaluation of the uncertainty of the parameter values

$$\begin{aligned} \sigma_{a_1}^2 &= g_{\mathrm{fit}} \cdot \frac{S_{\mathrm{xx}}}{S \cdot S_{\mathrm{xx}} - (S_{\mathrm{x}})^2} \\ &= g_{\mathrm{fit}} \cdot \frac{\sum_{i=1}^{N} w_i x_i^2}{\sum_{i=1}^{N} w_i \cdot \sum_{i=1}^{N} w_i x_i^2 - \left( \sum_{i=1}^{N} w_i x_i \right)^2} \end{aligned}$$

and

$$\begin{aligned} \sigma_{a_2}^2 &= g_{\mathrm{fit}} \cdot \frac{S}{S \cdot S_{\mathrm{xx}} - (S_{\mathrm{x}})^2} \\ &= g_{\mathrm{fit}} \cdot \frac{\sum_{i=1}^{N} w_i}{\sum_{i=1}^{N} w_i \cdot \sum_{i=1}^{N} w_i x_i^2 - \left( \sum_{i=1}^{N} w_i x_i \right)^2} \ . \end{aligned}$$

The goodness-of-fit $g_{\text{fit}}$

$$g_{\text{fit}} = \frac{\chi^2}{N_{\text{free}}} = \frac{1}{N_{\text{free}}} \cdot \sum_{i=1}^{N} w_i \cdot \left[ f(\mathbf{x}_i|\mathbf{a}) - y_i \right]^2 \ ,$$

compensates for the constant factor $k$ introduced by weights $w_i = k/\sigma_i^2$, see Chapter 4, eqs. (4.1) and (4.5).

## 7.5 Combined treatment of different model functions

The joint processing of different model functions becomes important (i) when these functions are dependent on at least one common parameter and/or (ii) the observations are not scalars $y_i$ but vectors $\mathbf{y}_i$ and weights have to be assigned to these vectors instead to their inseparable elements.

Both of these reasons are valid in the example of image alignment described in Subsection 2.6.7. Let us assume that we have taken two snap-shots from the same scene. The position of the camera, however, has slightly changed between the two shots in terms of translation in parallel to the image plane and rotation around the optical axis. Consequently, the second image is a translated and slightly rotated version of the first image.

If it is possible to identify pairs of corresponding points (landmarks), then the parameters of the camera movement can be estimated and the images can be aligned to each other.

The vectors $\mathbf{u}_i = (u_i \ v_i)^{\mathrm{T}}$ are the landmark coordinates in the first image (conditions) and the vectors $\mathbf{x}_i = (x_i \ y_i)^{\mathrm{T}}$ are the corresponding coordinates in a second image (observations), which were found, for instance, by a matching algorithm. The observations are points $(x_i, y_i)$ in two-dimensional space

$$\begin{pmatrix} x_i \\ y_i \end{pmatrix} = \begin{pmatrix} a_1 \\ a_2 \end{pmatrix} + \begin{pmatrix} \cos(a_3) & -\sin(a_3) \\ \sin(a_3) & \cos(a_3) \end{pmatrix} \cdot \begin{pmatrix} u_i \\ v_i \end{pmatrix} \ ,$$

depending on conditions $(u_i, v_i)$ which are coordinates as well. The parameter vector $(a_1 \ a_2)^{\mathrm{T}}$ describes the translational component, while the matrix

$$\begin{pmatrix} \cos(a_3) & -\sin(a_3) \\ \sin(a_3) & \cos(a_3) \end{pmatrix}$$

describes the rotation.

Actually, there are two model functions involved with $\mathbf{u} = (u \ v)^{\mathrm{T}}$, namely

$$f_{\mathrm{x}}(\mathbf{u}|\mathbf{a}) = \quad x \quad = a_1 + \cos(a_3) \cdot u - \sin(a_3) \cdot v$$

and

$$f_{\mathrm{y}}(\mathbf{u}|\mathbf{a}) = \quad y \quad = a_2 + \sin(a_3) \cdot u + \cos(a_3) \cdot v$$

which are linked via $a_3$. Based on an extension of the maximum-likelihood principle (see Section 6.2) towards two-dimensional normal distributions, the minimisation problem can be formulated as

$$\begin{aligned} \chi^2 &= \frac{1}{2} \sum_{i=1}^{N} w_i \cdot \left\{ [f_{\mathrm{x}}(\mathbf{u}_i|\mathbf{a}) - x_i]^2 + [f_{\mathrm{y}}(\mathbf{u}_i|\mathbf{a}) - y_i]^2 \right\} \longrightarrow \mathrm{Min} \\ &= \frac{1}{2} \sum_{i=1}^{N} w_i \cdot \left\{ [f_{\mathrm{x}}(\mathbf{u}_i|\mathbf{a}) - x_i]^2 \right\} + \frac{1}{2} \sum_{i=1}^{N} w_i \cdot \left\{ [f_{\mathrm{y}}(\mathbf{u}_i|\mathbf{a}) - y_i]^2 \right\} \longrightarrow \mathrm{Min} \end{aligned}$$

With respect to equation (2.6) for updating the model parameters, it is somewhat unclear in this setup how the Jacobian matrix and the vector of residuals, eqs. (2.3) and (2.4), should be filled. Instead, the direct use of Gauss-Newton method, eq. (6.20),

$$\mathbf{\Delta a} = -\mathbf{H}^{-1} \cdot \mathbf{g}$$

is proposed to solve this problem. The elements of $\mathbf{g}$ are equal to the derivatives of $\chi^2$

$$g_j = \frac{\partial \chi^2(\mathbf{a})}{\partial a_j} ,$$

i.e.,

$$\begin{aligned} g_j = & \sum_{i=1}^{N} w_i \cdot \left\{ \frac{\partial f_{\mathrm{x}}(\mathbf{u}_i|\mathbf{a})}{\partial a_j} \cdot [f_{\mathrm{x}}(\mathbf{u}_i|\mathbf{a}) - x_i] \right\} + \\ & \sum_{i=1}^{N} w_i \cdot \left\{ \frac{\partial f_{\mathrm{y}}(\mathbf{u}_i|\mathbf{a})}{\partial a_j} \cdot [f_{\mathrm{y}}(\mathbf{u}_i|\mathbf{a}) - y_i] \right\} , \end{aligned} \tag{7.17}$$

with $j$ comprising all parameters from both model functions. Analogously to eq. (6.21) this can be written in matrix notation

$$\mathbf{g} = -\mathbf{J}_{\mathrm{x}}^{\mathrm{T}} \cdot \mathbf{W} \cdot \mathbf{r}_{\mathrm{x}} - \mathbf{J}_{\mathrm{y}}^{\mathrm{T}} \cdot \mathbf{W} \cdot \mathbf{r}_{\mathrm{y}} , \tag{7.18}$$

where the indices ‘x’ and ‘y’ refer to the model functions $f_{\mathrm{x}}(\mathbf{u}_i|\mathbf{a})$ and $f_{\mathrm{y}}(\mathbf{u}_i|\mathbf{a})$, respectively. $\mathbf{W}$ is jointly used for both functions.

According to eq. (6.20), the elements of the Hessian matrix $\mathbf{H}$ are defined as

$$H_{jk} = \frac{\partial^2 \chi^2(\mathbf{a})}{\partial a_j \partial a_k} = \frac{\partial g_j}{\partial a_k}$$

leading to

$$\begin{aligned} H_{jk} \;=\; & \sum_{i=1}^{N} w_i \cdot \left\{ \frac{\partial^2 f_{\mathrm{x}}(\mathbf{u}_i|\mathbf{a})}{\partial a_j \partial a_k} \cdot [f_{\mathrm{x}}(\mathbf{u}_i|\mathbf{a}) - x_i] + \frac{\partial f_{\mathrm{x}}(\mathbf{u}_i|\mathbf{a})}{\partial a_j} \cdot \frac{\partial f_{\mathrm{x}}(\mathbf{u}_i|\mathbf{a})}{\partial a_k} \right\} + \\ & \sum_{i=1}^{N} w_i \cdot \left\{ \frac{\partial^2 f_{\mathrm{y}}(\mathbf{u}_i|\mathbf{a})}{\partial a_j \partial a_k} \cdot [f_{\mathrm{y}}(\mathbf{u}_i|\mathbf{a}) - y_i] + \frac{\partial f_{\mathrm{y}}(\mathbf{u}_i|\mathbf{a})}{\partial a_j} \cdot \frac{\partial f_{\mathrm{y}}(\mathbf{u}_i|\mathbf{a})}{\partial a_k} \right\} \end{aligned} \tag{7.19}$$

and

$$\mathbf{H} = \mathbf{Q}_{\mathrm{x}} + \mathbf{J}_{\mathrm{x}}^{\mathrm{T}} \cdot \mathbf{W} \cdot \mathbf{J}_{\mathrm{x}} + \mathbf{Q}_{\mathrm{y}} + \mathbf{J}_{\mathrm{y}}^{\mathrm{T}} \cdot \mathbf{W} \cdot \mathbf{J}_{\mathrm{y}} \; . \tag{7.20}$$

There are only two differences compared to the derivations in Section 6.4.2: (i) the sizes of $\mathbf{g}$ and $\mathbf{H}$ are based on the total number of parameters of both model functions and (ii) both, $\mathbf{g}$ and $\mathbf{H}$, are result of the summation of two components.

The next subsection will explain the combined treatment of model functions based on examples.

### 7.5.1 Example 1: Coordinate transformation

The concrete contents of $\mathbf{g}$ and $\mathbf{H}$ in the case of the aforementioned example of image alignment via coordinate transformation have to be derived based on the minimisation of

$$\begin{aligned} \chi^2 \;=\; & \frac{1}{2} \sum_{i=1}^{N} w_i \cdot \Big\{ [a_1 + \cos(a_3) \cdot u_i - \sin(a_3) \cdot v_i - x_i]^2 + \\ & [a_2 + \sin(a_3) \cdot u_i + \cos(a_3) \cdot v_i - y_i]^2 \Big\} \longrightarrow \mathrm{Min} \; . \end{aligned}$$

Let us define

$$\begin{aligned} \beta_1 &= [a_1 + \cos(a_3) \cdot u_i - \sin(a_3) \cdot v_i - x_i] \\ \beta_2 &= [a_2 + \sin(a_3) \cdot u_i + \cos(a_3) \cdot v_i - y_i] \; , \end{aligned}$$

then the elements of **g** can be written as

$$\begin{aligned} g_1 = \frac{\partial \chi^2}{\partial a_1} &= \sum_{i=1}^{N} w_i \cdot \beta_1 \ , \\ g_2 = \frac{\partial \chi^2}{\partial a_2} &= \sum_{i=1}^{N} w_i \cdot \beta_2 \ , \\ g_3 = \frac{\partial \chi^2}{\partial a_3} &= \sum_{i=1}^{N} w_i \cdot \{\beta_1 \cdot [-u_i \cdot \sin(a_3) - v_i \cdot \cos(a_3)] \\ &\qquad + \beta_2 \cdot [u_i \cdot \cos(a_3) - v_i \cdot \sin(a_3)]\} \ , \end{aligned}$$

and the elements of **H** ignoring the **Q** terms are

$$h_{11} = \frac{\partial^2 \chi^2}{\partial^2 a_1} = \sum_{i=1}^{N} w_i \ , \qquad h_{22} = \frac{\partial^2 \chi^2}{\partial^2 a_2} = \sum_{i=1}^{N} w_i$$

$$h_{12} = h_{21} = \frac{\partial^2 \chi^2}{\partial a_1 \partial a_2} = \frac{\partial^2 \chi^2}{\partial a_2 \partial a_1} = 0$$

$$\begin{aligned} h_{13} = h_{31} &= \frac{\partial^2 \chi^2}{\partial a_1 \partial a_3} = \frac{\partial^2 \chi^2}{\partial a_3 \partial a_1} \\ &= \sum_{i=1}^{N} w_i \cdot [-u_i \cdot \sin(a_3) - v_i \cdot \cos(a_3)] \ , \end{aligned}$$

$$\begin{aligned} h_{23} = h_{32} &= \frac{\partial^2 \chi^2}{\partial a_2 \partial a_3} = \frac{\partial^2 \chi^2}{\partial a_3 \partial a_2} \\ &= \sum_{i=1}^{N} w_i \cdot [u_i \cdot \cos(a_3) - v_i \cdot \sin(a_3)] \ , \end{aligned}$$

$$\begin{aligned} h_{33} = \frac{\partial^2 \chi^2}{\partial^2 a_3} &= \sum_{i=1}^{N} w_i \cdot [-u_i \cdot \sin(a_3) - v_i \cdot \cos(a_3)]^2 + \\ &\qquad \sum_{i=1}^{N} w_i \cdot [u_i \cdot \cos(a_3) - v_i \cdot \sin(a_3)]^2 \ . \end{aligned}$$

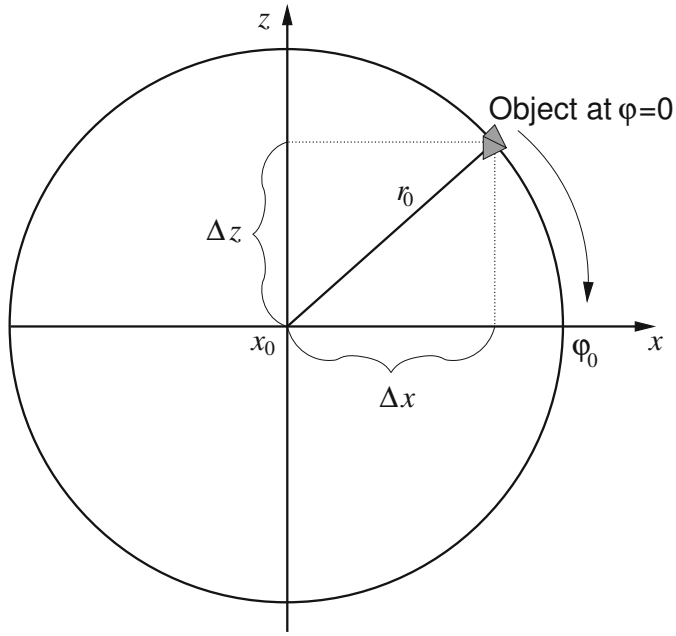


Figure 7.2: Circular movement of an object around the rotation axis ($y$ axis) perpendicular to the $x$ and $z$ axes. The direction of the projection is parallel to the $z$ axis.

### 7.5.2 Example 2: Circular movement

The modelling of circular object movements is a similar scenario (**Figure 7.2**). Let us imagine that only the projection of the object onto the $x$-$y$ plane can be observed by a camera and let us assume in addition that the camera is aligned such that the object moves along a horizontal line in the image, i.e., the $y$ coordinate is constant, whereas the $x$ coordinate follows the model function

$$x = x_0 + r_0 \cdot \cos(\varphi - \varphi_0),$$

which can be turned into a linear function (with respect to $\mathbf{a} = (a_1\ a_2\ a_3)^{\mathrm{T}}$)

$$x = a_1 + a_2 \cdot \cos(\varphi) + a_3 \cdot \sin(\varphi)$$

with

$$a_1 = x_0, \quad a_2 = r_0 \cdot \cos(\varphi_0), \quad \text{and} \quad a_3 = r_0 \cdot \sin(\varphi_0)\ ,$$

according to the expositions in Section 1.3.

If the observed coordinates $(x, y)$ have to be regarded as an inseparable unit, i.e., the $x$ value cannot be measured correctly if the observation of $y$ is wrong and vice versa, then the combined treatment should be applied. The minimisation problem for this example is

$$\begin{aligned}\chi^2 &= \frac{1}{2}\sum_{i=1}^{N} w_i \cdot \Big\{[f_x(\mathbf{u}_i|\mathbf{a}) - x_i]^2 + [f_y(\mathbf{u}_i|\mathbf{a}) - y_i]^2\Big\} \longrightarrow \text{Min} \\ &= \frac{1}{2}\sum_{i=1}^{N} w_i \cdot \Big\{[a_1 + a_2 \cdot \cos(\varphi_i) + a_3 \cdot \sin(\varphi_i) - x_i]^2 \\ &\qquad + [a_4 - y_i]^2\Big\} \longrightarrow \text{Min} \; .\end{aligned}$$

Using eqs. (7.17) and (7.19), the elements of $\mathbf{g}$ and $\mathbf{H}$ are

$$\begin{aligned}\frac{\partial\chi^2}{\partial a_1} &= \sum_{i=1}^{N} w_i \cdot [a_1 + a_2 \cdot \cos(\varphi_i) + a_3 \cdot \sin(\varphi_i) - x_i] \; , \\ \frac{\partial\chi^2}{\partial a_2} &= \sum_{i=1}^{N} w_i \cdot [a_1 + a_2 \cdot \cos(\varphi_i) + a_3 \cdot \sin(\varphi_i) - x_i] \cdot \cos(\varphi_i) \; , \\ \frac{\partial\chi^2}{\partial a_3} &= \sum_{i=1}^{N} w_i \cdot [a_1 + a_2 \cdot \cos(\varphi_i) + a_3 \cdot \sin(\varphi_i) - x_i] \cdot \sin(\varphi_i) \; , \\ \frac{\partial\chi^2}{\partial a_4} &= \sum_{i=1}^{N} w_i \cdot [a_4 - y_i] \; ,\end{aligned}$$

and

$$\begin{aligned}\frac{\partial^2\chi^2}{\partial^2 a_1} &= \sum_{i=1}^{N} w_i = S \; , \qquad \frac{\partial^2\chi^2}{\partial^2 a_2} = \sum_{i=1}^{N} w_i \cdot \cos(\varphi_i) \cdot \cos(\varphi_i) = S_{\text{cc}} \; , \\ \frac{\partial^2\chi^2}{\partial^2 a_4} &= \sum_{i=1}^{N} w_i = S \; , \qquad \frac{\partial^2\chi^2}{\partial^2 a_3} = \sum_{i=1}^{N} w_i \cdot \sin(\varphi_i) \cdot \sin(\varphi_i) = S_{\text{ss}} \; ,\end{aligned}$$

$$\begin{aligned}\frac{\partial^2\chi^2}{\partial a_1 \partial a_2} = \frac{\partial^2\chi^2}{\partial a_2 \partial a_1} &= \sum_{i=1}^{N} w_i \cdot \cos(\varphi_i) = S_{\text{c}} \; , \\ \frac{\partial^2\chi^2}{\partial a_1 \partial a_3} = \frac{\partial^2\chi^2}{\partial a_3 \partial a_1} &= \sum_{i=1}^{N} w_i \cdot \sin(\varphi_i) = S_{\text{s}} \; ,\end{aligned}$$

$$
\begin{aligned}
\frac{\partial^2\chi^2}{\partial a_1\partial a_4} = \frac{\partial^2\chi^2}{\partial a_4\partial a_1} &= 0\,, \\
\frac{\partial^2\chi^2}{\partial a_2\partial a_3} = \frac{\partial^2\chi^2}{\partial a_3\partial a_2} &= \sum_{i=1}^{N} w_i \cdot \cos(\varphi_i) \cdot \sin(\varphi_i) = S_{\mathrm{cs}}\,, \\
\frac{\partial^2\chi^2}{\partial a_2\partial a_4} = \frac{\partial^2\chi^2}{\partial a_4\partial a_2} &= 0\,, \\
\frac{\partial^2\chi^2}{\partial a_3\partial a_4} = \frac{\partial^2\chi^2}{\partial a_4\partial a_3} &= 0\,.
\end{aligned}
$$

The entire Hessian matrix is

$$
\mathbf{H} = \begin{pmatrix} S & S_{\mathrm{c}} & S_{\mathrm{s}} & 0 \\ S_{\mathrm{c}} & S_{\mathrm{cc}} & S_{\mathrm{cs}} & 0 \\ S_{\mathrm{s}} & S_{\mathrm{cs}} & S_{\mathrm{ss}} & 0 \\ 0 & 0 & 0 & S \end{pmatrix} = \begin{pmatrix} & [\mathbf{H}_{\mathrm{x}}] & & 0 \\ & & & 0 \\ & & & 0 \\ 0 & 0 & 0 & S \end{pmatrix}\,.
$$

Its inverse is equal to

$$
\mathbf{H}^{-1} = \begin{pmatrix} & \left[(\mathbf{H}_{\mathrm{x}})^{-1}\right] & & 0 \\ & & & 0 \\ & & & 0 \\ 0 & 0 & 0 & 1/S \end{pmatrix}\,.
$$

For equal weights $w_i = 1.0$ in this example, the combined treatment leads to exactly the same parameters $a_j$ as the separate fitting would. If, however, the observations $x_i$ and $y_i$ do have the same (but in $i$ variable) uncertainty per definition, then the application of combined fitting is mandatory.

## 7.6 Total least squares

Introducing the principle of data fitting in Chapter 1, one of the first assumption was that the condition vector $\mathbf{x}$ is known exactly. It may sometimes happen, however, that the conditions also have errors associated with them that are not negligible with respect to the errors in the observations. If, for instance, current and voltage have to be measured in order to determine the characteristic curve of the resistance of an electrical component, then it can be expected that both values are subject to random errors. These cases are referred to as 'errors in variables' or 'measurement error models' and typically the method of ordinary least squares is not appropriate (compare Section 2.1). Instead of minimising the squared distances between the observations and the model function, i.e. $[y_i - f(\mathbf{x}_i|\mathbf{a})]^2$, the shortest distance between the measured point $(\mathbf{x}_i, y_i)$ and the model function in

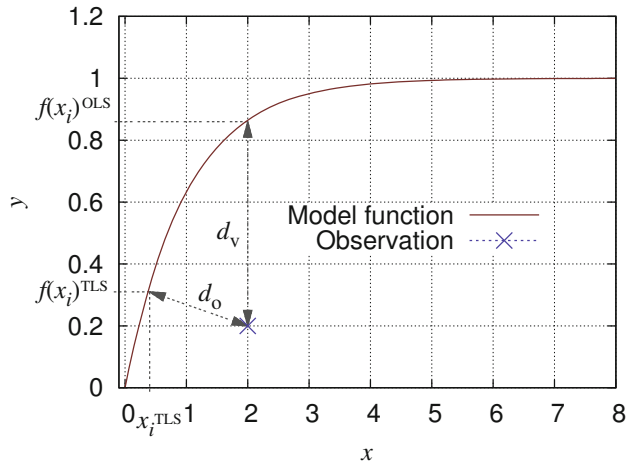


Figure 7.3: Distances between an observed point and model function: vertical distance $d_{\mathrm{v}} = f(x_i)^{\mathrm{OLS}} - y_i$ used in ordinary least-squares fitting (OLS), orthogonal distance $d_{\mathrm{o}} = \sqrt{(f(x_i)^{\mathrm{TLS}} - y_i)^2 + (x_i^{\mathrm{TLS}} - x_i)^2}$ used in total least-squares fitting (TLS)

point $(\mathbf{x}_{i,\mathrm{TLS}}, f(\mathbf{x}_{i,\mathrm{TLS}}|\mathbf{a}))$ should be taken into account (see **Figure 7.3**). Since the distances between observation and model function are determined orthogonal to the model graph, the total-least-squares fitting is also called *orthogonal least-squares fitting* or *orthogonal distance regression* (ODR).

### 7.6.1 Orthogonal fitting of a circle

For the case of fitting a circle, it is obvious that ideally the sum of the squared distance between the data points and the graph should be minimum (**Figure 7.4**). Looking for the best circle centre $(a_1, a_2)$ and radius $a_3$, the minimisation criterion consequently is

$$\sum_i \left[ \sqrt{(x_{1,i} - a_1)^2 + (x_{2,i} - a_2)^2} - a_3 \right]^2 \longrightarrow \mathrm{Min} \; .$$

In comparison to the definition of $\chi^2(\mathbf{a})$ (equation (2.2) on page 25), we can define

$$f(\mathbf{x}_i|\mathbf{a}) = \sqrt{(x_{1,i} - a_1)^2 + (x_{2,i} - a_2)^2} - a_3$$

and

$$y_i \equiv 0 \; .$$

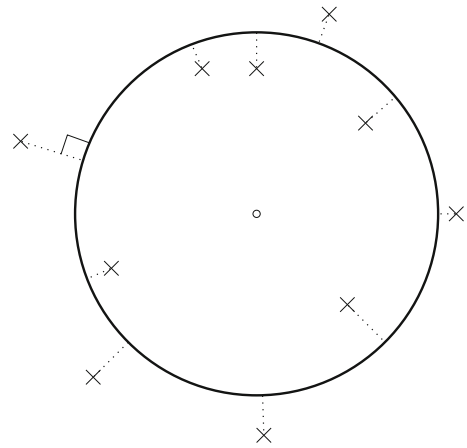

Figure 7.4: Orthogonal distances between observed points and graph of a circle

Hence, the underlying model function is

$$y_i = 0 = \sqrt{(x_{1,i} - a_1)^2 + (x_{2,i} - a_2)^2} - a_3 + \varepsilon_i \;, \tag{7.21}$$

which is obviously different from the model function (2.22) used in Subsection 2.6.10. Unfortunately, (7.21) is a real nonlinear function with respect to the vector of model parameters $\mathbf{a} = (a_1\ a_2\ a_3)^{\mathrm{T}}$ and has to be solved iteratively.

With

$$f \;=\; \sqrt{(x_1 - a_1)^2 + (x_2 - a_2)^2} - a_3$$

the partial derivatives are

$$\begin{aligned}
\frac{\partial f_i}{\partial a_1} &= \frac{a_1 - x_1}{\sqrt{(x_1 - a_1)^2 + (x_2 - a_2)^2}} \\
\frac{\partial f_i}{\partial a_2} &= \frac{a_2 - x_1}{\sqrt{(x_1 - a_1)^2 + (x_2 - a_2)^2}} \\
\frac{\partial f_i}{\partial a_3} &= -1 \;.
\end{aligned}$$

The computation of an initial guess for $\mathbf{a}$ was already explained in Subsection 2.6.10 (page 42). Applying this total least-squares approach to the problem discussed in Subsection 3.5.9 (page 97), the parameters change to $a_1 = 14.9609$, $a_2 = 15.3466$, $a_3 = 9.7200$, and the mean squared distance between observed data points an the graph of the approximated circle reduces from 0.7893 to 0.7851.

### 7.6.2 General approach

While in the example of circle fitting described above the TLS solution could be derived rather directly, the general case must treated in a much more complicated manner.

If the condition vector $\mathbf{x}_i = (x_1 \ \cdots \ x_k \ \cdots \ x_K)_i^{\mathrm{T}}$ has an associated error of $\underline{\delta}_i = (\delta_1 \ \cdots \ \delta_k \ \cdots \ \delta_K)_i^{\mathrm{T}}$, and the vector elements $\delta_k$ are normally distributed ($\delta_k \sim \mathcal{N}(0, \sigma_\delta^2)$), then the method of least squares results to the maximum-likelihood estimate for the parameters in $\mathbf{a}$ (compare also Section 6.2). Extending the derivations of [Bog87] towards multidimensional condition vectors ($x_i \mapsto \mathbf{x}_i$) the fitting problem given in (1.2) has to be changed to

$$y_i = f(\mathbf{x}_i + \underline{\delta}_i|\mathbf{a}) + \varepsilon_i = f(\mathbf{x}_i|\mathbf{a})^{\mathrm{TLS}} + \varepsilon_i \ . \tag{7.22}$$

The orthogonal distance regression searches for those parameters which cause the sum of the squared orthogonal distances $r^2$ from the observation points $(\mathbf{x}_i, y_i)$ to the model function $f(\mathbf{x}_i|\mathbf{a})$ to be minimised. Let $\delta_{k,i} = x_{1,i}^{\mathrm{TLS}} - x_{1,i}$ be the error assigned to the $k$th condition associated to the $i$th observation, then, the orthogonal distance is expressed by

$$\begin{aligned} r_i^2 &= \left[y_i - f(\mathbf{x}_i|\mathbf{a})^{\mathrm{TLS}}\right]^2 + \left[x_{1,i}^{\mathrm{TLS}} - x_{1,i}\right]^2 + \cdots \\ &\quad + \left[x_{k,i}^{\mathrm{TLS}} - x_{k,i}\right]^2 + \cdots + \left[x_{K,i}^{\mathrm{TLS}} - x_{K,i}\right]^2 \\ &= \varepsilon_i^2 + \sum_{k=1}^{K} \delta_{k,i}^2 \ . \end{aligned}$$

In order to minimise the distance $r^2$ we must sum over all $i$

$$\sum_{i=1}^{N} r_i^2 \ = \ \sum_{i=1}^{N} \left\{ \varepsilon_i^2 + \sum_{k=1}^{K} \delta_{k,i}^2 \, . \right\} \quad \longrightarrow \quad \mathrm{Min}$$

Introducing weights and eliminating $\varepsilon_i$ using equation (7.22) the minimisation problem is finally

$$\chi^2 \ = \ \frac{1}{2} \sum_{i=1}^{N} w_i \cdot \left\{ \left[y_i - f(\mathbf{x}_i + \underline{\delta}_i|\mathbf{a})\right]^2 + \sum_{k=1}^{K} v_{k,i} \cdot \delta_{k,i}^2 \right\} \longrightarrow \mathrm{Min}, \tag{7.23}$$

with $w_i = 1/\sigma_{\varepsilon_i}^2$ and $v_{k,i} = \sigma_{\varepsilon_i}^2 / \sigma_{\delta_{k,i}}^2$.

In comparison to the ordinary least-squares (OLS) approach, $N \cdot K$ new unknown parameters come into play, namely $\delta_{k,i}$ ($i = 1, 2, \ldots, N;\ k = 1, 2, \ldots, K$). [Bog87]

proposes to split (7.23) into sets of equations, similar to what we have used in Section 2.6.7 to combine the two model functions of the coordinate transform. The problem remains over-determined, since the generalisation to multi-dimensional conditions leads also to $K \cdot N$ new functions $g(\mathbf{x}|\mathbf{a}, \underline{\delta})$

$$\begin{aligned}
g_i(\mathbf{x}_i|\mathbf{a}, \underline{\delta}_i) &= w_i \cdot [y_i - f(\mathbf{x}_i + \underline{\delta}_i|\mathbf{a})]^2 && i = 1, \ldots, N \\
g_{i+N}(\mathbf{x}_i|\mathbf{a}, \underline{\delta}_i) &= w_i \cdot v_{1,i} \cdot \delta_{1,i}^2 && i = 1, \ldots, N \\
&\vdots \\
g_{i+k\cdot N}(\mathbf{x}_i|\mathbf{a}, \underline{\delta}_i) &= w_i \cdot v_{k,i} \cdot \delta_{k,i}^2 && i = 1, \ldots, N \\
&\vdots \\
g_{i+K\cdot N}(\mathbf{x}_i|\mathbf{a}, \underline{\delta}_i) &= w_i \cdot v_{K,i} \cdot \delta_{K,i}^2 && i = 1, \ldots, N
\end{aligned} \tag{7.24}$$

and we have to minimise

$$\chi^2 = \frac{1}{2} \sum_{i=1}^{(K+1)\cdot N} \{g_i(\mathbf{x}_i|\mathbf{a}, \underline{\delta}_i)\} \longrightarrow \text{Min}$$

which is an ordinary least-squares problem with $M$ parameters $a_j$, $K \cdot N$ parameters $\delta_{k,i}$ and $(K + 1) \cdot N$ observations.

**Example**: Straight-line fitting using TLS

Using the model function

$$y = a_1 + a_2 \cdot x \quad \mapsto \quad y_i = a_1 + a_2 \cdot (x_i + \delta_i) + \varepsilon_i \ ,$$

the condition vector $\mathbf{x}_i$ reduces to a scalar $x_i$ and its error $\underline{\delta}_i$ reduces to $\delta_i$. There are $N$ new parameters $\delta_i$ and, in total, two separate models (compare eq. 7.24) can be set up as

$$\begin{aligned}
g_i(\mathbf{x}_i|\mathbf{a}, \underline{\delta}_i) &= w_i \cdot [y_i - a_1 + a_2 \cdot (x + \delta_i)]^2 && i = 1, \ldots, N \\
g_{i+N}(\mathbf{x}_i|\mathbf{a}, \underline{\delta}_i) &= w_i \cdot v_i \cdot \delta_i^2 && i = 1, \ldots, N
\end{aligned}$$

It becomes apparent that, due to the parameters $\delta_i$, the fitting task has turned into a nonlinear problem. The required vector of residuals and the Jacobian matrix are

$$\mathbf{r} = \begin{pmatrix}
y_1 - a_1 + a_2 \cdot (x_1 + \delta_1) \\
y_2 - a_1 + a_2 \cdot (x_2 + \delta_2) \\
\vdots \\
y_N - a_1 + a_2 \cdot (x_N + \delta_N) \\
0 - \delta_1 \\
0 - \delta_2 \\
\vdots \\
0 - \delta_N
\end{pmatrix}$$

and

$$\mathbf{J} = \left(\begin{array}{cc|cccc} 1 & x_1+\delta_1 & a_2 & 0 & \cdots & 0 \\ 1 & x_2+\delta_2 & 0 & a_2 & \cdots & 0 \\ \vdots & \vdots & \vdots & \vdots & \ddots & \vdots \\ 1 & x_N+\delta_N & 0 & 0 & \cdots & a_N \\ \hline 0 & 0 & 1 & 0 & \cdots & 0 \\ 0 & 0 & 0 & 1 & \cdots & 0 \\ \vdots & \vdots & \vdots & \vdots & \ddots & \vdots \\ 0 & 0 & 0 & 0 & \cdots & 1 \end{array}\right) .$$

**J** comprises four blocks. The top left block corresponds to the Jacobian matrix of the OLS problem; the other three are result of the TLS derivations. The two blocks on the right-hand side are diagonal sub-matrices, because each row in **J** corresponds to a certain $i$. Row $i = 1$ of **J** contains the partial derivatives of the equation

$$y_1 = a_1 + a_2 \cdot (x_1 + \delta_1) + \varepsilon_1$$

which are

$$\frac{\partial y_1}{\partial a_1} = 1 \quad \frac{\partial y_1}{\partial a_2} = x_1 + \delta_1 \quad \frac{\partial y_1}{\partial \delta_1} = a_2 \, .$$

All other partial derivatives are zero

$$\frac{\partial y_1}{\partial \delta_j} = 0 \qquad \text{for} \qquad j > 1 \, .$$

The next row of **J** contains

$$\begin{aligned} \partial y_2/\partial a_1 &= 1 \\ \partial y_2/\partial a_2 &= x_2 + \delta_2 \\ \partial y_2/\partial \delta_1 &= 0 \qquad\qquad \delta_1 \text{ does not exist for } i = 2 \\ \partial y_2/\partial \delta_2 &= a_2 \, , \end{aligned}$$

and obviously it holds in general

$$\frac{\partial y_i}{\partial \delta_j} = 0 \qquad \text{if} \qquad j \neq i \, .$$

The bottom right block of **J** is diagonal for same reasons.
□□□

The major disadvantage of this approach is the large normal matrix $\mathbf{J}^{\mathrm{T}} \cdot \mathbf{W} \cdot \mathbf{J}$ whose size increases from $M \times M$ for OLS to $(M + N) \times (M + N)$ for TLS with one-dimensional conditions, i.e. $K = 1$. However, the special structure of $\mathbf{J}$ consisting of a zero block and two diagonal blocks can be exploited to reduce the amount of work to solve the TLS problem in about the same time as the corresponding OLS problem [Bog87].

## 7.7 Test questions

**7.1** In case of varying parameters, there is no constant parameter vector $\mathbf{a}$. Is optimisation still possible? If yes, how is it? If not, why?

**7.2** What are the three typical operations in an evolutionary approach to optimisation?

**7.3** If the gradients of the error surface are not known, how is it still possible to drive the optimisation towards the correct solution?

**7.4** What is the fundamental idea of Chauvenet's criterion?

**7.5** What are the drawbacks of outlier detection using Chauvenet's criterion?

**7.6** If an experiment is dependent on two measurement variables, both subject to errors, what is the resulting error variance of the experiment?

**7.7** How must data fitting be performed, if the result is based on two different model functions?

**7.8** What is the basic idea of TLS?

**7.9** How can total least-squares problems be solved? How does the Jacobian matrix look like for $f(x|\mathbf{a}) = a_1 + a_2 \cdot x + a_3 \cdot x^2$?

# Appendix A

# Comparison of Approaches to Outlier Detection

Based on Monte Carlo simulations, the cluster-based outlier detection (ClubOD) (see Subsection 3.4.2) is tested with different data distributions and compared with the method of standardised residuals ($z$-score). It is shown that the cluster-based approach identifies outliers more reliably, even for a normal data distribution, and the advantages are discussed in detail.

## A.1 Normally distributed data

It has been investigated whether the removal of observations according to the $\pm\kappa_\mathrm{O} \cdot \hat{\sigma}_\mathrm{y}$ rule of the standardised residuals method (eq. 3.15 on page 57) is in fact critical, and whether the described cluster-based approach leads to more reliable results. For different numbers $N$ of data points, $10^5$ sets of observations $y_i$, drawn from a normal distribution ($\sigma_\mathrm{y} = 1; \overline{y} = 0$), have been generated and analysed individually.

### A.1.1 Data sets without outliers

The method of standardised residuals has been tested in three modes: with a constant value of $\kappa_\mathrm{O} = 3.5$ and with two different adaptive values according to Chauvenet's approach, eq. (7.5), respectively. The cluster-based outlier detection (ClubOD) has been applied as described in subsection 3.4.2.

The average percentage of data sets having at least one data point declared as being an outlier has been recorded (**Figure A.1**). When using a constant value of $\kappa_\mathrm{O}$, the chance of classifying data points as outlier naturally increases with increasing $N$, since the tails of the Gaussian bell become more and more filled. The curve corresponding to $\nu_0 = 0.5$ does not seem to converge to the value of 50%. The reason for this lies in counting only the number of sets with outliers without considering the number of outliers per set. If one counts sets with two

T. Strutz, *Data Fitting and Uncertainty*, DOI 10.1007/978-3-8348-9813-5,

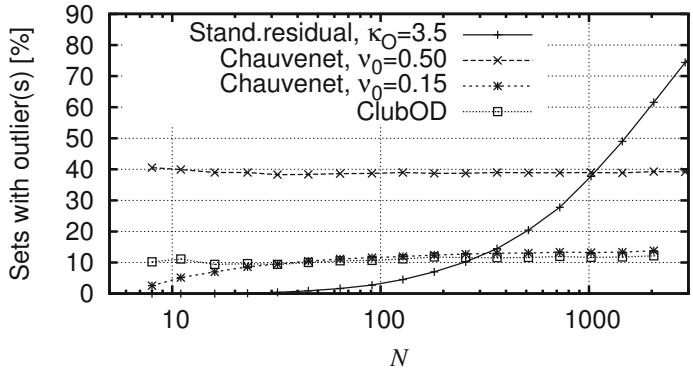


Figure A.1: Normally distributed observations: percentage of data sets with at least one observation classified as outlier.

outliers twice, sets with three outliers three times, and so on, the result will in fact converge towards 50%. According to the chosen thresholds $\kappa_1$ for the cluster-based method (ClubOD), each set shows on average 0.15 outliers leading to about 10% – 12% sets containing potential outliers.

The results of Figure A.1 reveal one major problem. Even though all values have been drawn from the same distribution, some of them have been classified as outliers by definition. The question is, does the removal of these falsely classified observations harm the data analysis, i.e. the estimation of the true value of $y$? In order to answer, the simulation mentioned above has also compared the mean value $\hat{y}$ of the entire set with the mean value $\hat{y}'$ of the reduced set, i.e. the set after removal of putative outliers. Theoretically, $\hat{y}$ should be equal to zero, due to the parameters of the normal distribution used. It has been found that the removal improves the estimate of the mean value of $y$ in less than fifty percent of all sets containing one or more observations classified as being contaminant (**Figure A.2**). There are no significant differences between all three cases, despite the different values of $\kappa_O$ or the different methods.

It follows that the removal of putative outliers actually yields poorer results when sets of normally distributed data are free of contaminants, whereas ClubOD shows less degradation than the method of standardised residuals for $N < 30$.

However, as the removal does not always negatively influence the estimate of $\hat{y}$, there is a chance that this relation will change in favour of removal where the presence of outliers can be expected.

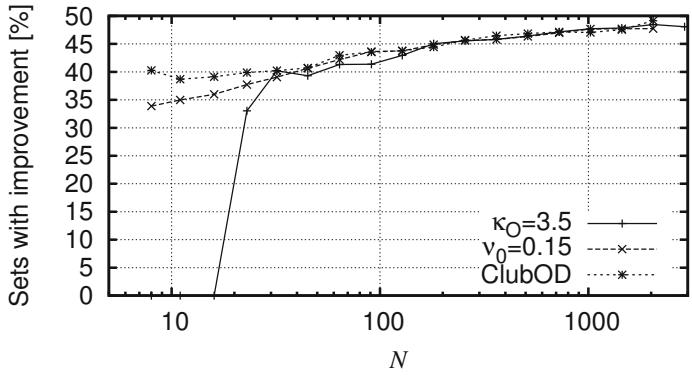


Figure A.2: Normally distributed observations: percentage of data sets with better estimates of $y$ after the removal of observations classified as outliers.

### A.1.2 Data sets containing outliers

In order to investigate the effects of real outliers, the simulations have been run again with one, two or three of the original observations substituted by some values drawn from a normal distribution with other parameters ($\sigma_y = 1, \overline{y} = 4.0$). **Figure A.3** shows the results in comparison to the outlier-free case. Naturally, the percentage of data sets with putative contaminants has increased. It is not 100% because the inserted outliers may have values similar to the other observations, and are not detected in these cases. Furthermore, the chance of detecting outliers with the method of standardised residuals decreases for small $N$ with an increasing number of inserted contaminants, because the estimate of $\sigma_y$ is strongly influenced by the outliers and it becomes less likely that the remaining 'good' observations will form a distinct unit.

The proposed cluster-based approach proves advantageous when detecting outliers in small data sets, because it is not dependent on the estimation of $\sigma_y$. In larger data sets, observations are more frequently located in the tails of the Gaussian distribution, closing the gap between the bulk of good observations and outliers. Consequently, fewer outliers are detected on average. This behaviour is also beneficial, as we have to ask ourselves whether the outliers deliberately included can still be regarded as contaminant when similar values are also common for true data points.

**Figure A.4** clearly shows that, as soon as outliers are present, the removal of outliers is statistically advantageous, especially for small data sets. It should

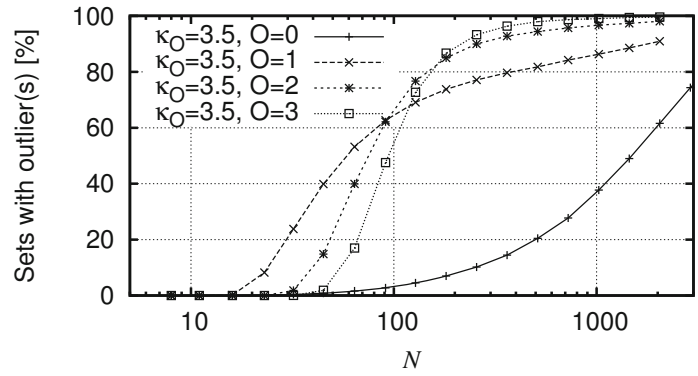


a)

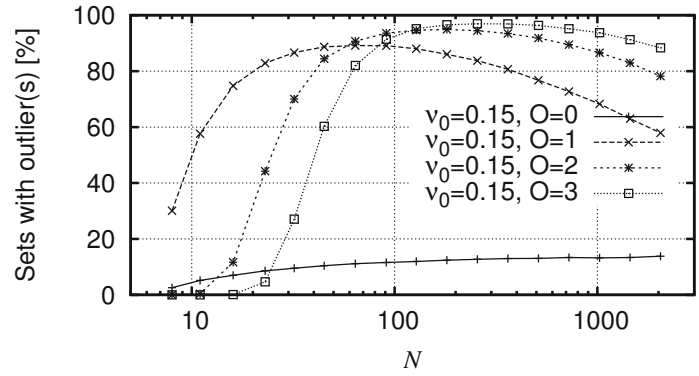


b)

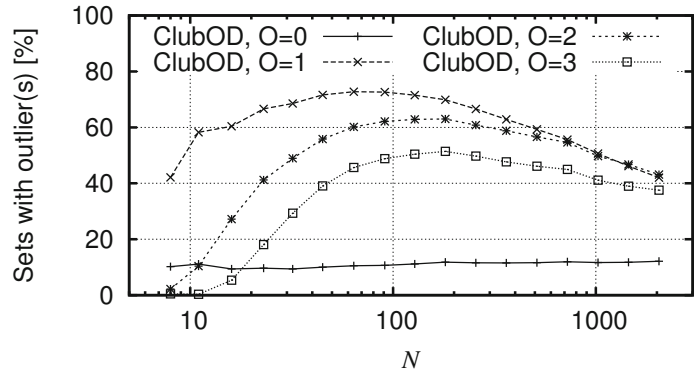


c)

Figure A.3: Normally distributed data: percentage of data sets with at least one observation classified as an outlier after insertion of one, two or three contaminants; a) $\kappa_O = 3.5$, b) Chauvenet's criterion $\nu_0 = 0.15$, c) cluster criterion.

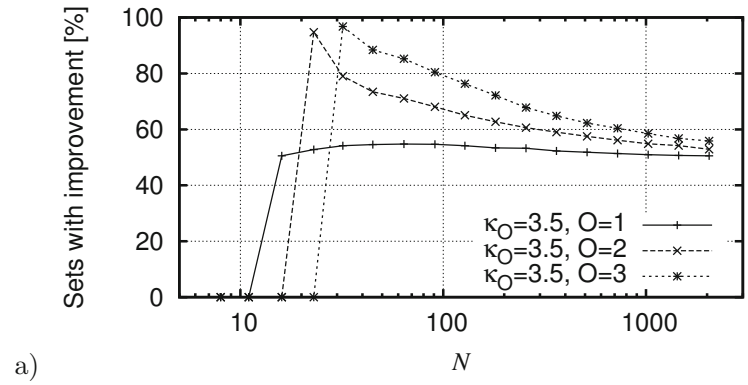


a)

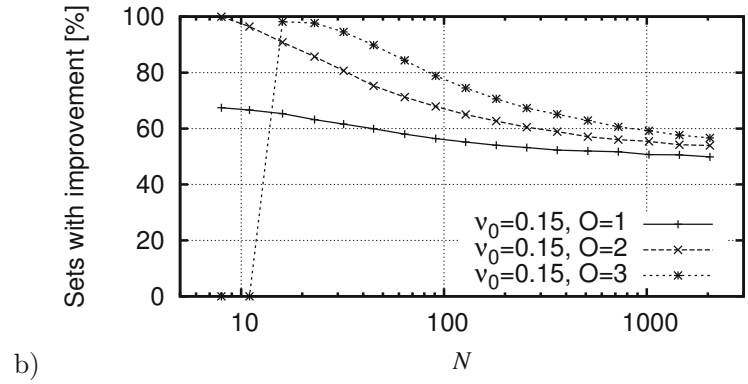


b)

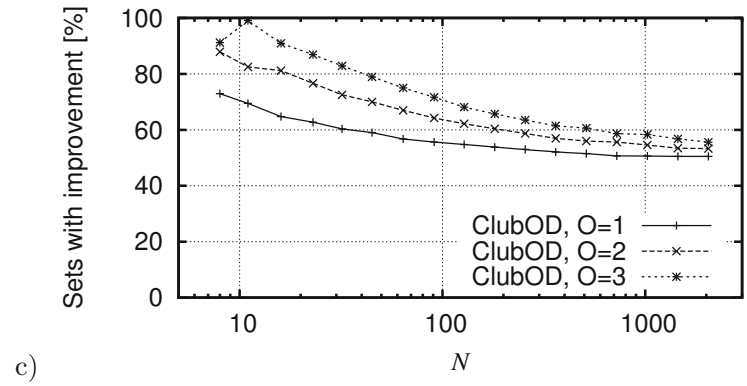


c)

Figure A.4: Normally distributed data: percentage of data sets with better estimates of $y$ after the removal of observations classified as outliers. Data sets with insertion of one, two or three contaminants; a) $\kappa_O = 3.5$, b) Chauvenet's criterion $\nu_0 = 0.15$, c) cluster criterion.

also be noted that the amount of improvement of the estimated value $\hat{y}$ is on average higher than its degradation (**Figure A.5**). The changes are given as absolute values. With increasing $N$, the influence of outliers on the estimation of $y$ decreases, and so do the changes.

## A.2 Non-Gaussian distribution

Albeit originally developed for normally distributed deviates, the cluster-based method also works well for other distributions. As a matter of course, the method of standardised residuals will fail in these cases. Two examples are discussed here.

### A.2.1 Laplace distribution

The Laplace distribution is a two-sided exponential distribution

$$f(\Delta) = \frac{1}{2 \cdot b} \cdot \exp\left(-\frac{|\Delta - \mu|}{b}\right)$$

which was investigated with $\mu = 0$ and $b = 1$. It turns out that the estimated standard deviation $\hat{\sigma}_\mathrm{y}$ is not suitable anymore as basis for discrimination of good observations and outliers. It causes the $\kappa_\mathrm{O} \cdot \hat{\sigma}_\mathrm{y}$ criterion to reject far too many observations with increasing $N$ (**Figure A.6**, in comparison with Fig.A.3, O=0). The cluster-based criterion, however, only shows a somewhat increased tendency to declare observations as contaminant. On average, only about 1.5 samples from the end of the tail are declared as contaminant per data set. That means, it is resistant to long tails in the distribution of deviates.

Most interestingly, the removal of putative outliers improves the estimated value on average. The proposed cluster-based method has here the highest percentage of improved data sets (**Figure A.7**).

### A.2.2 Uniformly distributed data

When applying both outlier detection schemes to uniformly distributed and outlier-free data ($-1 \leq y_i \leq +1$), almost no outliers are detected and the few cases of wrong classification mostly decrease the quality of the estimated $\hat{y}$. Using a fixed threshold $\kappa_\mathrm{O} = 3.5$, none of the observations is classified as an outlier.

After the insertion of outliers, uniformly distributed in the range of $2 \ldots 4$, the proportion of sets classified as containing at least one outlier significantly increases (**Figure A.9** a). Only in cases of small data sets, do the inserted outliers

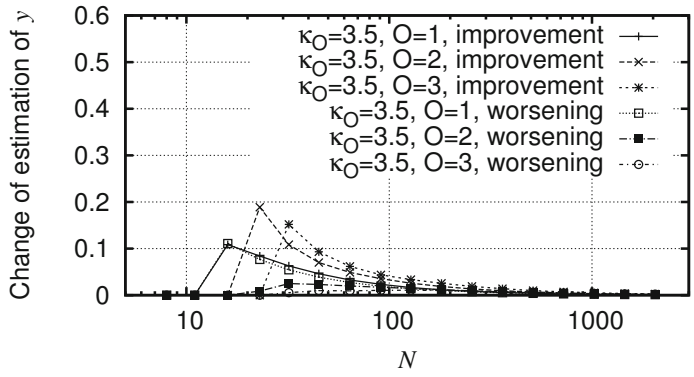


a)

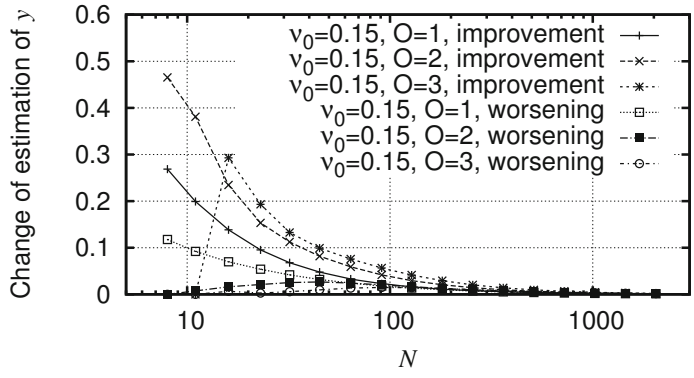


b)

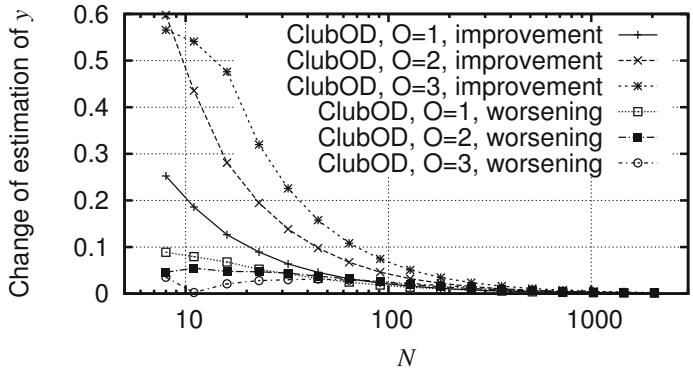


c)

Figure A.5: Normally distributed data: quantitative change of estimated $\hat{y}$ after the removal of observations classified as outliers. Data sets with insertion of one, two or three contaminants; a) $\kappa_{\mathrm{O}} = 3.5$, b) Chauvenet's criterion $\nu_0 = 0.15$, c) cluster criterion.

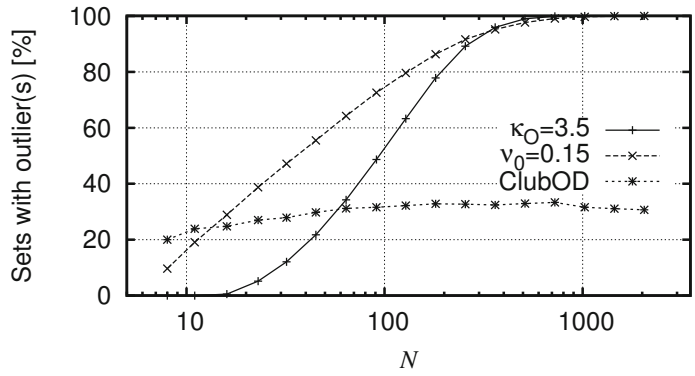


Figure A.6: Laplace distribution: percentage of data sets with at least one observation classified as an outlier.

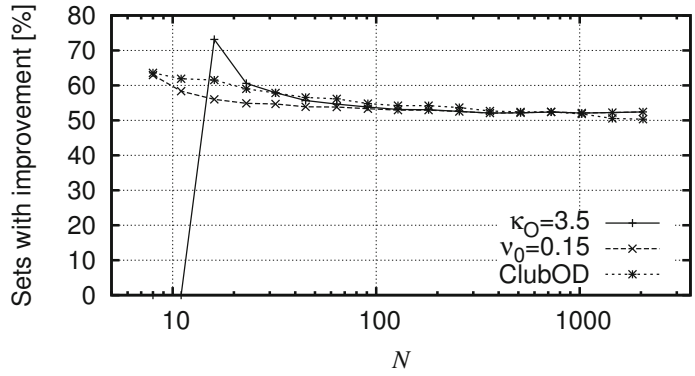


Figure A.7: Laplace distribution: percentage of data sets with better estimates of $y$ after the removal of observations classified as outliers.

influence the determination of $\sigma_\Delta$ (standardised residuals) or the computation of $d_{\text{glob}}$ (cluster-based approach) so strongly that the outliers are likely to become part of the cluster of 'good' observations. In terms of improvement after removal of putative contaminants, there is no significant difference between the approaches. That is why **Figure A.9** b) only shows the results based on a single inserted outlier.

It might be of interest that, if the data contains two outliers, the proposed approach typically finds both, whereas the method of standardised residuals often detects only one (**Figure A.10**).

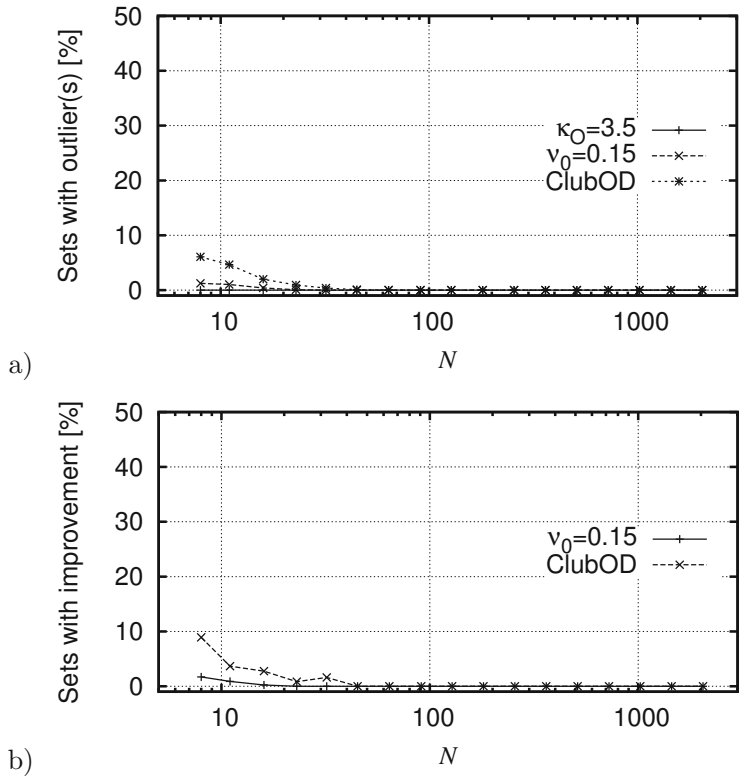


Figure A.8: Uniformly distributed observations: a) percentage of data sets with at least one observation classified as outlier; b) percentage of data sets with better estimates of $y$ after the removal of observations classified as outliers.

## A.3 Discussion

The Monte-Carlo simulations presented above underline numerically that the removal of observations decreases the estimation accuracy if normal distribution is assumed and the data set contains no outliers. This result can be generalised for any unbounded distribution. If any arbitrarily large value is an element of the distribution, none of the observations may be regarded as an outlier, regardless of the criterion that is used. The situation changes as soon the presence of outliers can be assumed. In the majority of cases, the removal of potential outliers improves the data analysis, and the improvements are higher than the effect, by which the estimation becomes worse.

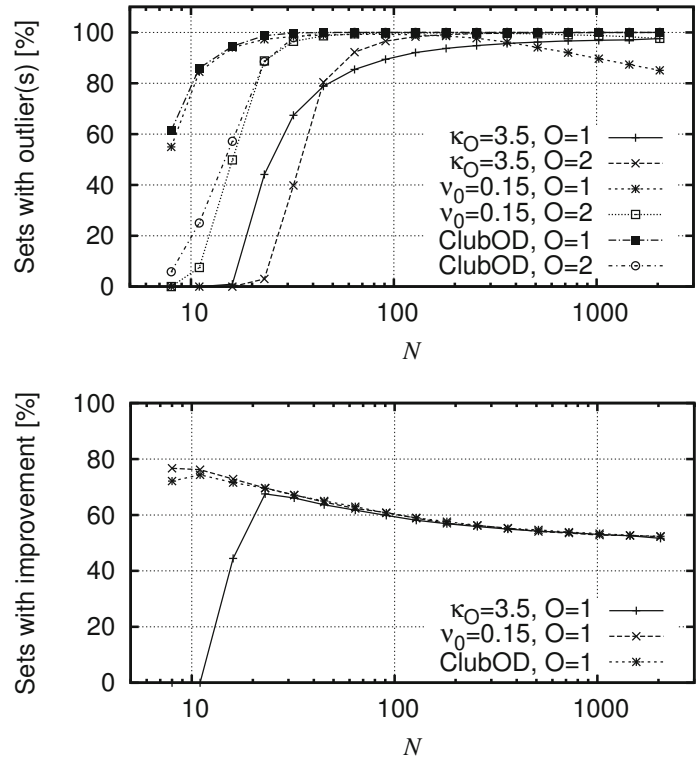


Figure A.9: Uniformly distributed observations: a) percentage of data sets with at least one observation classified as an outlier; b) percentage of data sets with better estimates of $y$ after the removal of observations classified as outliers.

The simulations have also revealed that the method of standardised residuals sometimes places the threshold $\lambda_O$ in between similar observations, which contradicts the intuitive decision as to the definition of outliers. In contrast, the cluster-based method considers the distances between deviates, and only removes those points that are in fact remote from the cluster of true observations. In addition, the cluster-based method is able to adapt itself to the possibly sparse distribution of deviates.

The benefits from the cluster-based approach become especially apparent, when the deviates are not normally distributed. In the case of Laplace distribution, the method of standardised residuals declares far too many observations as contaminant, whereas the proposed method is only slightly affected. In case of uniformly

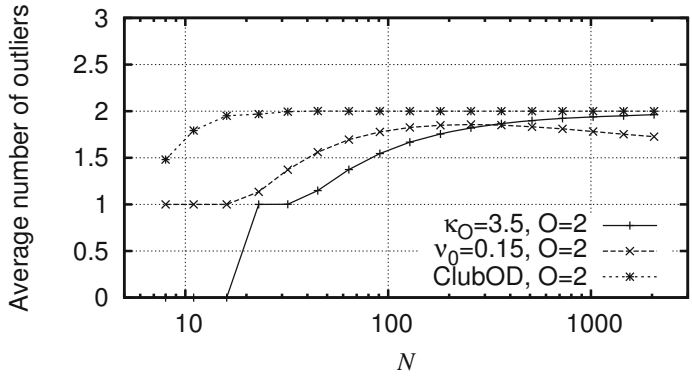


Figure A.10: Uniformly distributed observations: average number of detected outliers per data set, with two outliers inserted on purpose.

distributed data, only the proposed approach is able to detect true outliers with sufficient reliability, because it finds multiple outliers, while the method of standardised residual often only finds one out of two inserted outliers, for example.

The statistical relevance of results has been obtained by large scale tests based on simulated data. Presenting results of a particular data set from a concrete application would not prove or disprove the effectiveness of the approaches.

The inherent principle of the cluster-based method is generally compatible to any distribution of deviates, as soon as the deviates of outliers are more distant to others than the deviates of true data points, making it a very versatile method.

# Appendix B

# Implementation

## B.1 Functionality

The source code provided along with this book[1] addresses the tasks of linear as well as nonlinear data fitting using the method of weighted least-squares approximation as described in this book. It is by no means a software package for general purposes, but implements the discussed equations more or less in a one-to-one mapping. In other words: the implementation is neither optimised for speed nor for performance, but enables a maximum of understanding.

The software contains a selection of linear and nonlinear model function that were discussed in the previous chapters. The choice of arbitrary functions is not supported, however, with some basic programming skills in C, the interested reader should be able to add model functions of his or her needs.

The reader should be aware that there are other free software packages for least-squares optimisation available. Here only the 'fit' command of the gnuplot program [Gnupl] is mentioned. It enables the definition of arbitrary nonlinear functions. However, the conditions may appear in maximal three dimensions.

Please note that the packages known to the author do support neither the automated weighting nor outlier detection.

The next section explains the usage of the software. Special problems of implementation are discussed afterwards.

## B.2 Manual

The program can be called with a number options, most of them will discussed below in detail. **Figure B.1** and **Figure B.2** show the program output in case that a wrong option was given on the command line. Most options require an additional parameter. This is indicated by a following string starting with

[1] see 'OnlinePlus' area of the publishers website

T. Strutz, *Data Fitting and Uncertainty*, DOI 10.1007/978-3-8348-9813-5,

```
-i %s  ... input data file (compulsory)
-o %s  ... output file (compulsory)
-m  %d ... model function (compulsory)
       0 ... constant
       1 ... f(x|a) = a1 + SUM_j=2^M a_j * x_(j-1)
       2 ... f(x|a) = a1 + a2 * cos( x) + a3 * sin( x) [in degrees]
       3 ... f(x|a) = a1 + x[n-1] + a2 * x[n-1] + a3 * x[n-3]
       5 ... f(x|a) = a1 + a2 * cos( x - a3) [in degrees]
       6 ... f(x|a) = a1 + a2 * exp( a3 * x)
       7 ... f(x|a) = log( a1 * x)
       8 ... f(x|a) = a1 * exp( (x-a2)^2 * a3) +
                      a4 * exp( (x-a5)^2 * a6)
       9 ... f(x|a) = a1 * exp( a2 * x)
      10 ... ln(f(x|a)) = ln(a1) + a2 * x
      11 ... f(x|a) = a1 * exp( -|x|^a2 * a3)
      12 ... f(x|a) = a1 + a2 * x + a3 * cos( x - a4) [in radians]
      13 ... f(x|a) = a1 * exp( (x-a2)^2 * a3) +
      16 ... f(x|a) = a1 + a2 * x + a3 * x^2
      17 ... f(x|a) = a1 + a2 * x + a3 * x^2 + a4 * x^3
      18 ... f(x|a) = sum_{j=1}^M aj * x^(j-1) (linear)
      20 ... f(x|a) = a1 + a2*x1 + a3*x1^2 + a4*x2 +a5*x2^2
      21 ... f1(x|a) = a1 + cos(a3) * x1 - sin(a3) * x2 [in radians]
             f2(x|a) = a2 + sin(a3) * x1 + cos(a3) * x2 [in radians]
      22 ... f(x|a) = a1 + a2*cos(a3*x-a4)         [in radians]
      23 ... f(x|a) = a1 + a2*cos(a3*x-a4) + a5*cos(2*a3*x-a6)
      24 ... f(x|a) = 0 = (x1 - a1)^2 + (x2 - a2)^2 - a3*a3 (circle)
      25 ... f(x|a) = x1^2 + x2^2 = a1*x1 + a2*x2 - a3
                              (circle, linear)
      26 ... f(x|a) = 0 = (sqrt[(x1 - a1)^2 + (x2 - a2)^2] - a3)^2
                                        (circle, TLS)
      30 ... neural network 3x3x1, feed forward
      31 ... neural network 3x2x1
      32 ... neural network 1x2x1
      33 ... neural network 2x2x1
      34 ... neural network 1x3x1
      40 ... f(x|a) =(a1 + a2*x + a3*x*x + a4*x*x*x) /
                     (1 + a5*x + a6*x*x + a7*x*x*x)      NIST_THURBER
      41 ... f(x|a) = a1 * (x**2 + a2*x) /
                     (x*x + a3*x + a4)                   NIST_MGH09
      42 ... f(x|a) = a1 / (1 + exp(a2 - a3*x))          NIST_Rat42
      43 ... f(x|a) = a1 / [1 + exp(a2 - a3*x)]^(1/a4)   NIST_Rat43
      44 ... f(x|a) = a1 / a2 * exp(-0.5*((x -a3)/ a2)^2) NIST_Eckerle4
      45 ... f(x|a) = a1 * exp( a2 / (x+a3))             NIST_MGH10
      46 ... f(x|a) = a1 * (x+a2)^(-1/a3)                NIST_Bennett5
      47 ... f(x|a) = a1 *(1 - exp( -a2 * x)             NIST_BoxBOD
```

Figure B.1: Legal options of the fitting program (part 1)

```
-a  %d ... inversion algorithm (default: 1)
       0 - cofactor method
       1 - singular value decomposition
       2 - LU decomposition
-a[j]  %f ... provides initial value for  a_j (j=1,2,..,9)
-b  %d ... observations per bin, for '-w 2' (default: 50)
-c     ... enable scaling of conditions
-cc %s ... comma-separated list of column(s) containing
           conditions x (default: 1,2,...)
-co %d ... column containing observations y (default: 2)
-f     ... forget weights after outlier removal
-H     ... enable true Hessian matrix
-I %d   ... maximum number of iterations (default: 2000)
-M %d   ... number of parameters (for '-m 1' only)
-n     ... force usage of numerical derivation
-L     ... use Gaus-Newton instead of Levenberg-Marquardt
-s     ... use special SVD function for solving linear model
-t %f  ... target value for chisq (maximum error)
           default: iteration until convergence
-w %d   ... weighting  (default: 0)
       0 ... no weighting
       1 ... based on deviates
       2 ... binning
-x %d   ... outlier removal (default: 0)
       0 ... no outlier removal
       1 ... Chauvenet's criterion
       2 ... cluster criterion
```

Figure B.2: Legal options of the fitting program (part 2)

character '%'. If the next letter is 'd', then an integer number is expected, 'f' stands for a floating-point number, and 's' indicates that a string is required. There are only three mandatory options '-i', '-o', and '-m'. All other options are assigned a default value.

### B.2.1 Input and output

**Option '-i'** expects the file name of an ASCII text file containing the data to be processed. It must be organised in columns. Comment lines (lines starting with '#') and lines containing only white spaces (space, tabulator, line feed, carriage return) are ignored (**Figure B.3**).

Please ensure that all lines are finished with the *newline* (or *line feed*) character '\n' (ASCII code 10). Some text editors insert just single *carriage return* characters '\r' (ASCII code 13). These are not recognised by the C function `fgets()`, which is used for scanning the text. Wrong interpretation of the input data would be the consequence.

```
# This is comment line

# condition1 condition2   observation
  1           1.0             10.3
  1           2.3             11.5
  2           1               12.3
  2           2               14.4
# end of data
```

Figure B.3: Input example with conditions in columns one and two and observations in column three; neither option '-cc' nor '-co' are required

Based on the chosen model function (**option '-m'**), the program generally knows how many conditions have to be red. There are two exceptions. Model function '-m 1' activates multivariate regression

$$f(\mathbf{x}|\mathbf{a}) = a_1 + \sum_{j=2}^{M} a_j \cdot x_{j-1} \ .$$

The number of parameters (number of dimensions plus 1) must be given, in addition, via **option '-M'**. The same holds true for fitting a polynomial function ('-m 18' and '-m 19')

$$f(\mathbf{x}|\mathbf{a}) = \sum_{j=1}^{M} a_j \cdot x^{j-1} \ .$$

By default, the first condition $x_{1,i}$ is red from the first column, the second condition $x_{2,i}$ (if required) from the second column and so on. If the conditions are located differently, **option '-cc'** can be used to specify the corresponding columns. Let the two conditions $x_{1,i}$ and $x_{2,i}$ be located in columns two and three, for example, then '-cc 2' indicates the column of the first condition. The next condition is automatically taken from the next column. If, however, the conditions are not sorted in ascending order, then option '-cc' requires a comma-separated list of columns.

When the number of conditions is *cond_dim*, then the observations $y_i$ are expected in the column number *cond_dim*+1, otherwise the column must be specified using the **option '-co'**.

In the example of Figure B.3, the columns must not specified by neither option '-cc' nor '-co'. **Figure B.4** shows an input-file example with a different arrangement of columns. The columns deviate from the default settings and the

```
# this is file "dummy.txt"
# containing dummy observation and condition values
      # also comment followed by an empty line

# this is file "dummy.txt"
# containing dummy observation and condition values
  # also comment

# obs cond2  cond1  obs_exp
  1    2      3      3
  3    2      4      2
  4    2      5      1.5

# comment
  5    3      3      1
  7    3      4      0.8
  7    3      5      0.75
```

Figure B.4: Input example with conditions in unexpected order; option '-cc' and '-co' are required

corresponding **options '-cc 3,2'** and **'-co 1'** must be provided when calling the fitting program.

With the the option '-cc 0', the program assumes that no special condition values are provided and sequential numbers starting from $1, 2, \ldots$ are used as conditions, that means the condition is merely the number of the experiment.

The program writes the data-fitting results into a text file determined by **option '-o'**. Dependent on the chosen options, the content of this file can vary a lot. The output was designed to provide the user with a maximum of feedback about the convergence process. Especially, when using weights estimation in combination with nonlinear model functions, this file can be become rather long, because of the nested iterations. In order to make these files suitable as input for gnuplot ([Gnupl]), all non-empty lines start with '#' apart from the final values.

### Example 1

The command-line options "-i dummy.txt -o dummy_cc0_m0.txt -m 0 -cc 0" tell the program that the data has to be red from the text file "dummy.txt" (Figure B.4) and that none of the columns is used as condition values. '-m 0' indicates the fitting of a constant value, i.e. model function $y = a_1$. Despite

```
# main ================================
# use data file: dummy.txt
# constant function
# Number of observations: 6
# Number of parameters  : 1
# condition columns: 0
# observations column: 2
#
# fitting a linear system
# use special SVD based algoritm
#
#====================================
# main: approximation with final weights #: 0
#  -- ls - start  ------------------------------
#
#  singular values (thresh = 1E-012)
#  s1=2.4494897427832,
#  -- ls - end  --------------------------------
#
# main
# Parameters:  a1=2.500000,
#
# | chisq: 1.500000
# | mean of |deviates|: 0.500000
# | variance of |deviates|: 0.000000
# | goodnes of fit: 0.300000
# | number of outliers: 0
#
# evaluation of results
#  number of outliers: 0
#  parameters: a1=2.500000
#  chi square.................: 1.5
#  goodness of fit............: 0.3
#  uncertainty in observations: 0.547722557505
#
#  (co)variance of parameters:
#        0.167

#  (co)variance of parameters multiplied with goodness of fit
#        0.050

#  resulting uncertainty of parameters
#     0.223607
#        8.94%
#
# Final_Parameters a1= 2.5
#  cond1        observed     fitted   weight uncertainty glob.uncertainty difference
    1.000000     2.000000     2.500000    1.000000     1.000000  0.547723   -0.500000
    2.000000     2.000000     2.500000    1.000000     1.000000  0.547723   -0.500000
    3.000000     2.000000     2.500000    1.000000     1.000000  0.547723   -0.500000
    4.000000     3.000000     2.500000    1.000000     1.000000  0.547723   +0.500000
    5.000000     3.000000     2.500000    1.000000     1.000000  0.547723   +0.500000
    6.000000     3.000000     2.500000    1.000000     1.000000  0.547723   +0.500000
```

Figure B.5: Example 1: Output example for fitting a constant with '-cc 0'

the absence of conditions, the dimensionality of the condition space is set to $cond\_dim = 1$ for algorithmic reasons. Hence, the observations are expected in column $cond\_dim + 1 = 2$. The output of the fitting process is written to the text file "dummy_cc0_m0.txt", see **Figure B.5**. The output file starts with general information about the fitting process, i.e., which data file was used, which model function was approximated, how many observations were used, and how many model parameters had to be determined. This is followed by information about the iterated estimation of weights. Since weighting was not applied in this example, there is only a single run with number '# 0'. There is some feedback of the least-squares algorithm in each iteration. In the case of Figure B.5, there is

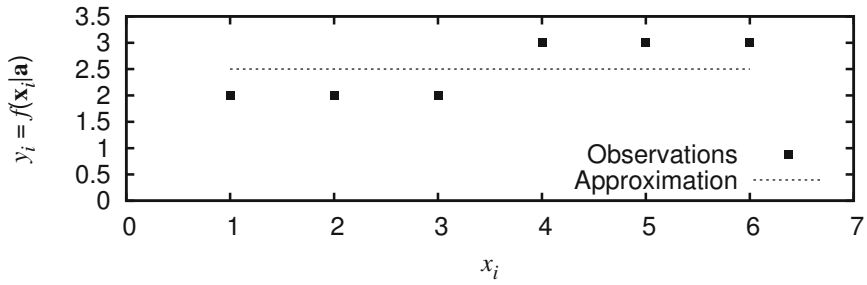


Figure B.6: Example 1: Comparison between observations and fitted model function

some information about the matrix inversion via singular value decomposition.

After the fitting process, the results are output ($\chi^2$, goodness-of-fit, number of outliers, standard uncertainty of observations $\sigma_\mathrm{y}$ and other). Of highest importance are probably the uncertainties of estimated parameters which are additionally given in percent. According to Chapter 4, this value should always be inspected. An uncertainty above 10% can indicate suspicious fitting results and the program outputs a warning also on the console.

The output finishes with a list of used data, the approximated observations ('fitted') and information about the estimated weights $w_i$, the estimated uncertainty $\sigma_i$ of each observation $y_i$, the global uncertainty $\sigma_\mathrm{y}$, and the difference between the approximated and measured observations $(y_i - \hat{y}_i)$ with $\hat{y}_i$ according to equation (3.4) on page 50.

**Figure B.6** shows the comparison between observations and fitted model function.

### Example 2

The command-line options "-i dummy.txt -o dummy_cc23_co1_m1_M3.txt -cc 2,3 -co 1 -m 1 -M 3" tell the program that the data must be red from the text file "dummy.txt" and has to be fitted against a plane. The input data is from the same input file as before (Fig. B.4). **Figure B.7** shows the corresponding output file. It contains similar information as Figure B.5. There are, however, two columns of conditions now, which are interpreted as raster points on a grid, while the observation is the value of elevation. The uncertainty of the parameters is indicated as suspicious. Obviously, the model function does not fit the data very well.

```
# main ================================
# use data file: dummy.txt
# linear in x, order 2
# Number of observations: 6
# Number of parameters  : 3
# condition columns: 2 3
# observations column: 1
#
# fitting a linear system
# use special SVD based algoritm
#
#====================================
# main: approximation with final weights #: 0
#  -- ls - start  ------------------------------
#
#  singular values (thresh = 1E-012)
#  s1=11.944357370871, s2=0.33724838998668, s3=1.4894933770784,
#  -- ls - end  --------------------------------
#
# main
# Parameters:  a1=-7.933333, a2=3.266667, a3=1.075000,
#
# | chisq: 0.204167
# | mean of |deviates|: 0.152778
# | variance of |deviates|: 0.010687
# | goodnes of fit: 0.068056
# | number of outliers: 0
#
# evaluation of results
#  number of outliers: 0
#  parameters: a1=-7.933333 a2=3.266667 a3=1.075000
#  chi square..................: 0.204166666667
#  goodness of fit.............: 0.0680555555556
#  uncertainty in observations: 0.260874597375
#
#  (co)variance of parameters:
#       8.333       -1.667       -1.000
#      -1.667        0.667       -0.000
#      -1.000       -0.000        0.250

#  (co)variance of parameters multiplied with goodness of fit
#       0.567       -0.113       -0.068
#      -0.113        0.045       -0.000
#      -0.068       -0.000        0.017

#  resulting uncertainty of parameters
#     0.753080     0.213003     0.130437
#       9.49%        6.52%       12.13%
# 1 parameter(s) have relative high uncertainty !
#
# Final_Parameters a1= -7.93333333333 a2= 3.26666666667 a3= 1.075
#  cond1        cond2        observed     fitted   weight uncertainty glob.uncertainty difference
    2.000000     3.000000     1.700000     1.825000    1.000000     1.000000  0.260875   -0.125000
    2.000000     4.000000     3.000000     2.900000    1.000000     1.000000  0.260875   +0.100000
    2.000000     5.000000     4.000000     3.975000    1.000000     1.000000  0.260875   +0.025000

    3.000000     3.000000     5.000000     5.091667    1.000000     1.000000  0.260875   -0.091667
    3.000000     4.000000     6.500000     6.166667    1.000000     1.000000  0.260875   +0.333333
    3.000000     5.000000     7.000000     7.241667    1.000000     1.000000  0.260875   -0.241667
```

Figure B.7: Example 2: Output example for fitting a plane with equal weights

In order to provide a proper input to gnuplot [Gnupl], rows with different condition one (cond1) are separated by an empty line. This enables to draw a plane mesh as can be seen in **Figure B.8**.

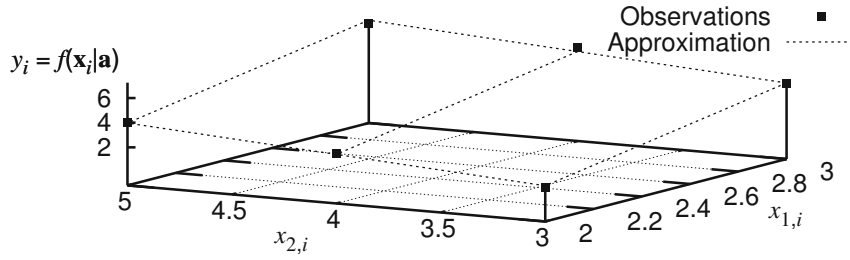


Figure B.8: Example 2: Comparison between observations and fitted model function

**Example 3**

The third example is to present a case of nonlinear data fitting. With the command-line options "-i dummy.txt -o dummy_cc0_co4_m9.txt -cc 0 -co 4 -m 9" the output in **Figure B.9** and **Figure B.10** is produced. As the parameters have to be estimated in an iterative manner, the generated output is much longer. In total, thirteen iterations are necessary to reach the convergence criterion. Figure B.9 shows only the results of iteration #1 and #11 – #13. The difference compared to the linear fitting starts with the output of the initially estimated parameter values. As can be seen in comparison to the final value, the initial value of $a_1$ is not very good. The reason lies in the assumption of the corresponding routine that the condition values start close to zero, while in the example the first condition is equal to one. Nevertheless, the algorithm finally approaches the global minimum.

In each iteration of least-squares approximation, the updates $\Delta a_j$, the resulting (intermediate) parameter estimates, and the value of $\chi^2$ are given. As expected, $\chi^2$ is decreasing in the course of iteration.

In case that the update does not lead to a decreasing $\chi^2$ in a particular round, the update is rejected (for example in iteration #11) and the parameter $\mu$ of the Levenberg-Marquardt method is increased in order to give the gradient-descent approach a higher weight (compare Subsection 6.4.4). The result of the fitting process is visualised in **Figure B.11**.

### B.2.2 Initialisation of model parameters

As pointed out in Section 2.3, it is required to initialise all parameters $a_j$ with a certain value, if the model function is nonlinear. Typically, the corresponding

```
# main ==============================
# use data file: dummy.txt
# exponential 2
# Number of observations: 6
# Number of parameters  : 2
# condition columns: 0
# observations column: 4
#
# algorithm for inversion: SVD
# fitting a nonlinear system
# use Levenberg-Marquardt method
# initial Parameters
# a1=1.660000000, a2=-0.271084337,
#
#==================================
# main: approximation with final weights #: 0
#  -- ls - start  -----------------------------
#
#  Iteration of least squares: 1
#  Updates:  da1=2.3233817125245, da2=-0.10885501320102,
#
#  Parameters:  a1=3.98338171252, a2=-0.37993935055,
#
#  chisq: 0.32117299135648  mu_fac: 1.000000e-004
#
#  Iteration of least squares: 2
#  Updates:  da1=0.069147985340399, da2=0.056935233145382,
#
#  Parameters:  a1=4.05252969786, a2=-0.323004117405,
#
#  chisq: 0.061775130101859  mu_fac: 5.000000e-005
    .
    .
    .
#  Iteration of least squares: 11
#  Updates:  da1=1.6863979690383E-010, da2=-2.1206452195462E-011,
#
#  rejection, chisq=0.059597741261129
#
#  Parameters:  a1=4.05787643972, a2=-0.328323111241,
#
#  chisq: 0.059597741261129  mu_fac: 3.164063e-005
#
#  Iteration of least squares: 12
#  Updates:  da1=1.6771781155617E-010, da2=-2.1142623269165E-011,
#
#  Parameters:  a1=4.05787643989, a2=-0.328323111262,
#
#  chisq: 0.059597741261129  mu_fac: 1.582031e-005
#
#  Iteration of least squares: 13
#  Updates:  da1=1.6346232385932E-012, da2=-1.4711255482683E-013,
#
#  Parameters:  a1=4.05787643989, a2=-0.328323111263,
#
#  chisq: 0.059597741261129  mu_fac: 7.910156e-006
#
#  convergence after 13 iterations
#  -- ls - end  -----------------------------
#
# main
# Parameters:  a1=4.057876, a2=-0.328323,
#
# | chisq: 0.059598
# | mean of |deviates|: 0.081178
# | variance of |deviates|: 0.003343
# | goodnes of fit: 0.014899
# | number of outliers: 0
    .
    .
    .
```

Figure B.9: Example 3: Output example for fitting a nonlinear model function (part 1)

```
    .
    .
    .
#
# evaluation of results
#  number of outliers: 0
#  parameters: a1=4.057876 a2=-0.328323
#  chi square.................: 0.0595977412611
#  goodness of fit............: 0.0148994353153
#  uncertainty in observations: 0.122063243097
#
#  (co)variance of parameters:
#        3.352       -0.303
#       -0.303        0.038

#  (co)variance of parameters multiplied with goodness of fit
#        0.050       -0.005
#       -0.005        0.001

#  resulting uncertainty of parameters
#     0.223477     0.023823
#        5.51%        7.26%
#
# Final_Parameters a1= 4.05787643989 a2= -0.328323111263
#  cond1        observed     fitted   weight uncertainty glob.uncertainty difference
    1.000000     3.000000     2.922200    1.000000     1.000000  0.122063   +0.077800
    2.000000     2.000000     2.104365    1.000000     1.000000  0.122063   -0.104365
    3.000000     1.500000     1.515417    1.000000     1.000000  0.122063   -0.015417
    4.000000     1.000000     1.091297    1.000000     1.000000  0.122063   -0.091297
    5.000000     0.800000     0.785876    1.000000     1.000000  0.122063   +0.014124
    6.000000     0.750000     0.565933    1.000000     1.000000  0.122063   +0.184067
```

Figure B.10: Example 3: Output example for fitting a nonlinear model function (part 2)

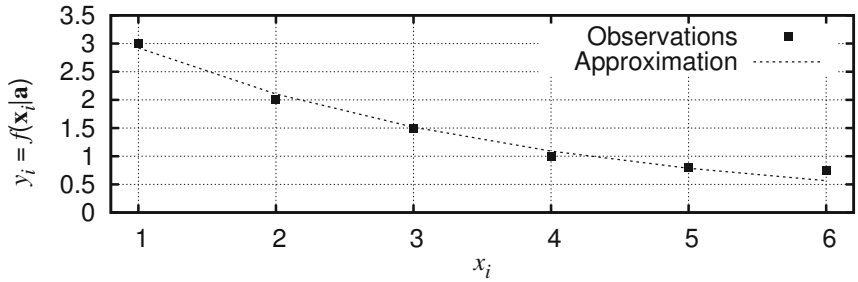


Figure B.11: Example 3: Comparison between observations and fitted model function

routines guess starting values from the observations themselves. In case that theses guesses are not sufficient and, for example, the algorithm does not find the global minimum, it is possible to provide initial parameter when starting the program using the **options '-a1', '-a2', . . . , '-a9'**.

### B.2.3 Processing control

There are some options controlling the kind of processing. **Option '-I'** allows for changing the maximum number of iterations (default is 2000). **Option '-s'** switches off the special SVD-based algorithm for the fitting of linear problems. Instead of equation (6.5), now equation (6.11) is used. In the case of nonlinear fitting, **Option '-L'** switches from the Levenberg-Marquardt approach, equation (6.26), to the Gauss-Newton method, equation (6.22).

### B.2.4 Weights and outliers

#### Example 1

**Option '-w'** enables the estimation of weights for each single observation. The choice of '-w 1' triggers the estimation based on the deviates (see Subsection 3.3.2). Based on the parameters "-i dummy.txt -o dummy_cc0_co1_m1_M2_w1.txt -co 1 -cc 0 -m 1 -M 2 -w 1", the programs output reflects this iterative estimation process (**Figure B.12** and **Figure B.13**)

The program starts with ordinary least-squares approximation, i.e. equal weights. The sorted deviates are inspected and the weights accordingly derived. After 12 cycles, weights estimations has converged and two out of the six observations are strongly down-weighted, as they are much more distant to the fitted straight line than the others. The thirteenth cycle is used to fit the data with the final weights. Please note that the minimisation target $\chi^2$ must not decrease with changing weights.

**Figure B.14** shows that the approximated line is dominated by the four observations owing high weights.

#### Example 2

Using the same options as in the previous example but including **option '-x'** enables the detection and removal of outlying observations. Independent of the detection scheme, the two down-weighted observations are identified as being contaminant and the fitting of the remaining four values yields a perfect straight-line fit.

The outlier detection is started directly after the convergence of the weights. **Figure B.15** shows the end of the programs output.

```
# main ==============================
# use data file: dummy.txt
# linear in x, order 1
# Number of observations: 6
# Number of parameters  : 2
# condition columns: 0
# observations column: 1
#
# fitting a linear system
# use special SVD based algorithm
#====================================
# main: weights iteration #: 0
#  -- ls - start  ------------------------------
#
#  singular values (thresh = 1E-012)
#  s1=1.0463419638985, s2=9.7931184254345,
#  -- ls - end  ------------------------------
#
# main
# Parameters:  a1=0.733333, a2=1.085714,
#
# | chisq: 0.204762
# | mean of |deviates|: 0.147619
# | variance of |deviates|: 0.012336
# | goodnes of fit: 0.051190
# | number of outliers: 0
#
# enter weight estimation
# -- est_weights1 - start ----------------------
#  Number of observations: 6
#  max_deviate: 0.338095
#  lambda_L = 0.119048
#
#  dev_sort[i],  weights[ idx[i] ]
#   0  9.523809524e-003      70.56000000
#   1  7.619047619e-002      70.56000000
#   2  9.523809524e-002      70.56000000
#   3  1.190476190e-001      70.56000000
#   4  2.476190476e-001      16.30917160
#   5  3.380952381e-001       8.74826423
# -- est_weights1 - end  -------------------------
#
# main
#  i       observ         calc      deviates    weights
#  0       1.70000      1.81905      0.11905      70.560000
#  1       3.00000      2.90476      0.09524      70.560000
#  2       4.00000      3.99048      0.00952      70.560000
#  3       5.00000      5.07619      0.07619      70.560000
#  4       6.50000      6.16190      0.33810       8.748264
#  5       7.00000      7.24762      0.24762      16.309172
#====================================
# main: weights iteration #: 1
#  -- ls - start  ------------------------------
#
#  singular values (thresh = 1E-012)
#  s1=7.5396235253955, s2=56.330172166194,
#  -- ls - end  ------------------------------
#
# main
# Parameters:  a1=0.724590, a2=1.080075,
#
# | chisq: 3.856002
# | mean of |deviates|: 0.146679
# | variance of |deviates|: 0.013516
# | goodnes of fit: 0.964000
# | number of outliers: 0
#
# enter weight estimation
# -- est_weights1 - start ----------------------
#  Number of observations: 6
#  max_deviate: 0.375037
#  lambda_L = 0.115261
#
   :
```

Figure B.12: Example for fitting with weights estimation based on deviates (part 1)

```
    :
# enter weight estimation
# -- est_weights1 - start ----------------------
#  Number of observations: 6
#  max_deviate: 0.499166
#  lambda_L = 0.024958
#
#  dev_sort[i]          weights[ idx[i] ]
#   0  2.410498630e-006    1605.35067674
#   1  8.387731592e-004    1605.35067674
#   2  1.670314822e-003    1605.35067674
#   3  1.675135820e-003    1605.35067674
#   4  2.974885015e-001      11.29951055
#   5  4.991660478e-001       4.01337669
# -- est_weights1 - end  -------------------------
#
# main
#  i       observ         calc      deviates    weights
#  0       1.70000      1.99749      0.29749      11.299511
#  1       3.00000      2.99832      0.00168    1605.350677
#  2       4.00000      3.99916      0.00084    1605.350677
#  3       5.00000      5.00000      0.00000    1605.350677
#  4       6.50000      6.00083      0.49917       4.013377
#  5       7.00000      7.00167      0.00167    1605.350677
#
# convergence of weights
#
#===================================
# main: approximation with final weights #: 12
#  -- ls - start  -----------------------------
#
#  singular values (thresh = 1E-012)
#  s1=28.754092057198, s2=331.76700514052,
#  -- ls - end  -----------------------------
#
# main
# Parameters:  a1=0.996652, a2=1.000836,
#
# | chisq: 2.010113
# | mean of |deviates|: 0.133474
# | variance of |deviates|: 0.038464
# | goodnes of fit: 0.502528
# | number of outliers: 0
#
# evaluation of results
#  number of outliers: 0
#  parameters: a1=0.996652 a2=1.000836
#  chi square.................: 2.010113
#  goodness of fit............: 0.502528
#  uncertainty in observations: 0.021643
#
#  (co)variance of parameters:
#   0.00114784155 -0.000264948098
# -0.000264948098 7.07291791E-005
#  (co)variance of parameters multiplied with goodness of fit
#  0.000576823 -0.000133144
# -0.000133144 3.55434E-005

#  resulting uncertainty of parameters
#    0.0240171358   0.00596182952
#           2.41%          0.596%
#
# Final_Parameters a1= 0.996652140 a2= 1.000836362
#  cond1        observed     fitted   weight uncertainty glob.uncertainty difference
    1.000000     1.700000     1.997489   11.299511     0.297489  0.021643   -0.297489
    2.000000     3.000000     2.998325 1605.350677     0.024958  0.021643   +0.001675
    3.000000     4.000000     3.999161 1605.350677     0.024958  0.021643   +0.000839
    4.000000     5.000000     4.999998 1605.350677     0.024958  0.021643   +0.000002
    5.000000     6.500000     6.000834    4.013377     0.499166  0.021643   +0.499166
    6.000000     7.000000     7.001670 1605.350677     0.024958  0.021643   -0.001670
```

Figure B.13: Example for fitting with weights estimation based on deviates (part 2)

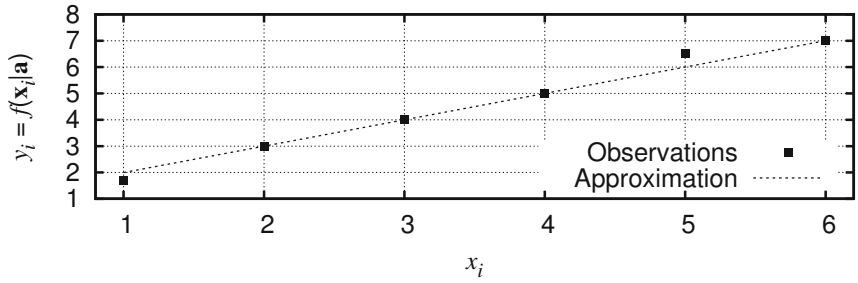


Figure B.14: Example 1: Comparison between observations and fitted model function when using estimation of weights

$\kappa_1$ is determined based on the number of observations, while $\kappa_2$ is set to a fixed value of 2. The routine for outlier detection outputs a table with sorted absolute deviates $\Lambda_s[n]$, the distances between the deviates $d[n]$, the global distance $d_{\text{glob}}[n]$, and the quotient $q[n] = d[n]/d_{\text{glob}}[n]$ (see Subsection 3.4.2). If $q[n] > \kappa_1$, then also the local distance $d_{\text{loc}}[n]$ and the quotient $r[n] = d[n]/d_{\text{loc}}[n]$ are computed. The final breakdown point is marked with a double-hash character. The table starts with $n = 4$ in this example, since sixty percent of the observations are assumed to be non-outliers. The weights of the contaminant data points are set to zero. The last cycle performs the least-squares approximation using the remaining observations and the actual weights.

**Example 3**

If sufficient observations under equal or similar conditions are available, then the standard uncertainty of observations can be reliably determined using the binning method (Subsection 3.3.1). **Figure B.16** contains the program output for such an example. In total, 500 data points were fitted to a polynomial function. The uncertainty of observation increases with the condition value and, in addition, they are influence by a positive bias.

First, observations from fifty consecutive conditions were fitted to straight lines, shown in the beginning of the output text file in Figure B.16. The deviation from this fit was taken as uncertainty for all of these fifty data points. The least-squares approximation then utilises the corresponding weights. The success is underlined by a goodness-of-fit value of $g_{\text{fit}} = 1.14$. However, the parameter $a_2$ shows a relative high uncertainty of about 12%. This indicates an inappropriate model function. The model function used for the fitting was $f(x|\mathbf{a}) = a_1 + a_2 \cdot x + a_3 \cdot x^2$, while the true process was $f(x|\mathbf{a}) = a_1 + a_3 \cdot x^2$, i.e. $a_2$ should be equal to zero.

```
          .
          .
          .
#
# convergence of weights
# -- outlier_detection2 - start ----------------------
#  Number of observations: 6
#  kappa1: 7.300000
#  kappa2: 2.000000
#
#   n   deviate    d[n]        d_glob       d[n]/d_glob    d_loc   d[n]/d_loc
# ------------------------------------------------------------------------------
#   4  2.975e-001  2.958e-001  5.00e-004    591.09  6.865e-006  43088.449324 * ##
#   5  4.992e-001  2.017e-001  1.02e-001      1.99
#
#  outliers detected !   lambda_0 = 0.297489
#
#   dev_sort[i]         dist_all[i]       weights[ idx[i] ]
#   0  2.410498624e-006 0.000000000e+000    1605.35067674
#   1  8.387731592e-004 8.363626605e-004    1605.35067674
#   2  1.670314822e-003 8.315416633e-004    1605.35067674
#   3  1.675135820e-003 4.820997248e-006    1605.35067674
#   4  2.974885015e-001 2.958133657e-001       0.00000000
#   5  4.991660478e-001 2.016775463e-001       0.00000000
# -- outlier_detection2 - end  ------------------------
#
#==================================
# main: approximation with final weights #: 12
#  -- ls - start  -----------------------------
#
#  singular values (thresh = 1E-012)
#  s1=28.642351244568, s2=331.5853018607,
#  -- ls - end  -----------------------------
#
# main
# Parameters:  a1=1.000000, a2=1.000000,
#
# | chisq: 0.000000
# | mean of |deviates|: 0.000000
# | variance of |deviates|: 0.000000
# | goodnes of fit: 0.000000
# | number of outliers: 2
#
# evaluation of results
#  number of outliers: 2
#  parameters: a1=1.000000 a2=1.000000
#  chi square.................: 2.5644567358E-026
#  goodness of fit............: 1.2822283679E-026
#  uncertainty in observations: 3.45721314435E-015
#
#  (co)variance of parameters:
#   0.00115684559 -0.000266964368
# -0.000266964368 7.11904981E-005

#  (co)variance of parameters multiplied with goodness of fit
# 1.48334E-029 -3.42309E-030
# -3.42309E-030 9.12825E-031

#  resulting uncertainty of parameters
# 3.85141563E-015 9.55418632E-016
#      3.85E-013%      9.55E-014%
#
# Final_Parameters a1= 1.000000000 a2= 1.000000000
#  cond1        observed     fitted   weight uncertainty glob.uncertainty difference
    1.000000     1.700000     2.000000    0.000000  9999.000000  0.000000   -0.300000
    2.000000     3.000000     3.000000 1605.350677     0.024958  0.000000   -0.000000
    3.000000     4.000000     4.000000 1605.350677     0.024958  0.000000   +0.000000
    4.000000     5.000000     5.000000 1605.350677     0.024958  0.000000   +0.000000
    5.000000     6.500000     6.000000    0.000000  9999.000000  0.000000   +0.500000
    6.000000     7.000000     7.000000 1605.350677     0.024958  0.000000   +0.000000
```

Figure B.15: Output example for fitting with outlier removal after estimation of weights

```
# main ================================
# use data file: polynom_biased.xy
# polynomial of 2nd order
# Number of observations: 500
# Number of parameters  : 3
# condition columns: 1
# observations column: 3
# fitting a linear system
# use special SVD based algoritm
#  -- est_weights2 - start ------------------------------
#  Number of bins: 10
#  bin number_of_observations   a1        a2             last_cond variance
#     0         50       9.9279e+000    2.3206e+000    1.3817e-001   8.412e-002
#     1         50       9.1731e+000    7.2364e+000    2.8010e-001   9.925e-002
#     2         50       7.7854e+000    1.1755e+001    5.0366e-001   5.764e-002
#     3         50       5.0093e+000    1.7649e+001    6.4755e-001   1.124e-001
#     4         50      -2.1232e+000    2.8296e+001    9.4245e-001   1.738e-001
#     5         50      -1.0234e+001    3.7062e+001    1.1285e+000   1.877e+000
#     6         50      -8.1908e+000    3.5651e+001    1.2778e+000   8.256e+000
#     7         50      -1.7926e+001    4.5995e+001    1.5758e+000   4.079e+001
#     8         50       1.3498e+001    3.1553e+001    1.7752e+000   1.295e+002
#     9         50      -1.0895e+002    1.0205e+002    1.9717e+000   2.689e+002
#  -- est_weights2 - end  ------------------------------
#====================================
# main: approximation with final weights #: 0
#  -- ls - start  ------------------------------
#  singular values (thresh = 1E-012)
#  s1=56.53362686549, s2=15.010473603365, s3=2.9327109772612,
#  -- ls - end  ------------------------------
# main
# Parameters:  a1=10.205032, a2=-2.092809, a3=18.615686,
# | chisq: 567.991503
# | mean of |deviates|: 3.613647
# | variance of |deviates|: 47.361795
# | goodnes of fit: 1.142840
# | number of outliers: 0
#
# evaluation of results
#  number of outliers: 0
#  parameters: a1=10.205032 a2=-2.092809 a3=18.615686
#  chi square.................: 567.991503173
#  goodness of fit............: 1.14284004663
#  uncertainty in observations: 1.06903697159
#
#  (co)variance of parameters:
#   0.00218900526  -0.00918148845   0.00795165394
#  -0.00918148845    0.0539568789   -0.0553097955
#   0.00795165394   -0.0553097955     0.064873586

#  (co)variance of parameters multiplied with goodness of fit
#   0.00250168    -0.010493   0.00908747
#    -0.010493    0.0616641   -0.0632102
#   0.00908747   -0.0632102    0.0741401

#  resulting uncertainty of parameters
#    0.0500168259     0.248322536     0.272286856
#           0.49%           11.9%           1.46%
# 1 parameter(s) have relative high uncertainty !
#
# Final_Parameters a1= 10.2050318876 a2= -2.09280850099 a3= 18.615685773
#  cond1        observed     fitted   weight uncertainty glob.uncertainty difference
    0.013620    10.002783    10.179981   11.888098     0.290031  1.069037   -0.177198
    0.013805     9.292838    10.179688   11.888098     0.290031  1.069037   -0.886850
    0.015035    10.121643    10.177775   11.888098     0.290031  1.069037   -0.056132
    0.015083     9.922627    10.177701   11.888098     0.290031  1.069037   -0.255074
    0.022013     9.813321    10.167984   11.888098     0.290031  1.069037   -0.354663
    :
    1.958257    76.087557    77.493657    0.003719    16.397803  1.069037   -1.406100
    1.960152   107.943153    77.627920    0.003719    16.397803  1.069037  +30.315233
    1.960207    94.607138    77.631819    0.003719    16.397803  1.069037  +16.975319
    1.960227    85.994650    77.633237    0.003719    16.397803  1.069037   +8.361413
    1.971709    99.422305    78.449640    0.003719    16.397803  1.069037  +20.972665
```

Figure B.16: Example for fitting with estimation of weights via binning

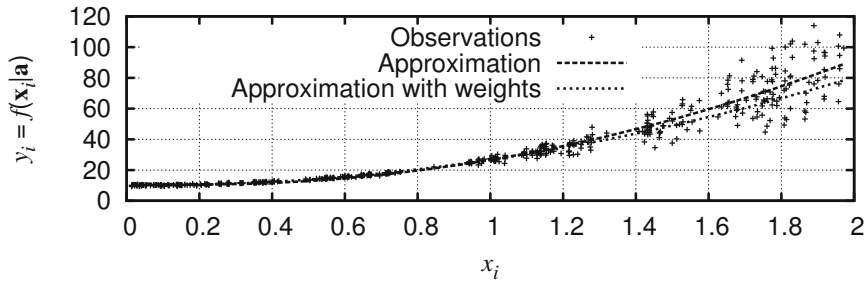


Figure B.17: Example 3: Comparison between observations and fitted model function when using estimation of weights

**Figure B.17** shows the approximated curves with and without the estimation of weights.

## B.3 General organisation of source code

The source code is organised in several '*.c' and '*.h' files.
The file `fitting.c` contains the main function. It

- reads the options from the command line,
- initialises the Jacobian matrix,
- initialises the model parameters, if a nonlinear model function was chosen,
- iterates the weights estimation,
- calls the least-squares routine with appropriate parameters,
- starts the outlier detection and removal after convergence of the weights estimation,
- re-runs the least-squares routine, if at least one outlier was found, and
- evaluates and outputs the results.

All functions not having a special header file have a prototype declaration in `prototypes.h`.

The least-squares fitting as such is encoded in file `ls.c`. All operations according to equation (2.6)

$$\boldsymbol{\Delta}\mathbf{a} = \left(\mathbf{J}^{\mathrm{T}} \cdot \mathbf{W} \cdot \mathbf{J}\right)^{-1} \cdot \mathbf{J}^{\mathrm{T}} \cdot \mathbf{W} \cdot \mathbf{r} \,. \tag{B.1}$$

are implemented here. Dependent on the chosen option '-a', one out of three different methods for the matrix inversion is used, i.e. cofactor method, LU decomposition, or singular value decomposition. The cofactor method, however,

is not computed recursively as described in Subsection 5.3.1, but uses formulae which are precomputed up to a matrix size of $5 \times 5$. Hence, it is only applicable for problems with less than six model parameters.

In the case of nonlinear model functions, the Levenberg-Marquardt method (page 158, eq. (6.26))

$$\mathbf{\Delta a} = \left(\mathbf{J}^{\mathrm{T}} \cdot \mathbf{W} \cdot \mathbf{J} + \mu \cdot \mathbf{I}\right)^{-1} \cdot \mathbf{J}^{\mathrm{T}} \cdot \mathbf{W} \cdot \mathbf{r} \quad . \tag{B.2}$$

is applied and the fitting is iterated until convergence. The convergence criterion is identical to eq. (2.8) with $\epsilon = 10^{-10}$ (defined in `macros.h`), i.e. when the correction terms $\Delta a_j$ for all parameters fall under a given threshold, the iteration is stopped. Only, if the provided target value for $\chi^2$ (option '-t') is not reached, then the parameters are randomised in order to escape a possible local minimum, see also Section B.4.4. If $\chi^2$ has dropped down to zero, the algorithm stops as well. The maximum number of repeated iterations, however, is limited to 2000, if not differently specified via option '-I'.

Linear fitting is performed via equation (6.11)

$$\mathbf{a} = \mathbf{V} \cdot \mathbf{S}^{-1} \cdot \mathbf{U}^{\mathrm{T}} \cdot \mathbf{\Sigma} \cdot \begin{pmatrix} y_1 & y_2 & \cdots & y_N \end{pmatrix}^{\mathrm{T}} \quad . \tag{B.3}$$

by default. The matrices $\mathbf{V}$, $\mathbf{S}$, and $\mathbf{U}$ are results of a singular value decomposition (see Subsection 5.3.4). $\mathbf{\Sigma}$ is a diagonal matrix containing the reciprocal uncertainties of the observations $y_i$ (see Section 6.3). This method is implemented in `solve_lin.c`, which is called from `ls.c`.

There is another fitting routine `ls_straighline.c` for the fitting of straight lines only. It is used for the piece-wise approximation of observations in the case of weights estimation via binning (Section 3.3.1) and uses eq. (7.16) from Section 7.4 with equal weights $w_i = 1.0 \; \forall \; i$.

The methods for weights estimation are encoded in file `est_weights.c` according to the explanations in Chapter 3. The file `outlier_detection.c` contains the algorithms for outlier detection.

`functions.c` contains all implemented model functions and/or their derivatives, respectively. They will be discussed below. The header file `functions.h` provides the corresponding prototypes of the functions.

As described in Section 2.3, the model parameters have to be initialised with reasonable values in the case of nonlinear model functions. This is done in special initialisation functions in the files `init_collection.c` and `init_gauss2.c` and will be described exemplarily below. The functions from the NIST data base (see

Section B.7) are encoded in separate files `functions_NIST.c`, `functions_NIST.h`, and `init_NIST.c`.

The matrix inversion via singular value decomposition is encoded in `svd_inversion.c`, which calls `singvaldec.c`. Other matrix operations can be found in `decomp_LU.c` and `matrix_utils.c`. The latter also contains special functions for the allocation of memory. It is accompanied with a header file `matrix_utils.h` for prototyping purposes.

`get_option.c` and `get_option.h` are responsible for the command-line parsing. All options start with a dash (minus sign) followed by one or more characters. The lists of available and compulsory options must be given in `usage.c`, which also provides help in cases of wrong command-line options.

`errmsg.c` and `errmsg.h` support a simple kind of error handling. The sorting of arrays of different types is possible using the functions in `heap_sort.c`.

Finally, there are two other header files, `macros.h` and `defines.h`, containing macros and definitions required in several functions.

## B.4 Model functions

The file `functions.c` contains all necessary information about the implemented model functions. Linear functions require simply the first partial derivatives with respect to the single model parameters. In contrast to this, fitting nonlinear functions additionally needs the model function as such.

### B.4.1 Numerical differentiation

In case of complicated nonlinear functions it might be simpler to use numerical differentiation instead of analytical determination of the partial first derivatives. This can be achieved by inspecting the functional course close to the actual parameter vector $\mathbf{a}$ using a distance $\delta_j$

$$\frac{\partial f}{\partial a_j} \simeq \frac{f(\mathbf{a} + \delta_j \mathbf{e}_j) - f(\mathbf{a} - \delta_j \mathbf{e}_j)}{2 \cdot \delta_j} \tag{B.4}$$

where $\mathbf{e}_j$ is the unit vector along $a_j$, i.e. as for instance $\mathbf{e}_1 = (1\ 0\ 0\ \ldots)^{\mathrm{T}}$ for $a_1$. $\delta_j$ should be only a portion of the parameter value. The implementation (function `f_deriv()`) uses $\delta_j = a_j/C$ with $C = 10^6$ yielding a variation of relatively small amounts. If $a_j = 0$, then $\delta_j$ is set to the arbitrary value of 0.001.

```
/*-------------------------------------------------------------
 * frotation()
 *     x = f1(u|a) = a1 + cos(a3) * u - sin(a3) * v
 *     y = f2(u|a) = a2 + sin(a3) * u + cos(a3) * v
 *-------------------------------------------------------------*/
double
frotation( int i, double *cond, double *a)
{
  if (i%2 == 0)
  {
    /* equation for x */
    return a[0] + cos(a[2]) * cond[i] - sin(a[2]) * cond[i+1];
  }
  else
  {
    /* equation for y */
    return a[1] + sin(a[2]) * cond[i-1] + cos(a[2]) * cond[i];
  }
}
```

Figure B.18: Source code example with interleaved access to conditions of a two-dimensional function

The drawback of the numerical differentiation is its computational complexity, since the model function has to be called twice with different parameter settings. In addition, the results of nonlinear approximation are somewhat less accurate than the results based on analytical derivations (see Section B.7).

### B.4.2 Handling of multi-dimensional conditions

The treatment of model functions with a single condition per observation is rather straightforward, since both, conditions $x_i$ and observations $y_i$, can be stored in one-dimensional arrays, '`cond[]`' and '`obs[]`'. The joint handling of these model functions with those having more than one condition requires the re-use of these arrays for multi-dimensional conditions. The implemented code writes the conditions $\mathbf{x}_i$ in alternating order into the array `cond[]`. If there are two conditions per observations, for example, the length of `cond[]` must be doubled. All functions accessing this array must increase the array index accordingly. This concerns, for example, the files `fitting.c` and `init_collection.c` (functions: `flin_deriv()`, `frotation()`, `fcircle()`). **Figure B.18** shows function `frotation()`, where the distinction between the interleaved conditions is made using the modulo-2 operation '`i%2`'.

### B.4.3 Limitation of parameter space

Section 2.3 had already discussed the problem of restricted ranges of allowed parameter values. The exponential function

$$y_i = a_1 \cdot \exp(a_2 \cdot x_i)$$

is one example, where the domain of definition has to be limited. The corresponding function is implemented in `fexpon2_deriv()` in file `functions.c`. If it is known that the observations describe a decaying process, then the parameter $a_2$ must be negative. In case that this parameter becomes non-negative in the course of optimisation, it is set virtually to zero by changing the partial derivatives for $a_1$ and $a_2$ according to

$$\frac{\partial f}{\partial a_1} = \begin{cases} \exp(a_2 \cdot x_i) & \text{if } a_2 < 0 \\ 1 & \text{otherwise} \end{cases}$$

and

$$\frac{\partial f}{\partial a_2} = \begin{cases} x_i \cdot a_1 \cdot \exp(a_2 \cdot x_i) & \text{if } a_2 < 0 \\ x_i \cdot a_1 & \text{otherwise} \end{cases} .$$

In doing so, the error surface is modified virtually and the optimisation does not walk into this direction.

If, however, the model function is only defined in a certain range as, for example, the logarithmic function

$$f(x|a_1) = \log(a_1 \cdot x) = \log(a_1) + \log(x) \qquad a_1 > 0 ,$$

then the parameter $a_1$ should be fixed before evaluating the function or its derivation.

### B.4.4 Initialisation of parameters

The proper initialisation can reduce the number of required iterations and might be even essential, if the error surface has many local minima. This problem was already addressed more in detail in Section 2.3. The responsible functions can be found in `init_collection.c` and `init_gauss2.c`. Two examples are discussed in the following.

**Example 1**: Fitting of a circle (`init_collection.c`)
Using the model function

$$(y_1 - a_1)^2 + (y_2 - a_2)^2 = r^2 ,$$

three parameters must be determined. Under the assumption that the sample points are evenly distributed on the circle, the centre coordinates $(a_1, a_2)$ can be estimated by

$$a_{1\text{init}} = \frac{1}{N} \cdot \sum_{i=1}^{N} y_{1i} \qquad \text{and} \qquad a_{2\text{init}} = \frac{1}{N} \cdot \sum_{i=1}^{N} y_{2i} \; .$$

The estimated radius is the averaged distance between all observed points and the estimated circle centre

$$r_{\text{init}} = \frac{1}{N} \cdot \sum_{i=1}^{N} \sqrt{(y_{1i} - a_{1\text{init}})^2 + (y_{2i} - a_{2\text{init}})^2} \; .$$

□□□

**Example 2**: Neural network (`init_collection.c`)
Initially all parameters are set to uniformly distributed random values in the range of $[-1; 1]$, if not specified differently on the command line. In order to keep the input of the hidden neurons also within $[-1; 1]$, the maximum and minimum condition values are determined and the parameter values accordingly normalised, see `init_NN3x3x1()` for example.
□□□

The provided source code supports the definition of a target value for $\chi^2_{\text{max}}$ (option '-t'), which can be used to escape local minima. If the actual value of $\chi^2$ is higher than $\chi^2_{\text{max}}$ after convergence or a maximum number of iterations, the parameters are re-initialised (`ls.c`, lines 541ff. and lines 614ff., respectively). However, calling the initialisation routines again only makes sense if they have a random component yielding different parameters in **a** for each call.

## B.5 Special algorithms

### B.5.1 LU decomposition

The LU decomposition described in Section 5.3.3 is performed using Crout's algorithm, see [Pre92] for details. The result is a single matrix, which contains

both, the $\lambda$'s and the $\upsilon$'s

$$\begin{pmatrix} \upsilon_{11} & \upsilon_{12} & \cdots & \upsilon_{1M} \\ \lambda_{21} & \upsilon_{22} & \cdots & \upsilon_{2M} \\ \vdots & \vdots & \ddots & \vdots \\ \lambda_{M1} & \lambda_{M2} & \cdots & \upsilon_{MM} \end{pmatrix} . \tag{B.5}$$

### B.5.2 Singular value decomposition

For a detailed description of the singular value decomposition see for instance [Bjo96]. The implementation in `singvaldec()` is based on a FORTRAN source code published on the internet [SVD]. The translation to C also takes into account that the indices are starting from zero in C and not from one as in the FORTRAN language.

### B.5.3 Sorting

The functions for weights estimation require the sorting of values at different stages. The file `heap_sort.c` contains two routines for the sorting based on the heap-sort algorithm. The function `heap_sort_d()` sorts the values in the input vector array `values[]`. A second routine `heap_sort_d_()` sorts in addition an index array. This is helpful, if the values must stay in their order and the sorted access is solely performed via the sorted index array. In this case, the value array passed to the heap-sort function must be a copy of the original vector array in order to keep the original values unsorted.

## B.6 Possible optimisations

It must be emphasised again that the provided source code is neither optimised for speed nor using elegant implementations, but is designed to be readable in connection with the text of this book.

Besides optimisations with respect to the speed of calculations, the user might be interested to have more influence on the performance of the data fitting. For instance the convergence criterion is hard-coded, but could be provided by the user via an additional program option. The same holds true for desired parameter ranges in terms of minimum and/or maximum values for all $a_j$.

Currently, the program does not support the usage of weights provided along with the observations. Also the combined fitting of two model functions as described

in Section 7.5 is not implemented yet. The total least-squares approach (Section 7.6) works only for the special case of fitting a circle.

The implementation of the neural networks based on the sigmoid function might be not optimal. The convergence process is highly dependent on the starting parameter values. Future implementations should consider to use radial basis functions as activation function for the neurons.

Suggestions by the reader towards the future improvement of the program are welcome!

## B.7 Performance Test

The National Institute of Standardization and Technology (NIST)[2] maintains a website containing statistical reference datasets [Strd].

In response to industrial concerns about the numerical accuracy of computations from statistical software, the Statistical Engineering and Mathematical and Computational Sciences Divisions of NIST's Information Technology Laboratory are providing datasets with certified computational results for a variety of statistical methods enabling the objective evaluation of statistical software.

Several datasets addressing linear as well as nonlinear problems are listed; either stemming from real world measurements or prepared by hand in order to stress the fitting algorithms. The datasets are labelled according to the level of difficulty as 'Lower', 'Average', or 'Higher'. All datasets are accompanied with the underlying model function $y = f(\mathbf{x}|\mathbf{a})$, certified model parameters $a_j$, which lead to the true global minimum, and their standard uncertainties $\sigma_{a_j}$. Producing correct results for all datasets in this collection will provide some degree of assurance, in the sense that a certain software package provides correct results for datasets known to yield incorrect results for some software. The certified values are 'best-available' solutions, obtained using 128-bit precision and confirmed by at least two different algorithms and software packages using analytic derivatives.

This section will evaluate the implemented algorithms using only the data with 'higher' difficulty. The NIST website states that "a good nonlinear least squares procedure should be able to duplicate the certified results to at least 4 or 5 digits".

The developed fitting software has been tested on a Pentium® 4 CPU (32 bit). Since the NIST datasets do not contain weights, $\sigma_i = 1.0$ is used for all tests.

[2] Founded in 1901, NIST is a non-regulatory federal agency within the U.S. Department of Commerce. NIST's mission is to promote U.S. innovation and industrial competitiveness by advancing measurement science, standards, and technology in ways that enhance economic security and improve our quality of life.

Table B.1: Results of fitting difficult linear model functions: number of correct digits in mantissae of estimated model parameters

| Dataset | Model type | $M$ | Default | '-s -a 1' | '-s -a 2' | '-c' | '-s -a 1 -c' |
|---|---|---|---|---|---|---|---|
| Filip | polynomial | 11 | 2 | failed | failed | 7 | 0 |
| Longley | multilinear | 7 | 9 | failed | 9 | 11 | 7 |
| Wampler 1 | polynomial | 6 | 10 | 3 | 5 | 10 | 6 |
| Wampler 2 | polynomial | 6 | 11 | 5 | 9 | 11 | 9 |
| Wampler 3 | polynomial | 6 | 7 | 3 | 5 | 10 | 7 |
| Wampler 4 | polynomial | 6 | 5 | 3 | 5 | 8 | 7 |
| Wampler 5 | polynomial | 6 | 3 | 3 | 5 | 6 | 6 |

### B.7.1 Fitting linear systems

The NIST data base contains seven linear problems of higher difficulty, two observed sets (Filip and Longley) and five artificially generated (Wampler1-5).

The default setup of the developed fitting software for solving linear problems is to apply the special SVD-based approach according to equation (B.3)

$$\mathbf{a} = \mathbf{V} \cdot \mathbf{S}^{-1} \cdot \mathbf{U}^{\mathrm{T}} \cdot \mathbf{\Sigma} \cdot \begin{pmatrix} y_1 & y_2 & \cdots & y_N \end{pmatrix}^{\mathrm{T}} ,$$

where $\mathbf{V}$, $\mathbf{S}$, and $\mathbf{U}$ are the matrices derived from the Jacobian matrix via singular value decomposition (see Subsections 5.3.4 and 6.3.2). The matrix $\mathbf{\Sigma}$ is a diagonal matrix containing the reciprocal uncertainties of the observations $y_i$ (see Section 6.3).

Alternatively, option '-s' switches to equation (B.1)

$$\mathbf{a} = \left(\mathbf{J}^{\mathrm{T}} \cdot \mathbf{W} \cdot \mathbf{J}\right)^{-1} \cdot \mathbf{J}^{\mathrm{T}} \cdot \mathbf{W} \cdot \mathbf{y} ,$$

where an explicit inversion of the normal matrix $\mathbf{N} = \mathbf{J}^{\mathrm{T}}\mathbf{W}\mathbf{J}$ is performed. The algorithm for inversion can be chosen via option '-a'. However, '-a 0' is only applicable for model functions with five parameters in maximum. The option '-c' enables the scaling of the condition values (see Subsection 6.3.3).

**Table B.1** indicates the number of correct digits in the mantissae of estimated parameter values. The numbers are approximate results, since the number of identical digits can vary for different $a_j$.

It can be clearly seen that the special SVD approach (column 'Default') outperforms the standard setup (option '-s') for all datasets. Polynomials of high

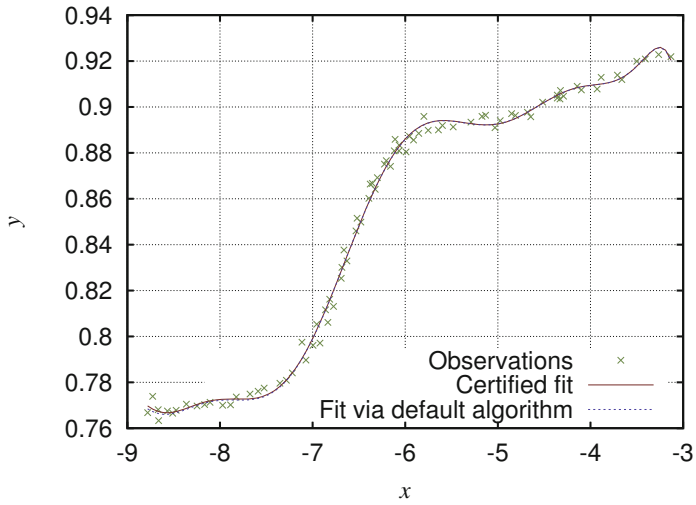


Figure B.19: Filip dataset and its approximation

order, as the Filip set, cannot be fitted via the normal matrix at 32-bit precision without special treating of the data. Even the special SVD approach yields only two correct digits. However, the visual quality of fitting is already rather good (**Figure B.19**).

When using option '-s' for the Filip data, the program outputs an error message, because at least one of the computed model parameter variance is negative, which indicates numerical instability. The same happens for the Longley dataset when using the options '-s -a 1'.

The Wampler datasets where designed to stress the fitting algorithms under test. The observations deviate more or less from a polynomial of fifth order. The model parameters are always equal to one or equal to $10^{-b}$ ($b \in \mathbb{N}$) in the case of the Wampler2 set. Albeit the results of the designed fitting program deviate somewhat from this exact solution, the plots are indistinguishable as can be seen for the case of Wampler4 (**Figure B.20**).

Interestingly, when using the standard approach, then the inversion via LU decomposition (option '-a 2') yields better results for all tested datasets than the inversion via singular value decomposition (option '-a 1').

The normalisation of the condition values by their absolute maximum before the least-squares approximation is applied (option '-c', see Subsection 6.3.3) distinctly increases the numerical accuracy. In addition, the standard approach (option '-s -a 1 -c') does not fail, neither in application to the Filip data nor to the Longley data. In general, the accuracy of the estimated parameters is increased compared

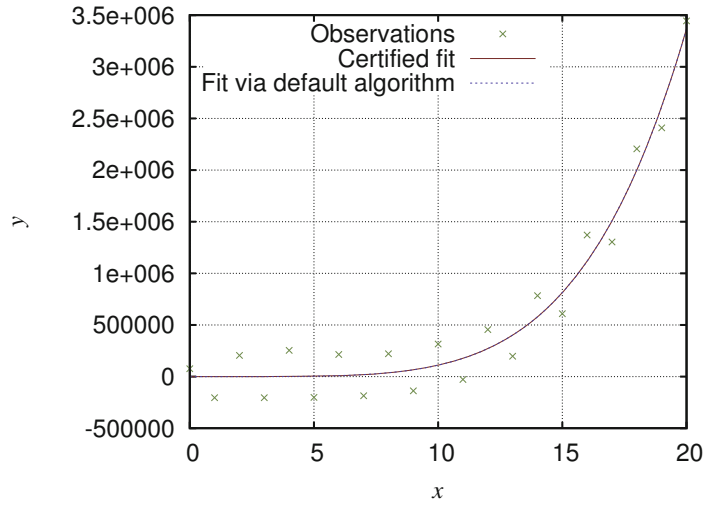


Figure B.20: Wampler4 dataset and fitted curves

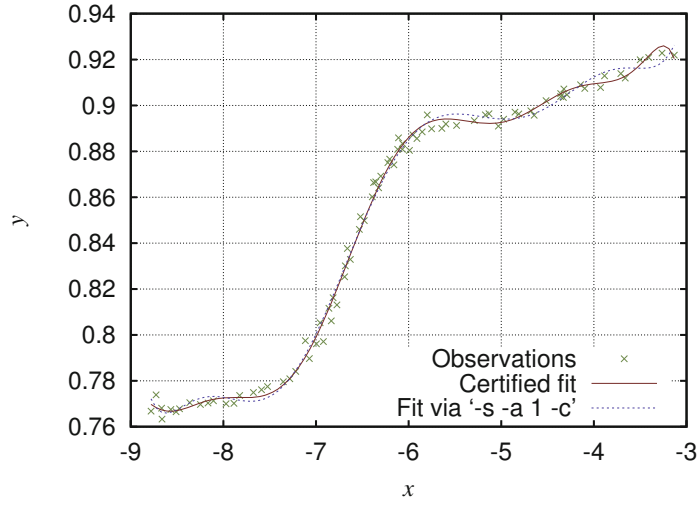


Figure B.21: Filip dataset fitted with options '-s -a 1 -c'

to column '-s -a 1'. Only the estimated parameters of the Filip data differ strongly from the true values. Nevertheless, the fitted curve is still close to the true one (**Figure B.21**).

### B.7.2 Fitting nonlinear systems

The robustness and reliability of nonlinear least squares software depends on the algorithm used and how it is implemented, as well as on the characteristics of the actual problem being solved. As already pointed out in Section 2.3, nonlinear least squares solvers are particularly sensitive to the starting values provided for a given problem. For this reason, the NIST website provides three sets of starting values for each problem: the first is relatively far from the final solution; the second relatively close; and the third is the actual certified solution.

**Table B.2** list the results of nonlinear fitting based on equation (B.2)

$$\mathbf{\Delta a} = \left(\mathbf{J}^{\mathrm{T}} \cdot \mathbf{W} \cdot \mathbf{J} + \mu \cdot \mathbf{I}\right)^{-1} \cdot \mathbf{J}^{\mathrm{T}} \cdot \mathbf{W} \cdot \mathbf{r} \quad .$$

The table contains at least two lines for each dataset corresponding to the two sets of initial parameter values, which are provided along with the data. The abbreviation 'st. 1' stands for the parameter set, which is far from the final solution. The lines 'st. 2' list the results stemming from initial parameter values close to the certified solution. The datasets BoxBOD and Eckerle4 have a third entry. As these model functions have a more or less simple structure, it is possible to guess suitable starting values directly from the observations.

Each column contains two values. The first one is the number of digits which are identical to the certified values; the second value in parenthesis is the number of iterations till convergence of the algorithm. Cases without convergence to a minimum are indicated by 'no conv.'.

As can be concluded from the column 'default', the developed software is very robust and reliable. There is only a single case (MGH10 start set 1) where the algorithm could not converge. In all other cases, the fitting program could determine the model parameter with sufficient accuracy.

Even though start set 1 defines initial parameter values, which are more distant from the global minimum than the values from start set 2, the number of iterations is not always higher. For the datasets Thurber and Bennett5, the algorithm converges faster, when starting from the remote point.

Five additional tests have been made in order to test single features of the fitting algorithm:

- '-n' ... usage of numerical derivation instead of analytical derivation,

Table B.2: Results of fitting difficult nonlinear model functions: number of correct digits in mantissae of estimated model parameters

| Dataset | Model | $M$ | Default | '-n ' | '-a 0 ' | '-a 2' | '-L' | '-L -a 2' |
|---|---|---|---|---|---|---|---|---|
| MGH09 st. 1 | rational | 4 | 8 (233) | 8 (231) | 8 (230) | 9 (232) | 0 (29) | failed |
| MGH09 st. 2 | rational | 4 | 9 (44) | 9 (47) | 8 (47) | 8 (46) | 0 (118) | 8 (46) |
| Thurber st. 1 | rational | 7 | 8 (72) | 8 (73) | / | 9 (73) | 0 (66) | 0 (46) |
| Thurber st. 2 | rational | 7 | 10 (83) | 9 (83) | / | 8 (82) | 11 (66) | 11 (66) |
| BoxBOD autom. | expon. | 2 | 10 (22) | 10 (23) | 10 (22) | 10 (22) | 11 (20) | 11 (20) |
| BoxBOD st. 1 | expon. | 2 | 8 (27) | failed/1/ | 8 (27) | 8 (27) | 11 (21) | failed/2/ |
| BoxBOD st. 2 | expon. | 2 | 11 (24) | 8 (26) | 11 (24) | 11 (24) | 11 (19) | 11 (19) |
| Rat42 st. 1 | expon. | 3 | 11 (28) | 8 (29) | 10 (30) | 11 (28) | failed/1/ | failed/1/ |
| Rat42 st. 2 | expon. | 3 | 10 (23) | 10 (23) | 10 (23) | 10 (23) | 11 (10) | 10 (10) |
| Rat43 st. 1 | expon. | 4 | 9 (34) | 8 (35) | 9 (34) | 10 (33) | 0 (5) | failed/1/ |
| Rat43 st. 2 | expon. | 4 | 10 (23) | 9 (26) | 9 (25) | 7 (24) | 10 (17) | 10 (17) |
| MGH10 st. 1 | expon. | 3 | 0 (no conv.) | 0 (no conv.) | 0 (no conv.) | 0 (no conv.) | 0 (9) | failed/3/ |
| MGH10 st. 2 | expon. | 3 | 7 (420) | 7 (419) | 7 (418) | 7 (420) | 11 (18) | 11(18) |
| Eckerle4 autom. | expon. | 3 | 11 (11) | 11 (8) | 11 (11) | 11 (11) | 11 (8) | 11 (8) |
| Eckerle4 st.1 | expon. | 3 | 11 (71) | 9 (75) | 11 (42) | 11 (71) | failed/4/ | failed/2/ |
| Eckerle4 st.2 | expon. | 3 | 11 (11) | 11 (10) | 11 (11) | 11 (11) | 11 (10) | 11 (10 |
| Bennett5 st.1 | misc. | 3 | 6 (1103) | 6 (1129) | 6 (1134) | 6 (1127) | 11 (45) | 11 (40) |
| Bennett5 st.2 | misc. | 3 | 6 (1754) | 6 (1752) | 6 (1754) | 6 (1753) | 11 (16) | 11 (34) |

- '-a 0' ... usage of direct inversion of the normal matrix instead of using the SVD,
- '-a 2' ... usage of LU decomposition for inversion of the normal matrix,
- '-L' ... usage of Gauss-Newton method instead of Levenberg-Marquardt,
- '-L -a 2' ... combination of Gauss-Newton method and LU decomposition.

Column '-n' proves that the implemented numerical derivation is accurate enough in general. Only fitting the BoxBOD dataset starting from the remote point fails. The failures are labelled in the table and the numbers have following meaning

- failed/1/ ... Result too large (CPU message),
- failed/2/ ... error message from LU decomposition "max. element is zero",
- failed/3/ ... error message from SVD "degraded matrix"[3],
- failed/4/ ... error message from SVD "singular matrix",

Column '-a 0' and '-a 2' show that there is only little advantage of SVD over other methods for matrix inversion. More interesting is the behaviour if the optimisation is performed without the Levenberg-Marquardt term $\mu \cdot \mathbf{I}$. The Gauss-Newtom method fails in two cases and does not converge to the desired minimum in five other cases. Then again, it leads to more accurate parameters values for the Bennett5 and MGH10 (start set 2) datasets using a fraction of iterations. If the Gauss-Newton method is accompanied with the LU decomposition for inversion of the normal matrix, the algorithm tends to fail instead to converge to a non-desired target.

The **Figures** B.22–B.25 show the fitting results (default approach) for selected datasets. The corresponding model functions are

- BoxBOD: $f(x|\mathbf{a}) = a_1 \cdot (1 - \mathrm{e}^{-a_2 \cdot x})$
- Thurber: $f(x|\mathbf{a}) = \dfrac{a_1 + a_2 \cdot x + a_3 \cdot x^2 + a_4 \cdot x^3}{1 + a_5 \cdot x + a_6 \cdot x^2 + a_7 \cdot x^3}$
- MGH10: $f(x|\mathbf{a}) = a_1 \cdot \mathrm{e}^{a_2/(x+a_3)}$
- Bennett5: $f(x|\mathbf{a}) = a_1 \cdot (a_2 + x)^{-1/a_3}$

[3] The failure message for MGH10 st.1 '-L -a 2' does not stem from the matrix inversion within the iterations, because the LU decomposition is used here. The SVD is required for the determination of the covariance matrix after a minimum was found.

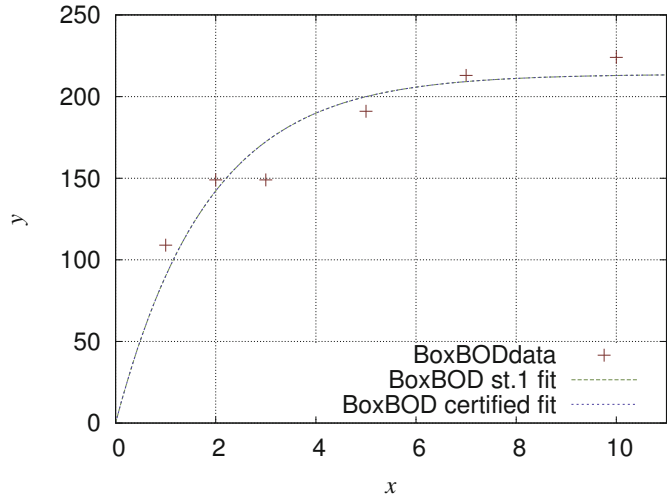


Figure B.22: BoxBOD dataset and fitted curve

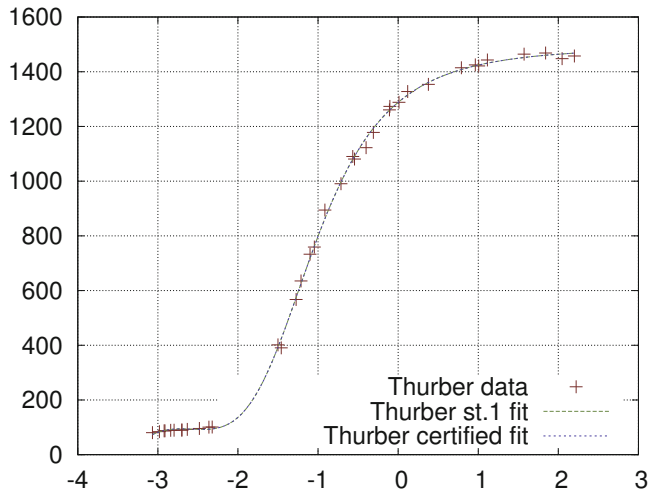


Figure B.23: Thurber dataset and fitted curve

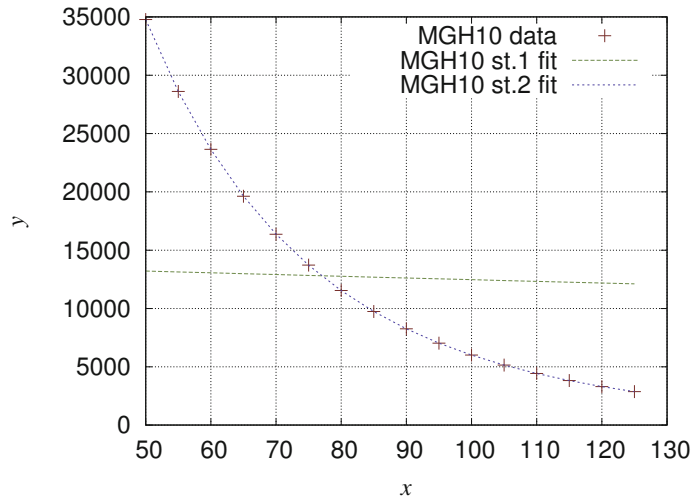


Figure B.24: MGH10 dataset and fitted curve

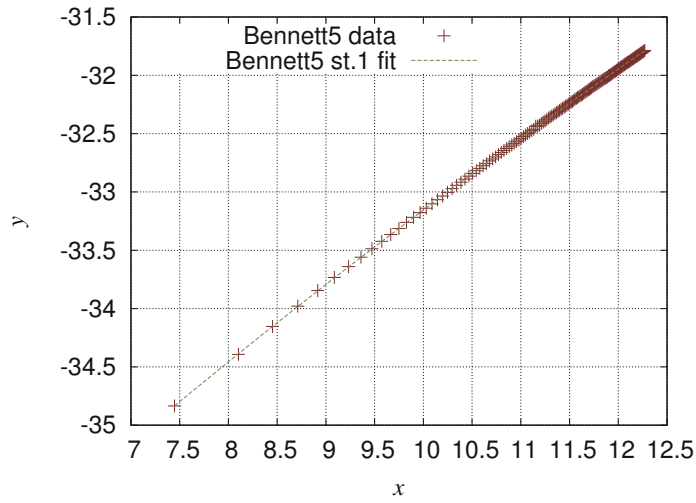


Figure B.25: Bennett5 dataset and fitted curve

# List of symbols

| | |
|---|---|
| $\in$ | is element of |
| $\forall$ | for all |
| $\approx$ | approximately equal |
| $\|g\|$ | absolute value of $g$ |
| $\|\|\mathbf{g}\|\|$ | (Euclidean) norm of vector $\mathbf{g}$; $\|\|\mathbf{g}\|\| = \sqrt{\mathbf{g}^{\mathrm{T}} \cdot \mathbf{g}}$ |
| $a_j$ | model parameter with $j = 1, 2, \ldots, M$ |
| $\Delta a_j$ | change of the model parameter $a_j$ |
| $\mathbf{a}$ | vector of model function parameters $(a_1 \ \ldots \ a_j \ \ldots \ a_M$ |
| $\boldsymbol{\Delta}\mathbf{a}$ | vector of model function parameters changes |
| $\hat{\mathbf{a}}$ | vector of estimated model parameters |
| $\mathbf{A} = (a_{ij})$ | matrix with elements $a_{ij}$ |
| $\mathbf{A}^{\mathrm{T}} = (a_{ji})$ | transposed matrix of $\mathbf{A}$ |
| $b_j$ | model parameter with $j = 1, 2, \ldots, M$ |
| $\mathbf{C}$ | covariance matrix |
| $\chi^2$ | value to be minimised in the course of least-squares approximation |
| $\Delta_i$ | deviate $y_i - \hat{y}_i$ |
| $\varepsilon_i$ | error in $y_i$ |
| $f(\mathbf{x}\|\mathbf{a})$ | model function |
| $f(x)$ | function of $x$ |
| $f'(x)$ | first derivative of function $f(x)$ |
| $f^{(\nu)}(x)$ | $\nu$th derivative of function $f(x)$ |
| $g_{\mathrm{fit}}$ | goodness of fit |
| $\mathbf{g}$ | vector of gradients $\mathbf{g} = \left(\frac{\partial\chi^2(\mathbf{a})}{\partial a_1} \ \ \frac{\partial\chi^2(\mathbf{a})}{\partial a_2} \ \ \ldots \ \ \frac{\partial\chi^2(\mathbf{a})}{\partial a_M}\right)^{\mathrm{T}}$ |
| $\mathbf{H}$ | Hessian matrix $\mathbf{H} = \left(\frac{\partial^2\chi^2(\mathbf{a})}{\partial a_j \partial a_k}\right)$ |
| $I$ | current |
| $\mathbf{I}$ | identity matrix |
| $i$ | number of an observation $i = 1, 2, \ldots, N$ |
| $\mathbf{J}$ | Jacobian matrix |
| $\mathbf{L}$ | lower triangular matrix |
| $\lambda_{\mathrm{L}}$ | threshold for discrimination between observations with equal weights and observations with adaptively estimated weights |
| $\lambda_{\mathrm{O}}$ | threshold for discrimination between good observations and outliers |
| $\Lambda_i$ | absolute deviate $\|y_i - \hat{y}_i\| = \|\Delta_i\|$ |

T. Strutz, *Data Fitting and Uncertainty*, DOI 10.1007/978-3-8348-9813-5,

| | |
|---|---|
| $\mu$ | mean value of a (Gaussian) distribution |
| $M$ | number of model parameters |
| $N$ | number of observations |
| $N_{\text{free}}$ | number of degrees of freedom, $N_{\text{free}} = N - M$ |
| $\mathcal{N}(\mu, \sigma^2)$ | Gaussian distribution |
| $\mathbf{N}$ | normal matrix |
| $\mathbb{N}$ | set of natural numbers |
| $r$ | radius |
| $\mathbf{r}$ | vector of residuals $(y_i - f(\mathbf{x}_i\|\mathbf{a}))$, $i = 1, 2, \ldots, N$ |
| $P$ | probability |
| $\prod_{i=0}^{p} b_i$ | product $b_0 \cdot b_1 \cdot b_2 \cdot \ldots \cdot b_p$ |
| $R$ | resistor |
| $\mathbf{S}$ | matrix of singular values |
| $\sigma$ | standard deviation of Gaussian distribution |
| $\sigma_\varepsilon^2$ | variance of normally distributed noise |
| $\sigma_{a_j}^2$ | variance of estimated parameter $a_j$ |
| $\sigma_i$ | standard uncertainty of of the parent distribution of $y_i$ |
| $\sigma_{\text{y}}$ | standard uncertainty of y |
| $\hat{\sigma}_{\text{y}}$ | estimated standard uncertainty of y |
| $\mathbf{\Sigma}$ | diagonal matrix of reciprocal uncertainties |
| $\sum_{i=0}^{p} b_i$ | sum $b_0 + b_1 + b_2 + \ldots b_p$ |
| $U$ | voltage |
| $\mathbf{U}$ | upper triangular matrix;<br>matrix resulting from singular value decomposition |
| $\mathbf{V}$ | matrix resulting from singular value decomposition |
| $w_i$ | weight assigned to observation $y_i$, $i = 1, 2, \ldots, N$ |
| $\mathbf{W} = (w_{ij})$ | matrix of weights |
| $x$ | condition, independent variable |
| $\mathbf{x}$ | vector of conditions $(x_1 \ \ldots \ x_k \ \ldots)$ |
| $\mathbf{x}_i$ | vector of conditions under which a particular value $y_i$ was observed |
| $\hat{x}[n]$ | estimated value of $x[n]$ |
| $y$ | dependent variable |
| $\overline{y}$ | mean value of $y$ |
| $y_i$ | value of a measurement, observation |
| $\hat{y}_i$ | estimate of $y_i$ based on the model function and estimated parameters $\hat{\mathbf{a}}$ |
| $\mathbf{y}$ | vector of observations $(y_1 \ldots y_N)^{\text{T}}$ |
| $\mathbb{Z}$ | set of integers |

# Bibliography

[Bar94] Barnett, V.; Lewis, T.: *Outliers in Statistical Data*. 3rd edition, WILEY, 1994, ISBN 0-471-93094-6

[Bec83] Beckman, R.J.; Cook, R.D.: Outliers. *Technometrics*, Vol.25, No.2, May 1983, 119–149

[Bev92] Bevington, P.R.; Robinson, D.K.: *Data reduction and error analysis for the physical science.*, 2nd edition, WCB/McGraw-Hill, 1992, ISBN 0-07-911243-9

[Bir32] Birge, R.T.: The calculation of errors by the method of least squares. *Physical Review* Vol. 40, April 15, 1932, 207–227

[Bis95] Bishop, C.M.: *Neural Networks for Pattern Recognition*. Oxford University Press, 1995, ISBN 0-19-853864-2

[Bjo96] Björk, Å.: *Numerical methods for least squares problems*. SIAM, Philadelphia, 1996, ISBN 0-89871-360-9

[Bog87] Boggs, P.T.; Byrd, R.H.; Schnabel, R.B.: A stable and efficient algorithm for nonlinear orthogonal distance regression. *SIAM J. Sci. Stat. Comput.*, Vol.8, No.6, November 1987, 1052–1078

[Bre00] Breuning, M.M; Kriegel, H.-P.; NG, R.T.; Sander, J, "LOF: Identifying density-based local outliers", *Proc. of the ACM SIGMOD Int. Conf. on Management of Data*, Dallas, Texas, 2000

[Car88] Carroll, R.J.; Ruppert, D.: *Transformation and Weighted Regression*. Chapman and Hall, New York, 1988

[Cha71] Chauvenet, W.: Method of Least Squares. Appendix to *Manual of Spherical and Practical Astronomy*, Vol.2, 4th edition, J.B. Lippincott & CO., Philadelphia, 1871, 469–566

[Coo93] Coope, I.D.: Circle Fitting by Linear and Nonlinear Least Squares. *Journal of Optimization and Applications*, Vol.6, No.2, February 1993, 381–388

[ESH07] *Engineering Statistics Handbook*. www.itl.nist.gov, visited 28 June 2007

T. Strutz, *Data Fitting and Uncertainty*, DOI 10.1007/978-3-8348-9813-5,

[Gel68] Gellert, W.; Küstner, H.; Hellwich, M.; Kästner, H. (eds.): *Mathematik – Kleine Enzyklopedie.* VEB Bibliographisches Institut Leipzig, 3. Auflage, 1968

[Goe89] Göhler: *Höhere Mathematik – Formeln und Hinweise.* VEB Deutscher Verlag für Grundstoffindustrie, Leipzig, 10. Auflage, 1989

[Gnupl] www.gnuplot.info, May 2007

[Ham71] Hampel, F.R.: A general qualitative definition of robustness. *Ann. Math. Stat.*, Vol.42, 1971, 1887–1896

[Ham86] Hampel, F.R.; Ronchetti, E.M; Rousseeuw, P.J.; Stahel, W.A.: *Robust Statistics: The Approach Based on Influence Functions.* Wiley, New York, 1986

[Hod04] Hodge, V.J; Austin, J., "A survey of Outlier Detection Methodologies", *Artificial Intelligence Review*, 2004, 22, 85–126

[Hol77] Holland, P.W.; Welsch, R.E.: Robust regression using iteratively reweighted least-squares. *Comm. Statist.-Theor. Meth.* Vol.A6(9), 1977, 813–827

[ISO00] ISO/IEC 14495-1, *Information technology – Lossless and near-lossless compression of continuous-tone still images: Baseline (JPEG–LS).* International Standard, corrected and reprinted version, 15 September 2000

[Jai88] Jain, A.K. and Dubes, R.C.: *Algorithms for Clustering Data.* Prentice Hall, Englewood Cliffs, New Jersey 07632, 1988, ISBN 013022278X

[Kas76] Kása, I.: A Circle Fitting Procedure and its Error Analysis. *IEEE Transactions on Instrumentation and Measurement* March 1976, 8–14

[Law95] Lawson, C.L.; Hanson, R.J.: *Solving Least Squares Problems.* SIAM Classics in Applied Mathematics, 1995, ISBN 0-89871-356-0

[Lev44] Levenberg, K.: A Method for the Solution of Certain Problems in Least Squares. *Quart. Appl. Math.* 2, 1944, 164–168

[Mad04] Madsen, K.; Nielsen, H.B.; Tingleff, O: *Methods for Non-Lineaer Least Squares Problems.* 2nd edition, published on the WWW, April 2004

[Mar03] Markou, M.; Singh, S.: Novelty Detection: A Review. Part I + II, *Signal Processing*, 2003, Vol.83, 2481–2521

[Mar63] Marquardt, D.: An Algorithm for Least-Squares Estimation of Nonlinear Parameters. *SIAM J. Appl. Math.* 11, 1963, 431–441

[Mey84] Meyer, E.F.: *A Practical Guide to Curve-Fitting for Chemists*. Chicago, 1984, ASIN B0007B77NK

[Mey01] Meyer, B.; Tischer, P.: Glicbawls — Grey Level Image Compression By Adaptive Weighted Least Squares. *Proc. of Data Compression Conference, DCC'01*, 27–29 March 2001, Snowbird, Utah, USA, 2001

[Pap01] Papula, L.: *Mathematik für Ingenieure und Naturwissenschaftler*. Bd.3, Vieweg, 4th edition, 2001, ISBN 3-528-34937-9

[Pot06] Pothineni, S.B.; Strutz, T.; Lamzin, S.: Automated detection and centring of cryocooled protein crystals. *Acta Crystallographica* D62, November 2006, 1358–1368

[Pre92] Press, W.H.; Teukolsky, S.A.; Vetterling, W.T.; Flannery, B.P.: *Numerical Recipes in C*. 2nd edition, Cambridge University Press, 1992, ISBN 0-521-43108-5

[Pri92] Prince, E.; Boggs, P.T.: Least squares. in *International Tables for Crystallography*. Vol.C, Mathematical, physical and chemical tables, 1992, ISBN 0-7923-1638-X, 672–682

[Rya97] Ryan, T.R.: *Modern Regression Methods*. John Wiley & Sons, Inc., 1997, ISBN 0-471-52912-5

[Sch89] Schwarzenbach, D., et al: Statistical Descriptors in Crystallography. *Acta Cryst.* A45, 1989, 63–75

[Strd] http://www.itl.nist.gov/div898/strd/index.html, visited 20 January 2010

[SVD] Singular Value Decomposition (SVD): `http://www.pdas.com/programs/fmm.f90`, visited 17 May 2007

[Str88] Strang, G.: *Linear Algebra and Its Applications*. 3nd edition, Brooks Cole, 1988, ISBN 0155510053

[Str09a] Strutz, T.: *Bilddatenkompression*. 4th edition, Vieweg+Teubner, Wiesbaden, 2009, ISBN 978-3-8348-0472-3

[Str09b] Strutz, T.: Adaptive Cluster-Based Outlier Detection. *EUSIPCO'09*, Glasgow, UK, 24-28 Aug 2009

[Tau91] Taubin, G.: Estimation Of Planar Curves, Surfaces And Nonplanar Space Curves Defined By Implicit Equations, With Applications To Edge And Range Image Segmentation. *IEEE Trans. PAMI*, Vol.13, 1991, 1115-1138

[Tay97] Taylor, J.R.: *An Introduction to Error Analysis*. 2nd edition, University Science Books, Sausalito, California, 1997, ISBN 0-935702-42-3

[Wei98] Weisstein, E.W.: *CRC Concise Encyclopedia of Mathematics.*, CRC Press, 1998, ISBN 0849396409

[Wri84] Wright, T.W.: *A Treatise on the Adjustment of Observations by the Method of Least Squares*. Van Nostrand, New York, 1884

# Index



T. Strutz, *Data Fitting and Uncertainty*, DOI 10.1007/978-3-8348-9813-5,